

Development and Evaluation of a Semi-active Suspension System for Full Suspension Tractors

vorgelegt von

M.Sc.

Shahriar Sarami

aus Teheran

Von der Fakultät V –Verkehrs und Maschinensysteme
der Technischen Universität Berlin
zur Erlangung des akademischen Grades

Doktor der Ingenieurwissenschaften

Dr.-Ing.

genehmigte Dissertation

Promotionsausschuss:

Vorsitzender: Prof. Dr.-Ing. P. U. Thamsen

Berichter: Prof. Dr.-Ing. Henning J. Meyer

Berichter: Prof. Dr.-Ing. P. Pickel

Tag der wissenschaftlichen Aussprache: 02. September 2009

Berlin 2009

D 83

Abstract

Conventional primary agricultural tractors have no suspension systems. Since the usage of suspension systems in tractors improves the ride comfort and dynamic behavior of them, modern agricultural tractors are equipped with different suspension systems such as seat, cabin, or chassis suspension. The technology of the suspension systems for tractors is developing. Recently, some tractor models are presented with the frame construction. These tractors can be equipped with both front and rear axle suspensions. However, the efficiency of the passive suspensions is limited, and the idea of active systems is considered nowadays with the aim of improving the performance of vehicle's suspensions. With recent progress in electronic technology, this idea is going to be more and more practicable.

In this investigation, utilization of the active suspension was considered along with development in the suspension technology of agricultural tractors. As the first step, the background of the research was studied that led to select semi-active suspensions as proper systems for agricultural tractors. In addition, as the control strategy of this system, on-off skyhook was selected. In order to evaluate this new system experimentally, a test-tractor was determined. This tractor, called TU-Trac was a full suspension test-tractor with hydro-pneumatic rear suspension. During this research work, the rear axle suspension was equipped with a semi-active control system.

In order to evaluate the new suspension system, two approaches of the computer simulation testing and experimental testing were used. For the first one, the computer model of the tractor and suspension system, using MATLAB-Simulink program, was built. For the second approach, the prototype of the new suspension system including a set of the sensors, hydraulic actuators, and electronic controller was developed, and then, they were installed on the tractor suspension.

After that, the test design and test plan of the simulation and experimental tests were determined. The suspension system was excited by three sets of impulse inputs, which were applied to the four tractor's wheels. Each test was performed once on the tractor with passive suspension mode, and then, the same test was performed this time with the semi-active suspension computer model. In the experimental tests, a suspension test rig was used to apply the test inputs to the tractor. This test rig is a part of the facilities at the TU Berlin -

Department Machinery System Design. The outputs of the tests were the acceleration data of the tractor body and wheels. These data were analyzed to obtain the time and frequency domain results of them. These results were used in two groups of the body accelerations and dynamic tire forces in order to evaluate the ride comfort and handling ability of the tractor.

Using these results, overall computer model was validated by comparing the simulation results with experimental one. Then, the comparative results of the passive and semi-active modes of the simulation and experimental tests were used in order to evaluate the performance of the new suspension system. This comparison demonstrated until 13 % reduction on the average of the tractor body accelerations that showed significant improvement in the ride comfort of the tractor. Additionally, the average of the dynamic tire force of the tractor was reduced until 6 % showing that tractor handling was not reduced, but also it was improved significantly. As conclusion, the overall performance of the tractor's suspension was increased by using the new suspension system.

Keywords: agricultural tractor, suspension, handling, ride comfort, hydro-pneumatic, passive, semi-active, control system, skyhook, model, simulation, prototype, experimental tests, test rig.

Deutsch

Entwicklung und Untersuchung eines semiaktiven Federungssystems für vollgefederte Traktoren

Federungssysteme können den Fahrkomfort und das dynamische Verhalten von Traktoren verbessern. Aus diesem Grund werden moderne landwirtschaftliche Traktoren mit verschiedenen Federungssystemen ausgestattet, wie Vorderachs-, Sitz- und Kabinenfederung oder der Federung des Aufbaus. Besonders bei der Vorderachsfederung kommen hauptsächlich passive Regelungssysteme zum Einsatz. Die Hinterachse ist bei Standardtrakoren in der Regel ungefedert.

In dieser Untersuchung wurde die Anwendung eines semiaktiven Federungssystems in landwirtschaftlichen Traktoren betrachtet. Hierzu wurde ein Testtraktor mit einem hydropneumatischem Federungssystem für die Hinterachse und einem konventionellen Vorderachsfederungssystem ausgerüstet. Gleichzeitig wurde von dem Traktor ein Simulationsmodell mit dem Programmpaket Matlab-Simulink erstellt. Mit Hilfe von Experimenten wurden Messungen mit der entwickelten semiaktiven und passiven Fahrwerksregelung auf dem hydraulisch angetriebenen Fahrbahnsimulator der TU Berlin durchgeführt und mit den Ergebnissen aus den Simulationsrechnungen verglichen. Hierbei wurde auch das entwickelte Modell verifiziert und validiert. Es konnte festgestellt werden, dass die Traktorbeschleunigungen mit dem semiaktiven System um bis zu 13 % verkleinert werden konnten. Die dynamische Reifenkraft konnte um 6 % gegenüber dem passiven System reduziert werden. Generell war festzustellen, dass mit einem semiaktiven System der Fahrkomfort und die Fahrsicherheit entscheidend verbessert werden können.

Schlagworte: Traktor, Federung, Handling, Fahrkomfort, hydropneumatische Federung, Regelung, Semiaktive Regelung, Skyhook, Modell, Simulation, Prototyp, Experimente, Versuchsstand.

Table of Contents

Abstract	I
List of Tables	VIII
List of Figures.....	IX
Nomenclature	XIII
1 Introduction.....	1
1.1 Motivation	1
1.2 Objectives	2
1.3 Approach	3
1.4 Outline	4
2 Background and Literature Review	6
2.1 Vehicle Suspension.....	6
2.1.1 Ride Comfort	7
2.1.2 Vehicle Handling.....	10
2.1.3 Passive Suspension Compromise	12
2.2 Active Suspension	13
2.2.1 Adaptive	14
2.2.2 Load Leveling	17
2.2.3 Fully Active	19
2.2.4 Semi-Active.....	22
2.2.5 Conclusion	26
2.3 Semi-active Control Strategies.....	28
2.3.1 Skyhook	28
2.3.2 Groundhook.....	31
2.3.3 Hybrid	33
2.3.4 Fuzzy	35
2.3.5 Preview	36
2.3.6 On-Off Damping	39
2.4 Hydro-pneumatic Suspension.....	41
2.5 Suspension System for Tractors.....	45
2.5.1 Suspension Characteristics of Tires	46
2.5.2 Seat Suspension.....	48
2.5.3 Cabin Suspension.....	51
2.5.4 Hitch Suspension	53

2.5.5	Front Axle Suspension	56
2.5.6	Full Suspension	60
2.5.7	Full Suspension TUB-Trac	65
2.5.8	Summary.....	69
3	Modeling of the Semi-active Suspension.....	72
3.1	Full Vehicle Model.....	73
3.1.1	Tire Model	73
3.1.2	Quarter Car Suspension Model	74
3.1.3	Full-Vehicle Model Degrees of Freedom	76
3.1.4	Physical Full Vehicle Model	78
3.1.5	Mathematical Full Vehicle Model.....	81
3.1.6	Simulink Full Vehicle Model	82
3.1.7	Front Suspension Model.....	85
3.2	Actuator Model.....	86
3.2.1	Hydro-Pneumatic Spring Model	87
3.2.1.1	Cylinder.....	87
3.2.1.2	Accumulator	89
3.2.1.3	Spring Model	91
3.2.2	Hydro-pneumatic Variable Damper Model	92
3.2.2.1	On-off Damper Structure	92
3.2.2.2	Throttle.....	94
3.2.2.3	Cylinder Port.....	95
3.2.2.4	Throttle Valve	97
3.2.2.5	Overall On-Off Damper.....	99
3.2.2.6	High-Low Damping Level	100
3.2.3	Cylinder Friction Model	103
3.2.4	Overall Hydro-pneumatic Suspension Model	105
3.3	Controller Model.....	107
4	Development of the Semi-active Suspension	113
4.1	Test-Tractor.....	114
4.2	Hydraulic Actuator	115
4.3	Velocity Sensors	120
4.4	Controller Hardware.....	121
4.4.1	A/D Converter.....	122
4.4.2	Interface Card.....	123

4.4.3	Electronic Relay System.....	125
4.5	Controller Software.....	126
4.6	Load Level Control.....	130
5	Simulation and Experimental Test	134
5.1	Test Design.....	134
5.1.1	Test Output.....	135
5.1.2	Data Reduction	135
5.1.2.1	Amplitude-Based Analysis	135
5.1.2.2	Frequency-Based Analysis	136
5.1.3	Test Input.....	138
5.1.4	Test Plan	140
5.2	Simulation Tests.....	141
5.2.1	Final Simulation Model.....	142
5.2.2	Simulation Test Performing.....	144
5.3	Experimental Tests	145
5.3.1	Full Suspension Test Rig	146
5.3.2	Data Acquisition System.....	147
5.3.3	System Operation Check	152
5.3.4	Experimental Test Performing.....	155
6	Result	158
6.1	Model Validation	158
6.1.1	Amplitude-Based Validation.....	159
6.1.2	Frequency-Based Validation.....	161
6.2	Ride Comfort Evaluation.....	164
6.2.1	Simulation Result.....	165
6.2.2	Experimental Result	167
6.3	Handling Evaluation	169
6.3.1	Simulation Result.....	170
6.3.2	Experimental Result	173
6.4	Suspension Travel Evaluation	175
6.5	Result Summary	177
7	Conclusion	181
7.1	Summary and Conclusions.....	181
7.2	Recommendations	183
	References.....	186

Appendices	193
Appendix A: Rest PSD Graphs	193
A.1: Passive, Experiment-Simulation.....	193
A.2: Simulation, Passive-Semi active	195
A.3: Experiment, Passive-Semi active.....	196
Appendix B: Suspension Test Rig	197
Appendix C: Measurement System	198
C.1: Accelerometer Sensor	198
C.2: Velocity and Position Sensor	200
C.3: Interface USB Card 6008/6009.....	201
C.3: BMCM PCI-BASE50/300 Data Acquisition Card.....	203
Appendix D: MATLAB M-files.....	205
D.1: Perform Simulink Model and Data Reduction	205
D.2: Data Acquisition System (for Experimental Data)	207
Appendix E: Vehicle-Suspension Model Parameters	209
E.2: Tractor Body Geometry, Mass and Inertia	209
E.2: Tire/Axle properties	212
E.3: Front Suspension Properties	212
E.4: Hydro-pneumatic Rear Suspension Properties	213
Appendix F: Technical Data of MB Trac 1600 Turbo Tractor	214

List of Tables

Table 2-1 The ranking of the different active suspension systems used for agricultural tractors.....	27
Table 2-2 The capability of different suspension systems used for agricultural tractors.	70
Table 3-1 Quarter-car suspension model parameters.	75
Table 3-2 Vehicle degrees of freedom.	77
Table 3-3 Considered degrees of freedom in the full-vehicle model.....	80
Table 3-4 The parameters and variables definition of the double-acting hydraulic cylinder.	88
Table 3-5 Parameters and variables definition of an accumulator.	90
Table 3-6 On-off damper components.....	93
Table 3-7 Parameters and variables of the throttle.	95
Table 3-8 Parameters and variables of a cylinder outlet.	96
Table 3-9 Valve switching delays.....	98
Table 3-10 Illustration of the working of on-off skyhook control strategy.	109
Table 3-11 On-off skyhook control commands for the double-acting hydro-pneumatic cylinder.	111
Table 4-1 Hydro-pneumatic suspension components in respect with figure 4-5.	116
Table 4-2 Technical data of the electronic relay system.....	126
Table 5-1 Three input modes used for the tests and the relevant pulses applying to the wheels....	139
Table 5-2 Detailed tests plan.....	141
Table 5-3 Simulink software configuration used for the simulation tests.	145
Table 5-4 Measured parameters of the test-tractor by data logger.	151
Table 6-1 Comparison between simulation and experimental results in the passive suspension mode.	160
Table 6-2 Comparison between simulation and experimental results of the semi-active suspension.	160
Table 6-3 Comparison between simulation and experimental natural frequencies of the tractor...	164
Table 6-4 Simulation RMS results of the tractor body accelerations with passive and semi-active suspension.....	165
Table 6-5 Experimental RMS results of the tractor body accelerations with passive and semi-active suspension.....	167
Table 6-6 Simulation results of the dynamic tire force in the passive and semi-active suspension mode.	170
Table 6-7 Experimental results of the dynamic tire force in the passive and semi-active suspension mode.	173
Table 6-8 Simulation results of the suspension travel in the passive and semi-active suspension mode.	176
Table 6-9 Experimental results of the suspension travel in the passive and semi-active suspension mode.	176
Table 6-10 Difference in performance of the semi-active suspension in the simulation and experimental tests.....	179

List of Figures

Figure 1-1 Block diagram showing the approach of this research.	3
Figure 2-1 The compromise present in passive suspension design.	13
Figure 2-2 A system of manually adjustable dampers for vehicle suspension (Barak P. , 1989).	15
Figure 2-3 Level tractor body in spite of load change in the tractor, created a load leveling control (FASTRAC, 2007).	19
Figure 2-4 Fully active suspension comparison with passive system.	19
Figure 2-5 Configuration of a low-bandwidth active suspension (Williams, 1994).	21
Figure 2-6 Semi-active suspension system.	22
Figure 2-7 Working area of the semi-active and fully active suspensions.	23
Figure 2-8 A hydro-pneumatic suspension as a semi-active suspension by using a controllable throttle.	24
Figure 2-9 Schematic Illustration of a MR damper (Paré, 1998).	24
Figure 2-10 Sky-hook damping approach.	29
Figure 2-11 Practicable implementation of sky-hook damping approach.	29
Figure 2-12 Ground-hook damping approach.	32
Figure 2-13 Hybrid damping approach.	33
Figure 2-14 Preview sensor for active suspension (Donahue, 1998).	37
Figure 2-15 Operating area of semi-active dampers a) continuously a) practicable continuously c) "On-Off" system.	41
Figure 2-16 Configuration of a hydro-pneumatic suspension system.	42
Figure 2-17 Capability of hydro-pneumatic suspensions in converting to different types of active system.	43
Figure 2-18 Hydro-pneumatic suspension with two-stage variable spring rate (Abd El-Tawwab, 1997).	44
Figure 2-19 Schematic of the hydro-pneumatic suspension interconnected in the pitch and roll planes (Chaudhary, 1998).	44
Figure 2-20 Suspension blockage mode by using the valves between the accumulators and cylinder (Bauer, 2007).	45
Figure 2-21 Single point contact modeling of tires.	46
Figure 2-22 Influence of the travel speed on tire suspension characteristics a) tire damping rate b) tire stiffness coefficient (Von Holst, 2000).	47
Figure 2-23 A "John Deere" modern seat using "active seat" technology (Jonh.Deere, 2005).	50
Figure 2-24 "Deutz" semi suspended cabin using pneumatic suspension units (Deutz, 2006).	52
Figure 2-25 A hydro-pneumatic shock absorber system applied to the tractor three-point hitch (Goehlich, 1984).	54
Figure 2-26 Full active vibration control system used for the tractor three-point hitch suspension (Hansson P. , 1995).	55
Figure 2-27 Typical standard and system constructive tractors.	57
Figure 2-28 Influence of seat position on seat vertical acceleration in "Standard" and "System" tractors with rigid and suspended front axle (Pickel P. , 1993).	58
Figure 2-29 A hydro-pneumatic front axle suspension used for 8020 series of John Deere tractors (Jonh.Deere, 2005).	59
Figure 2-30 Block construction of "Standard" tractors (Müller, 2001).	61
Figure 2-31 Half frame construction of a "Standard" tractor (Müller, 2001).	62

Figure 2-32 Full frame construction of fully suspension “JCB-FASTRAC” tractor (FASTRAC, 2007).....	63
Figure 2-33 Full frame construction of fully suspension “JCB- Fastrac, 7000 series” tractor (FASTRAC, 2007).....	64
Figure 2-34 MB-Trac 1600 tractor and relevant full frame construction equipped with front axle suspension.....	66
Figure 2-35 UNIMOG and relevant full suspension construction.	66
Figure 2-36 Amplitude spectrum of pitch movement of the tractor body for $v=30$ km (Lehmann, 2004).....	67
Figure 2-37 Constriction of the rear frame and rear axle suspension designed for the “TU-Trac” tractor (Thiebes, Müller, & Gericke, 2005).	68
Figure 2-38 Comparison of the vertical acceleration present on the seat of TUB-Trac with three different suspension modes: seat, Front Suspension, and full suspension (Hoppe, 2006).	69
Figure 3-1 Control loop in a tractor with active suspension system.....	72
Figure 3-2 Modeling procedure.....	73
Figure 3-3 Contact point tire model used for the simulation model.	74
Figure 3-4 Quarter-car model and relevant free body diagram.....	75
Figure 3-5 Vehicle-fixed coordinate system.....	76
Figure 3-6 Physical full-vehicle model with seven degrees of freedom.....	79
Figure 3-7 Full vehicle Simulink model.....	83
Figure 3-8 Vehicle sprung mass Simulink model.....	84
Figure 3-9 Vehicle unsprung mass Simulink model.....	84
Figure 3-10 Measured force-velocity characteristic of the dampers used for the front axle of the test-tractor.....	85
Figure 3-11 Damper model of the front suspension in full vehicle Simulink model.....	86
Figure 3-12 A variable hydro-pneumatic suspension as the actuator of the system.	86
Figure 3-13 Spring component of a hydro-pneumatic suspension with a double-acting cylinder.	87
Figure 3-14 A double-acting hydraulic cylinder.....	88
Figure 3-15 Simulink model of the double-acting cylinder.	89
Figure 3-16 A bladder accumulator using in hydro-pneumatic suspensions.	89
Figure 3-17 Accumulator Simulink model.	90
Figure 3-18 Simulink model of the hydro-pneumatic spring.	91
Figure 3-19 Stiffness-displacement curve of the hydro-pneumatic spring model.....	91
Figure 3-20 Using a variable throttle in hydro-pneumatic suspension in order to create a variable damping effect.	92
Figure 3-21 On-off damper components of the hydro-pneumatic suspension unit.....	93
Figure 3-22 On-off damper system with two level of a) high and b) low damping.	93
Figure 3-23 Physical model of the throttle.....	94
Figure 3-24 Simulink throttle model.	95
Figure 3-25 Hydraulic ports of a double-acting cylinder.	95
Figure 3-26 Cylinder outlet is considered as a throttle (Siekman, 2003).....	96
Figure 3-27 Simulink throttle model of a cylinder port.....	97
Figure 3-28 Switching characteristics of;.....	98
Figure 3-29 Simulink model of the throttle valve set and the equal hydraulic diagram.	99
Figure 3-30 Simulink model of the on-off hydro-pneumatic damper and the equal hydraulic diagram.	100
Figure 3-31 Hydro-pneumatic on-off damper characteristic.	102

Figure 3-32 Hydraulic cylinder and relevant sealing components.	104
Figure 3-33 Relation of coulomb and static friction forces with the slip velocity of a hydraulic cylinder.	104
Figure 3-34 Simulink model of the cylinder friction.	104
Figure 3-35 Circuit of the one unit of the controllable hydro-pneumatic suspension used for the tractor rear suspension.	105
Figure 3-36 Simulink model of the hydro-pneumatic actuator system.	106
Figure 3-37 Using of the model of the hydro-pneumatic suspension in the Simulink full tractor model.	107
Figure 3-38 Position of the controller and sensors in the overall control system.	108
Figure 3-39 Simulink model of skyhook on-off controller for one suspension unit.	111
Figure 3-40 Control command for the rod and head cylinder sides using two sinusoidal waves as the input of control.	112
Figure 3-41 Connection of the Simulink control model to the full tractor model.	112
Figure 4-1 Structure of the actual prototype of the control system.	113
Figure 4-2 Test-tractor with the conventional suspension of the front axle and the hydro-pneumatic suspension of the rear axle.	114
Figure 4-3 Hydraulic circuit of the hydro-pneumatic suspension with controllable damping system.	116
Figure 4-4 Hydraulic components of the hydro-pneumatic rear suspension with controllable damping system.	116
Figure 4-5 Position of the hydraulic cylinder in the rear axle suspension of the tractor.	117
Figure 4-6 Hydraulic cylinder and head/rod side ports.	118
Figure 4-7 A view of throttling system used for controlling the damping level of the suspension, T: throttles, V: valves, A: accumulators.	118
Figure 4-8 Throttle damping system with equivalent electrical circuit.	119
Figure 4-9 Using velocity sensors for the on-off semi-active control on the rear axle suspension. ...	120
Figure 4-10 Schematic of the control hardware of the semi-active suspension system.	122
Figure 4-11 Electronic circuit of a ADC unit.	123
Figure 4-12 Digital output of the ADC circuit, entering a sinusoidal wave input.	123
Figure 4-13 NI-DAC Interface card internal structure.	124
Figure 4-14 NI-DAC Interface card and relevant connection to the input-output devices.	124
Figure 4-15 The electronic relay circuit used for driving the solenoid valves of the actuators.	125
Figure 4-16 Developed electronic relay system.	126
Figure 4-17 Flowchart of skyhook on-off control strategy.	127
Figure 4-18 Block Diagram of the LabVIEW program of the semi-active controller.	128
Figure 4-19 Front panel of the LabVIEW program of the semi-active controller.	129
Figure 4-20 Effect of load changing on the tractor suspension	130
Figure 4-21 Block diagram of the load leveling control system.	131
Figure 4-22 Block diagram of the load leveling control system.	131
Figure 4-23 Block diagram of LabVIEW program of the load leveling controller.	132
Figure 5-1 Process of the test implementation.	134
Figure 5-2 Maximum peak-to-peak value of suspension travel.	136
Figure 5-3 Different input signal, used for the frequency response analysis.	138
Figure 5-4 The positive and negative pulse used for the test input.	139
Figure 5-5 Simulation test process.	142

Figure 5-6 The final Simulink model used for the simulation tests.....	142
Figure 5-7 Simulink model of the test input simulator with the relevant input-modes coefficients.	143
Figure 5-8 Simulink calculator of the dynamic tire force.	143
Figure 5-9 Flow chart of the MATLAB m-file used for simulation tests.	144
Figure 5-10 Experimental test configuration.	145
Figure 5-11 Test-tractor standing on the full suspension test rig.	146
Figure 5-12 Equipment of the control system of the full suspension test rig.	147
Figure 5-13 Components of the data acquisition system.	148
Figure 5-14 Schematic configuration of the data acquisition system (Thiebes P. , 2006).	148
Figure 5-15 Analysis procedure of the experimental data.....	149
Figure 5-16 The acceleration and displacement sensors used for data acquisition system.....	151
Figure 5-17 Configuration of the primary test of the control system.....	152
Figure 5-18 A result of the primary controller test, indicating mistakes in the relay signals due to the noise effect.	153
Figure 5-19 Semi-active close control loop.	154
Figure 5-20 Electronic equipment installed in the tractor cabin used for the experimental test.	155
Figure 5-21 Rear view of the test-tractor standing on the full suspension test rig used for the experimental tests.....	155
Figure 5-22 A view of the PC-based controller located in the test rig control cabin.	156
Figure 6-1 Model validation procedure.....	159
Figure 6-2 Comparison between the simulation and experimental frequency responses of the tractor body acceleration in the passive suspension mode.....	161
Figure 6-3 Comparison between the simulation and experimental frequency responses of the tractor body acceleration in the semi-active suspension mode.	162
Figure 6-4 Comparison between semi-active and passive frequency responses of the tractor body acceleration in the simulation test.....	166
Figure 6-5 Comparison between semi-active and passive frequency responses of the tractor body acceleration in the experimental test.	168
Figure 6-6 Comparison between semi-active and passive frequency responses of the dynamic tire force in the simulation test.	171
Figure 6-7 Comparison between semi-active and passive frequency responses of the unsprung mass (i.e. wheel) acceleration in the simulation test.....	172
Figure 6-8 Comparison between semi-active and passive frequency responses of the dynamic tire force in the experimental test.....	174
Figure 6-9 Comparison between RMS results of the tractor body accelerations in the simulation tests.	177
Figure 6-10 Comparison between RMS results of the tractor body accelerations in the experimental tests.	178
Figure 6-11 Comparison between the RMS results of the dynamic tire force in the simulation and experimental tests.....	178
Figure 6-12 Comparison between the MPTP results of the suspension travel in the simulation and experimental tests.....	179
Figure 7-1 Driver command sensors for the semi-active control loop in order to provide a more efficient control.	184

Nomenclature

Abbreviations

CG	Centre of gravity
DFT	Discrete Fourier transform
DOF	Degree of freedom
ER	Electro-rheological
MR	Magneto-rheological
RMS	Root mean square
FFT	Fast Fourier transformation
GND	Groundhook
SKY	Skyhook
MIN	Minimum
MAX	Maximum
FEM	Finite element method
ISO	International standard organization
CTIS	Central tire inflation systems
MBS	Multi-body system
TU-Berlin	Technischen universität berlin
MIMO	multiple-input and multiple-output
PSD	Power spectral density

Symbols

θ	Rotation along y-axis (Pitch)	<i>rad</i>
ξ	Damping ratio	-
φ	Rotation along x-axis (Roll)	<i>rad</i>
c	Damping coefficient	<i>Ns/m</i>
f	Frequency	<i>1/s , Hz</i>
F	Force	<i>N</i>
I_{xx}	Inertia along x-axis	<i>Kgm²</i>
I_{yy}	Inertia along y-axis	<i>Kgm²</i>
I_{zz}	Inertia along z-axis	<i>Kgm²</i>

k	Spring stiffness	N/m
m	Mass	Kg
t	Time	s
z	Vertical displacement	m
z'	Vertical velocity	m/s
z''	Vertical acceleration	m/s^2
m_1	Unsprung mass	Kg
m_2	Sprung mass	Kg
m_t	Tractor body mass	Kg
A_1	Piston area (head side)	m^2
A_2	Piston area (rod side)	m^2
p_o	Pre-charge accumulator gas pressure	$N/m^2 (Pa)$
p_1	Initial accumulator pressure	$N/m^2 (Pa)$
V_o	Accumulator volume	m^3
α	Flow reference number	-
ρ	Density of oil	kg/m^3
AT	Throttle cross-section	m^2
AP	Cylinder port cross-section	m^2
t_a	Valve switching-on time	s
t_b	Valve switching-off time	s
M_u	Tire /axle mass	kg
z_1	Unsprung mass vertical displacement	m
z_2	Sprung mass vertical displacement	m
z_0	Input vertical displacement	m
G	Constant gain for hybrid control	Ns/m
α	Relative ratio between skyhook and groundhook control	-
g	Acceleration due to gravity	m/s^2
l_f	Distance from CG to front suspension attachment point	m
l_r	Distance from CG to Rear suspension attachment point	m

t_r	Distance from CG to Right suspension attachment point	m
t_l	Distance from CG to Left suspension attachment point	m
Q	Volume flow rate	m^3/s
V	Volume	m^3
F_{co}	Cylinder coulomb friction force	N
F_{st}	Cylinder static friction force	N
v_o	Limit velocity of the static friction	m/s

Subscripts

cg	Centre of gravity
cr	Critical
f	Front suspension
r	Rear suspension
fl	Front left vehicle corner
fr	Front right vehicle corner
rl	Rear left vehicle corner
rr	Rear right vehicle corner
he	Heave
pi	Pitch
ro	Roll
r	Cylinder rod side
p	Cylinder head side
T	Tire
nf	Natural frequency
sky	Skyhook
gnd	Groundhook
ACC.	Acceleration

Chapter 1

Introduction

The purpose of this chapter is to provide an introduction showing the overview of this research. At the beginning of this chapter, the motivation of the research will be described. Then, the determined objectives and the approach of the research will be explained. The approach is planned based on the objectives. The chapter will be ended with classification of the manuscript.

1.1 Motivation

Operators of agricultural tractors are exposed with high level of vibrations. The operators work continuously many hours on the tractor, especially during the busy work season. These working conditions not only harm the health and physical condition of the operator, but also create early fatigue and reduce his efficiency. On the other hand, present necessities for more production with lower expense in agricultural applications leads to an important requirement for faster agricultural transportation. Under these circumstances, upgrading the ride comfort and ride safety of agricultural tractors is an important requirement. This improvement can be achieved by using a good suspension system.

Primary conventional tractors have only the tires as the elastic component between road and tractor, whereas tires are unable to provide proper suspension characteristics. Now, modern tractors are equipped with the different kinds of suspension systems, which are including from the simple seat suspension to the new chassis suspension. Seat and cabin suspensions are able to improve only the ride comfort, whereas chassis suspension can increase road stability besides the ride comfort of tractors.

Suspension systems for agricultural tractors have been one of the main research themes at the Institute of Agricultural Machinery of TU-Berlin for many years. The recent research in this area (Hoppe, 2006) was about a full suspension tractor with both rear and front suspensions. The results of this research showed that this full suspension tractor was able to provide a high norm for ride comfort and handling. However, there was still a need to

improve the performance of the suspension system, especially about the tractor body vibrations.

The efficiency of a passive suspension is principally limited. In order to achieve a better performance, the idea of electronic controlled active systems is considered recently. With the recent advancement in electronic technology, this idea is getting more and more practicable, especially for cars. In this thesis, the idea of active suspensions for agricultural tractors is considered.

1.2 Objectives

The primary objective of this research is to develop an active suspension for agricultural tractors with the aim of improving the dynamic behavior of them. In order to achieve this goal, these specific objectives are determined:

- To study the background of the suspension systems of vehicles, especially agricultural tractors.
- To study the background of active suspensions and their control strategies.
- To reveal proper active suspension and control strategy for the tractor.
- To define a test-tractor and relevant specifications.
- To build a mathematical and computer model of the overall system.
- To develop a prototype of the test-tractor tractor with the active suspension, including development of the components of the active suspension and installation of them on the test-tractor.
- To design the simulation and experimental tests.
- To perform the simulation and experimental tests.
- To validate the simulation model by comparing the simulation results with experimental results.
- To evaluate the new suspension by comparing the passive results with active suspension results.
- To determine the conclusion of research based on the whole results.

1.3 Approach

Figure 1-1 shows the general approach of this research. In this research, the motivation of the research is improvement the chassis suspension of agricultural tractors. With this motivation, the idea of using active suspension systems was considered. Proper active suspension was chosen and applied to a test-tractor, and in order to examine the performance of this new suspension, two approaches of the simulation and experiment were considered.

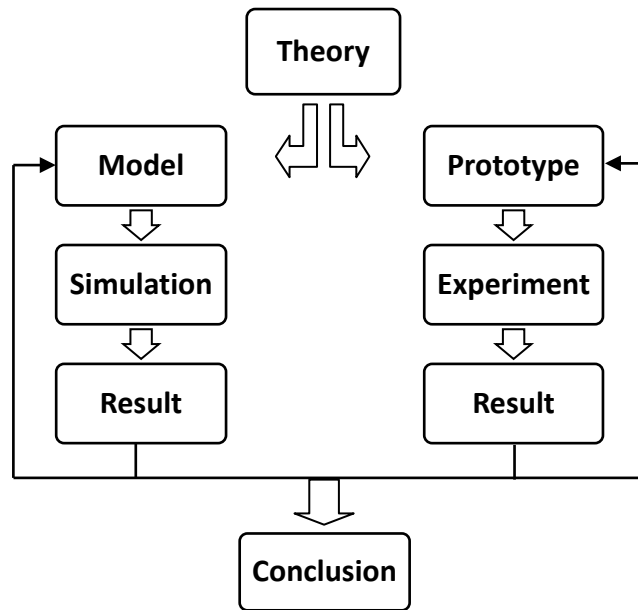


Figure 1-1 Block diagram showing the approach of this research.

The procedure of the computer modeling and prototype development had been influencing each other. On the one hand, the computer model was built based on the test-tractor, which was considered as prototype, and the parameters of the computer model were derived from the prototype model. On the other hand, the procedure of the computer modeling was used as pre-design for prototyping.

Finally, the results of these approaches were used to evaluate the new system. Furthermore, by comparing these two results, the validation of the computer model was performed with the aim of the obtaining a valid computer model for this study and future research works in this area as well. More details of the approach of this study are described in the next section as the outline of this thesis.

1.4 Outline

In order to achieve the objectives of this investigation, five steps were performed. In harmony with these steps, this thesis is organized in seven succeeding chapters. These steps and the relevant chapters are presented here in this section.

The first step of the study was the background and literature review of the investigation. This was made in the subjects of the suspension system of vehicles and agricultural tractors, active suspensions, control strategies, and hydro-pneumatic suspensions. These subjects are presented in the chapter 2 of this thesis. First, general definitions about vehicle suspension are presented. After that, different kinds of active suspensions and some related control-strategies are explained. Then, the actuator system of semi-active suspensions, and the hydro-pneumatic suspension are described. At the end of this chapter, different kinds of suspension systems used for agricultural tractors are discussed. Among these subjects, some details on the objectives of the research are also discussed. This study leads to determine a proper type of active suspensions and control strategies used for agricultural tractors. Also in this step, the specifications of a test-tractor used for the experimental study are revealed.

The second step was designing and modeling of a new suspension system. The modeling included the mathematical modeling, derived from a physical model and finally a computer model using MATLAB-Simulink program. These subjects are presented in chapter 3 of this thesis. At first, the model of the full suspension tractor is derived. After that, modeling of the hydro-pneumatic rear suspension is done. This includes also the model of the actuator. Next, the model of the control system is presented. At the end of this step, the overall model involving all sub-models is completed.

The third step was the development of the prototype of the suspension system. The prototype was used for the experimental study of this research. This step is described in chapter 4 of the thesis. At first, the control system, including hardware and software components is explained. The controller was a personal computer with proper software. This computer was connected to the system's inputs (i.e. sensors) and outputs (i.e. actuators) by using an interface card. After the control system, the building the hydraulic actuator system and relevant installation on the hydro-pneumatic rear suspension of the test-tractor is presented.

The fourth step was the test design and test setup. The test design was similar for the simulation and experimental tests. It included the determination of the test input, which used for the excitation of the suspension, and the test output, which used for the derivation of the test results. Unlike the test design, the test setup of the simulation and experimental tests were different. For the simulation test, a MATLAB m-file program was used to conduct the simulation process. For the experimental tests, the suspension test rig at the TU Berlin - Department Machinery System Design was employed in order to apply the test input to the tractor. In addition, a data acquisition system attached with acceleration sensors was used in order to save the output parameters of the test.

In chapter 5 of this thesis, the fourth step of the study is presented. This step is the test design and test setup. At the first part of this chapter, the test input and output, and the analysis methods of the output data are determined. Then the test setup of the simulation tests and the test setup of the experimental tests are presented separately. For the experimental test, a suspension test rig and a data acquisition system were used. These equipments are described at the end of this chapter.

The fifth step was the study of the results of the simulation and experimental tests. These results were derived from the amplitude and frequency based data analysis. By comparing the simulation results with experimental results, the validation of the model was performed. After that, performance of the semi-active suspension was investigated by comparing the passive and semi-active results. Two series of the results related to the tractor body acceleration and the tire dynamic force were used in order to illustrate the ride comfort and handling ability of the tractor. At the end, all results were used in order to determine the conclusion of this study and provide some recommendations for future works.

The results of the tests are presented in chapter 6. At first, the results of the model validation are given. After that, two series of the evaluation results related to the ride comfort and handling of the tractor are presented. Finally, in chapter 7 the results of this study are concluded. The highlights, significant results, and the summary of the main works are presented. At the end, recommendations for future work are given.

Chapter 2

Background and Literature Review

In this chapter the background of this investigation and the literature review are presented. At first, general definitions related to vehicle suspensions such as ride comfort, handling, and passive suspension are described. Then active suspensions and different types of them are explained. It follows a description of the control strategies for semi-active suspensions. These suspensions are the systems that were selected as the proper active suspensions in this investigation. On the other hand, this new system was applied to a hydro-pneumatic suspension. These suspensions are explained in this chapter. As the final point, the different types of suspension systems of agricultural tractors are described.

2.1 Vehicle Suspension

On a road with smooth surface, there is no need for a suspension system to provide ride comfort for the passengers of a vehicle. However, there are various types and roughness of road surfaces in reality, and a suspension system is necessary in order to isolate the vehicle from the exciting vibrations of the road unevenness. Besides this function, suspension systems should maintain a permanent contact between tires and road surface so as to provide good ride stability for vehicle. This ability is particularly important as vehicle is turning, accelerating, or braking. Briefly, a vehicle suspension provides ride comfort and driving stability for the vehicle. They are also necessary for protecting the road surface from excessive tire forces and pavement damage.

The typical construction of the suspension system of a vehicle consists of the suspension units, which place at the vehicle corners and connect the vehicle chassis to the vehicle wheels via a linkage system. Each suspension unit is comprised of two basic suspension elements of the spring and the damper, setting in parallel. Springs absorb the shock-excitations, which is caused by the road surface roughness. As the suspension meets a bump, the spring gets compressed and stores the energy of the shock. After that, it expands and releases the absorbed energy gradually to the vehicle body. On the other hand, the

function of a damper is to dissipate the energy of suspension vibrations. As the suspension meets a bump, the damper damps directly a part of the shock energy. In addition, it dissipates the stored energy in the spring. In this way, it controls the action of the springs. Likewise, springs and dampers control the motion of the vehicle body, caused by driving maneuvers.

In most of the vehicles, steel springs are used for the suspension system, which comes in three types of coil, torsion bar, and leaf springs. Pneumatic and hydro-pneumatic springs are also used in some vehicles. The details of these systems will be described in the following sections. Dampers in vehicle suspension systems are mostly hydraulic dampers. The working principle of the hydraulic dampers is similar. As the damper compresses or expands, a hydraulic fluid is forced through a throttle. The created pressure-drop in this throttle creates the damping force. The size of the throttle determines the damping coefficient of these dampers.

In the following sections, ride comfort and vehicle handling as the two main functions of the suspension systems will be described. In addition, the limitations of the conventional suspensions in achieving these functions, and available solutions will be discussed.

2.1.1 Ride Comfort

Ride comfort is considered as the first objective of the suspension systems of vehicles. Ride comfort is an important characteristic of vehicles that indicates how much riding is comfortable for passengers. Ride comfort is very important for agricultural tractors, because the acceleration transmitting to the driver compared with other vehicles is very high (Horton & Crolla, 1984). In addition, the operators of agricultural tractors spend many hours in the field during peak working seasons. These conditions can affect the comfort, efficiency, alertness, and health of the operators.

Vibration sources that affect ride comfort are categorized generally into two classes, namely on-board sources and road sources (Jamei, 2002). On-board sources arise from the rotating components including the wheels, the driveline, and the engine. These sources caused aural vibrations in the frequency region of 25 - 20,000 Hz, which are called "noise" (Gillespie, 1992). These two frequencies are the lower and higher frequency thresholds of human hearing. The second category of the vibration sources of vehicles is the road source, referring to the road roughness and maneuver excitations. Frequency range of these

excitations is between 0 and 25 Hz. This range including the natural frequencies of human tactile and visual is the most sensitive frequency areas to human body. For that reason, the road excitation source is considered as the most important factor in affecting ride comfort of a vehicle.

Suspension systems are considered as the foundation of vehicles ride comfort. The frequency area of suspension systems is in the range of lower than 25 Hz. In the case of vehicle dynamics, "ride comfort" is related to only this part of the frequency range (Gillespie, 1992). Ride comfort depends particularly on the dynamic behavior of the vehicle body (i.e. sprung mass). Vibrations on the body of a vehicle are the combination of the vertical vibration of heave, and the angular vibrations of pitch and roll.

The vibration effect on human body, particularly about the passengers of a vehicle, have been examined in many investigations (Bastow, 1987). The human body shows different sensitivity to vibrations. This sensitivity is dependent on the direction and frequency content of vibrations. In general, the human body is more sensitive in horizontal directions compared with the vertical direction. In the vertical direction, the most sensitive range of the body is 4 - 8 Hz corresponding to the resonant frequencies of the organs in the abdominal cavity. The sensitivity in the horizontal directions is highest in the range of 1 - 2 Hz (SAE, 1992). The range 0.5 - 0.75 Hz can be also associated with motion sickness or "seasickness" (Barak P. , 1991). As a result, the most uncomfortable frequencies to humans and those that a suspension system needs to control are in the 0.5 - 10Hz range (Barak P. , 1991). Based on this conclusion, performance of the suspension system in this thesis was evaluated in the mentioned frequency range.

In order to quantify the ride comfort of a vehicle, vibrations of the vehicle body should be measured in two directions of vertical (i.e. heave) and horizontal (i.e. roll, pitch and yaw). The most commonly used measurement methods is the RMS acceleration. Root Mean Square (RMS) acceleration is defined as:

$$RMS(a) = \sqrt{\frac{1}{T} \int_0^T a^2(t) dt} \quad 2-1$$

With (T) being the total sample time, (a) the sprung mass acceleration, and t the time. This measurement must be performed for both directions. However, to simplify the measurement, just the body vertical acceleration (i.e. heave) is often measured. In this

study, in order to evaluate the ride comfort, the RMS accelerations of both the vertical and horizontal directions were measured. More detail will be presented in chapter 5.

With the purpose of considering the factor of vibration frequency in ride comfort measurement, a weighted form of accelerations can be used in equation 2-1 instead of the plain acceleration. In this method, a weighting curve, which is created base on the human sensitivity of different vibration frequencies, determines a weighting factor for the amplitude of each acceleration data respect to the frequency of this acceleration data. More detail in this subject can be found in the reference of (Thoresson, 2003). In another method, with the aim of considering the frequency factor, the acceleration data of the sprung mass is filtered by a Human Response Filter (i.e. HRF) (Donahue, 1998).

In general, the mentioned formulation of the RMS acceleration is used in order to evaluate the ride comfort capability of the suspension systems. The focus of some studies is the human exposure to the vehicle vibrations. For these studies, other methods are needed to involve some related variables in measurement of ride comfort. The important variables are the magnitude, frequency, direction, and duration of vibrations. For example, There are some standards defined concerning with the measurement of ride comfort of agricultural vehicles and the acceptable levels of the acceleration transmitted to their operators. Among them two ISO standards are usually preferred for the agricultural vehicles (Adams, 2002).

The first standard is ISO 2631, which was initially issued in 1974. This standard is a general norm used for three main issues of vibration measurement, human exposure to the whole body vibration, and acceptable vibration levels relative to the health risk (Pickel P. , 1993). In this standard, a vector is used as the weighed factor for evaluating the total load, which contains the loads of vibrations in all three linear directions (Hansson P. A., 1995). In addition, this standard considers the factor of time limitation in order to define the acceptable vibration levels of human.

Another standard is ISO 5008 issued initially in 1974. This standard describes a method for the measurement and analysis of the vibration load on the driver of an agricultural tractor (Hansson P. , 1995). This standard presents a rough and a smooth test-track, which are designed in order to imitate normal driving conditions in agricultural applications. In addition, ISO 5008 recommends that the test-tracks should be traversed at 5 km/h and 12 km/h (Adams, 2002). This standard makes use of the ISO2631/1 standard in order to weight the frequency information of accelerations. Then, it integrates the values

overall frequencies in order to form a single root mean square (RMS) value for acceleration (Adams, 2002).

2.1.2 Vehicle Handling

Handling is a characteristic of a vehicle that provides stable and safe driving that can be created via a steady contact between the tires and road surface. In some references, handling is called also with other names such as road holding, ride stability, and driving safety, implying the same meaning. The handling capability of a vehicle is important during maneuvers such as cornering, braking, or accelerating. In these extreme situations, weak handling reduces the control ability of the vehicle and can affect the safety of the passengers. Due to this fact, handling is considered as an important capability for vehicles, and beside the ride comfort, it is considered as the main target of using the suspensions in vehicles.

Handling is related to the tire contact force that is influenced by two factors: wheel and vehicle body vibrations. Vertical motion of the wheels is affected mainly by road roughness, and body motions are produced mainly by vehicle directional changing. The maneuvers changing of vehicles are considered as the major challenge for the handling characteristic of a vehicle. For example during cornering, the centrifugal forces push vehicles. This must be resisted by the tire contact forces. In the same time, the centrifugal force causes load shift on the tires from one side of the vehicle to another side. This leads to major reduction in the tire contact forces and provides consequently a poor handling performance. Likewise, as a vehicle brakes or accelerates rapidly, a critical handling state is created. In this condition, extra traction forces on the tires are needed, whereas because of the weight transfer from back to front or conversely, tire contact force cannot be created optimally.

The handling capability of a vehicle is affected by different characteristics of the vehicle. The main one is the characteristic of the vehicle suspension. A good suspension provides strong resistance to the vehicle body motion (i.e. roll, pitch and heave) and prevents excessive weight transfer in the vehicle body, which increase the vertical loads of the wheels and affects the handling negatively. In addition, an effective suspension can control the vertical vibration of the wheels (i.e. wheel hop), which are produced by the road roughness and have direct influence on the tire contact force and consequently on handling of the vehicle.

As mentioned above, vehicle handling and ride comfort are the two main functions of the vehicle suspension. In order to evaluate a suspension system, these two characteristics must be measured and examined. Unlike ride comfort, which was explained before, there is no standard to quantify or formulate the vehicle handling. This makes the qualification of the handling complicated. However, there are some methods for indirect measurement of handling. Good handling can be provided by stable tire contact forces, and high variation of the tire force reduces the handling capability of the vehicles.

As a result, variation of the contact force between the tires and road surface corresponds directly to the vehicle handling, and it can be used for the quantification. The term of tire contact force is equal to the vertical tire force. As a result, the tire force variation or dynamic tire force can be used in order to measure the handling. Lower dynamic tire force means better handling and higher dynamic tire force indicates worse handling. In experimental works, the direct measurement of the vertical tire force is difficult. Measuring the deflection of tires is often an alternative. Due to the elasticity of tires, this deflection is proportional to the vertical tire force.

(Mitschke, 1984) defined a factor called RLF “Radlastfaktor” in order to quantify vehicle handling. In calculating this factor, the vertical static tire force was considered in addition to the vertical dynamic tire force. RLF factor is equal to the value of the dynamic tire force over the value of the static tire force. Greater value of this factor means higher instability in the tire contact, implying worse handling. In another related study about tractor dynamics, RLF factor was used also for examining handling of tractors. The conclusion of this investigation is that the handling of tractors is acceptable if the RLF value is lower than 0.33 (Ulrich, 1983). This factor was also used by (Hoppe, 2006) in order to evaluate the handling capability of a full suspension tractor.

Handling capability for the agricultural tractors is particularly important. A comparison of agricultural tractors with automobiles shows that the position of the center of gravity is higher. Further differences are the higher body mass and the lacking chassis suspension. As a result, tractors have normally poor roll and pitch stability. In extreme situations poor handling may lead to very weak steering and braking control ability of the vehicle. On the other hand, effective agricultural processes need a higher tractor velocity. This demand leads to an increasing importance of the handling capability for agricultural tractors.

In the investigation of (Simon, 2001), it was concluded that the limit of the handling performance of automobiles is characterized by the loss of the yaw stability, whereas this limitation in off-road vehicles should be characterized by the loss of the roll and pitch stability. In this investigation, the main objective was improvement of the tractors handling. It was concluded that this can be achieved via providing a better control on the vibrations of the tractor body (i.e. roll, pitch, and heave) by using an effective chassis suspension for the tractor.

2.1.3 Passive Suspension Compromise

Usual suspension systems of vehicles are passive suspensions. In these systems, the characteristics of the suspension elements are constant. In the design of these systems, there is an inherent compromise between good ride comfort and vehicle stability as the two main goals of the design. A vehicle suspension with stiff spring and firm damper is referred as 'hard' suspension. This provides good control on the vehicle body motion and wheels vibration, and it creates optimal handling. However, this system is unable to offer effective body isolation. On the other hand, a suspension with low stiffness and soft damping, called 'soft' suspension provides effective body isolation from road unevenness and creates good ride comfort. However, this system cannot control the motions of the vehicle body and wheels effectively. Therefore, in the design of conventional passive suspensions, a compromise has to be made between good handling and ride comfort. This limits the performance of passive suspensions.

Figure 2-1 indicates the compromise in suspension design due to the damping ratio. In suspension design, the main way to specify the suspension is the tuning of the damping rate, because the selection of the spring stiffness is generally based on the vehicle's weight. A suspension with high damping ratio damps the resonance of the sprung mass effectively. However, it increases the transmissibility of the road roughness and provides a poor ride comfort for the vehicle. Conversely, low damping ratio decreases the transmissibility of the road roughness. However, it is not able to damp the resonance of the sprung mass effectively and provides a poor handling capability.

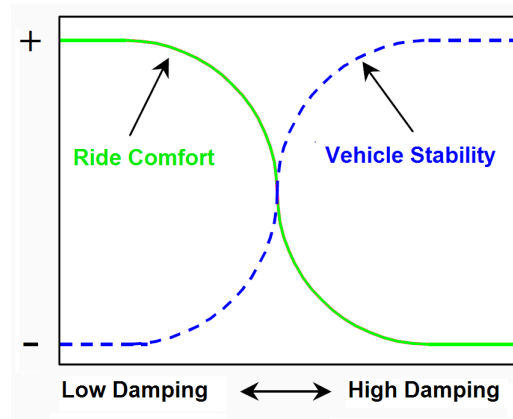


Figure 2-1 The compromise present in passive suspension design.

Even a good design for passive suspensions cannot remove this trade-off, but also it can only optimize one set of the driving conditions. For example, sports cars with a hard suspension provide a good handling capability and safe fast cornering, which is achieved at the cost of relative uncomfortable ride for driver. Conversely, city buses with a soft suspension provide a comfortable ride for passengers achieving at the cost of having poor handling capability. Therefore, designers must decide about the priority of ride comfort or handling based on the purposed application of the vehicle.

In order to overcome against the drawback of passive suspensions caused by the inherent compromise, active suspensions are considered as the key of this problem, presenting the possibility of optimizing both ride comfort and handling. These systems will be described in the following sections.

2.2 Active Suspension

In a passive suspension system, springs store and dampers dissipate the energy of the vibration. The parameters of these elements are generally fixed and are chosen in order to achieve a certain level of the compromise between road holding and ride comfort of the vehicle. This compromise limits the performance of the passive suspension. In order to eliminate this limitation, other types of suspensions with beyond the passive components are expected. Advance in electronic technology has recently provided new facilities for improvement in the suspension of vehicles.

Modern suspensions are equipped with electronic control systems that control the operation of the suspension elements. They have not a limited performance like passive suspensions and create a new advancement in removing the drawback of the design compromise present in passive suspensions. This optimizes both the ride comfort and

handling capability of vehicles. Therefore, active suspension systems are considered as a proper solution in order to increase the performance of conventional suspensions and create an effective suspension for vehicles. The idea of active suspension has been also considered in this investigation with the aim of improving the performance of the chassis suspension of agricultural tractors. The term of “active suspension” is used in this thesis for referring to each type of the modern suspension that uses an electronic system for controlling the suspension. These systems are different from passive systems that have constant characteristics.

There are different types of active suspension. They could be relative simple such as manual adjustable systems or relative complicated such as fully automatic systems. They may use open loop controls or use sensory feedback loop controls. Their bandwidth could be low, covering a part of the suspension vibrations, or it could be relative high, covering all the suspension vibrations. They could work just by dissipating the suspension energy or work by consumption of extra energy. In this script, all these advanced suspension systems are classified to the four categories: adaptive, load leveling, semi-active, and fully active suspension. Each one will be described in the following sections. In addition, these suspension systems will be compared to one another in order to choose the proper system for the chassis suspension of agricultural tractors.

2.2.1 Adaptive

In the design of passive suspension systems, there is an inherent compromise between ride comfort and handling as two main design goals. The priority of these two goals of suspensions is dependent on the operation conditions of the suspension. For example, as a vehicle is driving on a rough road, ride comfort should be considered as the priority of the vehicle suspension. On the other hand, as the vehicle arrives to a smooth road with many corners, the priority shifts to handling rather than ride comfort. Therefore, a suspension system that can adapt its parameters to the different operation modes is able to offer an efficient performance. This system is called adaptive suspension system. They work normally alike a passive system, until a change in operating condition of the suspension appears. This system recognizing the change modifies the parameters of the suspension respect to the change and adapts the suspension to the new condition.

In simple type of adaptive suspensions, change in operation condition of the suspension is recognized directly by the driver of the vehicle, and the modification in the suspension parameters is also performed directly by the driver manually. Figure 2-2 illustrates one of these systems that let driver choose one of three suspension modes of “soft”, “medium”, and “firm”. These modes are in fact three damping levels for the suspension. For example, driver can choose the soft suspension mode as the vehicle is running on a rough road. This provides a better ride comfort capability. In contrast, during driving on a highway at high speed, firm suspension mode can be selected in order to provide better ride stability. Advantage of these systems is the considering of the driver impression. However by such a manual system, fast control cannot be provided, and proper reaction to the short time changes in the operating condition of the suspension is impossible. Therefore, instead of manual control, the automotive control systems are employed in the advanced adaptive suspensions.

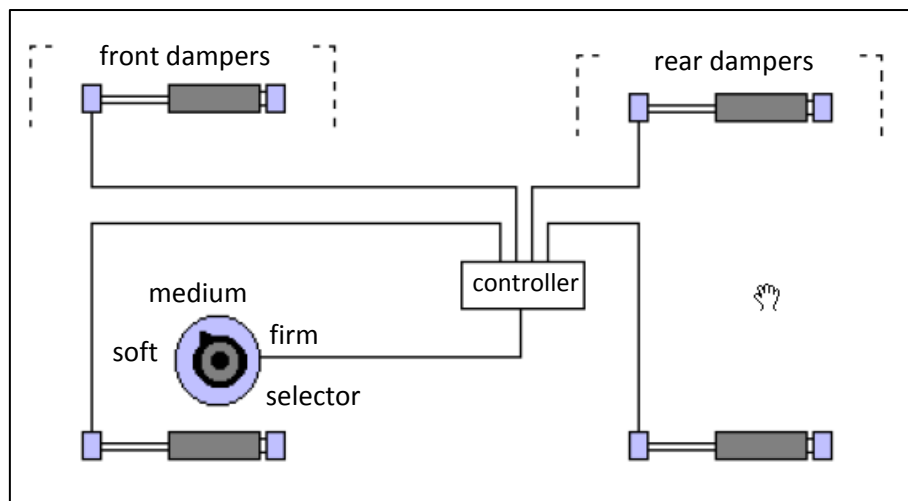


Figure 2-2 A system of manually adjustable dampers for vehicle suspension (Barak P. , 1989).

In automotive adaptive systems, the operating condition of the suspension is distinguished based on the sensory information. After that, controller accomplishes the necessary change in the suspension parameters. There are different ways for detecting the operating condition of a suspension. In one system, the driver commands such as gas, brake, and steering commands are measured. The achieved signals are used as the inputs of adaptive control, and based on them; the controller can recognize the maneuver conditions. For example, intense and frequent driving commands infer a severe maneuver condition. This condition needs high ride stability, which can be provided by a firm suspension.

In another type of adaptive systems, the maneuver condition and road surface quality are recognized by analysis of the accelerations of the vehicle which are measured by proper accelerometers. The amplitude and frequency analysis of the vertical, longitudinal, or lateral accelerations are considered. The analysis can be also performed based on the suspension deflection of the vehicle (Lizell, 1990). In some other systems, the travel speed of the vehicle is measured as input of the adaptive control. High speed driving on the straight and even roads implies the need to better ride stability, which can be provided by high handling capability of vehicles (Williams, 1994).

The output of an automatic adaptive suspension is indeed to make the proper changes in suspension parameters. Similar to the manual system, this is performed often by changing the damping level of the suspension. However, the output of a type of these systems is the stiffness of the suspension. In this system, which is called load-leveling system, the stiffness is determined based on the static load of the vehicle. The details of this system will be described in the next section.

For an adaptive suspension system, just a low bandwidth for the controller is needed, because an adaptive suspension system reacts only to the steady form of the changes in operating condition of the suspension, for example, entering of a vehicle from a smooth road to a rough road. In the new adaptive systems, the bandwidth of the controller is increased in order to create the ability of fast responding to the suspension inputs such as a bump or sudden brake. However, the bandwidth of these systems is still lower than the natural frequencies of the vehicle body, and their performance is limited. Higher control bandwidths are used in other types of active suspension systems such as semi- active and fully active suspension systems. These systems will be described in the next sections.

In the study of (Karnopp & Margolis, 1984) , a fast adaptive system was investigated. Quick changes was performed in suspension parameters of the hydro-pneumatic suspension system of a vehicle. This performed on both the damping and stiffness level. The input of the control system was the frequency response of the vehicle body vibration. Examination of this system showed the high potential of this system in improving both the ride comfort and handling of the vehicle.

Adaptive suspension systems have a high potential for agricultural tractors. These vehicles works in a wide range of different operating conditions from the field work to the driving on the normal asphalt roads. By using adaptive suspension, the suspension

parameters can be tuned proportional to different conditions. This provides an efficient suspension for tractors in all working conditions.

2.2.2 Load Leveling

Normally, static changes in the load of vehicles create steady changes in the vehicle height, which is unwanted. A load leveling control system provides a constant vehicle height in spite of these changes. This system detects the changes and tunes the springs's stiffness of the vehicle proportionally in order to correct the suspension height, and in this way, the vehicle height stays invariable. These systems react only to the static inputs and have a low control speed, but they still provide noticeable benefits for vehicle suspensions and improve their performance. The advantages of load leveling control systems can be stated as follow:

1- In a passive suspension, until 50% of the suspension strike may be absorbed after increasing the vehicle load, and just remained value can be used against dynamic inputs from the road. While by using load-leveling system, the whole suspension strike stays usable despite the different static loads (Eulenbach, 2003).

2- In a passive suspension, considering the maximum static loads, relative hard springs are used. This reduces ride comfort of vehicles, particularly as a vehicle is running with a low value of loading. Whereas by using load leveling system, softer springs can be used in the suspension. These springs can be until six times more flexible than conventional suspension and provide obviously better ride comfort for the vehicle (Williams, 1994).

3- In principle, the natural frequencies of the body of vehicles depend on the vehicle load and suspension stiffness. The stiffness is constant in a passive suspension. As a result, with change in the vehicle load, the natural frequencies of the vehicle body are changed. This affects negatively the suspension performance and decreases ride comfort and handling capability of the vehicle. While using a proper load leveling system, the spring's stiffness is tuned proportional to the change in the vehicle load. In this way, the dependency of the vehicle natural frequencies to the vehicle load is nearly eliminated, and the suspension performance is improved consequently.

Load leveling controller is a sensory feedback loop controller, which uses displacement sensors for measuring the suspension height. The signals of these sensors are passed first through a low-pass filter in order to remove the signals related to the dynamic changes in the suspension height. In this way, the static suspension height is just used as the

input of control. The load leveling control system responds just to the static changes of the suspension height, and it has a low speed controller. In practice, the bandwidth of this system is usually less than 0.25 Hz (Burton, Truscott, & Wellstead, 1995). This low bandwidth leads to an uncomplicated construction and low energy consumption of this system. These facts have converted the load leveling system to the most practicable active suspensions in vehicles (Williams, 1994).

The load leveling control is especially practicable by pneumatic and hydro-pneumatic suspension systems. In these systems, the stiffness can be adjusted by charging and discharging oil or air to the system, which leads to correct the suspension height. These systems need an external power source to drive oil or air pump to the system. This power source is provided from the vehicle engine. However, there are also self-energized systems using relative suspension movement to pump oil to the system (Meller, 1987).

The load leveling system keeps the suspension height in a constant primary value. By adjusting of this value with respect to the driving condition, operation of the suspension can be developed. This can be performed manually by driver or automatically by a control system. The automatic system uses sensory information to recognize the driving condition and determine the proper primary suspension height. For example, as a vehicle is driving with high speed on a flat highway, the center of gravity of the vehicle can be shifted lower by reducing the primary height. This improves ride stability of the vehicle. In addition, the aerodynamic resistance of the vehicle is decreased (Giliomee, 2003). On the other hand, driving on uneven roads needs a higher suspension height to prevent hitting of the chassis with the road surface.

Load-leveling systems have been used widely for heavy vehicles that work usually with a wide range of load variation. A group of these vehicles is agricultural tractors that have great potential to benefit from load leveling systems. A load leveling system used for the front axle suspension of an agricultural tractor was described in the investigation of (Marsili, Ragni, Santoro, & Servadio, 2002). This system was adjusted so as to react only to the more than 2cm change in the suspension height. The change had to be survived for at least 3.5 second. This proved that the change was a static type.

An example of manufactured tractors using this system is “Fastrac” from “JCB” Company. This tractor is a full suspension tractor with the hydro-pneumatic rear suspension that is equipped with a load leveling control system. Figure 2-3 illustrates the working of this

system that keeps the tractor height invariable in spite of the change in the static load. More detail about this tractor will be given in section 2.6.6.

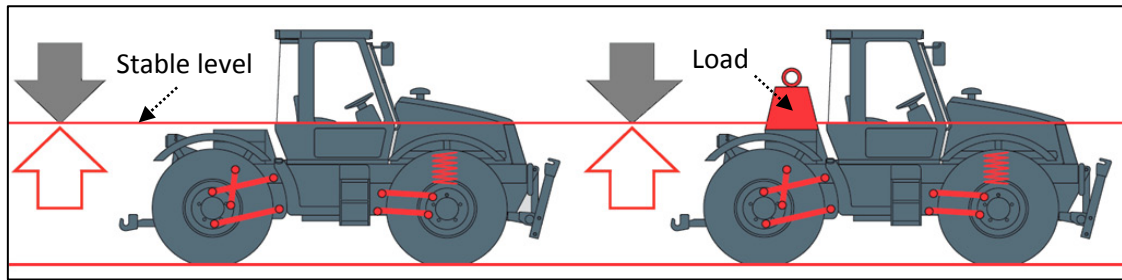


Figure 2-3 Level tractor body in spite of load change in the tractor, created a load leveling control (FASTRAC, 2007).

2.2.3 Fully Active

Conventional passive suspension unit works by storing vibration energy via a spring and dissipating via a damper, whereas a fully active suspension is able also to inject energy into the system. This is performed by using a force actuator, which is directly placed between the sprung mass and unsprung mass of the vehicle (Fig. 2-4). Unlike passive suspension elements, the created force by this actuator does not depend directly on the relative displacement or velocity of the suspension, but also, it is determined by a sensory feedback controller working based on a special control strategy.

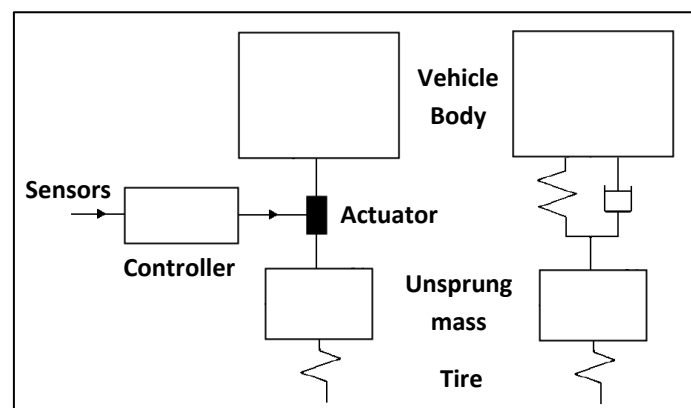


Figure 2-4 Fully active suspension comparison with passive system.

A fully active system is designed to control the suspension over the full bandwidth of the system. In particular, this means that the goal is to improve the suspension response around the natural frequencies of the vehicle body and wheels. These natural frequencies of typical vehicles are 1-3 Hz of the vehicle body and 5-15 Hz of the wheels (Williams, 1994).

These systems cover the full bandwidth of the suspension system and are able to perform a complete control on the vibrations. This provides good ride comfort and road stability for vehicle. However, the high bandwidth control leads to a significant quantity of power consumption, which is approximately until 10 kW for the normal automobiles. This high power consumption can affect negatively the overall performance of the vehicle and increases the fuel consumption in the range of 10 – 15 % (Williams, 1994).

On the other hand, the high bandwidth of these systems means that more accurate and faster components especially wide bandwidth actuators are required. This leads to the relative complexity and high expense of these systems. The relatively high level of noise is another weakness of these systems due to the disability in isolating the high frequency vibrations. These systems generate themselves also undesired noise causing from the fast action of their actuators. This affects negatively the ride comfort of the vehicles. However, this problem can be reduced by placing rubber elements in series with the actuators in the system.

Since in a fully active suspension, the passive suspension elements are replaced by an actuator, the actuator force has a central role in suspension performance. In this condition, the failure modes of the actuator can affect critically the suspension. For example, an error in operation of the controller in determining the actuator force may cause a major failure in producing damping or stiffness force in the system. This leads to a major drop in ride quality and road handling of the vehicle. On the other hand, a strong wrong force by an actuator may cut the tire contact from the road surface and reduce critically the stability and controllability of the vehicle. Such situation may lead to create dangerous modes for vehicle and passengers.

Considering these weaknesses of fully active suspensions, in spite of the high performance of these systems, they are not used generally for the normal vehicles, and just for luxury or special vehicles are employed. In order to have a more practicable system of the fully active suspension, low-bandwidth type of these systems is presented. In this system, the actuator is placed in series with a passive spring and, in some cases, in series with a passive damper (Fig. 2-5). Unlike fully active system, this system is not designed to control the suspension vibrations over the full bandwidth of the system. On the contrary, the goal is to improve the suspension response just around the natural frequencies of the body of vehicles, with the typical range of 1 – 3 Hz, because these frequencies area has the main

role in both ride comfort and handling of vehicles. At higher frequencies, the actuator does not work effectively, and the wheel-hop motion is controlled only by the passive elements.

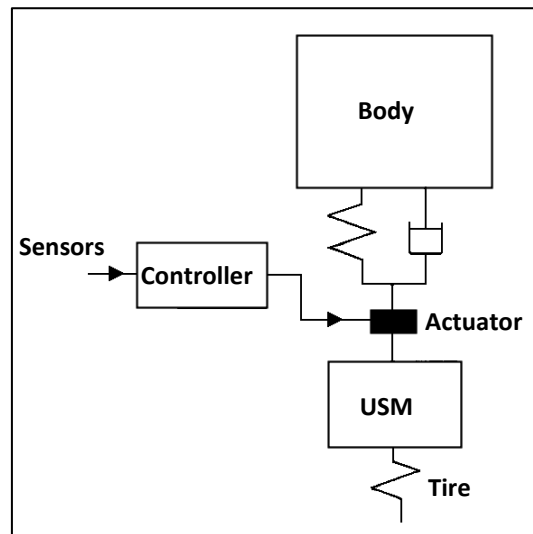


Figure 2-5 Configuration of a low-bandwidth active suspension (Williams, 1994).

In practice, in spite of the lower bandwidth, performance of the low-bandwidth active suspensions is relative similar to fully active systems in providing good ride quality and handling capability for vehicles (Williams, 1994). These systems are able to create significant reduction in the body roll and pitch motions during vehicle maneuvers such as cornering and braking. This efficiency is achieved with lower energy consumption than high bandwidth systems. In addition, since in these systems, passive suspension elements are employed beside the actuator, the failure modes in system are not critical such as high-bandwidth systems. These capabilities of these active systems have led to their application for automobiles. The major motor manufacturers, such as Jaguar, BMW, Mercedes Benz, and Toyota have already presented their own fully active suspension systems.

Many research works have been already conducted in this area with the purpose of performance evaluation of fully active suspensions. One of these investigations is the basic research work of (Chalasani R. , Dec.1986) that applied a low-bandwidth active suspension to a quarter-car model. He examined the suspension system by using white noise as the road input of the suspension. After the examination, he concluded that the RMS value of the sprung mass acceleration was 20% reduced in comparison with a passive system. This was achieved without negative effect on the unsprung mass vibration and suspension travel.

Power consumption of low-bandwidth fully active systems is lower than the high-bandwidth systems. However, this consumption is still considerable, especially about heavy

vehicle. In the research work of (Deakin, Crolla, & Shovlin, 1997), the power consumption of a military heavy vehicle, equipped with low-bandwidth active suspension, was examined. The result of this investigation showed that until 25 % power of the vehicle engine could be spent for the active suspension. However, this value for smooth roads was just 3 %. In a similar investigation (Donahue, 1998), a low-bandwidth active suspension was applied to a military off-road heavy vehicle “HMMWV”. The tests showed that until 30 HP of 150 HP engine power was used by the active suspension. This led to considerable increase in the fuel consumption of the vehicle.

Fully active systems provide high performance, but they are not used for the chassis suspensions of the heavy vehicles such as agricultural tractors. Fully active systems in these high masse vehicles consume considerable energy. However, for the partial suspension of heavy vehicles, the fully active systems have been already used successfully. For example, these systems have presented a good efficiency in the seat and cabin suspension of tractors.

2.2.4 Semi-Active

In a fully active suspension, a force generator using extra energy source is put in the passive suspension with the purpose of improving its performance. In a semi-active suspension, the active force generator is replaced with an adjustable damper. Using this damper, the rate of energy dissipation can be changed depending on the instant condition of the suspension motion. Figure 2-6 shows the construction of a semi-active suspension. In this suspension, the passive damper is replaced with an adjustable damper that its damping rate is determined by a controller with closed loop control, using sensory information as feedback.

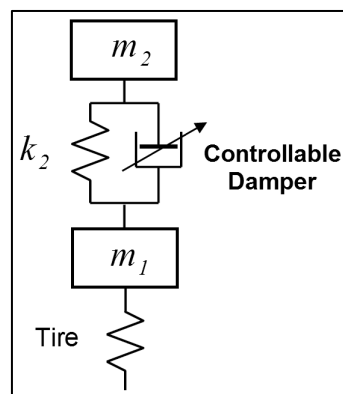


Figure 2-6 Semi-active suspension system.

In order to clarify the difference between the operation of semi-active and fully active suspensions, the working area of these two systems are illustrated in figure 2-7. In a fully active system, the four operation areas are covered, because the force of the actuator can be applied to the system in direction or against the direction of the suspension movement. In spite of this, in a semi-active system, the force of the adjustable damper can be applied to the system only against the direction of the suspension movement. Thus, just two areas of the four operating areas are covered by this system.

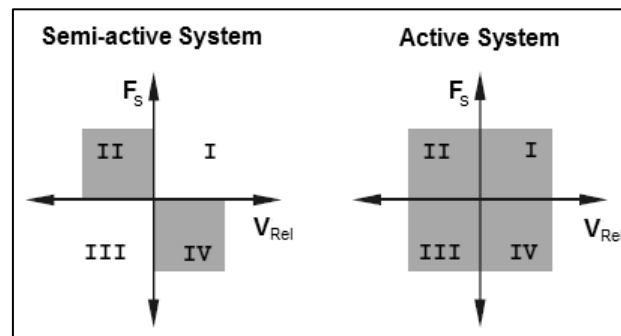


Figure 2-7 Working area of the semi-active and fully active suspensions.

Basic theory of a semi-active suspension is the controlling of the damping level of the suspension. However, there are different strategies to perform this control. A semi-active control approach determines the damping level based on the sensory information. These strategies will be described in the next sections.

The main difference in the construction of a semi-active suspension with a fully active suspension is the actuator of the system. The actuator of a semi-active suspension is in fact a controllable damper with a relative simple construction in comparison with the force actuator of a fully active system. A controllable damper is made normally based on the common hydraulic dampers. In these dampers, the damping force is created based on the throttling the hydraulic fluids. Two main methods are used in order to control the damping rate of the controllable dampers.

In the first method, the controlling of the damping rate is created by adjusting the cross area of a throttle. The hydro-pneumatic suspensions are the proper systems for performing this method, because they can be equipped with a controllable throttle-valve between the cylinder and accumulator (Fig. 2-8). This method was used in this investigation as the actuation system of a semi-active suspension. More details about these systems will be presented in the next parts.

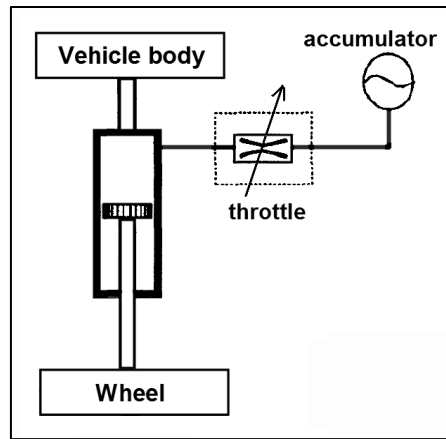


Figure 2-8 A hydro-pneumatic suspension as a semi-active suspension by using a controllable throttle.

The second method for creating a variable damper is based on the viscosity property of the hydraulic oil instead of cross-area of the throttle of a damper. There are two kinds of such fluids. The first one is electro-rheological (ER) fluid. Viscosity of this fluid can be changed by electrical field. The second fluid-type is magneto-rheological (MR) fluid. Viscosity of this fluid can be controlled by magnetic field. A schematic illustration of a controllable damper working with the MR fluid is shown in figure 2-9.

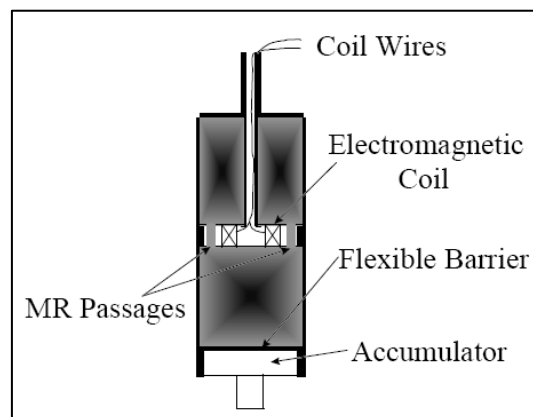


Figure 2-9 Schematic Illustration of a MR damper (Paré, 1998).

Advantage of these MR dampers is in their high-speed response, which is in the range of millisecond. This is important in a semi-active control system, because among all components of this control system, the time response of the actuator is the most limiting factors in order to create the proper control bandwidth (Mäkelä, 1999). A feature of these dampers is their form and their dimension that is similar to the typical passive dampers, and so, they can be simply installed in their place. MR dampers has priority to the ER dampers in

practicable application (Goncalves, 2001), because they can be directly operated by the electricity source of a vehicle. In addition, they provide a wide range of damping rate.

Many research works have been conducted about semi-active suspension since its introducing in early 1970's. The primary researches investigated this idea theoretically by using simple car models. Later, the practicable application of the system was also investigated for the different types of vehicles such as motorcycle, automobile and heavy vehicle. Some of these research works proved that the performance of semi-active suspensions can be considerable and competitive with fully active suspensions. For example, in the analytical investigation of (Margolis D. , 1982), performances of semi-active suspensions were compared with active suspensions. As result, some control strategies for a semi-active suspension were presented. With these strategies, the semi-active suspension offered comparable performance to fully active suspensions. In another research work (Karnopp, Crosby, & Harwood, 1974), it was concluded that a continuous semi-active suspension can achieve an acceptable performance near a fully active suspension.

In most of the studies about the semi-active suspensions, the efficiency of this system are examined only in providing good ride comfort for vehicles. However, because of the well-known compromise present in the suspension design, the handling of vehicles should be also examined besides the ride comfort. To be exact, after achieving improvement in ride comfort, the change in vehicle handling should be studied. In the research work of (Heo, Park, & Hwang, 2000), both of these two criteria were considered for examining a semi-active suspension. This suspension was applied to an automobile with some different control strategies. The results of this investigation showed that this system was able to improve the ride quality without aggravating the handling capability of the vehicle.

In another research work (Margolis & Nobles, 1991) , it was concluded that by using semi-active suspensions for heavy vehicles, the vibrations control of the body of these vehicles such as roll and heave control was improved. In addition, this improvement affected the handling capability of the vehicles positively. In the work of (Yi & Hedrick, 1993) the influence of semi-active suspensions on the dynamic tire force of vehicles was investigated. The dynamic tire-force was considered as the criterion of the handling capability. Using the prototype of a vehicle, some experiments were performed on a suspension test rig. The results of these tests showed that improvement in ride comfort of the vehicle was achieved

without rise in the dynamic tire force. In other words, improvement in ride comfort was accomplished without drop in the handling capability of the vehicle.

Failure modes of semi-active suspension systems are less than fully active systems, because their operation is simpler. In these systems, just damping force is controllable, and error modes just lead to create a passive damping mode in the suspension. This decreases its efficiency without creating a critical situation in the vehicle. Besides this advantage, semi-active suspensions have low energy consumption, and these systems have not complicated construction and high cost. These properties beside the notable performance make these systems as a practicable system and are usually preferred over fully active suspensions. These semi-active suspensions are considered and employed in the new vehicles by most of the famous companies.

For the heavy vehicles, semi-active suspensions are preferred particularly as a practicable way in order to improve their suspension performance (Efatpenah, Beno, & Nichols, 2000). Application of fully active suspensions for heavy vehicles, which have high mass and inertia, leads to unacceptable high-energy consumption. In an investigation (Nobles & Miller, 1985), efficiency of semi-active suspensions for military heavy vehicles was studied. For this purpose, a tank was considered, and the four wheels of its ten wheels were equipped with the semi-active suspensions. Performance of this tank was tested on a virtual road. In this evaluation, the energy absorption of the body vibration was considered as the criteria of ride comfort.

The results showed a significant reduction (13-40%) in this criterion, indicating a significant improvement in ride comfort. An agricultural tractor is also a heavy vehicle used for agricultural applications. Semi-active suspensions having low energy consumption are proper systems for these vehicles, especially for the chassis suspension of the tractors. However, the application of semi-active systems in the chassis suspension is still in research stage. At this time, the semi-active suspension is used in practice for the secondary suspension of tractors, such as seat and cab suspension. The proper active suspension for agricultural tractors that was a key theme in this study will be discussed in the next section.

2.2.5 Conclusion

In this investigation, it was intended to improve the performance of the chassis suspension of agricultural tractors by way of using active suspensions. This began with

determining the proper type of the active suspension. In recent sections, different types of active suspension were described, and the related capabilities and limitations were studied. In order to conclude this study and compare these active systems, their characteristics are summarized in table 2-1. In this table, some criteria are considered, and for each one a weighting ratio indicating their importance is determined.

High efficiency of each suspension system is considered as the main strength of it. In opposition, the factors of the energy consumption, complexity, and cost of the system are considered as the main weakness of each system. Other considered characteristics are the control bandwidth, operation condition consideration, and failure mode problem. For each type of active suspension, the considered factors are quantified by ranking. By adding all these ranks, a sum point is achieved for the active suspension, which shows the overall potential of the system for the chassis suspension of agricultural tractors.

Table 2-1 The ranking of the different active suspension systems used for agricultural tractors.

Factor	Weight	Adaptive		Level-Control		Semi-Active		Fully Active	
Efficiency	(+3)	low-medium	6	low	6	high-medium	9	high	12
Energy consumption	(-2)	low-medium	-4	low	-2	low-medium	-4	high	-8
Complexity and cost	(-2)	low-medium	-4	low	-2	low-medium	-4	high	-8
Control bandwidth	(+2)	low-medium	4	low	2	high	8	high	8
Operation condition consideration	(+1)	high	4	low-medium	2	low	1	low	1
Failure mode problem	(-1)	low	-1	low-medium	-2	low-medium	-2	high	-4
Sum point:	-		5		4		8		1

Fully active suspensions have the least ranking among active suspensions in the table, because in spite of the best efficiency, high-energy consumption of this system is a major weakness. In contrary, semi-active suspensions provide good performance and need less energy. The controllable damper used for this system is not complicated and expensive, unlike to the force actuator of fully active systems. In addition, the probable failure modes of

a semi-active suspension are not critical. Therefore, semi-active suspensions gain the best ranking, and they are considered as the proper choice.

The two other systems (i.e. adaptive and load leveling systems) offer acceptable efficiency, but not as well as the semi-active system. These systems have a ranking between fully active and semi-active systems. Because of the special function of these systems, they can be employed beside the semi-active suspension. This is particularly useful for agricultural tractors that work in wide different operating conditions. Adaptive suspension systems are able to involve the factor of suspension operating condition, and load leveling control system can remove the negative influence of the load variation on suspension systems.

2.3 Semi-active Control Strategies

For each type of active suspensions, many different control approaches has been used. Active suspensions are usually considered as the first practicable system for the examination of the modern control theories, because a vehicle suspension, with some simplifications and linearizations, symbolizes a true MIMO-system that its mathematical model can be simply derived. In addition, ground vehicles are quite familiar example for people, because almost everybody has an experience with driving an automobile. In most of the investigations about the modern control theories, a linearized quarter model of the vehicle suspension is used. By using this model, different control methods and their basic features can be derived without creating complexity (Elmadany & Abduljabbar, 1999).

The semi-active suspension is the system that was used in this study. Main practicable control approaches of semi-active suspensions will be reviewed in this part. With small changes, these methods can be also used for fully active systems. At first skyhook-based strategies of “skyhook”, “groundhook” and “hybrid” will be presented. After that, fuzzy control method and preview control method will be reviewed. Finally, the on/off damping control approach will be described

2.3.1 Skyhook

Skyhook is one of the most famous control methods for active suspensions and is considered today as a classical method. This method was introduced for the first time in 1974 by (Karnopp, Crosby, & Harwood, 1974). Skyhook was derived by LQR calculation from the optimal control method, as the control aim was to minimize the RMS value of the sprung mass acceleration of the suspension. As from the name of “Skyhook” can be realized, the

vibration of the sprung mass in this method is damped by a damper that is connected to a fixed point in space (Fig. 2-10).

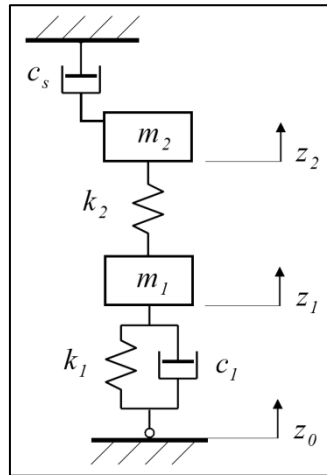


Figure 2-10 Sky-hook damping approach.

Force of the skyhook damper can be defined mathematically as:

$$F_{sky} = c_s \dot{z}_2 \quad 2-2$$

However in sky-hook approach, the damper connection to the fixed point can be performed only in a stationary system. In mobile systems like vehicle suspensions, a force actuator between sprung and unsprung masses is used to simulate the skyhook damper force. In a fully active suspension, a force actuator generates the sky-hook force by using an external power source, whereas in a semi-active suspension, a controllable damper is used as the force actuator (Fig. 2-11). This damper simulates the skyhook damper force without using external power source, just by dissipating the suspension energy.

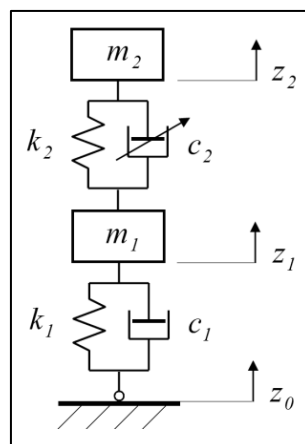


Figure 2-11 Practicable implementation of sky-hook damping approach.

The generated force by the practicable damper with coefficient of c_2 is calculated as:

$$F_d = c_2(z'_2 - z'_1) \quad 2-3$$

This force must be equal to the skyhook damper. Therefore, considering equation 2-2, the damping coefficient of the practicable damper can be calculated as:

$$F_d = F_{sky} \rightarrow c_2(z'_2 - z'_1) = c_s z'_2 \rightarrow c_2 = \frac{c_s z'_2}{(z'_2 - z'_1)} \quad 2-4$$

However, a damper generates the damping force always in inverse direction of the suspension movement. As this force is not in the demand direction, the damper must be shut off. The following switching law performs this consideration in the damper equation:

$$F_d = \begin{cases} c_2(z'_2 - z'_1) & z'_2(z'_2 - z'_1) \geq 0 \\ 0 & z'_2(z'_2 - z'_1) < 0 \end{cases} \quad 2-5$$

Because of the strengths of skyhook control strategy, this method is usually considered as a reference for evaluation of the other control strategies. However, this method is not perfect and has some weaknesses. As mentioned, sky-hook method was derived with the purpose of controlling the sprung mass vibration. In the skyhook construction, the damper is connected just to the sprung mass, and the control is focused on it. With this construction, the unsprung mass vibration remains without damping force.

Therefore, reduction of the unsprung mass vibration is achieved at the cost of the rising sprung mass vibration. In the vehicle suspensions, this problem causes high wheels bouncing and leads to a poor tire contact with road surface. As a result, this control strategy is useful when the vibration control of the sprung mass or the ride comfort of a vehicle is in priority. However, in the practicable implementation of skyhook, the damper is placed between the two masses, and using this construction, this problem is moderated. This subject will be discussed in the next chapter.

Another weakness of skyhook strategy is the high level of jerk in the sprung mass of suspension. This is created because of the switching law of this method that causes a rapid variation in the body accelerations. In vehicle suspension, this phenomenon has negative effect on the ride quality of vehicles (Karnopp, Crosby, & Harwood, 1974). However, this

problem can be moderated by limiting the maximum and minimum level of the damping in suspensions.

The skyhook control strategy is usually used for two main objectives. First, it is used as the ideal model with the purpose of evaluating other control strategies. Second, it is used as a practicable control method for the active suspensions (Valášek, Novak, Sika, & Vaculin, 1997). In the investigation of (Al-Holou, Joo, & Shaout, 1996), a fuzzy logic control method for active suspensions was evaluated by comparing with a skyhook control method in addition to a passive suspension. On the other hand, in the research work of (Satoh, Fukushima, Akatsu, Fujimura, & Fukuyama, 1990), skyhook method was used as the control method of a fully active suspension for an automobile. This system could provide a good control on the vibration of the body and wheels of the vehicle. In addition, in comparison with passive suspension, a significant improvement in ride quality and road stability was achieved.

In another research work (Miller, 1988); a quarter car model was used to study the performance of the passive, semi-active, and fully active suspensions. For the semi-active suspensions, the used control algorithm was skyhook method. This control approach was created based on the control feedbacks of the absolute and relative velocities. In order to evaluate this suspension system, ride comfort, road holding, and suspension travel were considered. The suspension was excited by a random velocity-input with the frequencies of less than 100 Hz as the simulation of the road roughness.

The results of the evaluation of the semi-active system showed that the RMS values of the body acceleration were reduced significantly. However, the suspension deflection and tire contact force were both increased in comparison with the passive suspension. As another result, it was found that the limitation of the maximum and minimum values of the skyhook damping force had important influence on its performance, particularly on the tire contact force of the vehicle.

Based on the skyhook control strategy, some other strategies such as groundhook and hybrid are derived. These methods will be described in the following sections.

2.3.2 Groundhook

Groundhook is a control strategy similar to skyhook strategy with the difference that instead of the sprung mass, the unsprung mass is connected to the damper fixed to the

space point (Fig. 2-12). This control method is focused on the unsprung mass and provides optimal vibrations control on it. This decreases the dynamic load of the tires directly and leads to an improvement in handling capability of the vehicle and reduction in the road damage.

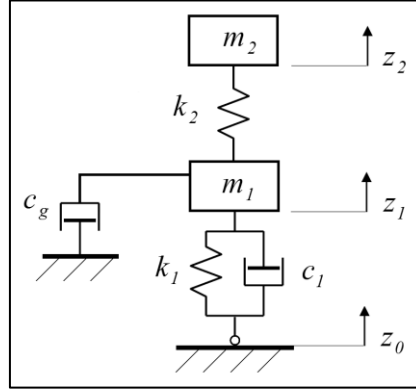


Figure 2-12 Ground-hook damping approach.

Looking at figure 2-12, the groundhook damper force with the coefficient of c_g is defined as:

$$F_{gnd} = c_g z_1' \quad 2-6$$

In the practicable implementation of groundhook strategy, the damper is placed between the two masses of the suspension (refer to Fig. 2-11). This damper is used to generate the same force as the groundhook damper. Therefore, its damping coefficient can be calculated as:

$$F_d = F_{gnd} \rightarrow c_2(z_2' - z_1') = c_g z_1' \rightarrow c_2 = \frac{c_g z_1'}{(z_2' - z_1')} \quad 2-7$$

The damper force is related to the movement direction of the two masses of the suspension. When this force is in the opposite direction of the simulating groundhook force, the damper must be switched off. This consideration can be performed by this switching law:

$$F_d = \begin{cases} c_2(z_2' - z_1') & -z_1'(z_2' - z_1') \geq 0 \\ 0 & -z_1'(z_2' - z_1') < 0 \end{cases} \quad 2-8$$

In this method, the focus is on the control vibration of the unsprung mass, and the groundhook damper is connected just to this mass and, no damping force enters to the sprung mass. In this way, the reduction in the vibration of the unsprung mass is achieved at the cost of increased vibration in the sprung mass. However in the practicable implementation of groundhook, a damper is placed between the two masses and simulates

the groundhook damping force. This damper provides a partial damping force for the unsprung mass vibration and moderates the problem.

Based on the related investigations, usage of the groundhook control reduces the road damage, created by the vibration of the wheels. In addition, usage of this strategy decreases the tire-road force and enhances the driving safety of the vehicle. However, this can be achieved only at the cost of reduced ride comfort (Valášek, Novak, Sika, & Vaculin, 1997). Overall, this control strategy is useful as the vibration control of the unsprung mass is the priority of the control.

2.3.3 Hybrid

Hybrid is the combination of two suspension control methods of skyhook and groundhook. While skyhook control focus on the sprung mass vibration, and groundhook strategy concentrates on the unsprung mass vibration, hybrid provides a balance between these two methods. Figure 2-13 illustrates the configuration of this control strategy.

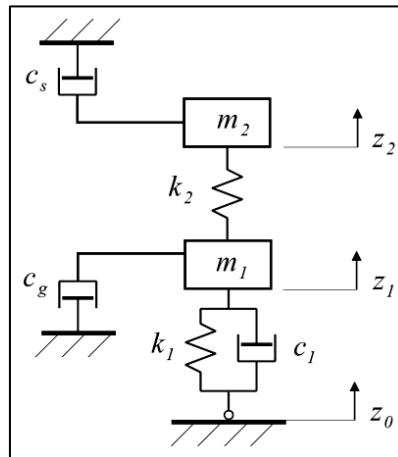


Figure 2-13 Hybrid damping approach.

As stated before, the forces of the skyhook and groundhook dampers are defined as:

$$F_{sky} = c_s \dot{z}_2$$

$$F_{gnd} = c_g \dot{z}_1$$

In the practicable implementation of hybrid strategy, a damper between the sprung and unsprung masses generates the hybrid damping force (refer to Fig. 2-11).

The hybrid damping force can be expressed mathematically as follows:

$$F_d = G[\alpha\sigma_{sky} + (1-\alpha)\sigma_{gnd}] \quad 2-9$$

$$\sigma_{sky} = \begin{cases} z'_2 & z'_2(z'_2 - z'_1) \geq 0 \\ 0 & z'_2(z'_2 - z'_1) < 0 \end{cases} \quad \sigma_{gnd} = \begin{cases} z'_1 & -z'_1(z'_2 - z'_1) \geq 0 \\ 0 & -z'_1(z'_2 - z'_1) < 0 \end{cases}$$

Where, G is the damping coefficients of the skyhook and groundhook dampers, which are assumed equivalent as:

$$c_s = c_g = G$$

In addition, the coefficient of α is defined as a ratio that determines the tendency of hybrid strategy to the skyhook and groundhook methods. Also, σ_{sky} and σ_{gnd} are the switch variables of the skyhook and groundhook strategies, came out from the equations of 2-5 and 2-8.

The tendency of hybrid control method to skyhook and groundhook can be adjusted by changing the ratio of α , which has a value between zero and one. With the value of one, the hybrid converts completely to skyhook, and with the value of zero, it converts completely to groundhook control strategy. Between these two values, the hybrid approach is a combination of the two control strategies. Indeed, this value defines the priority of the control design. By selecting a proper value for α , the hybrid approach is capable to offer the benefits of both the skyhook and groundhook methods and provide good control on the vibration of both the sprung and unsprung masses.

Performance of three control policies of the skyhook, groundhook, and their hybrid, were compared experimentally with one another in the research work of (Ahmadian & Pare, 2000). It was concluded generally that the skyhook control improves ride comfort, and conversely the ground-hook control improves vehicle stability and reduces the road damage. Whereas a hybrid of these policies is capable to improve ride comfort, vehicle stability and provide road protection in the same time. However, besides these advantages, some aspects should be considered about this strategy.

The performance of this method is related closely to the ratio of α in equation 2-9, which is considered difficult to be determined correctly. In addition, in this control method, unlike skyhook and groundhook methods, it is needed to measure the absolute velocity of both the masses. On the other hand, by looking at the formulation of this control method, this strategy cannot be performed in the on/off form, and just in continuous form by using

continuous controllable dampers can be executed. These issues are considered technically as complexity of this system.

2.3.4 Fuzzy

Fuzzy control is a control theory based on “fuzzy logic”, which was introduced first by “Lotfy Zadeh” in 1965 (Zadeh, 1965). This control method is particularly proper for the systems with complex modeling (Carter, 1998). Since there are some nonlinear characteristics in suspension systems, accurate modeling of them are complicated as well, and fuzzy control can be considered as a proper strategy for the active suspensions.

Fuzzy logic runs basically by executing some rules that link the controller inputs to the desired outputs. These rules are not derived based on the complicated mathematical equations but also are created through the perception or knowledge of the proficient operators of the system. There are three main steps for designing a fuzzy logic controller: the fuzzification of the controller inputs, the execution of the rules, and the defuzzification of the output. More detail about the theoretical and practicable background of fuzzy logic control can be found in the reference of (Carter, 1998).

Fuzzy control method has been used for vehicle suspensions in practice only in recent years. This control can be used directly for calculating of the damping coefficients for semi-active systems (Al-Holou, Joo, & Shaout, 1996) or for calculating of the force of the actuators of active suspensions (Barr & Ray, 1996). Most of the studies in this area are simulation-based. However, there are also some experimental cases. Overall result of these investigations implies high potential of this control method for active and semi-active vehicle suspensions.

One feature of this method is its special flexible design. In the simulation study of (Titli & Roukieh, 1995), a semi-active system with fuzzy logic control was applied to a quarter-car model. The design goal of the fuzzy logic control was reduction of the compromise between ride comfort and vehicle handling. For this purpose, a three-section controller was created. This controller was consisted of two sub-controllers, namely “comfort” and “handling”, and a fuzzy supervisor. Each sub-controller had two inputs. The suspension deflection and body speed were used as the inputs of the ride comfort controller, and tire deflection and tire speed were used as the inputs of the handling sub-controller.

On the other hand, the fuzzy supervisor had the special inputs including vehicle travel speed, longitudinal acceleration, braking pressure, steering angle, and body height. Based on these inputs, the supervisor could recognize the priority of the ride comfort and handling and created two weighting factors for the corresponding sub-controllers. In order to evaluate this semi-active suspension system, its performance was compared with the passive system using step suspension input. In comparison with a passive suspension, about 50% reduction in the percent overshoot of the transient responses of the body and wheel displacements was achieved.

In another investigation (Al-Holou, Joo, & Shaout, 1996), a fuzzy logic-based controller was developed for a semi-active suspension system. In order to evaluate this controller, the results of this system were compared with another semi-active system with on-off skyhook strategy in addition to the passive system. The simulation results showed a major improvement over passive suspensions. This improvement was achieved in both the areas of the body acceleration and dynamic tire contact force. However, over the semi-active suspension with skyhook strategy only minor superiority was achieved. This was attained only because of a slight priority in improving the body acceleration, whereas in the dynamic tire contact force, no priority was observed.

2.3.5 Preview

The road surface input is the main excitation source that affects ride quality of a vehicle. As a vehicle with an active suspension, drives on the road irregularities, the dynamic behavior of the vehicle will be influenced by these irregularities. Sensors of the active suspension system detect the created changes in the dynamic of vehicle. Base on the sensors signals, the controller react against the changes. With this working procedure, vehicle is always influenced by the first effect of the road irregularities. This is especially problematic as the first effect is intense, like as vehicle meets a sudden bump or pothole on the road surface. If prior knowledge of the obstacles and rough patches on the road surface would be available, the controller can enter this additional information into the control loop. With this information, controller has enough time to response properly to the road inputs. This leads to raise the performance of the suspension system. In order to acquire the preview information, there are two methods.

In the first method, the preview sensors are used for collecting the road profile ahead of vehicles (Fig. 2-14). This sensory information can be used for both the front and rear suspensions of the vehicles. For that reason, this system has high potential in improving the performance of vehicle suspensions. However, it needs an advanced sensory set-up and complex algorithm system in order to derive the road profile from the sensory information (Baillie, 1999). Different kinds of sensors can be used for this system such as optical, ultrasonic, and radar technology. In this method, the derivation of the road profile from the sensory information is the main challenge of the system, and it is often executed with errors. For example, a pothole filled with water may not be distinguished from the road surface and cardboard box may not be distinguished from a piece of stone.

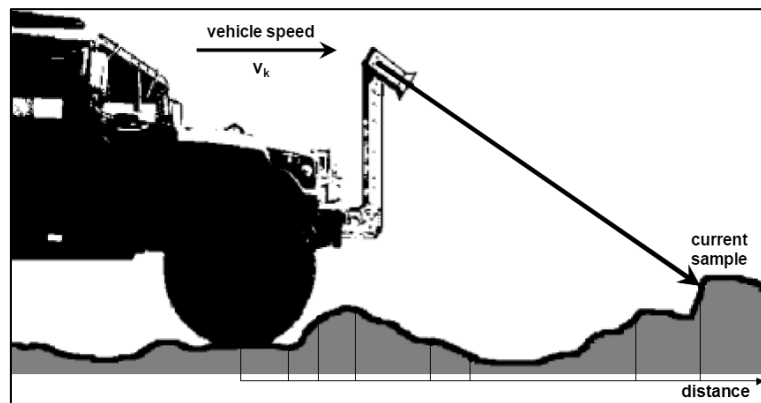


Figure 2-14 Preview sensor for active suspension (Donahue, 1998).

Theoretical investigations about this kind of preview control have considered significant potential profits for these systems, such as the investigation of (Soliman & Crolla, 1996). In spite of this, the experimental investigations have reported some practical difficulties in achieving these benefits. For example, in the practicable investigation of (Langlois, Anderson, & Hanna, 1991), an ultrasonic height sensor was used as a look-ahead preview sensor for an off-road military vehicle, which was equipped with an active suspension. After testing the vehicle over a rounded bump with 50mm height, the results showed that the preview control system provided a reduction of 15 % in the RMS acceleration of the body in comparison with a passive suspension, whereas this system could offer only 4 % improvement over the active system without preview.

In the second type of preview control systems by measuring the dynamic variables at the front axle, the road profile under the rear wheel is predicted. The moment that the roughness reaches to the front wheel can be calculated based on the vehicle speed and

wheelbase. For that reason, this method is called wheelbase preview control. As an advantage of this system, they do not need to the complex sensory system in the front of the vehicle. However, in this system, the preview information is only available for the rear suspension. The investigations about wheelbase preview control have considered grate potential benefits for this system. For example, in the research work of (Crolla & Abdel-Hady, 1991), the capability of the wheelbase preview system was evaluated by applying it to the rear semi-active suspension of a vehicle. Based on the results of this investigation, it was concluded that semi-active systems with preview control strategy have the potential to achieve a performance over fully active systems.

The research work of (Hansson P. , 1996) is a rare research work in the theme of active suspensions for fully suspension agricultural tractors. In this research work, a preview control approach was used for the rear adaptive suspension of a tractor in order to modify its performance. The primary adaptive suspension of this tractor was not enough fast to deal with sudden changes in ground roughness, such as potholes. Especially, sudden roughness on a smooth surface produced a high level of vibration, because on the smooth surface, the dampers were normally set on the high damping mode by the controller. As the sudden rougher area reached, the adaptive control was unable to create fast major change in the damping gain. In this condition, result might be a suspension over-travel, inducing extreme vibration levels at the driver.

Hansson found that the solution of this problem was to use a preview control system in order to recognize the sudden road roughness previously. Since the first kind of preview control with the look-ahead preview sensor was considered too complicated and expensive for a tractor, the wheelbase preview-control system was chosen. In this system, the accelerations at the front axle was measured and filtered in order to pre-estimate the ground roughness under the rear wheel. Using this preview information, the damping controller was able to determine the optimal damping degree so that, the rear suspension could use the available travel space in an optimal way. In this way, rear suspension was able to react effectively to the sudden road inputs.

In summary, employing the preview controls in advanced suspensions provides encouraging results in improving their performance. However, the technical difficulties are considered in the practicable application of these systems, particularly about the look-ahead preview sensors.

2.3.6 On-Off Damping

In a semi-active suspension, dampers are able to generate force only in the opposite direction of the suspension, and the control strategy includes always a switching law in order to turn the damper off, as the damping force is in the inverse direction. Because of this switching, the damping forces are discontinuous in these systems. This issue leads to create rapid changes in the vehicle body accelerations and consequently, increase the problem of the jerk and noise. This phenomenon affects negatively its ride quality and handling. This issue has been also addressed in some research works such as (Karnopp, Crosby, & Harwood, 1974) and (Hauck, 2001). In order to regulate this problem, the difference between maximum and minimum value of the damping forces should be reduced. The formulation of the skyhook control strategy was presented before in section 2.3.1. By limiting the values of the damping coefficients, the formulation of the control strategy can be modified as follows:

$$c_2 = \begin{cases} c_s z'_2 / (z'_2 - z'_1) & z'_2 (z'_2 - z'_1) \geq 0 \\ c_{\min} & z'_2 (z'_2 - z'_1) < 0 \end{cases} \quad (c_{\min} < c_2 < c_{\max}) \quad 2-10$$

As seen, in the “off” mode, a minimum value for damping coefficient is defined instead of the zero value. In addition, the lowest and highest values of the “on” mode are also limited.

Looking at equation 2-10 as a typical formulation of a continuous semi-active suspension, it can be realized that a continuous controllable damper is needed in order to perform a continuous semi-active system. In addition, in order to perform this system, both the absolute and relative velocities of the suspension must be measured, because the damping coefficient of the continuous damper is calculated based on these velocities. However, these conditions can be changed totally with a simple change in the control strategy.

By looking again at the semi-active strategy, it can be found that this approach works in this principle that as the damping force is useful for the damping of vibrations, the damper coefficient is increased to the specific values. Alternatively, as damping force is in the wrong direction, the damper is turned off to a minimum value for its coefficient. Now, if for the “on” mode of the damper similar to the “off” mode, just one coefficient would be considered the major simplification would be achieved. This new strategy is called “on-off damping” approach and can be defined mathematically as:

$$c_2 = \begin{cases} c_{high\ state} & z'_2(z'_2 - z'_1) \geq 0 \\ c_{low\ state} & z'_2(z'_2 - z'_1) < 0 \end{cases} \quad 2-11$$

The modes of “off” damping and “on” damping are called respectively as “low state” and “high state”, referring to the low and high levels of the damping in system. The switching law of this formulation is based on the skyhook approach, and because of this, it can be called “on-off skyhook damping” control strategy. However, the switching law can be defined differently based on the different on-off damping strategies.

On-off damping strategy provides major simplification in the application of a semi-active system namely in the actuator, sensors, and controller components of the system. In these systems unlike the continuous systems that need continuous controllable dampers, just dampers with two levels of damping are necessary. On the other hand, the formulation of this system implies that the measures of the relative velocity and absolute velocity are needed in a continuous strategy, whereas just the signs of these velocities are necessary in on-off strategy.

These simplifications are considered as the main advantage of this strategy in comparison with the continuous method. These systems can be considered as proper option for the semi-active suspensions used for agricultural tractors. A new system for these vehicles, which work under severe operating conditions, should have a relative simple and robust construction in addition to the good performance. In this research work, this was considered also as the motivation of choosing on-off skyhook as the proper control strategy for the semi-active suspension of agricultural tractors.

However, the probable weaknesses of this system should be studied as before to ensure that this strategy provides a good efficiency for the system. Because of the phenomenon of the discontinuous damping force in the on-off strategy, the most challenging problem is the increasing jerk and noise in the system. “Miller” and “Nobles” in their investigation (Nobles & Miller, 1985) tried to find a solution in order to overcome against this problem in semi-active suspensions. They found finally that the method of creating a limitation for the damping force range was completely effective in both continuous and on-off semi-active suspensions. As a result, in order to overcome against this problem in on-off strategy, a more limited range for the high and low level of damping should be defined as:

$$c_{high\ state} < c_{max} \ , \ c_{min} < c_{low\ state} \quad 2-12$$

The operating areas of semi-active dampers in continuous and on-off systems are indicated in figure 2-15. In a continuous semi-active suspension, dampers works only in the two areas of the quadratic operating areas (Fig. 2-15 a), because they are not able to generate the damping force in the direction of the suspension movement. In order to reduce the jerk and noise in the continuous semi-active suspension, minimum and maximum values are defined for the damping coefficients, and the damping force can be changed only in a limited area (Fig. 2-15 b). On the other hand, in an on-off semi-active system, there are only two levels of damping for the suspension (Fig. 2-15 c). These levels are more close to one another in comparison with a practicable continuous system.

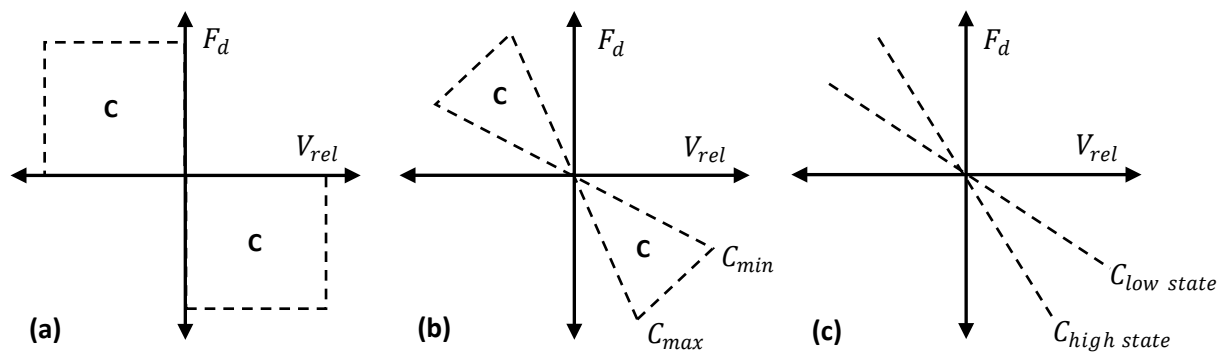


Figure 2-15 Operating area of semi-active dampers a) continuously a) practicable continuously c) “On-Off” system.

Because of the limited range of the damping levels in the on-off semi-active suspensions, it is expected that the performance of these systems would be less than continuous systems. Some researchers have already considered this issue in their investigations. For example, in the investigation of (Fodor & Redfield, 1995), it was concluded directly that the performance of an on-off semi-active suspension was close to the performance of a continuous semi-active system. In general, the results of these research works showed that the performance of on-off systems is less than continuous system, but the difference is not in practice considerable. Since the on-off semi-active system was used in this research work, this strategy will be studied in more details in the next sections of this thesis.

2.4 Hydro-pneumatic Suspension

Hydro-pneumatic suspensions were introduced first in the 1950's, when the hydro-pneumatic struts were installed on the prototype of a heavy tracked vehicle. This was the

result of an investigation with the purpose of using compressible fluids in suspension systems, conducted by two German companies (Hilmes, 1982). After that, hydro-pneumatic suspension was used for automobiles by Citroen Company as the first time in the mid-1950's. In this way, the superior capability of this system for the automobiles was proved as well as in heavy vehicles. However, in the beginning, there were some shortages such as the problems of improper sealing and heat influence of the system. During the next years, by using new hydraulic technology, the problem of sealing was solved, and the temperature influence was removed by employing the load leveling control system (Giliomee, 2003).

The principle of a hydro-pneumatic suspension is illustrated in figure 2-16. A hydraulic cylinder is placed between the chassis and wheel of the vehicle instead of the spring and damper in conventional suspensions. This cylinder has a hydraulic connection to an accumulator through a throttle. As the cylinder is compressed, oil is forced to the accumulator through the throttle. This condenses the gas inside the accumulator and produces a pressure in the accumulator that appears as the stiffness force on the cylinder. On the other hand, the pressure drop on the throttle creates the damping force on the cylinder. More detail of this system will present in chapter 2.

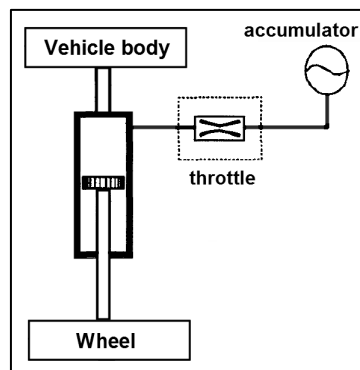


Figure 2-16 Configuration of a hydro-pneumatic suspension system.

Since the stiffness property of a hydro-pneumatic suspension is created based on the gas compression, unlike steel springs, the stiffness is not linear, and it rises progressively with increase in the suspension displacement. This characteristic decreases the influence of the load variation on the natural frequencies of the vehicle body. In addition, the overload capability of this suspension type is improved, because the stiffness of the suspension rises largely at the end of its strike.

One important feature of hydro-pneumatic suspensions is the controllability of this system that can be equipped with different types of control systems. Figure 2-17 illustrate the methods of converting this system to an active suspension. In figure 2-17 (a), a controllable throttle valve is used between the cylinder and accumulator in order to control the damping level of the suspension. This mechanism can be used as the actuation system of semi-active or adaptive suspensions. On the other hand, by applying the pressurized oil from a hydraulic pump to the hydro-pneumatic suspension, this system can be used as an actuation system for fully active or for a load leveling suspension systems (Fig 2-17, b).

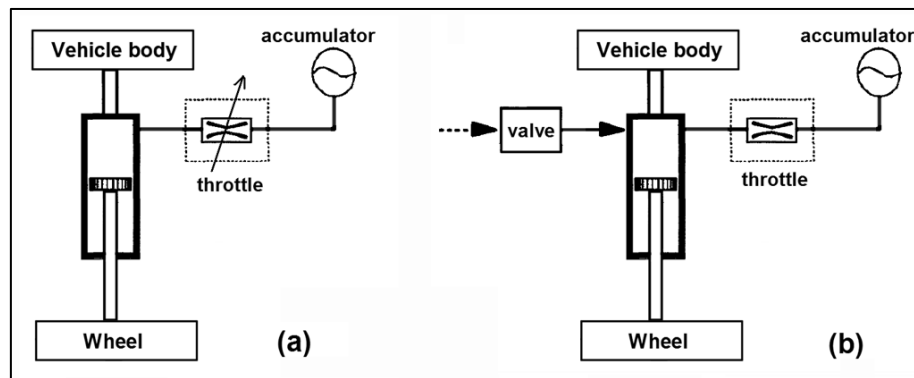


Figure 2-17 Capability of hydro-pneumatic suspensions in converting to different types of active system.

In hydro-pneumatic suspensions, variable stiffness can be also provided in addition to the variable damping mechanism. This ability is created by changing the primary pressure of the gas in the accumulator, which can be performed by pressurizing oil to the cylinder or pulling oil out from it. In order to create major changes in the level of stiffness, extra accumulators can be used. These accumulators are connected to the cylinder via the on/off valves. Vehicle load leveling system is an application of the variable stiffness. In addition, the variable stiffness can be used in order to create an adaptive suspension system like in the research work of (Abd El-Tawwab, 1997). In this investigation, in addition to use a throttle valve for creating a controllable damping system, an on/off valve with an extra accumulator was used in order to create a controllable stiffness mechanism (Fig. 2-18).

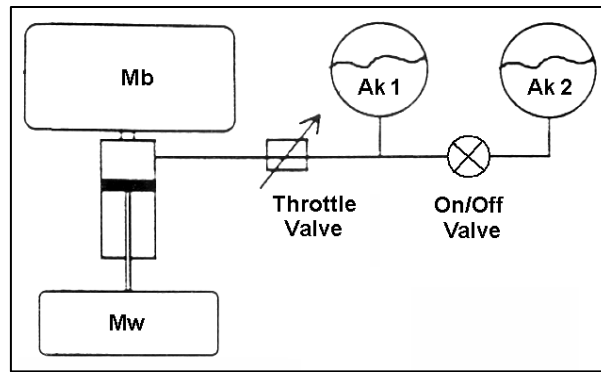


Figure 2-18 Hydro-pneumatic suspension with two-stage variable spring rate (Abd El-Tawwab, 1997).

Hydro-pneumatic suspensions of the vehicles can be equipped with an interconnection system more simple and effective than conventional suspension. The interconnection mechanism is applied by creating special hydraulic connections between left-right and front-rear suspension units (Fig. 2-19). This mechanism called fluidic interconnections provides higher stiffness and damping against body motion. This improvement is specially valuable, because it is created without increasing the stiffness and damping of the overall suspension, which has negative effect on its ride comfort. By employing this system for a vehicle, the pitch, and roll motions of its body are reduced, particularly during the maneuvers such as braking, accelerating, and cornering. Using this system has also the advantage that it works passively and does not need any control system (Chaudhary, 1998).

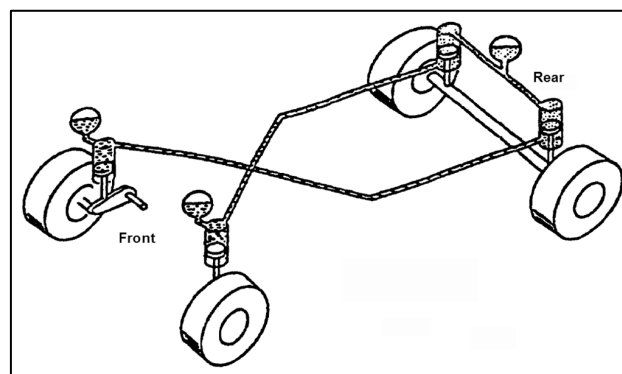


Figure 2-19 Schematic of the hydro-pneumatic suspension interconnected in the pitch and roll planes (Chaudhary, 1998).

One feature of hydro-pneumatic suspensions is its compact and flexible design. This is particularly notable for the suspension systems of heavy vehicles that consist of heavy and large steel springs. Different advantages of hydro-pneumatic suspensions have led to the

frequent use of this system for different vehicles. For example, these suspensions are employed widely for the agricultural tractors, because of their compact and flexible design and also their control ability. In these vehicles, the auto leveling system, which is needed especially because of their wide range of loads, can be applied simply to the hydro-pneumatic suspension. In addition, for station work or extreme working condition of tractors, suspension blockage mode is necessary. This mechanism can also be added simply to a hydro-pneumatic suspension by using hydraulic valves, so as to block the oil in the cylinders (Fig. 2-20).

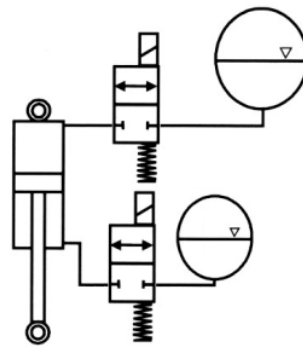


Figure 2-20 Suspension blockage mode by using the valves between the accumulators and cylinder (Bauer, 2007).

In this investigation, a semi-active control system was applied to the hydro-pneumatic suspension of the rear axle of an agricultural tractor. For that reason, in the next sections of this thesis, more theory and practical details will be presented about the hydro-pneumatic suspension systems.

2.5 Suspension System for Tractors

In the previous sections, the suspension system of vehicles was studied in general. Now, in this part, employment of the suspension systems for agricultural tractors is considered. The early agricultural tractors had no suspension systems, and different types of suspension systems were employed in them gradually with time. The primary systems were seat suspensions, which were used with the aim of improving ride comfort of tractors. Along with the development in tractors technology, chassis suspensions were also used for these vehicles.

These systems were able to improve the handling of tractors besides the ride comfort of them. This provided more safety and stability for tractors, and their travel speed was increased. In this part of thesis, suspension systems used for agricultural tractors are studied.

This begins with characteristics of tires, and suspensions of seat and cabin. Then, the chassis suspension systems of tractors including front axle and full suspension are explained. Finally, as the summary of this part, the general characteristics of these systems are presented.

2.5.1 Suspension Characteristics of Tires

When in the early 30th, the pneumatic tires were used first time for agricultural tractors, ride comfort and handling were improved, and the travel speed of tractors was increased until 20 km/h (Hoppe-01, 2004). Tires are the first elastic elements between a vehicle and the ground surface. For that reason, the suspension properties of the tires have an important role in the dynamic behavior of tractors, particularly for tractors having no other suspension systems.

The suspension characteristic of a tire can be demonstrated by a simple model, which is constructed of a spring and a damper in parallel (Fig. 2-21). Based on this model, figure 2-22 presents the measured stiffness and damping characteristic of a typical tire for agricultural tractors. As shown, the stiffness and damping coefficients of the tire are correspondingly too high and too low than typical suspension characteristic needed for a tractor. Therefore, tires are not able to work lonely as a proper suspension system, because high stiffness of tires is equal to a very hard suspension that is unable to provide good ride comfort. On the other hand, with very low damping capacity of tires, they are not able to provide effective control on vibrations.

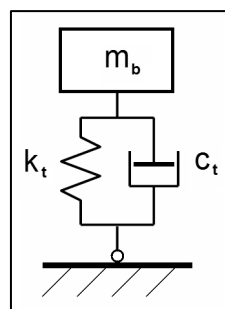


Figure 2-21 Single point contact modeling of tires.

In addition to the improper value of stiffness and damping coefficient of tires, these characteristic are not constant and depend on the inflation pressure and speed of tires. All these factors cause a poor dynamic behavior for the conventional tractors that have no primary suspension, and the tires are the only elastic element working as a suspension for them. This is particularly considerable in the heave and pitch vibration of the tractors in the

high travel speed (Von Holst, 2000). With the raise in the travel speed of them, the road excitations are increased, and in the same time, the damping coefficient of the tires is reduced. The speed range of 50 - 60 km/h is reported as the critical driving condition of conventional tractors on the standard roads (Vessonen & Järviluoma, 2001). In the worst case, because of the resonance phenomenon, the vibration amplitude can be increased until 15 times and reach to the limit where the wheels lose their contact to the road surface. This may reduce largely the steer ability of the tractors and creates an unsafe mode for them.

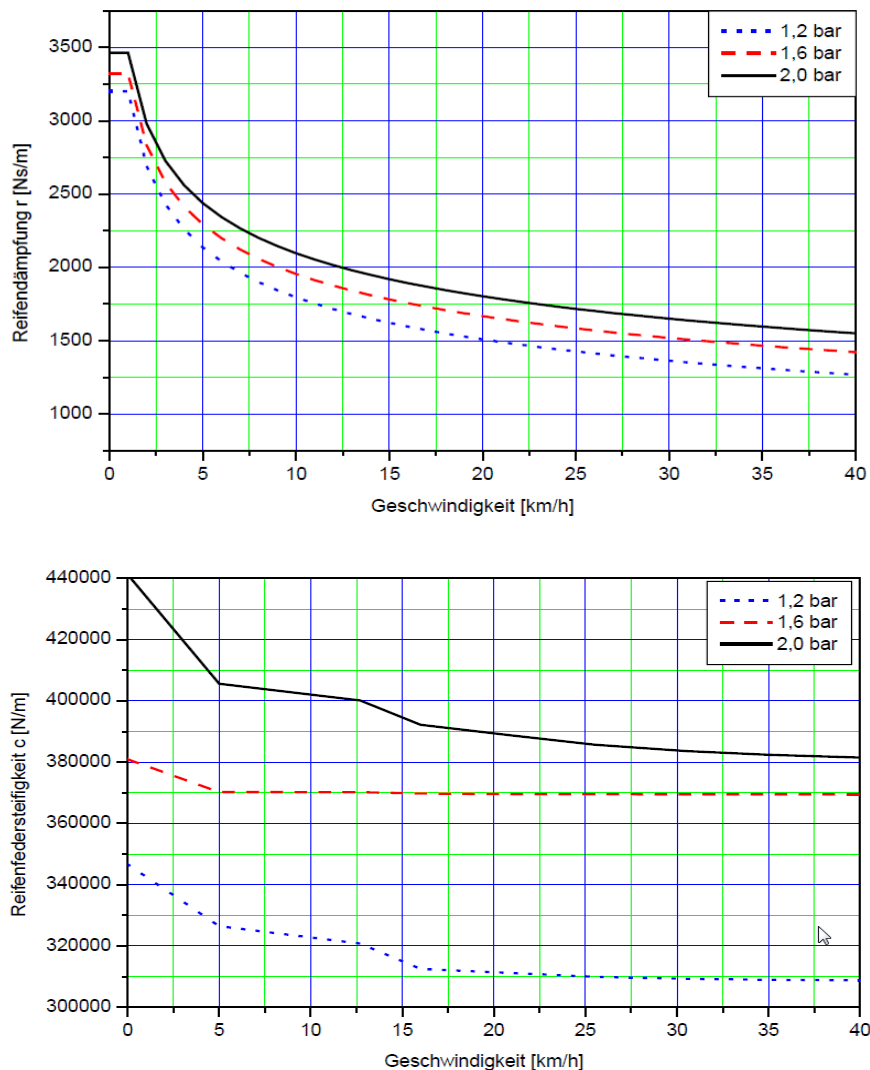


Figure 2-22 Influence of the travel speed on tire suspension characteristics a) tire damping rate b) tire stiffness coefficient (Von Holst, 2000).

As whole, in the lacking of a primary suspension, the insufficient suspension property of tires creates these consequences for conventional tractors (Von Holst, 2000):

- Low handling, which causes low driving safety and low travel speed.

- Poor ride comfort, which decreases driver efficiency and can harm his healthy.
- Pavement damage, which is particularly problematical for the public asphalt roadways used for the transportation.

As mentioned, the inflation pressure of a tire has significant influence on its characteristics. Based on this fact, some research works have been conducted with the theme of “Central Tire Inflation Systems” (CTIS). In these investigations, it was intended to improve dynamic behavior and traction power of the tractors via an optimal control on the tires inflation pressure. These investigations were confirmed that a significant improvement in ride comfort of tractors could be achieved as the inflation pressure was optimally controlled (Ulrich, 1983).

In addition, in the research work of (Kaczmarek, 1984) it was shown that the handling capability of a vehicle could be improved also by this system. This improvement could be created by modifying the natural frequency of the vehicle via an optimal control of the tires stiffness. However, in spite of these achievements by the CTIS systems, the tires are not still able to provide a good dynamic behavior, and this implies that the suspension systems are totally needed for the agricultural tractors. The different suspension systems that are employed in the agricultural tractors will be explained in the following sections.

2.5.2 Seat Suspension

Problem of the vibration transmitted to the operators of agricultural tractors has been widely discussed over the last 40 years (Marsili, Ragni, Santoro, & Servadio, 2002). Operators of conventional agricultural tractors are exposed to a high level of vibrations during typical farm operations (Scarlett, Price, & Stayner, 2007). On the other hand, they work normally for a long time on the tractors particularly during intensive working seasons. The high level of vibrations experienced by an operator is harmful for his health and creates an early fatigue. This consequence decreases the efficiency of operators.

In order to overcome against this problem and decrease the vibration transmitted to the operators, employment of suspension systems has been considered. The first system used for this purpose is the suspension for the seat of the operator. This system is placed directly between the driver seat and tractor body, and it affects directly driver comfort and reduces the vibration experienced by him. Seat suspensions are uncomplicated, inexpensive and have a robust construction. For these reasons, they are employed now for nearly the

whole modern agricultural tractors. A suspension seat is made of typically a foam cushion suspended on a parallel spring and damper set. Type of suspension systems may be mechanical, pneumatic, hydraulic, hydro-pneumatic, or a combination of these systems.

In order to improve the performance of seat suspensions, active suspension technology have been employed. For example in the investigation of (Hauck, 2001), a semi-active suspension with a MR damper as the actuator was employed in the seat suspension of the agricultural tractors. This system was evaluated by both computer simulation and experimental testing. In the experimental part, the tests were performed by use of a suspension test rig. According to the simulation tests, a reduction until 22 % was achieved in seat RMS acceleration in comparison with passive damping. However, in the experimental tests, this improvement was fallen into 9 % improvement.

Considering the low total mass of a seat and driver, using fully active systems for seat suspensions causes no high extra consumption of energy. Therefore, these systems have been also considered as practical systems in order to improve the performance of the seat suspensions. In this theme, (Stein & Ballo, 1991) conducted a research project with the purpose of measuring the required energy for an active seat suspension. For this purpose, they considered a low bandwidth fully active seat suspension, which used a hydraulic force actuator combining with a passive spring-damper system. As a result, this system could provide full vibration isolation until 3 Hz by consuming the maximum power of 2.2 kW.

The application of active suspension systems for the seat suspension has been considered by most of the well known agricultural tractor companies with the aim of offering a high level of ride comfort for the operators of tractors. Figure 2-23 shows a modern seat from John Deere with an active seat technology. This seat technology uses a full active hydro-pneumatic suspension. This system receiving 200 Hz sensory inputs is able to reduce the excessive vertical movement of the seat. This provides more comfortable ride, and consequently, the operator can travel faster in hard field conditions.



Figure 2-23 A “John Deere” modern seat using “active seat” technology (Jonh.Deere, 2005).

“Air-ride seat” from New Holland is another active seat system, constructed based on a pneumatic suspension. This system uses an adaptive control system that adjusts the parameters of the suspension relative to the driver’s weight. Another example of the modern seats is the semi-active system produced by the tractors manufacturer of Valtra. This system is equipped with a pneumatic spring and a MR damper, which works as the actuator of the system. The controller of this system is able to sense the vertical acceleration of the tractor body with sample rate up to 500 Hz. Based on the control strategy of the system, controller changes the damping ratio of the MR shock absorber in order to provide optimal damping ratio for the suspension. In addition, the controller of this system is able to recognize the ground conditions based on the sensory information and involves them in the control strategy.

Besides the seat suspension, which has major role in providing ride comfort for the driver, some other characteristics influence on the ride comfort. For example, size, design, and materials of a seat have important role in sitting perception. In addition, dimension adjustment is influential on the sitting perception, as they allow a seat to accommodate people with different sizes in a fixed workspace. For example, John Deere “active seat” (Fig. 2-23) is a fully adjustable seat providing nine adjustment points. On the other hand, a proper seat cushion can affect the sitting perception by damping the high frequency vibrations, and also a seat climatic system can absorb the seat moisture that is particularly effective while the driver stay on the seat for a long time.

Seat suspensions have some characteristics that limit their performance. For example, maximum stroke of a typical seat suspension must be restricted so as to prevent

the suspension from excessive displacement between the driver and the vehicle control equipments (Boileau & Rakheja, 1990). In order to restrict the travel of the seat suspension, rubber bump-stops are often used. However, contact with the bump stops can lead to a higher level of vibrations on the seat over than the vehicle floor (Gunston, 2000). In order to avoid this experience, a stiffer spring should be used. However, this increases the resonant frequency of the seat closely to the resonant frequency of the vehicle. This leads to a higher transmission of the vibrations to the seat, and it is the main restriction of the seat suspensions.

On the other hand, whereas seat suspension is able to reduce effectively the vertical vibration of the tractor body, it is very difficult to achieve effective vibration isolation by seat suspension in horizontal and rotational directions. These vibrations are particularly important, because they have high amplitude on the body of agricultural tractors and have a significant influence on ride quality (Suggs & Huang, 1969). In order to remove these weak points and achieve better performance, besides the seat suspension, the other types of suspension systems such as cabin and chassis suspension should be used.

2.5.3 Cabin Suspension

In modern agricultural tractors, a cabin is used in order to isolate the driver from the outside, and it protects the driver from the annoying environmental conditions, dust, and noise. Using a suspension system for the cabin, driver place could be isolated from the tractor vibrations as well.

A cabin suspension can offer more benefits than a seat suspension and provide better ride comfort for the driver. These advantages can be stated as follow:

- It provides vibration isolation for both the driver and the control equipments beside him. In this way, the problem of the relative movement between the driver and the control equipments is eliminated (Hansson P. , 1995).
- Cabin suspension decreases the structurally transmitted noise to the drivers.
- Cabin suspension is able to isolate the driver from the rotational vibrations of the tractor body in addition to the vertical vibrations.
- Since the mass of a cabin is greater than a seat, the natural frequency of cabins is lower than the one of seat suspensions. This leads to provide better vibration isolation (Von Holst, 2000).

- Because of the greater mass of a cabin, the variation in the drivers' weight has less influence on the performance of the cabin suspension.

The manufactured cabin suspensions of the agricultural tractors can be categorized in two groups of semi suspended and fully suspended. In the first group, the rear side of the cabin is connected to the chassis by means of two suspension units in its corners. In spite of this, the front side is connected to the tractor chassis without suspension and only via a joint-type link. This type is often used for the tractors with front axle suspension. In this system, body vibrations appear on the cabin as pitch rotational movement, and response of this system to the roll movement of the tractor body is very limited.

An example of this system is the cabin suspension of Deutz Agrotron tractors. The suspension units used for this system are pneumatic-type (Fig. 2-24). This suspension is controlled by an adaptive control system that adjusts the stiffness of suspension relatively to the load of the cabin. Benefiting this control system, the used suspension stroke is just 40 mm.



Figure 2-24 “Deutz” semi suspended cabin using pneumatic suspension units (Deutz, 2006).

Another type of the cabin suspensions is the fully suspended cabin, which is constructed by four suspension units in the corners of the cabin. With this construction, this system is capable to damp all six degrees of vibrations of the dimension and rotational directions (Goehlich, 1984). This type of cabin suspensions have already used by tractor companies of “Class” and “Renault” for their productions.

The cabin suspension of the agricultural tractors has been already the theme of some research works such as (Kauss & Weigelt, 1980) and (Hilton & Moran, 1975). All these investigations confirmed the capability of the cabin suspensions in providing good ride comfort, especially as it was compared with seat suspensions. However, the cabin

suspension still suffers from the same problem of high natural frequencies due to the limited travel space. These resonant frequencies are close to those of the tractor body and causes high vibration transmitting.

In order to improve the performance of the cabin suspensions, the idea of active suspensions can be considered. In this theme, there are some research projects, such as the work of (Hansson P. , 1995). In this investigation, a combination of the adaptive and fully active suspension was used for a cabin suspension intended primarily for the agricultural tractors. In this system, based on a linear optimal control technique, the feedback gains of the controller was varied iteratively so that the controller always strived to make the optimum use of the available travel space. The efficiency of this system was evaluated in the terms of the vibration isolation and power consumption. Based on the positive results and low power consumption, the active cabin suspensions are recommended for the practicable application. In addition to these investigations, the active cabin suspension has been already employed by tractor companies such as Fendt and Deutz for their productions.

Cabin suspensions have no considerable influence on the dynamic behavior and handling capability of the tractors, because the mass of the cabins (300-600 kg) is very low in comparison with the total mass of the tractors. In this condition, the cab suspension can create only a small reduction in the natural frequency of the tractors. However, in the investigation of (Von Holst, 2000), it was concluded that the handling capability of the rear axle in a conventional tractor can be affected significantly by the cab suspension, because in these tractors, the cabin places on the rear axle, and the handling effect of the cabin suspensions is focused on this axle.

As conclusion, a cabin suspension provides good ride comfort but have no significant influence on the handling of the tractors. In order to provide both good ride comfort and good handling, in addition to the secondary suspensions, the primary suspensions is needed. The secondary suspension is referred here to the cabin and seat suspensions, and the primary suspension is referred to the chassis suspensions, which will be described in the following sections.

2.5.4 Hitch Suspension

During transportation, tractors are often mounted with heavy implements. These heavy implements change largely the mass characteristics of the tractors, and influence

mainly the dynamic behavior of the tractors. On the other hand, tractors have typically no axle suspensions, particularly no one for the rear axle. Without the primary suspension, the tires are the only elastic elements that affect the handling of the tractors, whereas the tires have no required suspension properties. Under these conditions, the dynamic behavior of the tractor becomes worse under the influence of the attached implements, particularly the bounce and pitch movement of the tractor are increased. This situation causes a fall in the control ability of the tractor, which especially during high-speed transports leads to unsafe modes.

In order to reduce the effect of the mounted implements on the tractors and in order to control their vibration, a suspension system can be used in the connection between them and the tractors. Since the implements are normally mounted on a tractor via the three-point hitch, this suspension is applied to this mechanism and called “hitch suspension”. Figure 2-25 illustrates such a system that employs a hydro-pneumatic suspension in damping the pitch vibration of the implement. As shown, a hydraulic actuator is used instead of the upper link in this system. This actuator is connected to a hydraulic accumulator through a throttle valve and works as a hydro-pneumatic suspension.

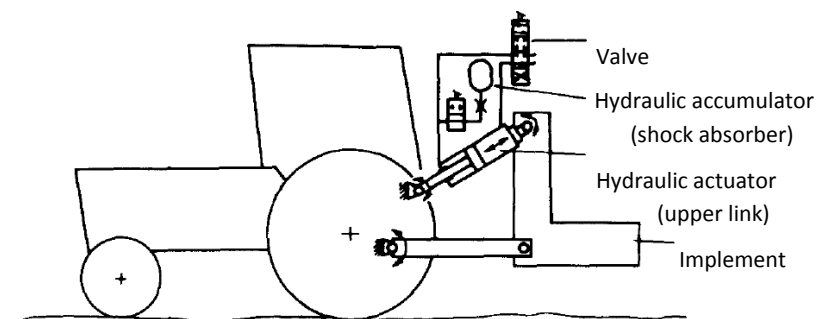


Figure 2-25 A hydro-pneumatic shock absorber system applied to the tractor three-point hitch (Goehlich, 1984).

In order to improve the performance of hitch suspensions, the active suspensions can be used. All types of active suspension such as fully active, semi-active, and adaptive control could be applied to a hitch suspension. Since the primary hitch suspensions are usually hydro-pneumatic, the actuation system of the active systems can be performed typically by using an adjustable throttle between the cylinder and accumulator for semi-active system and energizing oil to the cylinder for fully active system. According to the natural frequency

of a hitch suspension, the control system of these active suspensions works with the bandwidth of less than 3 Hz (Hoppe-01, 2004).

There are some research works in this area like the research work of (Hansen & Andersen, 2003). In this investigation, in order to damp the pitch vibration of the tractor body, a fully active hitch suspension was used for controlling the vibrations of the mounted implements. Figure 2-26 shows the components of this system. A plough used as the implement of the system was hung from the rear end of the tractor via a three-point hitch linkage. This linkage was typically actuated by two so-called hitch hydraulic cylinders, which were used as the actuator of the active hitch suspension. It was intended that for damping the pitch movement of the tractor body, the actuators were controlled to move the implement appropriately to the vibration of the tractor body in order to neutralize it. For controlling the cylinders forces, the directional solenoid-valves were used to control the connection of the cylinders to the hydraulic pump and the tank.

Hansen considered two different control strategies for the system. The first one was based on measuring the cylinders oil pressure, and the second one was based on measuring the pitch angle of the tractor body. The first control strategy strived to maintain the derivative of the pressure signal substantially constant at the value of zero, and the second control strategy strives to keep the derivative of the pitch angle at the value of zero. After evaluation of the system, it was concluded that both the strategies created significant improvement in performance of the hitch suspension in comparison with the non-controlled system.

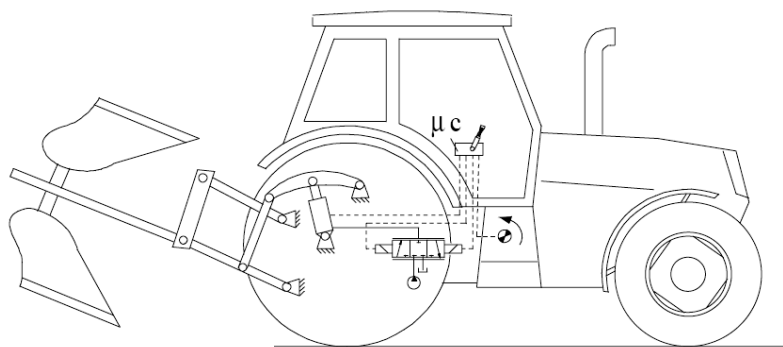


Figure 2-26 Full active vibration control system used for the tractor three-point hitch suspension (Hansson P. , 1995).

The influence of the hitch suspension on the dynamic behavior of tractors is dependent on the quantity of the mass and moment of inertia of the mounted implement.

For the heavy implements, experimental and analytical studies have shown that the rear hitch suspension modifies the vibration behavior of the tractors significantly, and in this way first, they have a great positive influence on the steering and drive safety of the tractors, and secondly, they improve the ride comfort of tractors (Ulrich, 1983) & (Von Holst, 2000).

For adding a hitch suspension system to a tractor, the main structure of the typical three-point hitch can be employed, and in this manner, no constructional change is necessary, and this suspension can be added to the tractors relative simply with low expense, whereas they can create large improvement in the vibration behavior of the tractor. Presently, most of the modern tractors are equipped with this kind of suspension system.

2.5.5 Front Axle Suspension

During the late 1980's, four Wheel Drive (4WD) tractors became popular due to the better traction performance. Using these tractors, the front wheels acquired a new role in the traction capability of the tractors and also in the steering ability of them. In this condition, the typical problem of the pitch movement of the tractors was more noticeable, because it created a load variation on the front tires and caused the problem of bouncing, particularly during the pulling heavy loads by tractors. This produced a traction variation effect, called "power hop," that was not only uncomfortable for the operator, but also caused a major loss in the traction efficiency of the tractors.

In order to overcome against this problem, the front axle suspension was used for tractors. This suspension provided a stable contact between the front tires and ground that leads to a significant improvement in the traction and steering capability of tractors. Because of this advantage, front axle suspension has become a common option in 4WD tractors now. In addition, the front wheels are the navigating wheels. They take the major steering and brake loads of a tractor. Front suspension by keeping front tires in firm contact with the ground, allows better steering control and brake efficiency. This promotes the handling capability and increases consequently the travel speed of a tractor. The improvements created by using front suspensions have been confirmed also in some references such as (Rhenius, 1983), (Weigelt, 1987) and (Rill, Slag, & Wilks, 1992).

However, influence of the front suspension on ride comfort of tractors is not notable as much as the influence of this system on the handling of tractors. In the research work of

(Weigelt, 1987) a front suspension was applied to a test-tractor with standard construction (i.e. typical tractor construction with rear big wheels (Fig 2-27)). The evaluation of the dynamic behavior of this tractor showed that by using front suspension, the handling of the tractor was improved significantly. But, the influence of the front suspension on the vertical acceleration of the seat was not considerable. This occurred, because in standard constructive tractors, seat position is on top of the rear axle, and the front suspension had no effect on the bouncing movement of the rear part of tractors body and only reduced the pitching movement of the tractors.



Figure 2-27 Typical standard and system constructive tractors.

As mentioned, in the standard constructed tractors, using the front suspensions does not reduce the vertical acceleration of the driver's seats. In the investigation of (Pickel P. , 1993), the influence of the seat position on the vertical acceleration was investigated. Figure 2-28 indicates the result of this investigation that is presented as the RMS value of the vertical acceleration of the seat. This value is presented in respect to the position of the seat on the tractor body. The examination was performed for the standard and system types of tractors in the two modes of the suspended front axle and rigid front axle. System tractors are the tractors that have the same rear and front tire size, and the seat is located in a position between two axles and standard tractors are the typical tractors with rear big wheels (Fig. 2-27).

As shown in this graph, the front axle suspension has a minor effect on the vertical acceleration of the seat, which is located nearly over the rear axle. On the other hand, position of the seat in a system tractor is between two axles, and the front axle suspension can reduce the vertical acceleration of the seat considerably. Therefore, when the front suspensions are employed with the aim of improving the ride comfort, the system tractors have priority over standard tractors. However, in order to convert a standard tractor to a

system tractor, major constructional changes are necessary. Theme of a proper suspension system for standard tractors will be discussed in the next section.

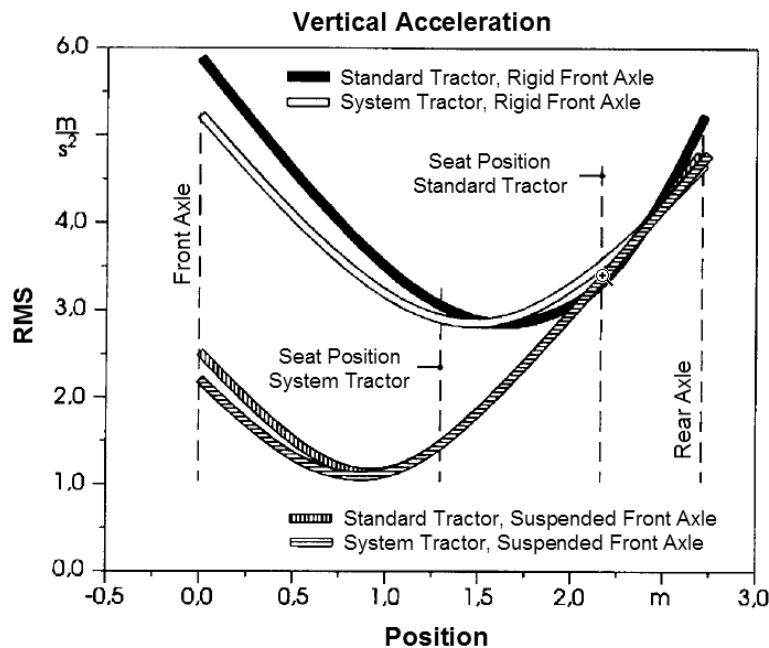


Figure 2-28 Influence of seat position on seat vertical acceleration in “Standard” and “System” tractors with rigid and suspended front axle (Pickel P. , 1993).

Despite the results about the minor influence of the front suspension on the ride comfort, driving with front suspension is in practice more comfortable. This perception is achieved because of the reduction in the horizontal accelerations, which has an important influence on ride quality. The reduction of the horizontal accelerations is created, due to the capability of the front suspension in effective damping of the pitch motion of tractor (Pickel, Kaplick, & Göhlich, 1990). Compatible with this explanation, the results of the investigation of (Lehtonen & Juhala, 2006) showed that by using front suspension for a tractor, both drivers’ comfort and driving performance of the tractor were improved.

In this work, a MBS model of an independent front axle suspension was built and added to the validated MBS model of an agricultural tractor. The simulations were performed on the different test-tracks, and the results were analyzed according to the related standards. Finally, it was concluded that the ride comfort for driver was improved significantly in the tractor equipped with the front axle suspension, even though the driver's seat was located above the non-suspended rear axle of the tractor. Likewise, in the investigation of (Rill, Slag, & Wilks, 1992), it was concluded that with a tuned front axle suspension, both ride comfort and ride safety could be improved significantly.

Adding a front axle suspension to a standard tractor does not need constructional change, because the front axle of these tractors is connected to the block chassis via a “hanging” construction, and it can be exchanged simply with a suspended axle. There are different linkage-types for the front axle of agricultural tractors. The list of these linkages with relevant schematic demonstrations is presented in the reference of (Göhlich, Hauck, & von Holst, 1999).

The primary suspension systems used for front axle was mechanical type, but in most of the new modern tractors, the hydro-pneumatic suspensions are preferred. These suspensions provide some advantages over the mechanical type. The hydro-pneumatic suspensions can be equipped simply with leveling control and suspension blockage systems. In addition, having a compact and flexible design, this suspension is adaptable with almost all kinds of front axle mechanisms. Figure 2-29 shows a hydro-pneumatic suspension system used for the front axle of 8020 series of John Deere tractors. This system is outfitted with auto leveling control and suspension blockage systems.



Figure 2-29 A hydro-pneumatic front axle suspension used for 8020 series of John Deere tractors (Jonh.Deere, 2005).

As stated, front suspensions improve the handling capability of the tractors and have a positive effect on their ride comfort. However, in order to achieve to a more effective suspension providing good handling beside the good ride comfort, the rear axle suspension can be used for the tractors in addition to the front axle suspension. In the following section, the theme of fully suspension tractor will be discussed.

2.5.6 Full Suspension

Higher travel speed is taken into consideration for the modern tractor design, because road vehicles such as trucks do not fulfill all the necessities of the agricultural transport-purposes. This led to try for development of high tractor speeds, which are able to cover the transportation needs of agricultural applications (Goehlich, 1984). As mentioned, employment of the front suspensions in tractors provided a major benefit regarding to the high travel speed. However, front axle suspensions can be sufficient just to reach to a limited maximum speed. In order to achieve a higher speed, the unique approach can be found in employment of the full suspension in tractors. A full suspension tractor is a tractor equipped with both rear and front axle suspensions. These tractors can provide improvement on both driving behavior and ride comfort, promising the possibility for the rise in the driving speed.

Tractors with only front suspensions cannot present a perfect dynamic characteristic. As mentioned, the influence of the front suspensions on ride comfort of the tractors is not significant, especially on the vertical vibration of the seat. In addition, this influence depends on the position of the seat between two axles. About the handling capacity of tractors, front suspensions have a good efficiency. However, disadvantageously, the front axle suspension affects negatively the vibration behavior of the unsuspended rear axle, which keeps more than half of the load of the tractor, because by using front axle, rotation axle of the pitch body oscillation shifts to the rear axle. This increases the bounce of the rear wheels and decreases consequently the tires contact to the road surface.

On the other hand, the front suspensions have significant effects only on the pitch and longitudinal vibration of the tractors, whereas the rear suspension influences the vibrations in most of the directions, particularly in the important vertical direction (Hansson P. , 1996). After all, using the rear axle suspension besides the front suspensions can end these problems by creating an essential contribution in vibration isolation at both the rear and front axles. In this way, a full suspension system provides both safe driving and good ride comfort for the tractors. The previous research works also have already illustrated the superior characteristics of the full suspension tractors (Claar, Sheth, Marley, & Buchele, 1980).

Despite of the advantages of the full suspension tractors, adding the rear suspensions to the conventional tractors is not as simple as the front suspensions. This is originated from the typical structure of the conventional or standard tractors, which are about 80 % of the

whole agricultural tractors (Kaplick C. , 1995). These tractors have a similar construction and called block construction (Fig.2-30). These tractors have a block construction, instead of the chassis construction. This construction is formed by connecting the three blocks of engine, transmission, and rear axle unit. Since primary types of these tractors have just rear drive wheels, in order to achieve optimal traction, at least 60% of their weight stands on the rear axle, and the rear wheels are selected bigger and heavier than the front wheels.

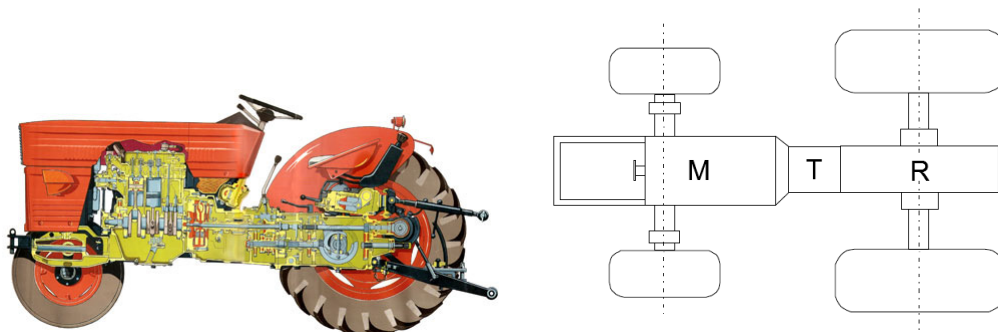


Figure 2-30 Block construction of “Standard” tractors (Müller, 2001).

In these tractors, front axle is linked to the block via a hanging-type junction and driver seat is positioned over the rear axle (Fig. 2-30). Adding front axle suspension to this structure is simply possible and needs no major changes. In the case of the rear axle suspension, the issue is not simple. In a standard tractor, axle of the rear wheels is fixed directly to the block of the tractor, and in this way, it is related directly to the transmission. With this structure, in order to add rear axle suspensions to standard tractors, basic changes in the construction of these tractors are necessary. The block structure of these tractors is not just for the rear suspension problematic. Each modification on the main components of these tractors, such as engine and transmission is not simply possible. Therefore, tractor manufacturers have recently tried to change the block construction of the tractors in order to provide more flexibility in their systems.

First attempt to modify the block construction of the standard tractors was to use a framework in the front part of them. In these tractors, the engine and front axle are mounted on this frame, but the transmission and rear axle units have still their block construction (Fig. 2-31). The engine is mounted on the frame. The connection between it and the transmission block is made by using a universal shaft. The advantage of the tractors with the semi-frame construction is their flexibility in employing the different type of front axle mechanisms and engine models.

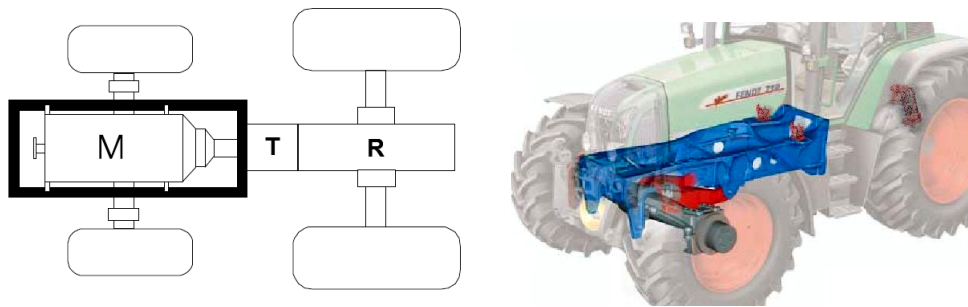


Figure 2-31 Half frame construction of a “Standard” tractor (Müller, 2001).

An example of the manufactured tractors with the half frame construction is John Deere 6030 series, which is called wrongly as a full frame tractor by its company. This manufacture is mentioned some special benefits for this half frame tractor as follow (Jonh.Deere, 2005):

- To optimize weight distribution for traction, steering, and implement handling.
- All components have a dedicated function, and they can be designed without compromise.
- It allows a compact modular construction.
- Modular design enables the option flexibility of drive train units and components.
- Low weight, high payload tractor handles larger and heavier implements with ease.
- Isolated engine mounting and transmission mounting reduces noise and vibrations transmitted to the cab.
- Integrated frame mounting points carry higher payloads without stressing the engine and drive train.

However, after all these advantages, since the construction of the rear axle unit is still block type, the complexity of adding the rear axle suspension to these tractors is still remained.

In the way of modifying the block-type construction of the standard tractors, finally, the tractors with full frame-type construction were presented. These tractors, similar to automobiles have a chassis that all the components of a tractor such as motor, transmission, cabin, and axles are installed on it. All benefits mentioned for the half frame tractors are presented more advantageously by these tractors. These tractors are four wheels drive with the usually same size of the rear and front wheels. Weight of the tractor is distributed on the wheels almost equally, causing optimal traction. Position of the driver seat and cabin is shifted from the rear part of the tractors to the mid-point of them between two axles. This

leads to provide better ride comfort, even if the tractor is equipped just with front axle suspension.

As an individual characteristic of the full frame tractors, the rear axle is separated from the chassis, and it is connected to the transmission via a universal shaft. With this construction, these tractors can be equipped simply with the rear axle suspensions. Therefore, along with presenting the full frame tractors, the idea of the full suspension tractors gets more practicable. On the other hand, some primary weaknesses of the full suspension tractors has solved by employing of the hydro-pneumatic suspension systems, giving the possibility of the self-leveling control and suspension blockage.

Nevertheless, most of the prepared full frame tractors have been already used just as prototype for the research purposes, and only some rare full suspension models of tractors have been already presented on the market. The best known of these tractors are the “Fastrac” tractors from JCB Company. Figure 2-32 shows a typical model of these tractors that are equipped with both rear and front axle suspensions. The rear suspension of these tractors is hydro-pneumatic suspension regulated by a self-leveling control system. These tractors provide great ride comfort and handling so that a high travel speed of between 60 to 80 km/h can be achieved by them.

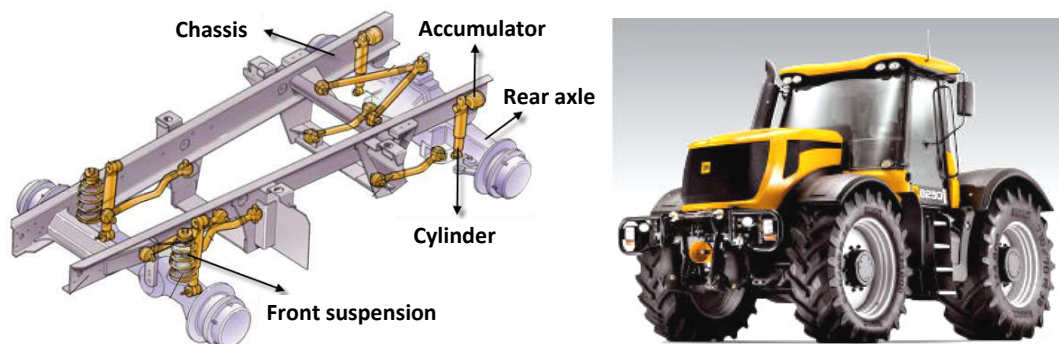


Figure 2-32 Full frame construction of fully suspension “JCB-FASTRAC” tractor (FASTRAC, 2007).

In 7000 series of these full suspension tractors, both of the axles are equipped with the hydro-pneumatic suspension regulated by a self-leveling control system. The form of 7000 series of these tractors has been changed unpredictably near the conventional tractors, having big rear wheels (Fig. 2-33). This change has been probably done with the aim of satisfying customers who believe wrongly that the conventional tractors with the rear big and heavy wheels present better traction and power.

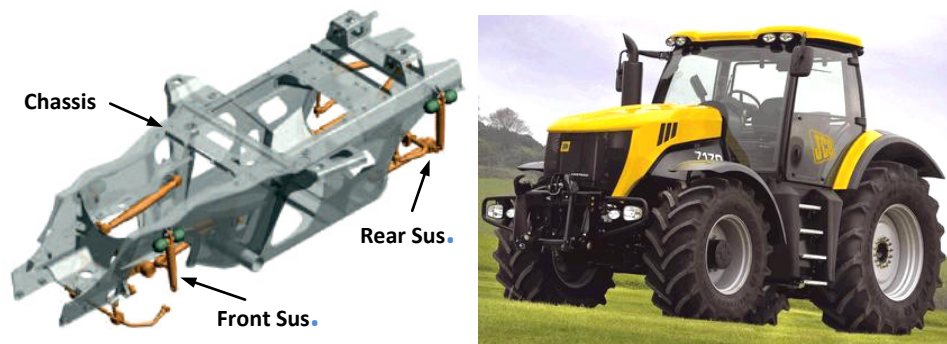


Figure 2-33 Full frame construction of fully suspension “JCB- Fastrac, 7000 series” tractor (FASTRAC, 2007).

In Fastrac tractors, coupling devices are mounted on the rear axle and not on the body of the tractor. This means that attached implements are not suspended. The weak point of this technique is that the natural frequency of the rear axle can be changed mainly by the attached implements, because by mounting these devices, the value of the unsprung mass is changed mainly. In addition, the whole weight of the implements is carrying by rear tires. (Pickel P. , 1993) was also mentioned this problem for JCB-Fastrac; the relative small rear tires of these tractors are not able to carry heavy implements. On the other hand, the typical big agricultural tires are not also recommended for them because of their high travel speed. However, JCB Company in “7000” series of Fastrac has overcome this problem. This tractor using relative big rear tires is able to drive until 70 km/h, and at the same time, it can carry loads until 9100kg on the rear linkage system (FASTRAC, 2007).

The method of the mounting the coupling devices on the rear axle is also confirmed in the research work of (Hansson P. , 1996). In this investigation, it was concluded that attaching the heavy implements to the suspended body of a full suspension tractor causes a major change in the total ratio of the sprung mass to the unsprung mass of the tractor. He considered also that the suspension would be controlled by a load-leveling device. But, this solution was found to place a very high demand on a full suspension tractor. Therefore, mounting the coupling devices on the rear axle was considered finally as the practicable solution, because it does not affect directly the suspension system of the tractor.

With the purpose of improving the suspension efficiency of the full suspension tractors, some research works has been already conducted. For example in the investigation of (Hansson P. , 1996), a computer model of a full axle suspended tractor was built as a virtual prototype of these tractors. Using this model, the characteristics of these tractors with differently adjusted passive suspensions and slow load leveling devices were examined.

One conclusion of the results was that the most important dynamic behaviors of full suspension tractors are determined by the characteristics of rear axle suspension.

In continue of this investigation, the various types of controlled damping system for the rear axle of the full suspension tractors were considered, and the potential of these control systems in providing an efficient control on the tractor body vibrations were investigated. Based on the simulations results, it was shown that the new systems, with the bandwidth of 5-10 Hz outperform the passive system with the fixed damping constants.

In addition to the semi-active suspension, a new type of the adaptive control was presented for the rear axle suspension. This control system was designed to tune the dampers in the way that, the available travel space of the suspension would be used always optimally, in spite of the inconsistent driving speed and ground roughness condition. The algorithm used for this system was a preview control strategy. In this strategy, the measured information of the ground roughness at the front wheel was used as basics for the adaptation of the rear suspension. The final evaluation results of the simulation tests showed that this system offered good characteristics in vibration control of the tractor body.

In this thesis, improving the dynamic behavior of the tractors is considered also as the objective of the research. For this purpose, the idea of using active suspensions for tractors was chosen, because these systems provide high efficiency for the suspension systems. Since the full suspension tractors present the most highly developed suspension system for the tractors, the active suspension was decided to employ in these tractors. For this purpose a test tractor with the name of TUB-Trac, which was a full suspension tractor, was selected as the prototype for this investigation. This tractor will be described in the following section.

2.5.7 Full Suspension TUB-Trac

Full suspension TUB-Trac is a prototype tractor-model at the TU Berlin - Department Machinery System Design. This prototype model is derived from MB-Trac 1600 tractor, which is a full frame agricultural tractor (Fig. 3-34). MB-Trac tractor series are developed by Mercedes-Benz Company based on their Unimog platform (Fig. 3-35). This tractor is crossed the Unimog technology of all-wheel drive and a power transmission to four large equal-sized wheels. In contrast to conventional tractors, the cabin of this tractor is situated between the axles. MB-Trac tractor has a front axle suspension, but the rear axle is not suspended.

However having full frame construction, it can be converted to a full suspension tractor without constructional change.

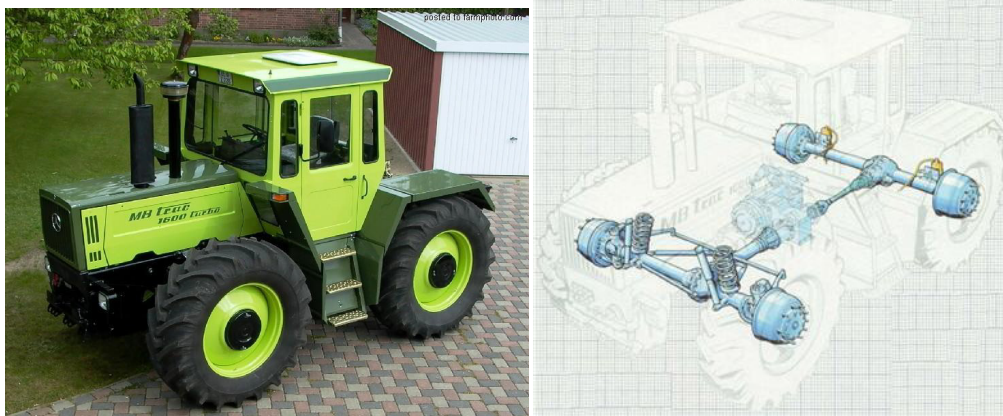


Figure 2-34 MB-Trac 1600 tractor and relevant full frame construction equipped with front axle suspension.

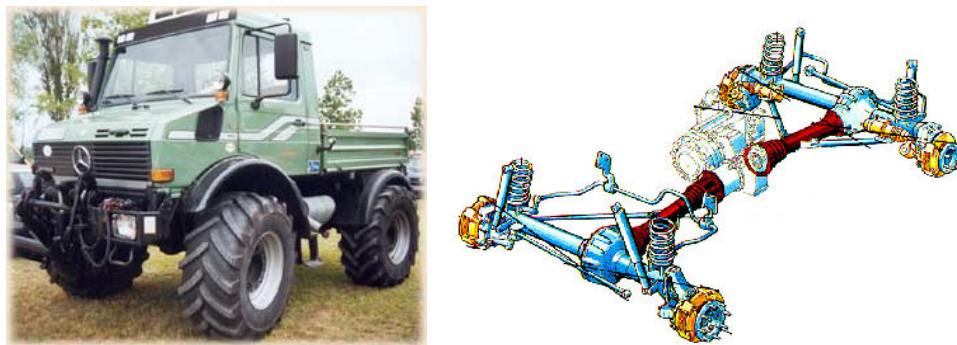


Figure 2-35 UNIMOG and relevant full suspension construction.

This potential was used during some research projects at the TU Berlin - Department Machinery System Design, and the tractor was equipped with a rear axle suspension. Because of the features of hydro-pneumatic suspensions in the agricultural tractors (refer to the section 2.4), this system was chosen as the proper suspension for the rear axle of MB-Trac 1600 in order to convert it to a full suspension tractor. In addition to this issue, the driving characteristics of this full suspension tractor were examined during these research works, with the purpose of recognizing the potentials of the full suspensions tractors.

As the first step, a virtual prototype of the full suspension TUB-Trac was created by (Lehmann, 2004). He built a model of the hydro-pneumatic rear suspension by MATLAB-Simulink software. Then, he added this model to the MBS simulation model of the MB-Trac,

which was made by “DADS” MBS software. By joining these two models together, he created the overall model of the full suspension TUB-Trac. Finally, he performed some primary simulation tests by using this model. In these tests, he considered four test modes: the tractor without ballast, front ballast, rear ballast, and full ballast.

Figure 2-36 shows one of the results derived from these tests showing the frequency response of the tractor in the two modes of the rear and front ballast. This graph indicates that how the ballast of the tractor body influences on the natural frequency of the pitch movement. At the end of this research work, it was recommended to employ the active suspension systems, particularly the auto-leveling system. This system was considered for the rear axle suspension of the tractor in order to improve its efficiency.

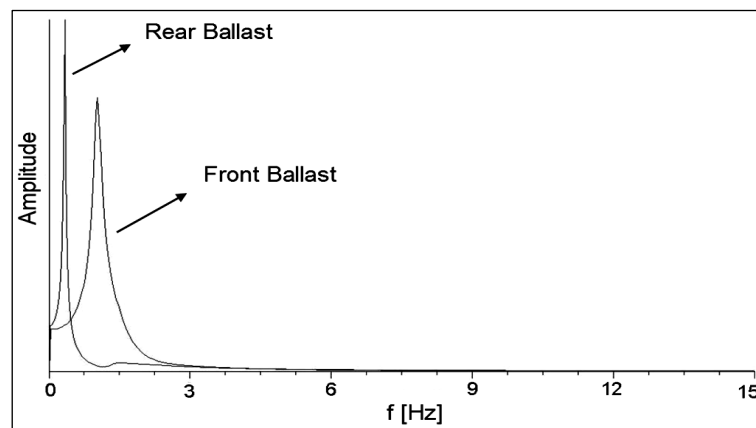


Figure 2-36 Amplitude spectrum of pitch movement of the tractor body for $v=30$ km (Lehmann, 2004).

After this model study, another research work was conducted by (Thiebes, Müller, & Gericke, 2005) with the objective of preparing the MB-Trac for adding a hydro-pneumatic suspension to its rear axle, including design and constructing a rear framework for it. Figure 2-37 shows the designed rear frame that was assembled to the main frame of the tractor. Axle suspension was connected to this frame via a four bar linkage. This provides a degree of freedom for the vertical movement of the axle. After this study, in the research work of (Hoppe, 2006) the hydro-pneumatic rear suspension was designed and an actual prototype was built, and then was installed on the MB-Trac tractor and in this way the full suspension TUB-Trac was created. The details of this tractor and its rear suspension system will be given in the next chapters.

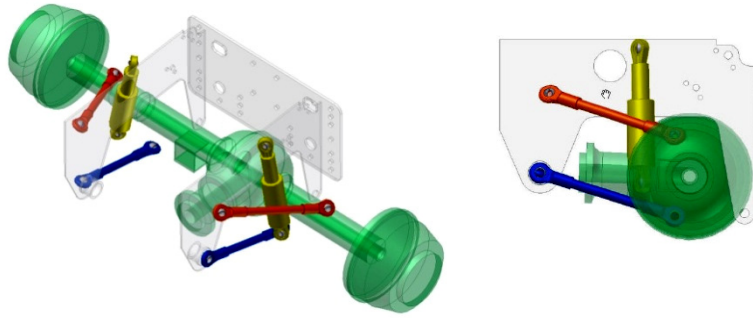


Figure 2-37 Constriction of the rear frame and rear axle suspension designed for the “TU-Trac” tractor (Thiebes, Müller, & Gericke, 2005).

After creating this actual prototype model, it was used in the investigation by (Thiebes P. , 2006) in order to validate the corresponding virtual prototype model, which was built in the previous research works. For this purpose, he conducted some similar tests by using both the real prototype and the virtual prototype of TUB-Trac. He executed these tests with the different parameters of the travel speed, tire pressure, ballast, and the static gas pressures of the accumulator. He considered these factors in order to investigate the influence of them on the dynamic behavior of the tractor. After that, he compared the results of the simulations with the measured data of the experiments to make a statement on the quality of the model, and in order to derive the information about the validity of the model. In this way, he decided when the modification of the model should be stopped and the validated model was achieved.

Using the validated model, (Hoppe, 2006) examined the driving properties of fully suspended tractors. He focused on the capability of the full suspension tractors in modifying the ride comfort and driving stability of the tractor. For this purpose, he considered the wheel-loading factor (RLF) and the driver seat RMS acceleration as the evaluation criteria. In addition, he used an optimal algorithm to find the optimal suspension parameters that provides the best compromise between the handling and ride comfort of the full suspension tractor. At the end, he recommended to employ active suspension systems in the axles in order to achieve better suspension performance. Figure 2-38 shows a result of this project, indicating the priority of the full suspension over the front and seat suspensions.

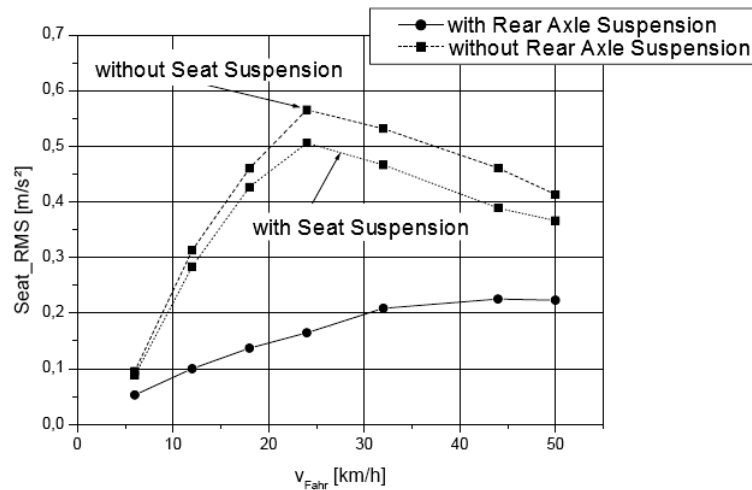


Figure 2-38 Comparison of the vertical acceleration present on the seat of TUB-Trac with three different suspension modes: seat, Front Suspension, and full suspension (Hoppe, 2006).

The main objective of the mentioned research works at the TU Berlin - Department Machinery System Design was the improvement of the driving characteristics of the agricultural tractors by using efficient suspension systems. Considering this objective, this Ph.D. thesis was conducted with the theme of active suspension for the full suspension tractors, as it was also recommended in the previous investigations. This project was performed on the TUB-Trac, by applying an active suspension to the rear axle suspension of this tractor, which was a hydro-pneumatic type.

2.5.8 Summary

In the previous sections, the characteristics of the different suspension systems of agricultural tractors were described. In this part, these characteristics including positive and negative features are summarized.

In order to determine the priority of the different suspension systems for agricultural tractors, some research works has already been conducted. These investigations achieved finally some useful results. However, they could not conclude directly about the priority of the suspension systems. The reason was that they did not examine all these suspension systems by similar tractors, but also they used different tractor models for each type of suspension system. Since the qualities of the suspension systems in these tractors independent of their type were not similar, it was not possible to achieve a clear conclusion about the priority of suspension systems.

One of these investigations is the work of (Scarlett, Price, & Stayner, 2007) that was conducted to quantify emission of the whole-body vibration (WBV) of agricultural tractors. For this purpose, exposure levels found upon a range of modern agricultural tractors with different suspension systems were estimated. The considered systems were seat suspension, seat plus cabin suspension, seat plus cabin plus front axle suspension, and seat plus fully suspension. The evaluation tests were operated in some determined conditions, and the test-tracks were the traversing ISO ride vibration types.

In addition, the conditions of performing selected agricultural operations and performing identical tasks during 'on-farm' were considered. Finally in this investigation, the whole RMS-results of the WBV for the different test conditions were presented. However, the clear conclusion about the priority of the suspension systems was not achieved. It was just founded that the emission-level of the WBV of tractors was very dependent upon the nature of field operations, and in opposition, the emission-level was largely independent of the capability of the vehicle suspension due to the dominance of the horizontal vibration. However, during on-road transport, all these trends were reversed.

Based on the study about the different suspension systems used for agricultural tractors, table 2-2 is derived, which shows a valuation of these systems. The judgment about the capability of the suspension systems is issued based on their positive influence on the ride comfort and handling of tractors. In addition, the complexity and the cost of adding the suspension system to standard tractors is considered as a negative factor.

Table 2-2 The capability of different suspension systems used for agricultural tractors.

Suspension	Influence on		Expenditure
	Ride Comfort	Handling	
Seat	<i>middle</i>	<i>slight</i>	<i>low</i>
Cabin	<i>high</i>	<i>low</i>	<i>middle</i>
Hitch	<i>low-middle</i>	<i>low-high</i>	<i>low</i>
Front axle	<i>low</i>	<i>high</i>	<i>middle</i>
Full axle	<i>high</i>	<i>high</i>	<i>high</i>

As explanation of the grading for the suspension systems in this table, an abstract about their capabilities and weaknesses are given again in this part. First systems are the seat suspension systems that are relatively inexpensive and have robust construction. These systems are the first choices in order to improve the ride comfort of tractors. Even if in

tractors equipped with other kinds of suspension systems, the seat suspension is not removed. On the other hand, cabin suspension has been used as the next option in order to provide better ride comfort. In addition to the driver, a cabin suspension isolates all equipment present in the cabin from the chassis vibrations, and so, it reduces structurally the transmitted noise to the driver and provides better ride comfort. However, these two suspensions have no considerable influence on handling capability of tractors.

In order to promote the handling capability of the tractors, the axle suspension systems are considered. In this way, front axle suspension is the first choice, because adding a front axle suspension to a standard tractor does not need constructional change, and it can be performed simply, whereas for adding rear axle suspensions to these tractors, a major constructional change is needed. However, the influence of the front axle suspension on ride comfort in standard tractors is not considerable. Combination of the cabin suspension with front axle suspension can be considered as the best choice for the standard tractors, as the cabin suspension provides good ride comfort and front axle suspension provides good handling for the standard tractors (Von Holst, 2000), (Hauck, 2001), (Hoppe- & Meyer, 2005) and (Profi, 2007).

Full frame construction presents different advantages in agricultural tractors. This caused that the production of these kinds of tractors is developing, particularly about large 4WD tractors. For these tractors, full suspension is surely the best choice, because, on the one hand, the conversion of these tractors to full suspension tractors can be performed without complexity. On the other hand, a full suspension tractor provides high level of ride comfort and handling capability leading to a high travel speed until 80 km/h, which is especially a big advantage for transport purposes. Other type of suspension used for tractors is the hitch suspension. This suspension can be added simply to the 3-point hitch system. The hitch suspension can provide a big benefit for the tractors by improving their handling as well as the ride comfort, particularly for the tractors working with heavy implements such as heavy plough.

In this chapter, the background of the study was presented. As mentioned, the purpose of this investigation is to employ active suspensions in the full suspension tractors in order to improve their suspension efficiency. The procedure of this investigation will be described next in the different chapters. As the first step, the model study will be presented in the following chapter.

Chapter 3

Modeling of the Semi-active Suspension

In the previous chapters, the background and literature review of the investigation were presented, and the proper active suspension and related control strategy for this investigation were determined. In addition, it was proposed that the new suspension system is examined by applying it to a test agricultural tractor. This examination was not performed only by a practicable experience, but also a computer simulation was planned in order to examine the new system. For this purpose, a computer model of all system components is needed. This chapter explains the details of this modeling.

The total model includes two main components. The first one is the model of the semi-active suspension including three sub-models: controller model, actuator model, and sensor model. This semi-active suspension is applied to the test-tractor. Therefore, the second model component is the model of this test-tractor. In figure 3-1, the structure is illustrated. As shown, the whole system works in a close loop. The dynamic behavior of the tractor is scanned by the sensors. After that, this information is sent to the controller. Based on the relevant control strategy, the controller sends the commands to the actuator and in this way, changes the parameters of the tractor suspension.

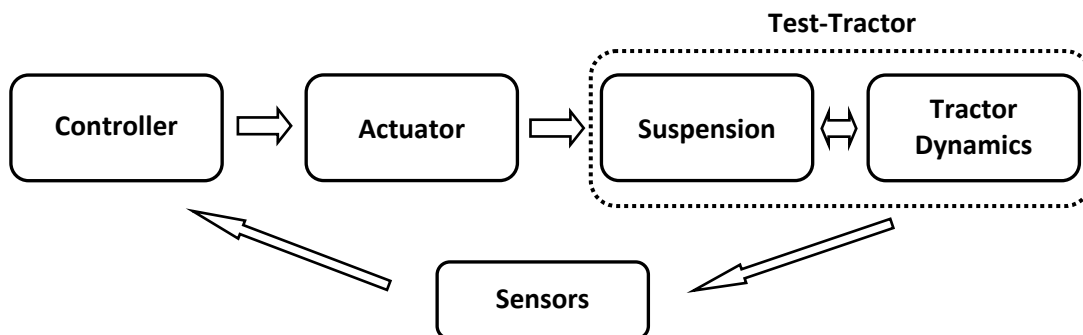


Figure 3-1 Control loop in a tractor with active suspension system.

For modeling of the components, a similar routine is used. Figure 3-2 illustrates the four steps of the modeling process. In the first step, the real system is known in details. Then

based on this knowledge, the physical model of the system is created, and after that by deriving the equation of this model, the mathematical model is produced. In the last step, the computer model is developed from the model equations by using MATLAB-Simulink program.

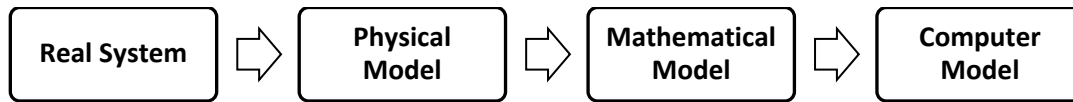


Figure 3-2 Modeling procedure.

The modeling part of the research project is performed in three steps. At the first step, the model of the tractor is built. Then, the model of the actuator system including the hydro-pneumatic rear suspension of the tractor is created. In the last step, the controller and sensors are modeled. In conclusion, after all these steps, the simulation model is developed by connecting all models together.

3.1 Full Vehicle Model

In the first step of the modeling, the full vehicle model of the tractor is developed. This model includes the sub-models of the tire, tractor body, wheels, and tractor suspension, which will be explained in this part.

3.1.1 Tire Model

Tires are the first elastic element between the road surface and vehicle that have an important role in providing effective isolation from the road disturbances, particularly the high frequency road input that is not damped effectively by a suspension system. On the other hand, the tires characteristics are related closely to the quality of the tire-road contact and the vehicle handling.

A precise modeling of tires is complicated, because the stiffness and the damping characteristics of tires are not constant and are affected by different factors such as static load, inner pressure, temperature, rotational speed, and excitation frequency (Von Holst, 2000). In order to consider all these effects, some complicated models are presented. For example, some of them use FEM modeling that defines a little bit of the tire as the basic element of the modeling. In this way, they consider the effect of the vertical, lateral, and longitudinal tire forces and also, the effect of these forces on one another (Blundell, 1999).

In this investigation, a complicated tire model is not necessary. The experimental tests are considered as the reference of the simulation tests. Since the experimental tests are performed on a test rig, some simplifications are possible in tire modeling. For example, just vertical tire force is concerned from all force directions. In addition, factors such as the temperature and rotational speed of the tire are not considered. The tire model used for this study is a linear “point contact” model. This simple model is capable to simulate the suspension characteristics of tires correctly. The model consists of a spring and a damper element in parallel that are connected to a single point of ground (Fig. 3-3). These two elements are linear with constant stiffness and damping coefficient.

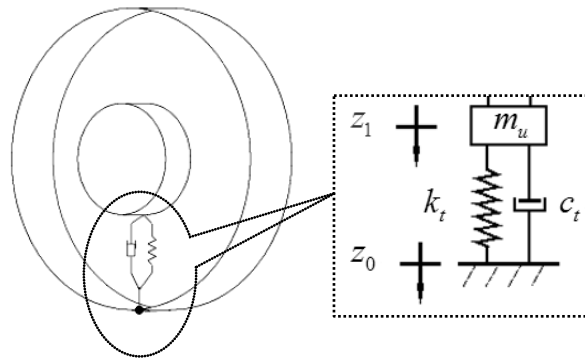


Figure 3-3 Contact point tire model used for the simulation model.

So, the mathematical model of a tire is presented as:

$$F_{tire} = k_t(z_1 - z_0) + c_t(z_1 - z_0)' \quad 3-1$$

The road contact of the tire can be lost for a moment. In this case, the calculated tire force would be an impossible negative value. Because of this, a limitation is added to the first equation as follows:

$$(z_1 - z_0) < 0 \rightarrow F_{tire} = 0$$

3.1.2 Quarter Car Suspension Model

The quarter-car model is shown in figure 3-4. It is called quarter-car, because it seems to represent one of the four vehicle suspension units. It is a simplified model with lumped masses and linearized elements. This may appear to be an oversimplification model for a vehicle suspension system. However, the origins of the many ideas come from the fundamental work using this model. Particularly, this model is used in the area of modern control strategies for active and semi-active suspensions. In this study, the quarter-car model

is also used as basics for deriving of the full vehicle. The fundamental parameters of a suspension system can be defined by this model. These parameters are presented in table 3-1.

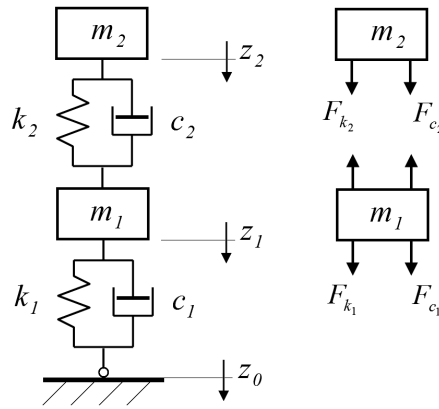


Figure 3-4 Quarter-car model and relevant free body diagram.

Table 3-1 Quarter-car suspension model parameters.

Symbols	Description	Symbols	Description
m_1	Unsprung mass (i.e. wheel assembly)	z_1	Unsprung mass displacement
m_2	Sprung mass (i.e. vehicle body)	z_2	Sprung mass displacement
k_2	Suspension stiffness	z_0	Road input displacement
c_2	Suspension damping	$(z_2 - z_1)$	Suspension travel
k_1	Tire stiffness	$(z_1 - z_0)$	Tire deflection
c_1	Tire damping		

Figure 3-4 shows the free body diagram of the quarter-car model. Looking at this model, the equations of the sprung mass and unsprung mass motions can be derived in two parts as follow:

First, sprung mass equation,

$$\begin{aligned}
 +m_2 z_2'' + F_{k_2} + F_{c_2} &= 0 \mapsto \\
 +m_2 z_2'' + k_2(z_2 - z_1) + c_2(z_2' - z_1') &= 0
 \end{aligned}
 \tag{3-2}$$

Then, unsprung mass equation,

$$\begin{aligned}
 +m_1 z_1'' + F_{k_1} + F_{c_1} - F_{k_2} - F_{c_2} &= 0 \mapsto \\
 +m_1 z_1'' + k_1(z_1 - z_0) + c_1(z_1' - z_0') - k_2(z_2 - z_1) - c_2(z_2' - z_1') &= 0
 \end{aligned}
 \tag{3-3}$$

The motions of the sprung and unsprung masses (*i.e.* z_1, z_2) can be determined by solving the system of these two differential equations. In the following sections, full-tractor suspension model will be described. The quarter-car model and relevant equations will be used as the basics of this full-tractor model.

3.1.3 Full-Vehicle Model Degrees of Freedom

The quarter-car model can be used in order to evaluate the main characteristics of vehicle suspensions. However, a model with the two degrees of freedom of the sprung and unsprung masses covers just the vertical motions of a vehicle, and in order to study the rotational motions, other models with more degrees of freedom are necessary. A full-vehicle model is able to cover all needed degrees of freedom. As before, it is necessary to define a proper coordinate system for dynamics of a tractor.

For this purpose, there are two kinds of coordinate systems: space-fixed and vehicle-fixed system. The first one fixing at one point in space determines the position and orientation of a vehicle. This system is used in order to define the maneuver path of a vehicle. In opposition, vehicle-fixed coordinate system is originated at the center of gravity (CG) of a vehicle and travels with it. In the study of suspensions, the vehicle-fixed system is used in order to define a relative coordinate system for the dynamics of the suspension components. This coordinate system is shown in figure 3-5.

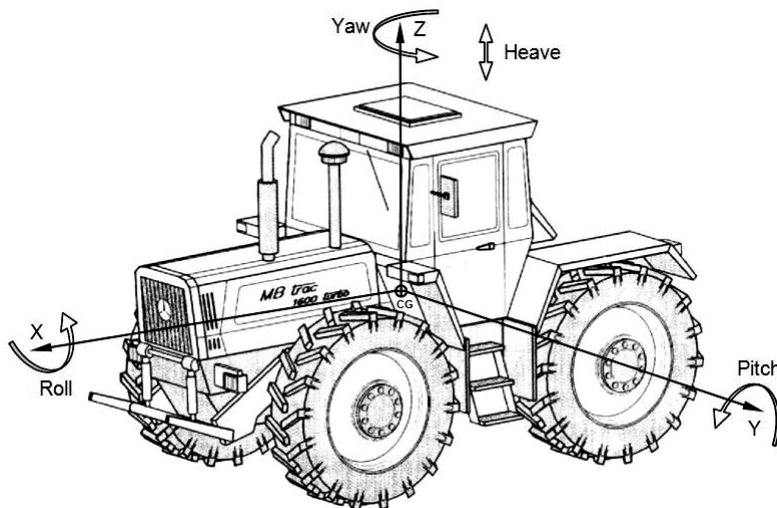


Figure 3-5 Vehicle-fixed coordinate system.

According to the ISO convention, the positive directions of the axes are defined as follow:

- 1- x-axis: straight to the forward from the vehicle.

2- y-axis: straight to the left from the vehicle.

3- z-axis: straight to the upwards from the vehicle.

Now with respect to the vehicle fixed coordinate system, the vehicle motions can be described. There are six degrees of freedom (6DOF) related to the vehicle body motions including three dimensional and three rotation degrees of freedom. In addition, there are four dimensional degrees of freedom related to the unsprung masses, which is the number of the vehicle wheels. These vehicle motions and relevant terminology are mentioned frequently in this thesis. Thus, these motions of the vehicle body are described in this part. Table 3-2 illustrates the list of the complete degrees of freedom for a four-wheel vehicle. These degrees of freedom are explained as follow:

1- Longitudinal: It is the body motion in x-axis dimension or forward/backward. For example as a vehicle accelerates or brakes, its body is exited with forces in this direction called longitudinal forces.

2- Lateral: It is the body motion in y-axis dimension or left/right. An example for this direction is the centrifugal lateral force entering to the vehicle during turning.

Table 3-2 Vehicle degrees of freedom.

No.	Vehicle Part	Degree of Freedom	Motion	Axis
1	body	longitudinal	dimension	x-axis
2	body	lateral	dimension	y-axis
3	body	vertical(heave)	dimension	z-axis
4	body	roll	rotation	x-axis
5	body	pitch	rotation	y-axis
6	body	yaw	rotation	z-axis
7	wheel-1	vertical	dimension	z-axis
8	wheel-2	vertical	dimension	z-axis
9	wheel-3	vertical	dimension	z-axis
10	wheel-4	vertical	dimension	z-axis

3- Vertical: It is the body motion in z-axis dimension or up/down. Upward and downward motion of the vehicle body caused by uneven road is an example for this case. This motion is also referred to as "heave" or in some references as "bounce". This motion is usually measured at the mass center of the vehicle body and is considered as an important

parameter of the performance of a suspension. Among these three-dimensional motions of the vehicle body, just vertical direction is related to the suspension operation, and because of this, only this motion is studied in modeling of the tractor.

4- Roll: It is the rotation body motion about x-axis (Fig. 3-6 and 3-7). Leaning of the vehicle body during cornering is an example for the excitation of the roll motion. As a vehicle turns a corner, the centrifugal force entering to the vehicle body is resisted by the tires road contact force. Interaction of these two forces creates torque at the vehicle body that causes a vehicle weight transfer on one side, and the vehicle leans consequently towards the outside of the curve. This is what is called body roll. The extreme amplitude of the body roll causes a critical situation for vehicle stability. The performance of the suspension system has the main role in providing the roll stability for a vehicle.

5- Pitch: It is the rotation body motion about y-axis (Fig. 3-6 and 3-7). The dive of the vehicle body during braking is a typical example for the excitation of the pitch body motion. As a vehicle brakes, the inertia of the vehicle body causes transfer of the center of gravity (CG) of the body, and vehicle dives forward, and the weight on the rear tires transfers to the front tires. This causes a critical moment in controlling of a vehicle.

6- Yaw: It is the rotation body motion about z-axis (Fig. 3-6 and 3-7). The spinning motion of a vehicle is an example for the yaw motion. This instability mode may occur during cornering on slippery surfaces. In this situation, the decreased traction forces of the rear tires are not able to resist against centrifugal force, and tires slip, and vehicle turns violently around itself. This body motion is not related directly to the suspension system of a vehicle, and so that, it is not considered in the full-tractor model.

7- Wheel hop: It is the unsprung mass motion in z-axis dimension or up/down. In addition to the body motions, the wheel motion is also important in the study of vehicle dynamics. This motion is in z-axis direction and referred usually as “wheel hop”. This motion affects directly the tire-road connections and influences consequently the vehicle stability. Using the definitions of the coordinate systems and vehicle motions, physical model of the tractor will be derived in the following sections.

3.1.4 Physical Full Vehicle Model

As mentioned before, a quarter-car model is not able to simulate all important vehicle motions considered in the suspension system. Thus, another model with more

degrees of freedom is needed. In this section, a full-vehicle model is used for simulation the tractor dynamic behavior in respect to the suspension system. Figure 3-6 shows this physical full-vehicle model. This model consists of a body sub-model and four sub-models of the wheels. Each wheel model is a lumped-mass quarter-car model, which is connected to the corners of the body. The whole model is able to simulate each one of the seven needed degrees of freedom (illustrated in table 3-3). Other used symbols in figure 3-6 are explained in the nomenclature part of this script.

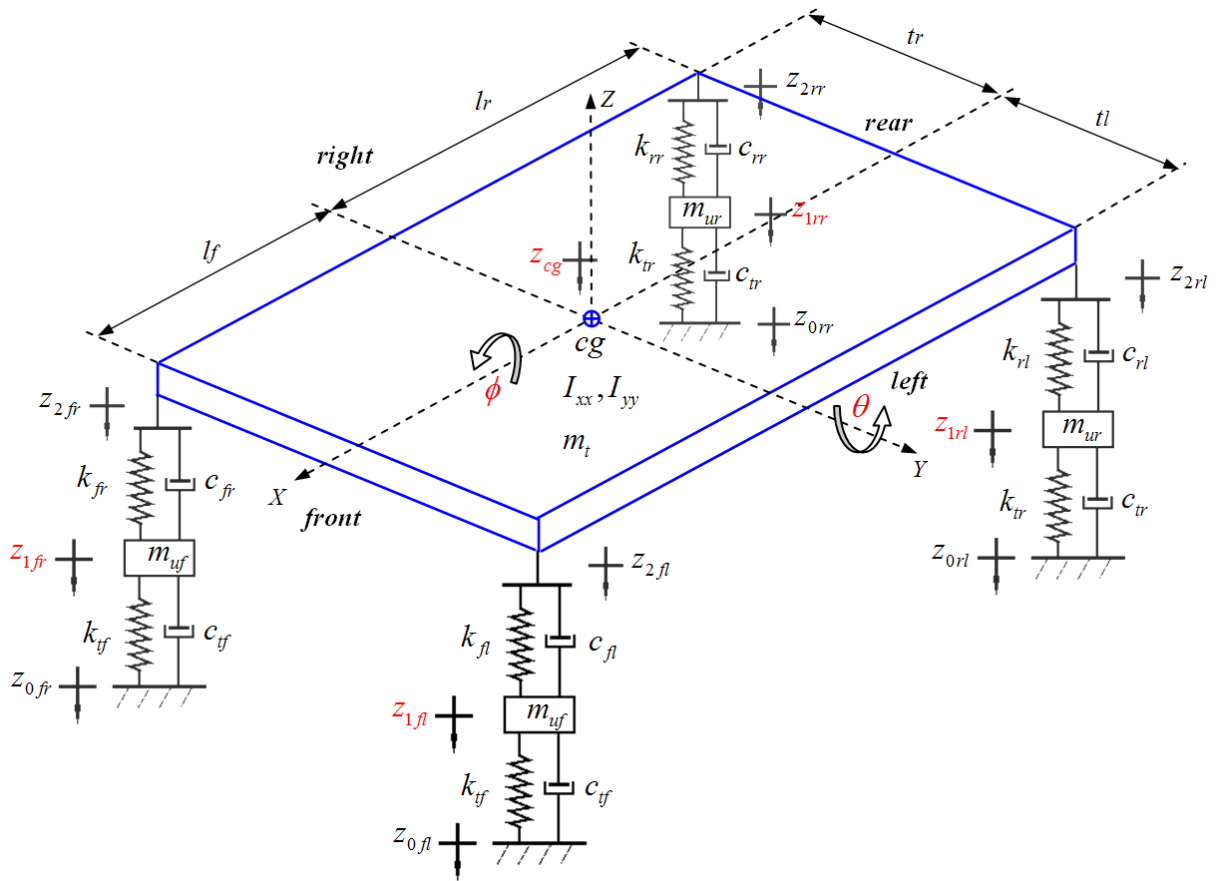


Figure 3-6 Physical full-vehicle model with seven degrees of freedom.

The physical full-vehicle model consists of four components: 1- tire model 2-front and rear suspension units model 3-wheel (unsprung mass) model 4-tractor body (sprung mass) model. The model of tires is the contact point model (stated in section 3.1.1). The model of a suspension unit consists of a spring and a damper model, which are placed between the wheel and tractor body. Each one of these models is indeed comparable with a quarter-car model. However, this model is completed later during model modification.

Table 3-3 Considered degrees of freedom in the full-vehicle model.

Nr.	Symbol	Description
1	θ	pitch angle at center of gravity
2	φ	roll angle at center of gravity
3	z_{cg}	heave displacement at center of gravity
4	z_{1fl}	front-left unsprung mass vertical displacement
5	z_{1fr}	front-right unsprung mass vertical displacement
6	z_{1rl}	rear-left unsprung mass vertical displacement
7	z_{1rr}	rear-right unsprung mass vertical displacement

Similar to the procedure of all other modeling, there are some assumptions and simplifications in this modeling. The tractor axles are like a link between the right and left units. In spite of this, in the models of the unsprung masses, it is assumed that the suspension units are independent, and the effects of the axles are ignored. Similar to quarter-car model, the unsprung mass is considered as lumped-mass. The parameters of the unsprung mass are calculated by adding the wheel mass and a part of the axle mass.

In full vehicle model, tractor body is also modeled as a rectangular form of lumped-mass models. This mass form has specific dimensions determining the position of the center of gravity and position of the four suspension units standing on the corners of the body. In this modeling, it is also supposed that the axes of the roll and pitch cross the center of gravity (Fig. 3-5). This model presents a proper simplification. However, it is needed that the related mass and inertia parameters to be calculated accurately. In the reality, tractor body involves different masses standing on different position. In order to accurate the model parameters, the body of the tractor is considered a multi-rigid body mass. This mass consists of some main mass-components such as engine, chassis, transmission, and cabin.

In appendix E1, there are more information about the parameters of the rigid multi-body model including the mass and position of the body components. In addition, the methods of calculating total mass and moment of inertia are indicated. It should be also considered that the body model is still a solid model, and there is no consideration for elastic connections among body components. In the following section as the next step of modeling, equations derivation of the model will be explained.

3.1.5 Mathematical Full Vehicle Model

In mathematical modeling, the suspension between the tractor body and wheels are modeled by simple linear spring and damper elements, whereas some of these elements in the test-tractor are hydraulic or hydro-pneumatic elements with non-linear characteristic. Using simple linear model for these elements provides proper simplifications for the primary full tractor model. In the following steps of the modeling, the non-linear elements will be modeled separately. Then, these new models will be replaced with the simple primary models.

In mathematical modeling, the motion equations for each one of seven degrees of freedom are derived. These motions are four unsprung masses motions along with the three motions of the sprung mass. As the first stage, the differential equations of the tractor's four unsprung masses are derived based on the equations of the quarter-car model (refer to section 3.1.2). The equations of the tractor's four unsprung masses are with respect to figure 3-6 as follow:

$$\begin{aligned}
 fl: & \\
 & + m_{uf} z_{1fl}'' + c_{tf}(z_{1fl} - z_{0fl})' + k_{tf}(z_{1fl} - z_{0fl}) - c_{fl}(z_{2fl} - z_{1fl})' - k_{fl}(z_{2fl} - z_{1fl}) = 0 \\
 fr: & \\
 & + m_{uf} z_{1fr}'' + c_{tf}(z_{1fr} - z_{0fr})' + k_{tf}(z_{1fr} - z_{0fr}) - c_{fr}(z_{2fr} - z_{1fr})' - k_{fr}(z_{2fr} - z_{1fr}) = 0 \\
 rl: & \\
 & + m_{ur} z_{1rl}'' + c_{tr}(z_{1rl} - z_{0rl})' + k_{tr}(z_{1rl} - z_{0rl}) - c_{rl}(z_{2rl} - z_{1rl})' - k_{rl}(z_{2rl} - z_{1rl}) = 0 \\
 rr: & \\
 & + m_{ur} z_{1rr}'' + c_{tr}(z_{1rr} - z_{0rr})' + k_{tr}(z_{1rr} - z_{0rr}) - c_{rr}(z_{2rr} - z_{1rr})' - k_{rr}(z_{2rr} - z_{1rr}) = 0
 \end{aligned} \tag{3-4}$$

After the unsprung mass, equations of the unsprung mass are derived. For this purpose at first, the unsprung mass motion on the center of gravity is decomposed to the three components: heave, pitch, and roll motions. After that, the equations of all motions are derived separately, and finally by adding the effect of all these motions, the equations of the body motions are achieved. First, it is supposed that the displacements are small (i.e. $\sin \alpha \approx \alpha$). The equations are derived similar to sprung mass equation in the quarter-car model (refer to equation 3-2). For each equation, the effects of all four unsprung mass forces are considered.

After some manipulations, these equations are presented as follow:

Heave,

$$z_{cg}'' = \frac{1}{m_t} [c_{fl}(z_{fl1} - z_{fl2})' + k_{fl}(z_{fl1} - z_{fl2}) + c_{fr}(z_{fr1} - z_{fr2})' + k_{fr}(z_{fr1} - z_{fr2}) + c_{rl}(z_{rl1} - z_{rl2})' + k_{rl}(z_{rl1} - z_{rl2}) + c_{rr}(z_{rr1} - z_{rr2})' + k_{rr}(z_{rr1} - z_{rr2})] \quad 3-5$$

Pitch,

$$\theta'' = \frac{1}{I_{yy}} [l_f \cdot c_{fl}(z_{2fl} - z_{1fl})' + l_f \cdot k_{fl}(z_{2fl} - z_{1fl}) + l_f \cdot c_{fr}(z_{2fr} - z_{1fr})' + l_f \cdot k_{fr}(z_{2fr} - z_{1fr}) + l_r \cdot c_{rl}(z_{2rl} - z_{1rl})' + l_r \cdot k_{rl}(z_{2rl} - z_{1rl}) + l_r \cdot c_{rr}(z_{2rr} - z_{1rr})' + l_r \cdot k_{rr}(z_{2rr} - z_{1rr})] \quad 3-6$$

Roll,

$$\varphi'' = \frac{1}{I_{xx}} [-t_l \cdot c_{fl}(z_{2fl} - z_{1fl})' - t_l \cdot k_{fl}(z_{2fl} - z_{1fl}) + t_r \cdot c_{fr}(z_{2fr} - z_{1fr})' + t_r \cdot k_{fr}(z_{2fr} - z_{1fr}) - t_l \cdot c_{rl}(z_{2rl} - z_{1rl})' - t_l \cdot k_{rl}(z_{2rl} - z_{1rl}) + t_r \cdot c_{rr}(z_{2rr} - z_{1rr})' + t_r \cdot k_{rr}(z_{2rr} - z_{1rr})] \quad 3-7$$

After all by considering the dimensions of the tractor body (Fig. 3-6), the effect of all these sprung mass motions are added together in order to calculate the vertical accelerations of the body's corners as follows:

$$\begin{cases} z_{2fl}'' = z_{cg}'' - l_f \cdot \theta'' + t_l \cdot \varphi'' \\ z_{2fr}'' = z_{cg}'' - l_f \cdot \theta'' - t_r \cdot \varphi'' \\ z_{2rl}'' = z_{cg}'' + l_r \cdot \theta'' + t_l \cdot \varphi'' \\ z_{2rr}'' = z_{cg}'' + l_r \cdot \theta'' - t_r \cdot \varphi'' \end{cases} \quad 3-8$$

In this section, the mathematical full-vehicle model was created. This model included the equations of the vertical or rotational motion of the unsprung masses (i.e. wheels) and sprung mass (i.e. body). These equations will be used as the basics of the full-vehicle computer model presenting in the next section.

3.1.6 Simulink Full Vehicle Model

Figure 3-7 shows the computer model of the mathematical full vehicle model created by MATLAB-Simulink program. This model consists of the two sub-models: unsprung mass and sprung mass. Because of the direct relation between these two masses, their models are also joined together. The input of the model is a road profile that enters to the unsprung mass sub-model. Outputs of the model are some model variables that are used in order to

evaluate the suspension. In addition, some of these variables are used as the input of the controller. These inputs and outputs of the model will be described in the next sections.

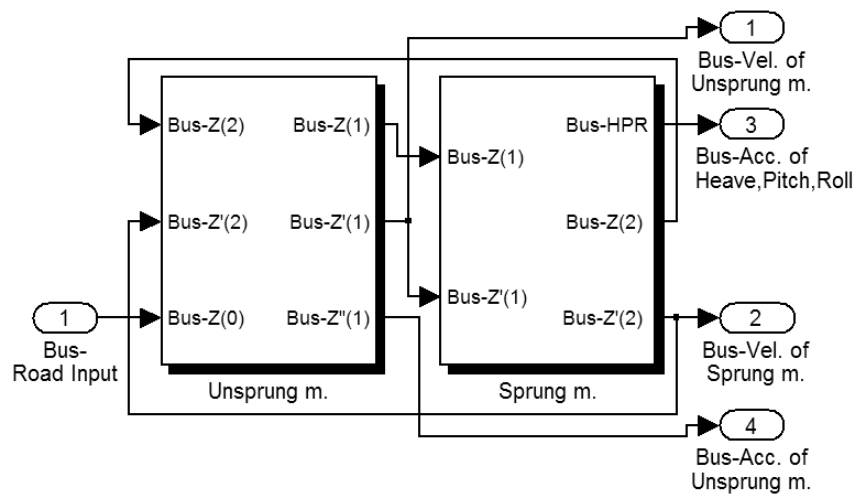


Figure 3-7 Full vehicle Simulink model.

The sprung mass model is shown in figure 3-8. This model simulates the motions of the vehicle sprung mass. As explained before about the mathematical model, the sprung motion is decomposed initially to the heave, pitch, and roll motions. As shown in this figure, the Simulink model consists of three blocks: heave, pitch, and the roll motions of the sprung mass. These blocks are based on the equation 3-5, 3-6, and 3-7.

The motions are summed by the “sum” block, which is based on equation 3-8. In addition, this block produces the displacements and velocities of the vertical motion of the body corners, which are used as the inputs of the unsprung mass model. Unsprung mass model is shown in figure 3-9. This model simulates the vertical motions of the four vehicle wheels. As shown in this figure, this model consists of the four blocks of the unsprung masses of the vehicle created based on the equation 3-4.

As conclusion, the full vehicle simulink model of the tractor was presented in this section. This model is used as the foundation of the overall model. As shown in figure 3-1, the overall model consists of some other components that will be added to the full vehicle Simulink model later. These rest components will be presented in the following sections of this chapter.

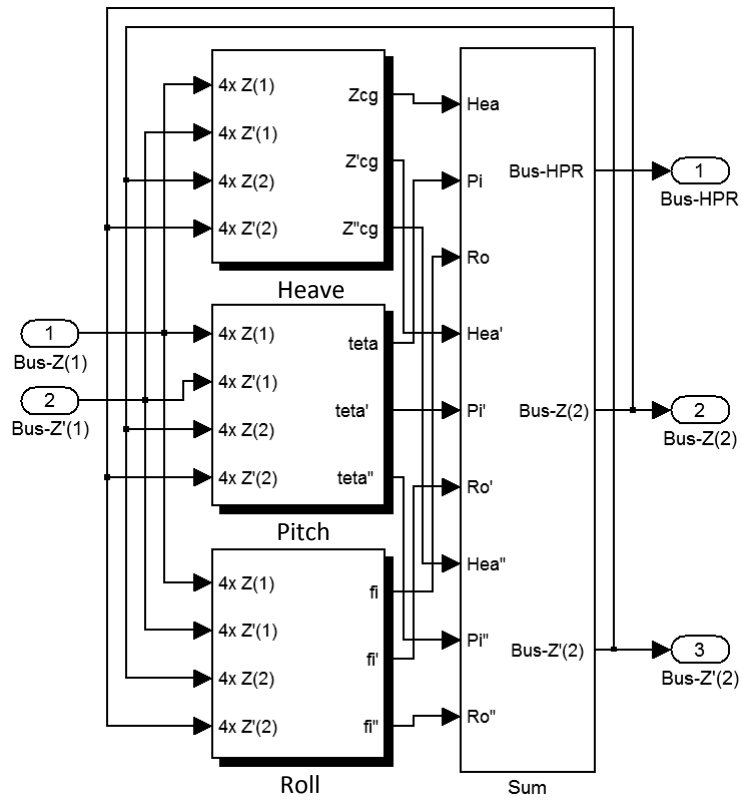


Figure 3-8 Vehicle sprung mass Simulink model.

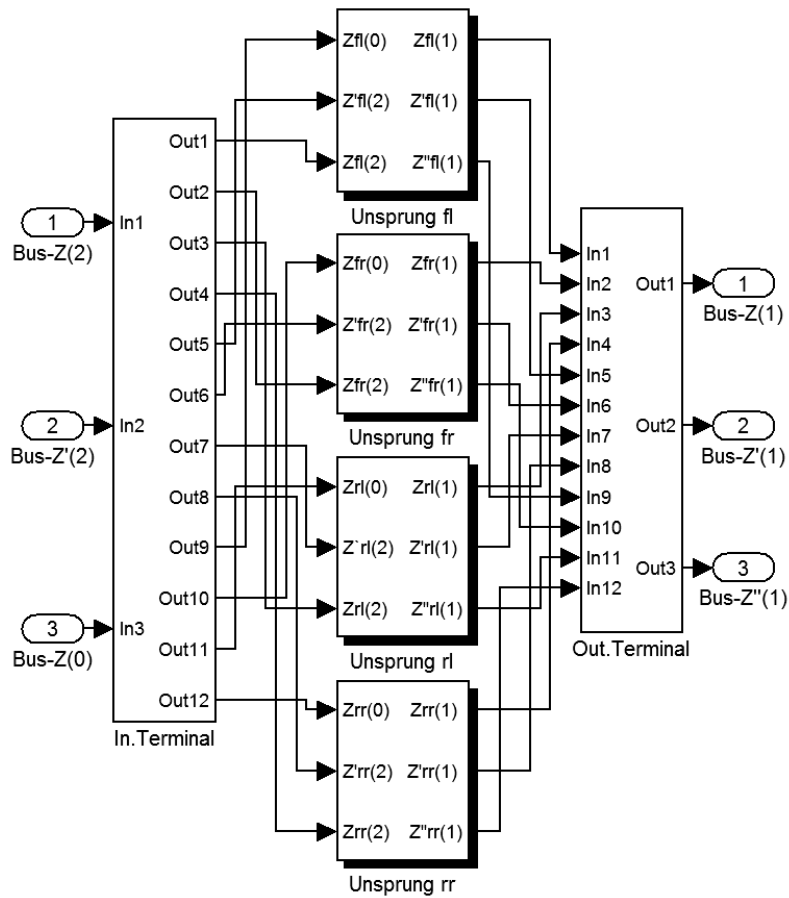


Figure 3-9 Vehicle unsprung mass Simulink model.

3.1.7 Front Suspension Model

The dampers of the tractor front suspension are hydraulic dampers with non-linear characteristic. In the full vehicle model, these dampers are simulated with a simple linear model to prevent the model equations from complication. After building the Simulink full vehicle model, a more accurate model for the dampers of the front suspension are presented in this section. Figure 3-10 shows the force-velocity characteristic of these dampers. This graph is achieved from the experimental data of the real damper, presenting the real characteristic of the dampers.

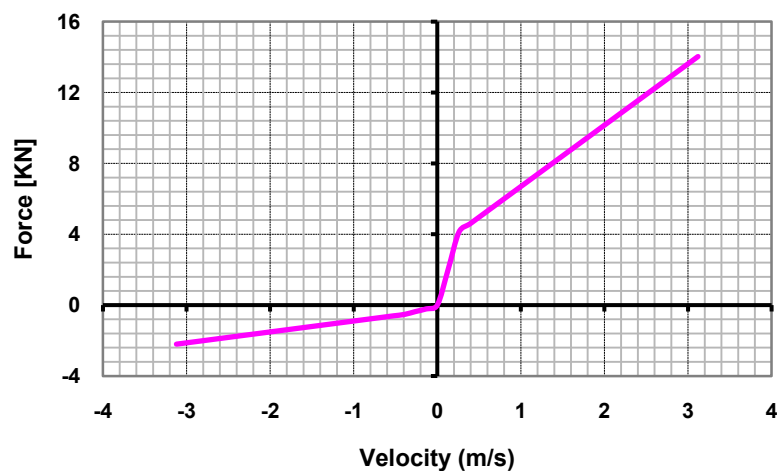


Figure 3-10 Measured force-velocity characteristic of the dampers used for the front axle of the test-tractor.

By inserting this information into a Simulink “Lookup Table”, a one-dimensional function is created to approximate the damper force with respect to the damper cross velocity. This new function replaces the primary simple linear function, and so, an accurate model for the damper is provided. Figure 3-11 shows the use of this new damper model in the full vehicle Simulink model.

After the modification of the front suspension model, derivation of a more accurate model is considered for the hydro-pneumatic rear suspension. This model is an important part of the overall model, because it is indeed the actuator system of the semi-active suspension. In the following sections, the parts of this modeling will be described.

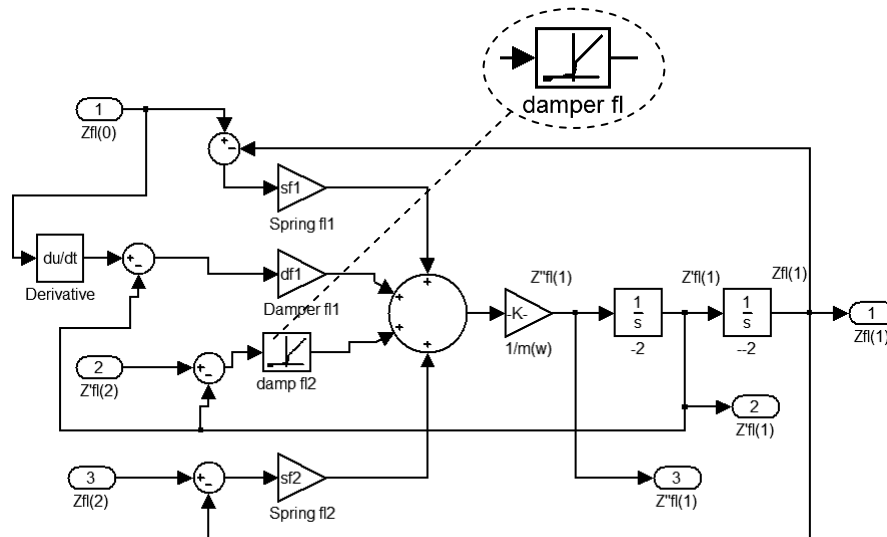


Figure 3-11 Damper model of the front suspension in full vehicle Simulink model.

3.2 Actuator Model

In a vehicle with an active suspension system, the actuators are the components that work between the controller and the tractor suspension (refer to Fig. 3-1). It receives the control commands from the controller and applies the forces to the suspension. In this way, it can modify the vehicle dynamics. The actuator is indeed a part of an active suspension system with the parameters that can be changed by the command of a controller. In this investigation, the semi-active suspension system is used for the hydro-pneumatic rear suspension of the test-tractor. The variable damper of this hydro-pneumatic suspension is indeed the actuator of the system. Using this part, the damping level of the suspension can be changed by the order of the controller.

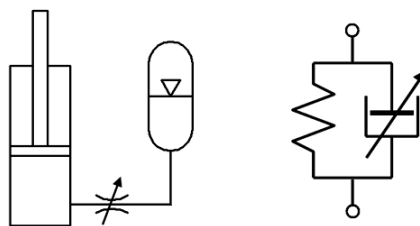


Figure 3-12 A variable hydro-pneumatic suspension as the actuator of the system.

Hydro-pneumatic suspension can be modeled as a set consists of a spring and a damper. The stiffness effect of the system creates by the compressed gas of the accumulator, and the damping effect of the system creates by throttling the flowing oil between the cylinder and accumulator. In order to use this system as the actuator, a

controllable throttle is added to this system (Fig. 3-12). In order to build the model, the function of the actuator is divided into the two parts of the spring and variable damper. The first part generates the stiffness force and the second one generates the controllable force damping force of the suspension. These two components are modeled separately. By joining these two models, the hydro-pneumatic actuator model is created.

3.2.1 Hydro-Pneumatic Spring Model

The stiffness effect of a hydro-pneumatic suspension is produced by compressing the gas in accumulators. The hydro-pneumatic cylinder forces oil to the accumulator and compress the gas inside the accumulator. The produced pressure is transferred to the cylinder via a pipe. This pressure is proportional to the piston displacement. Therefore, stiffness force is produced in the cylinder. In the hydro-pneumatic suspension of the test-tractor, a double-acting cylinder is used (Figure 3-13). Both side of this cylinder are connected to two accumulators, which generate the stiffness force of the suspension.

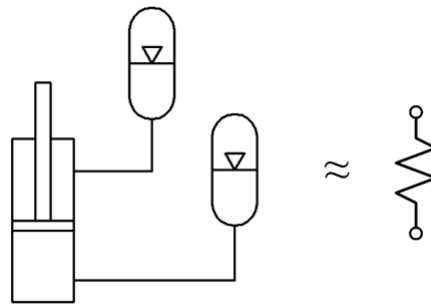


Figure 3-13 Spring component of a hydro-pneumatic suspension with a double-acting cylinder.

By removing the throttle from a hydro-pneumatic suspension, only the stiffness effect is remained. In the following sections, the spring components of the hydro-pneumatic suspension will be modeled. First, the cylinder and accumulator are modeled separately. Then, these two models are joined together in order to create the model of the hydro-pneumatic spring.

3.2.1.1 Cylinder

In a hydro-pneumatic suspension, the cylinder converts the hydraulic pressure to the stiffness and damping forces. Then, the cylinder producing the stiffness and damping forces works alone instead of both the spring and damper in a conventional suspension. The cylinders used in the hydro-pneumatic suspension of the test-tractor are a double-acting

cylinder. Respecting to figure 3-14, the parameters and variables of the cylinder are presented in table (3-4).

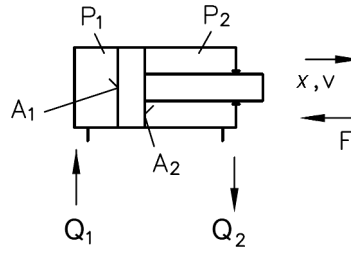


Figure 3-14 A double-acting hydraulic cylinder.

Table 3-4 The parameters and variables definition of the double-acting hydraulic cylinder.

Symbol	Parameter	Symbol	Variable
A_1	piston area (head side)	x, v, F	travel, velocity, force
A_2	piston area (rod side)	P_1, P_2	pressure head/rod side
		V_1, V_2	volume, head/rod side
		Q_1, Q_2	flow rate, head/rod side

The relations between these parameters and variables are presented by the following formulas:

$$F = p_1 \cdot A_1 - p_2 \cdot A_2 \quad 3-9$$

$$Q_1 = A_1 \cdot v, Q_2 = A_2 \cdot v \quad 3-10$$

$$\Delta V_1 = A_1 \cdot \Delta x, \Delta V_2 = -A_2 \cdot \Delta x \quad 3-11$$

Based on these formulas, the Simulink model of the double-acting cylinder is built (Fig. 3-15). This model is used as a component of the spring model. As shown, the outputs of this model are: cylinder force, cylinder volume alternation, and cylinder volume flow rate. The force is indeed the output of the suspension, and volume alternation output is connected to the accumulator model. The output of the volume flow rate of the cylinder is also applied to the throttle model. The inputs of the cylinder model are the cylinder pressures, piston displacement, and velocity. The dynamics inputs are the functional road inputs, and the pressure input comes from the accumulator model.

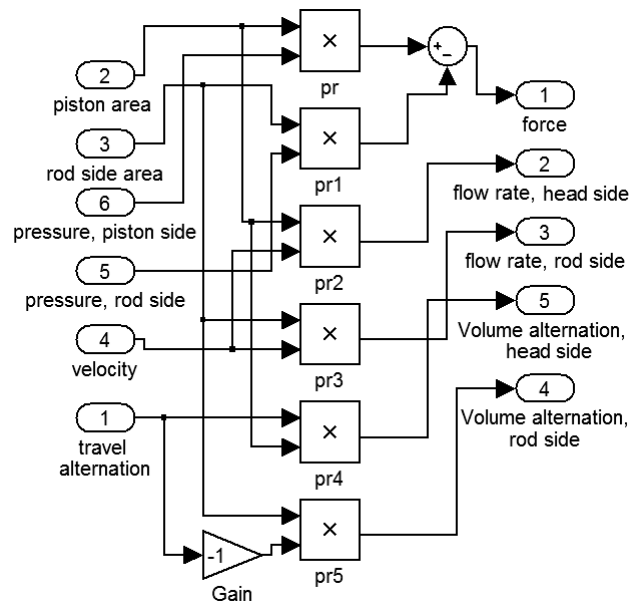


Figure 3-15 Simulink model of the double-acting cylinder.

3.2.1.2 Accumulator

As oil enters to an accumulator, the gas inside the accumulator becomes compressed. In this way, the accumulator is used in the hydraulic systems in order to reserve the pressurized oil. In a hydro-pneumatic suspension, the accumulator is connected to the cylinder, and the cylinder converts the oil pressure of the accumulator to the spring force. Accumulators have a dynamic function in a hydro-pneumatic suspension. Therefore, the bladder-type of accumulators is employed in the tractor suspension (Fig. 3-16). The parameters and variables of the accumulator are presented in table 3-5.

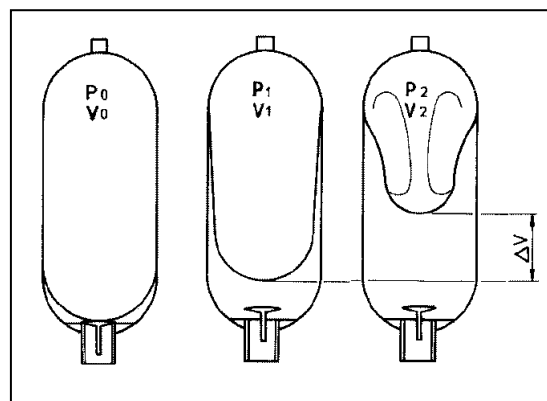


Figure 3-16 A bladder accumulator using in hydro-pneumatic suspensions.

Table 3-5 Parameters and variables definition of an accumulator.

Symbol	Variable	Symbol	Parameter
p_2	operating pressure	p_0	pre-charge gas pressure
ΔV	volume alternation	p_1	initial pressure
		V_0	accumulator volume
		V_1	initial volume

The relations between the parameters and variables are presented by the following formulas. First, the primary volume is calculated based on the initial volume, initial pressure, and primary pressure of the accumulator as follows:

$$V_1 = \frac{p_0 \cdot V_0}{p_1} \quad 3-12$$

Then, operating pressure is calculated from the initial volume, operating volume, and initial pressure of the accumulator as follows:

$$p_2 = p_1 \cdot \left(\frac{V_1}{V_1 + \Delta V} \right)^k \quad 3-13$$

In this formula, k is the polytrophic constant with the value of 1.35, which is often used in modeling of hydro-pneumatic springs (Meller, 1987). Based on these two formulas, the Simulink model of the accumulator is built (figure 3-17). As shown, the outputs of this model is the operating pressure which is applied to the cylinder model, and the input of the model is volume alternation, entering from the cylinder model.

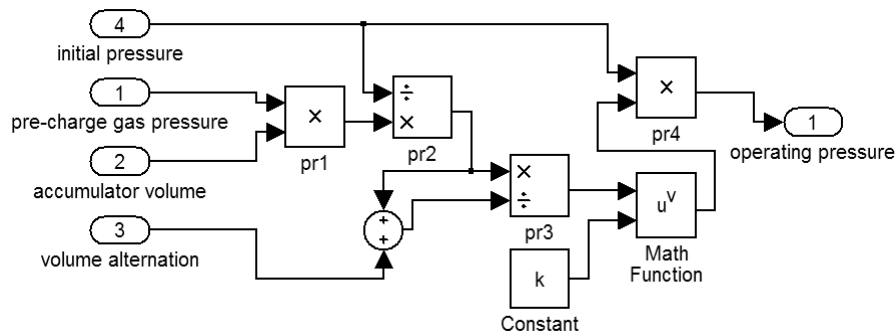


Figure 3-17 Accumulator Simulink model.

3.2.1.3 Spring Model

After building the models of the cylinder and accumulator, these two models are joined together to create the hydro-pneumatic spring model (Fig. 3-18).

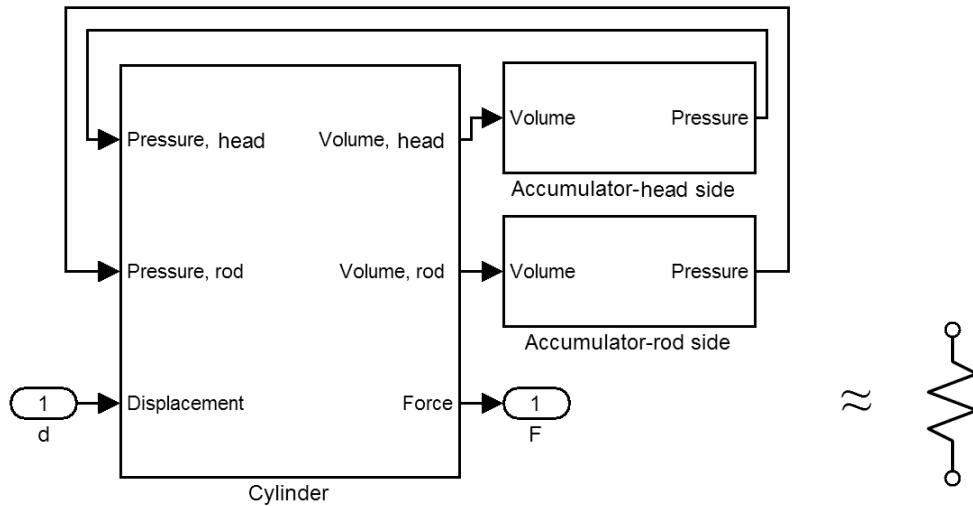


Figure 3-18 Simulink model of the hydro-pneumatic spring.

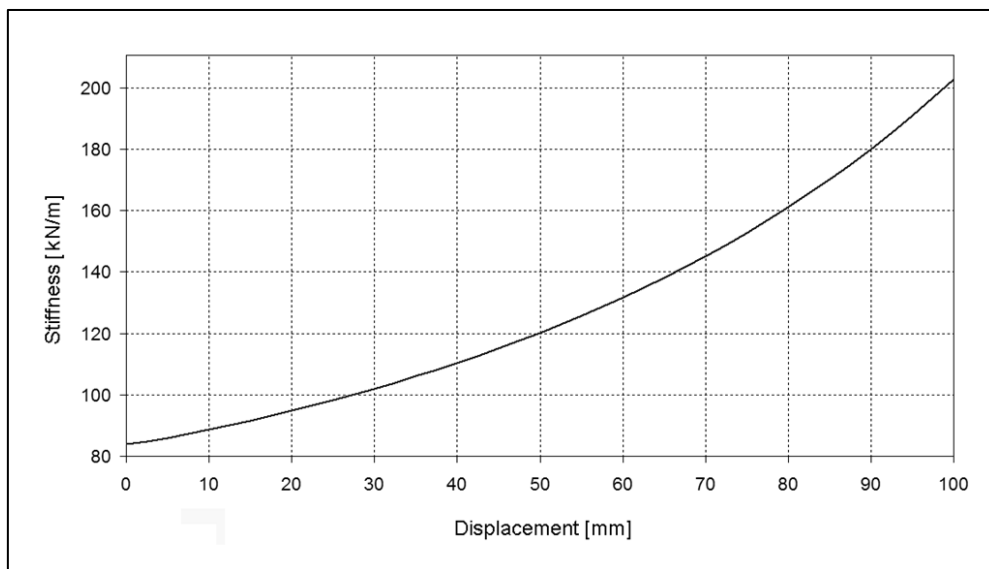


Figure 3-19 Stiffness-displacement curve of the hydro-pneumatic spring model.

As shown, the volume outputs of the cylinder are connected to the volume inputs of the accumulator, and the pressure outputs of the accumulator are connected to the pressure inputs of the cylinder. The output and input of the overall model of the hydro-pneumatic spring are the displacement and force. These parameters are identical to the output and input of a typical spring model.

In order to demonstrate the simulation characteristic of the hydro-pneumatic spring, the stiffness-displacement curve of the overall model is created by applying the simulation parameters (Fig. 3-19). Unlike a conventional spring, the stiffness is not constant and rises progressively with increasing of the spring displacement. After modeling of the hydro-pneumatic spring, the next step is to derive the model of the hydro-pneumatic variable damper presented in the next sections.

3.2.2 Hydro-pneumatic Variable Damper Model

In a hydro-pneumatic suspension, the damping effect is created by using a throttle between the cylinder and accumulators (Fig. 3-20). As oil flows through this throttle, a pressure drop proportional to the flow rate is created. This pressure appears on the piston as the damping force, which is proportional to the piston velocity and the. In a hydro-pneumatic suspension with semi-active control, damping force is controllable by using a variable throttle.

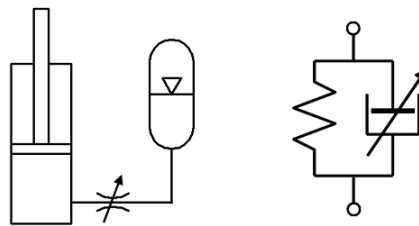
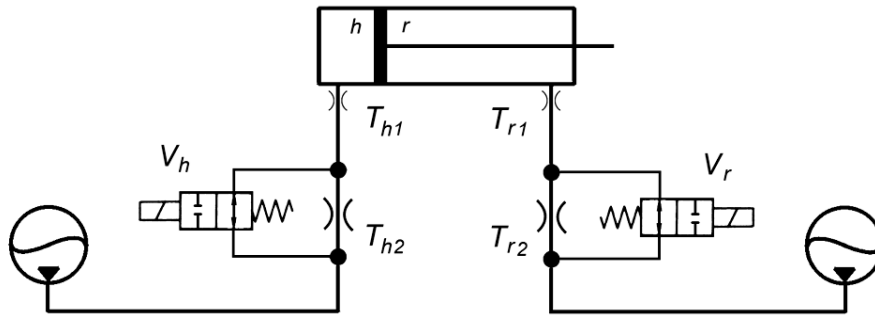


Figure 3-20 Using a variable throttle in hydro-pneumatic suspension in order to create a variable damping effect.

After modeling of the spring component, the variable damper is modeled to complete the overall model of the actuator. The variable damping system and the relevant derived models are described in the following sections.

3.2.2.1 On-off Damper Structure

There are two kinds of actuator systems in semi-active suspensions: continuous and on-off variable damper. The used system in this study is on-off damper, which works in just two levels of low and high damping. Figure 3-21 shows the hydro-pneumatic suspension unit of the tractor including the variable on-off damping system. The components of this system are presented in table 3-6.



.Figure 3-21 On-off damper components of the hydro-pneumatic suspension unit

Table 3-6 On-off damper components.

Symbol	Description
T_{h1}, T_{r1}	cylinder ports
T_{h2}, T_{r2}	throttles
V_h, V_r	valves

The throttles and valves are attached together in parallel, and they stand between the cylinders and accumulators. As a valve is turned off, the oil flows through both the throttle and cylinder port, and damping effect is created by both of them (Fig. 3-22-a). In opposition, as the valve is on, the oil flows through the parallel valve as well as the throttle. This deports the damping effect of the throttle from the system. Therefore, the damping effect in this mode is created just by cylinder port, and the lower damping level is created in this way (Fig. 3-22-b). To sum up, the “off” valve creates the high damping level, and “on” valve creates the low damping level in the suspension system.

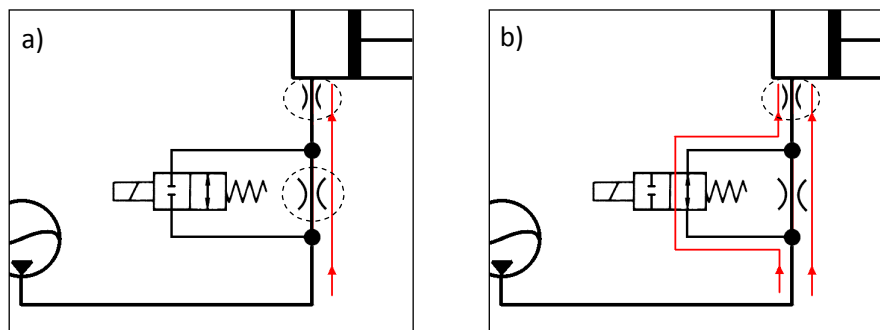


Figure 3-22 On-off damper system with two level of a) high and b) low damping.

In the hydro-pneumatic suspension of the tractor, a double-acting cylinder is used (refer to Fig. 3-21). For generating the high damping mode, the control strategy determines the activation method of the throttle systems of the head side and rod side of the cylinder. The damping forces of the throttle system are calculated on both the cylinder sides as follow:

Damping forces in “on” mode,

$$DF_r = A_r \cdot \Delta P_{Tr1} \quad DF_h = A_h \cdot \Delta P_{Th1} \quad 3-14$$

Damping forces in “off” mode,

$$DF_r = A_r \cdot (\Delta P_{Tr1} + \Delta P_{Tr2}) \quad DF_h = A_h \cdot (\Delta P_{Th1} + \Delta P_{Th2}) \quad 3-15$$

Where,

Symbol	Description
DF_r, DF_h	Damping forces (rod & head sides)
A_r, A_h	Piston areas (rod & head sides)
$\Delta P_{Tr2}, \Delta P_{Th2}$	Pressure drop on the throttles (rod & head sides)
$\Delta P_{Tr1}, \Delta P_{Th1}$	Pressure drop on the cylinder ports (rod & head sides)

This subject will be described in the following sections. In the following sections, the on-off damper components including the throttle, cylinder ports, and valves will be modeled.

3.2.2.2 Throttle

In a hydro-pneumatic suspension, the throttle produces a pressure drop that is proportional to the flow rate and appears on the piston as the damping force. This pressure drop occurs by a sudden change in the flow cross-section in the oil pipeline illustrated in figure 3-23. The parameters as well as the variables of this throttle are presented in table 3-7.

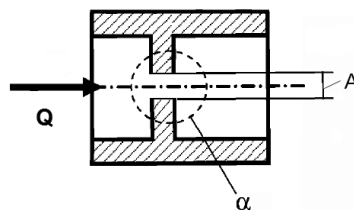


Figure 3-23 Physical model of the throttle.

Table 3-7 Parameters and variables of the throttle.

Symbol	Variable	Symbol	Parameter
Q	volumetric flow rate	A	throttle cross-section
Δp	pressure drop	ρ	density of the oil
		α	flow reference number

The following equation presents a proper mathematical model for a throttle (Festo, 2003).

$$\Delta p = \frac{\rho \cdot Q^2}{2 \cdot \alpha^2 \cdot A^2} \quad 3-16$$

As shown, pressure drop of a throttle is directly proportional to the square of the flow rate. Based on this formula, the Simulink model of the throttle is derived (Fig. 3-24).

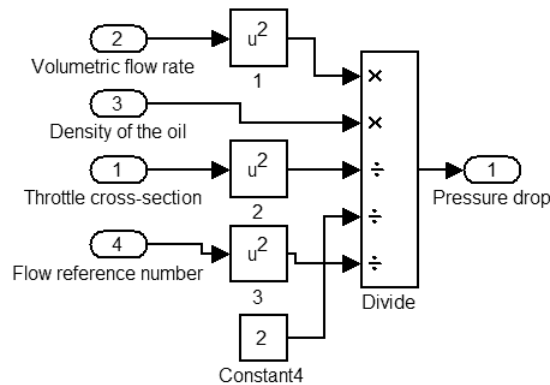


Figure 3-24 Simulink throttle model.

In this model, flow rate and pressure drop are the input and output of the model, which are connected to the cylinder model of the hydro-pneumatic suspension. The input of the flow rate is provided from the output of the cylinder model, and the pressure drop of the throttle is added to the pressure input of the cylinder model.

3.2.2.3 Cylinder Port

Cylinder ports are the outlet and inlet of a hydraulic cylinder (Fig. 3-25).

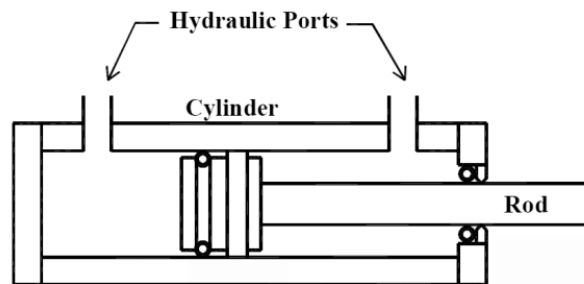


Figure 3-25 Hydraulic ports of a double-acting cylinder.

As mentioned before, ports of the cylinder works as a throttle in the hydro-pneumatic suspension and affects the damping level of the system. A cylinder port is in fact a throttle with a sudden change in the flow cross-section, producing pressure drop in hydraulic system. As oil is leaving the cylinder through its port, a main reduction in the flow cross-section occurs.

In opposition, as oil is flowing through the port to the cylinder, the change in the flow cross-section is increased mainly. This means that the drop pressure in the outlet is completely higher than the drop pressure in the inlet. Based on this fact, the throttling effects of the cylinder ports are modeled only as oil is flowing out from the cylinder. Figure 3-26 shows the physical model of the cylinder outlet throttle. The parameters as well as the variables of this model are presented in table 3-8.

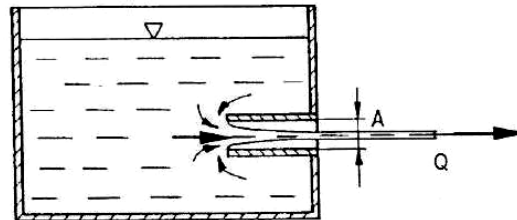


Figure 3-26 Cylinder outlet is considered as a throttle (Siekmann, 2003).

Table 3-8 Parameters and variables of a cylinder outlet.

Symbol	Variable	Symbol	Parameter
Q	cylinder volumetric flow rate	A	cylinder port cross-section
Δp	pressure drop	ρ	density of the oil

The throttle effect of a cylinder outlet is calculated by the following equation (Siekmann, 2003).

$$\Delta p = \frac{3 \cdot \rho \cdot Q^2}{2 \cdot A^2} \quad 3-17$$

From this formula, the Simulink model of a cylinder port is derived (Fig. 3-27). In this model, flow rate and pressure drop are the input and output of the model that they are connected to the cylinder model of the hydro-pneumatic suspension. The input of the flow rate is provided from the output of the cylinder model, and the pressure drop of the cylinder port is added to the pressure input of the cylinder.

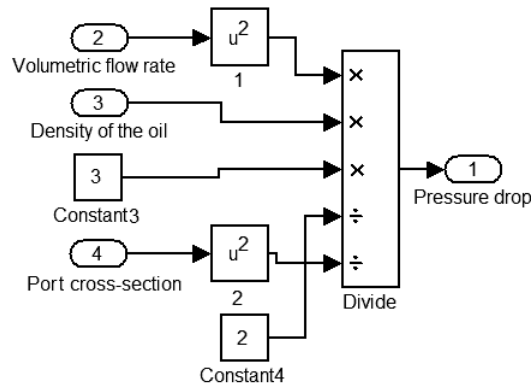


Figure 3-27 Simulink throttle model of a cylinder port.

3.2.2.4 Throttle Valve

Damping level of the suspension is determined by the electric commands, coming from the controller. These commands are applied to the valves, which are the only electric components of the actuator system. As mentioned, the second way for oil flow between the cylinder and accumulator is provided by the valve that is attached in parallel to the throttle. As the valve is turned on, the oil flows through the valve as well as the throttle. In this mode by selecting a proper valve, the pressure drop of the throttle is removed from the system, and just the throttle effect of the cylinder ports is remained.

Solenoid valves work in practice with a delay, and the related timing should be considered in their modeling. Figure 3-28 and table 3-9 illustrates the timing of a valve after applying on-off command to it. A valve does not react at once, as it receives the command (Fig. 3-28-a). The first delay is the switching time of the valve, and the second one is changing pressure time (Fig. 3-28-b). In order to build a model for this timing of the valve, a simplified physical model is created, considering the delay of the switching and delay of the pressure change in the valve. However, in this model, the pressure changing is supposed to be sharp, and it occurs in the middle of the delay of the pressure changing (Fig. 3-28-c). Based on this simplification, the new delays are formulated as:

$$t_a = t_1 + \frac{t_2}{2} , \quad t_b = t_3 + \frac{t_4}{2} \quad 3-18$$

Table 3-9 Valve switching delays.

Symbol	Parameter
t_1	switching-on delay
t_2	switching-on pressure decrease delay
t_3	switching-off delay
t_4	switching-off pressure increase delay
t_a	simplified switching-on delay
t_b	simplified switching-off delay

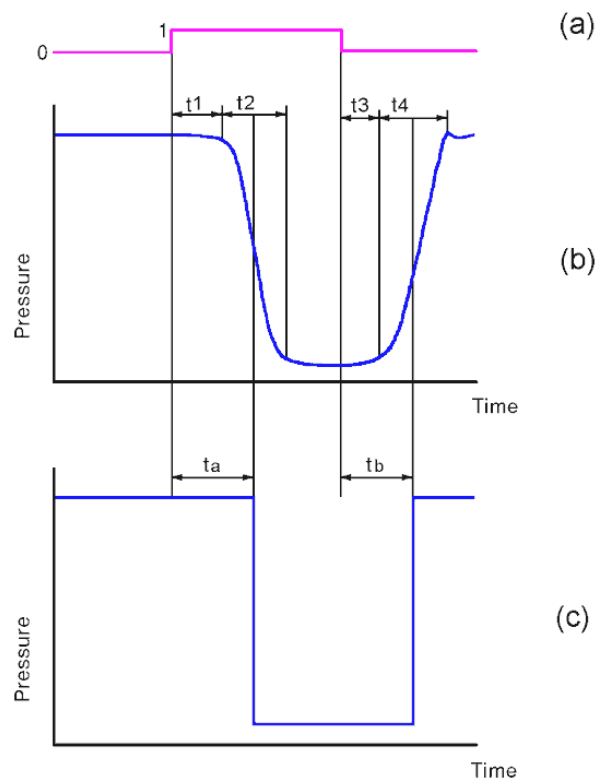


Figure 3-28 Switching characteristics of;
a) input pulse b) real timing chart c) simplified timing chart.

As mentioned, the set of the valve and throttle construct a system that works as a controllable on-off throttle system. Figure 3-29 shows the Simulink model of this system including the throttle and valve timing models. The inputs of this model are the valve command and flow rate, and the output of the model is the pressure drop. The input command is kept for especial delay by this model and then is applied to the switch block. As command is “off,” this block delivers pressure drop calculated by the throttle model to the

output of the model, and when command is “on”, none pressure drop is delivered to the output of the model by switch block. The delay is also used based on the model of the valve timing.

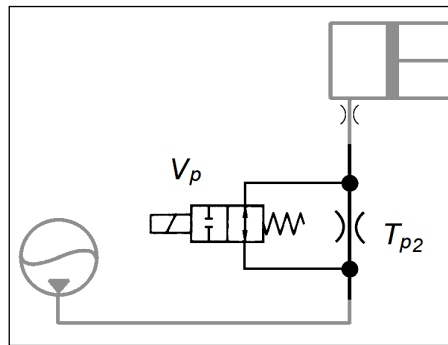
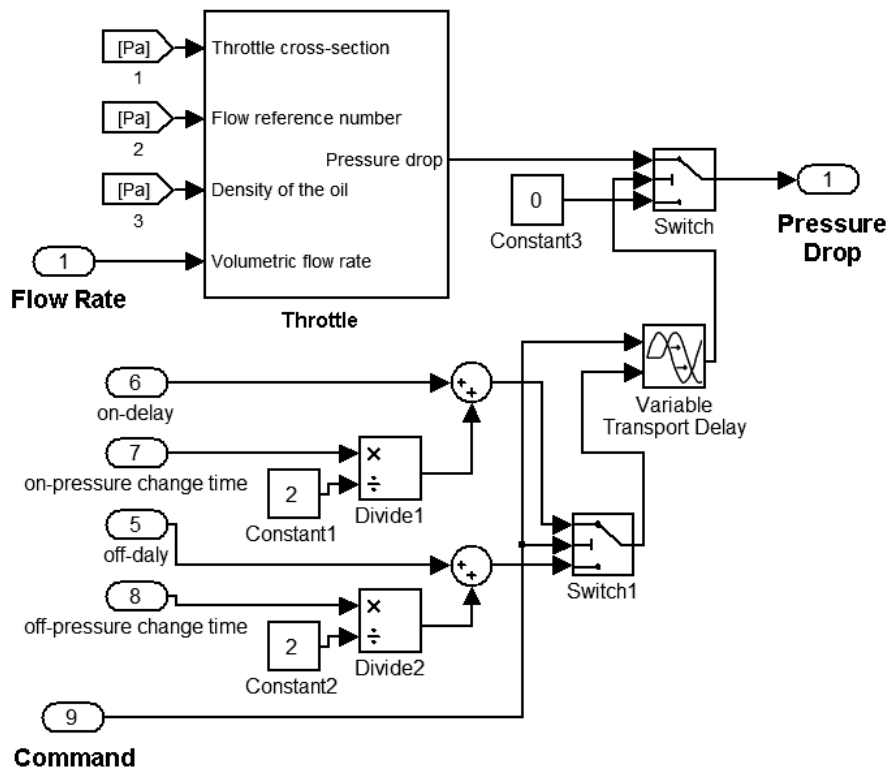


Figure 3-29 Simulink model of the throttle valve set and the equal hydraulic diagram.

3.2.2.5 Overall On-Off Damper

By joining the cylinder port model and the throttle valve model, the Simulink model of the on-off damper is built (Fig. 3-30). The inputs of this model are the damper command and flow rate, and output of the model is the pressure drop. As damper command is “off”, pressure drop output is produced just by the cylinder port model, because the model of the throttle valve set deliver none pressure drop in this mode. In opposition, when command is

“on”, pressure drop output is calculated by adding the outputs of the cylinder port to the outputs of the throttle valve set models.

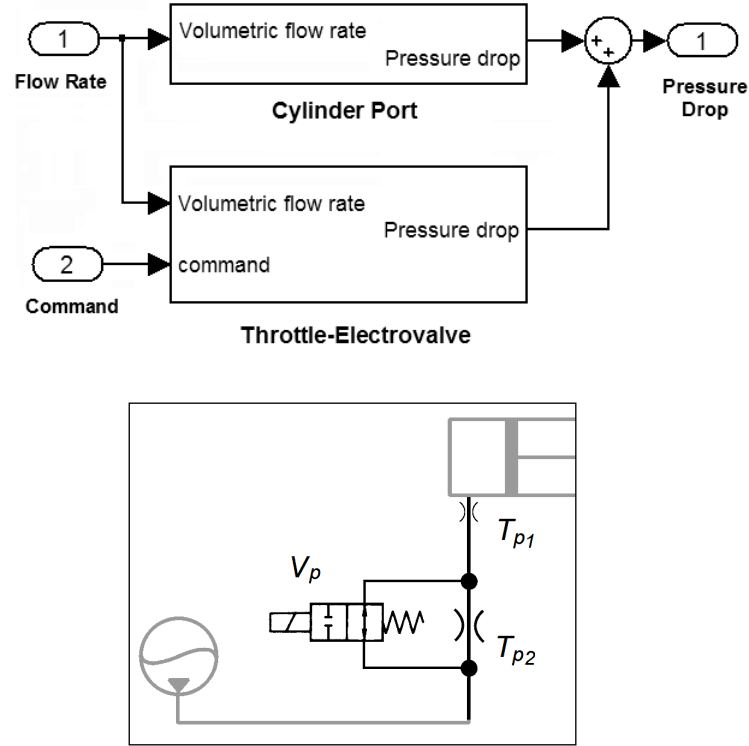


Figure 3-30 Simulink model of the on-off hydro-pneumatic damper and the equal hydraulic diagram.

In the next sections, the on-off damper model will be joined to the hydro-pneumatic spring model with the intention of building the overall hydro-pneumatic actuator model. As before, the proper damping level of the suspension system will be discussed.

3.2.2.6 High-Low Damping Level

As explained in section (2-3-1) about skyhook control strategy, vibration damping is performed by a damper connected between the sprung mass and a constant point in space (refer to Fig. 2-8). The damping coefficient of the skyhook damper is determined by multiplying the damping rate by critical damping as:

$$c_{sky} = \xi_{sky} \cdot c_{cr} \quad 3-19$$

Where, the critical damping is related to the spring stiffness and sprung mass of a suspension as follows:

$$c_{cr} = 2\sqrt{k \cdot m} \quad 3-20$$

In the theoretical approach of skyhook, damping ratio is near one (Karnopp, Crosby, & Harwood, 1974).

$$\xi_{sky} \cong 1 \quad 3-21$$

In practicable skyhook control strategy for semi-active suspension, a damper installing between sprung mass and unsprung mass simulates the skyhook damper. The coefficient of this damper is not constant and depends on the damper velocity. This coefficient can be defined by multiplying the damping ratio by critical damping. The damping ratio is theoretically between zero and one.

$$c_2 = c_{sky} \cdot f(z') = \xi_2 \cdot c_{cr} \quad 0 < \xi_t < 1 \quad 3-22$$

Using the theoretical range in vehicle suspensions does not provide a good efficiency. The values of damping ratio is near zero. This increase the vibration of the unsprung mass, because with this ratio, there is no damping force to control the unsprung mass vibration. On the other hand, zero damping ratio for sprung mass is also not permitted, with a technical failure happens in the semi-active system, a lack of damping force will be happened in suspension that can lead to an unsafe situation.

A value near one is also an inappropriate damping ratio in vehicle suspension, because it creates a big difference between the low and high level of damping that means a great change in the damping force. This increases the stroke and jerk level of the masses. In addition, because of the technical consideration, this damping ratio is not permitted, and it reduces the efficiency of a semi-active suspension, especially in situations such as facing with a sudden road excitation.

As a result, another damping range for the skyhook semi-active suspension of vehicles is necessary. Therefore, proper minimum and maximum values are determined for the damping ratio. These edges are called ride ratio as the minimum damping ratio and handling ratio as the maximum damping ratio. Ride damping is indeed a practicable damping level that provides an optimal ride comfort for vehicles at the cost of minimum road stability. In opposition, the handling damping is a practicable damping level that provides the best road stability for vehicles at the cost of having minimum ride comfort. So, acceptable damping ratio can be determined as:

$$\xi_{Ride} \leq \xi_p \leq \xi_{Handling} \quad 3-23$$

Based on the different research references, the value of these two limits are declared as 0.2 till 0.3 for ride damping ratio and 0.7 till 0.8 for the handling damping ratio (e.g. (Hyvärinen, 2004), (Jalili, 2002), (Standards, 2004), (Masi, 2001)). In on-off skyhook semi-

active suspension, the damper has just two modes of “off”, which is the suspension mode with maximum damping, and “on”, which is the mode with minimum damping. Therefore, handling and ride damping ratio can be determined for these two damping levels as follow:

$$\begin{aligned}\xi_{on} &\cong \xi_{ride} \\ \xi_{off} &\cong \xi_{handling}\end{aligned}\tag{3-24}$$

In order to reduce the stroke phenomenon of on-off skyhook semi-active suspension, the range of the damping should be determined more limited. Therefore, the handling ratio of 0.7 and ride comfort ratio of 0.3 are selected for this suspension system. However, it should be noted that the critical damping and damper coefficient of a hydro-pneumatic suspension are not constant, but also they depend on the displacement and velocity of the suspension. In these circumstances, suspension parameters should be selected in the way that even the maximum and minimum values of the damper coefficient would be set in the determined range.

$$\begin{aligned}c_{on} &\geq (0.3) \cdot \min(c_{cr}) \\ c_{off} &\leq (0.7) \cdot \min(c_{cr})\end{aligned}\tag{3-25}$$

By considering the values of the high and low levels of damping, proper parameters for the model of on-off hydro-pneumatic damper are selected. Based on these parameters, damping characteristic of the damper is presented by a force-velocity graph (Fig. 3-31).

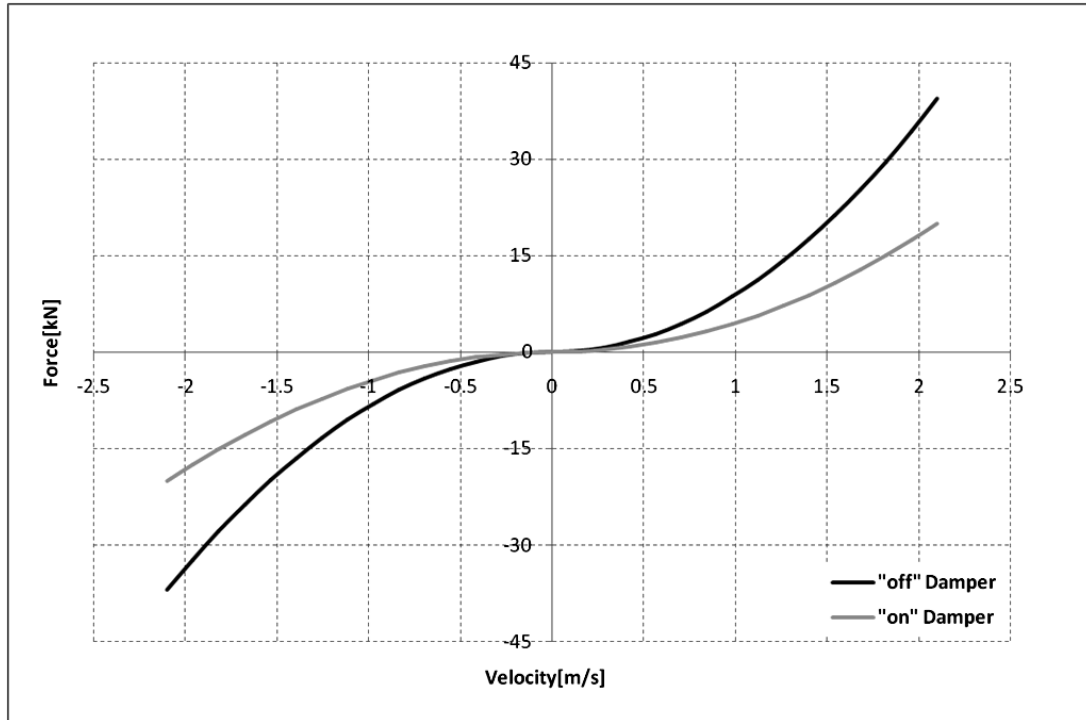


Figure 3-31 Hydro-pneumatic on-off damper characteristic.

As shown, the velocity-force curves of the hydro-pneumatic damper are not linear and rise in a progressive way. It means that damper coefficient is not constant, but also it increases with raising the damper velocity.

3.2.3 Cylinder Friction Model

In this section, the modeling of the friction effect in the hydro-pneumatic suspension is considered. Friction is an unwanted effect in a suspension system and reduces its performance. Similar to damping force, the friction force is always in the opposite direction of the suspension movement. There are two kinds of frictions in a hydro-pneumatic suspension.

The first kind of friction is created by the contact of oil with the inner area of other components like pipe, cylinder, and throttle. This friction produces a pressure drop proportional to the velocity of the suspension. Then, the cylinder converts this pressure to a force similar to the damping force of the system. The example of this case is the friction effect of the throttle that is the source of the damping force in a hydro-pneumatic suspension. In this study, this kind of friction was also considered in the damper model. Therefore, this kind of friction is considered as a useful effect, because it can be estimated in the damping design of the system.

The second kind of friction is created by the contacts among the solid components of a suspension, like the contact between a piston and the cylinder body or the contacts among components of the mechanical mechanism of a suspension. This kind of friction is harmful, because firstly, this friction is difficult to be calculated, and secondly, it is not proportional to the suspension velocity and cannot be considered as the damping effect of the system. Among these kinds of frictions, the static friction is particularly problematic, because it appears at the beginning of the motion of the suspension, as no damping force is needed. The cylinder is one component of a hydro-pneumatic suspension that produces this kind of friction. This friction occurs because of the contact between the piston and cylinder body through their sealing set (Fig. 3-32).

In order to consider the friction effect in the suspension model, in this section, the model of the friction effect in the cylinders is built. For this purpose, the well-known friction model of Coulomb is used. In this model, the friction force is independent of the slip velocity. However, the friction coefficient with the slip velocity near zero is in practice higher (Fig 3-

33). This primary friction, calling as static friction, is more effective in suspension performance, and it should be considered particularly in the friction model of the cylinder.

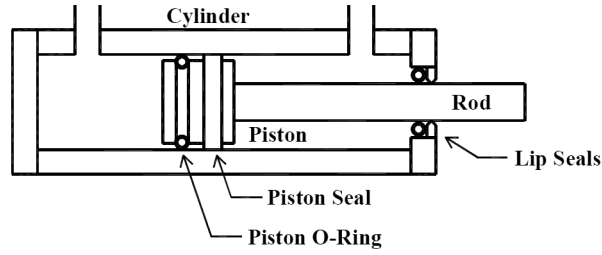


Figure 3-32 Hydraulic cylinder and relevant sealing components.

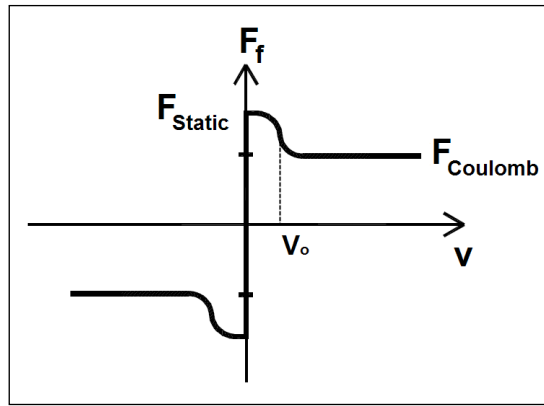


Figure 3-33 Relation of coulomb and static friction forces with the slip velocity of a hydraulic cylinder.

Since coulomb and static friction are constant. The friction model of the cylinder is indeed a switch that determines which one of these two friction forces adds to the cylinder force. The mathematical model of the cylinder friction is defined as:

$$F_f = \begin{cases} F_{static} & (|v| - v_o) \leq 0 \\ F_{static} + F_{coulomb} & (|v| - v_o) > 0 \end{cases} \quad 3-26$$

In this formula, v_o is the symbol for the limit velocity of the static friction. Based on this formulation, the Simulink model of the cylinder friction is built (Fig. 3-34).

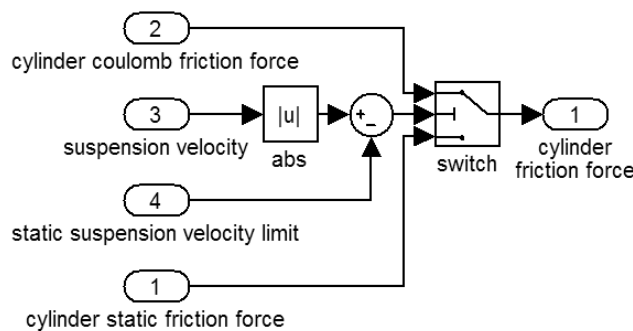


Figure 3-34 Simulink model of the cylinder friction.

As mentioned, the coulomb friction force, static friction force, and static limit velocity are constant values, and they are considered as the model parameters. In simulation, it was supposed that the coulomb friction force of the hydro-pneumatic cylinder was negligible, and the static friction force were determined via experimental measurement on the cylinder of the prototype model. The Simulink model of the cylinder friction will be used in the model of the hydro-pneumatic rear suspension presenting in the following section.

3.2.4 Overall Hydro-pneumatic Suspension Model

As was explained, in this investigation, the hydro-pneumatic rear suspension of the tractor was equipped with a controllable damping system in order to be used as the actuator for the semi-active suspension system. Figure 3.35 shows the circuit of the one unit of this hydro-pneumatic suspension. For the modeling of this system, the hydro-pneumatic suspension is divided into the two components: the hydro-pneumatic spring and the hydro-pneumatic variable damper. The spring model consists of two components of the cylinder and accumulator models, and variable damper consists of three components: throttle, cylinder port, and valve models. Modeling of all these components was presented in the previous sections. The final model of the actuator is created by joining all these components. In this section, this model is presented.

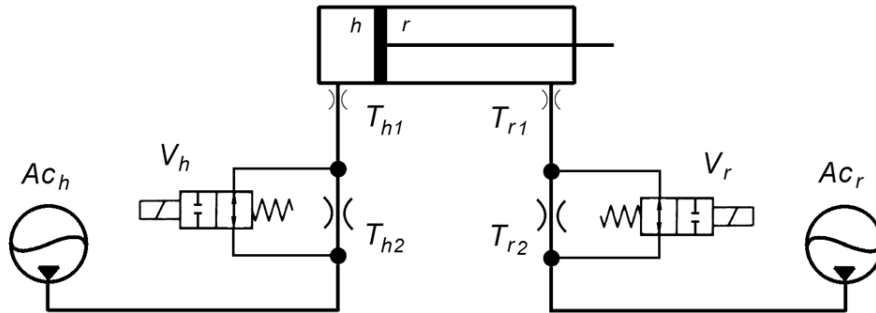


Figure 3-35 Circuit of the one unit of the controllable hydro-pneumatic suspension used for the tractor rear suspension.

Figure 3-36 shows the final Simulink model of the hydro-pneumatic actuator unit, which consists of four sub-models: cylinder, accumulator, throttling system, and cylinder friction. Main component of this model is the cylinder model. This model receives the displacement and the velocity of the suspension as the model inputs and delivers the suspension force as the model output. By receiving the suspension input, the cylinder model

calculates the oil volume variation of both sides of the cylinder and sends these values to the accumulator models.

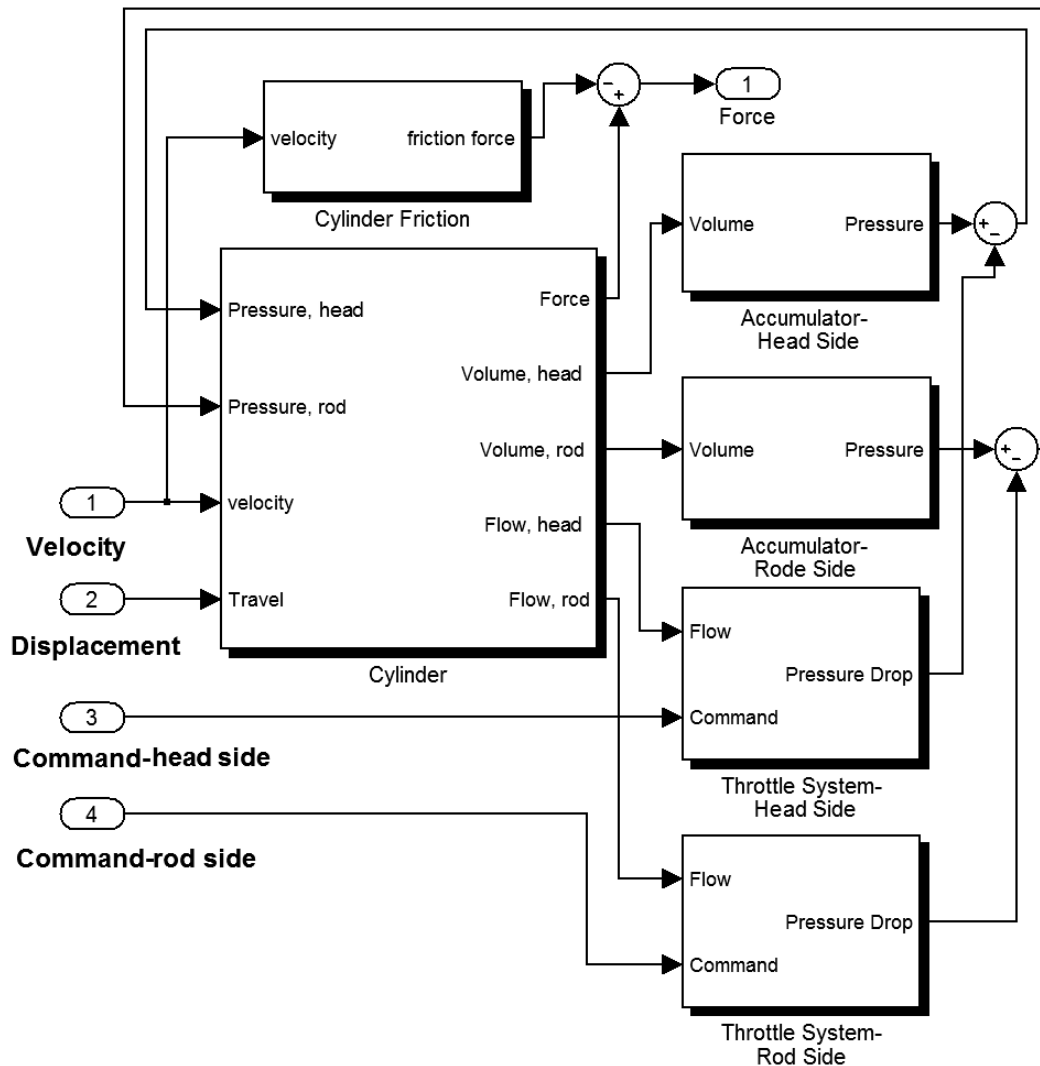


Figure 3-36 Simulink model of the hydro-pneumatic actuator system.

On each side of the cylinder, the accumulator model calculates the created pressure and sends it back to the cylinder model. This model can convert the received pressure to the cylinder force. However, the effect of the throttle system on this pressure drop must be considered before. For this purpose, the throttle model receives volumetric flow from the cylinder model and based on the control command, determines the created pressure drop. Now, total pressure of the cylinder can be calculated by subtracting this pressure drop from the accumulator pressure. Based on this pressure, the cylinder model calculates the output force. In the same time, the cylinder friction model calculates the friction force based on the

cylinder velocity. Therefore, the final suspension force is achieved by subtracting the friction force from the cylinder force.

After building the hydro-pneumatic suspension model, this model can be applied to the full tractor model. For this purpose, the simple linear model for the rear suspension units is replaced by the hydro-pneumatic suspension model (Fig. 3-37).

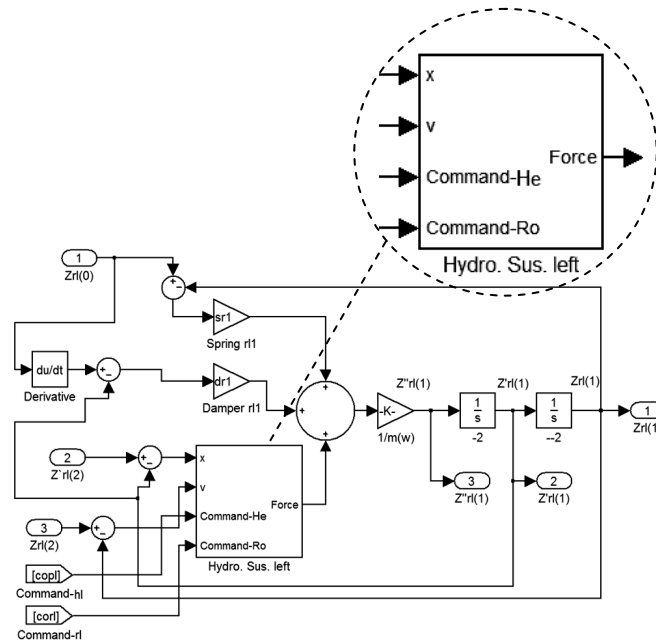


Figure 3-37 Using of the model of the hydro-pneumatic suspension in the Simulink full tractor model.

After this modeling, the last step is remained to complete the final simulation model. This step is to create the controller model, and it will be presented in the following section.

3.3 Controller Model

The structure of the semi-active suspension system is illustrated in figure 3-38. This structure consists of four components: tractor dynamics, actuator, sensors, and controller. These components work all in a close loop. The controller monitors the dynamic behavior of the tractor via the sensors. Then, based on the relevant control strategy, it produces the control commands and sends them to the actuator in order to improve tractor dynamics.

In the previous sections, building the vehicle model and actuator model were presented. Now in this section, modeling of the rest components of the system, namely sensors and controller are considered. The sensors measure the vehicle dynamics

parameters. The signals of these parameters are prepared by the signal conditioning system and are sent to the controller. With ignoring the probable errors of the sensors, there is no need to model this part of the system, because the parameters of the tractor dynamics can be read directly from the full vehicle model and sent to the controller. Therefore, modeling of the sensors is not covered in this study. On the other hand, the second part is the controller, which has an important role in the overall system. Model of the controller receiving the sensors information, produces the control commands based on the control strategy and send them to the actuators.

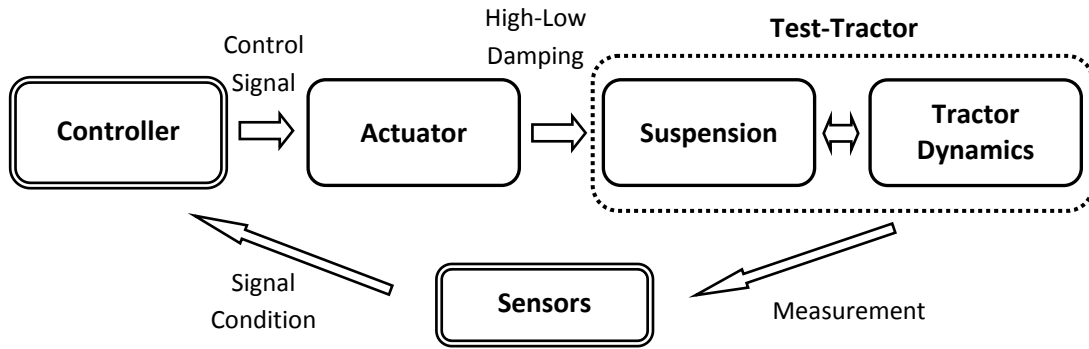


Figure 3-38 Position of the controller and sensors in the overall control system.

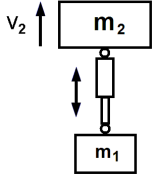


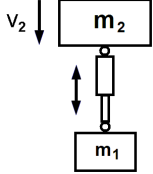


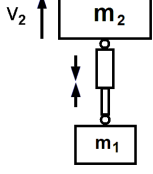


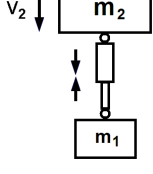


As mentioned before, the control strategy used in the study is the on-off skyhook strategy presented in details in section (2.2.5). This control strategy uses the same control conditions as the classic skyhook strategy, which is based on the control inputs of the absolute velocity of the sprung mass and the relative velocity of the unsprung mass. However, the output of this strategy is not continuous similar to classic skyhook strategy, and it is limited only to the two high and low levels of damping. The formulation of this strategy can be presented as:

$$c_2 = \begin{cases} c_{high\ state}, & \dot{z}_2 (\dot{z}_2 - \dot{z}_1) \geq 0 \\ c_{low\ state}, & \dot{z}_2 (\dot{z}_2 - \dot{z}_1) < 0 \end{cases} \quad 3-27$$

Based on this formulation, the working of this control strategy is illustrated in table 3-10. In this table, based on the movement direction of the sprung mass (i.e. m_2) and unsprung mass (i.e. m_1), four working phases are defined, and in each one, operation of the semi-active damper is compared with the operation of the passive one. In the first phase, the sprung mass moves upwards and two masses separate. In this condition, damper is

expanded, and sprung mass is pulled down. This means that the damping force works usefully against sprung mass movement. Therefore, control strategy switches to the high level of damping in order to magnify the useful damping force.

Table 3-10 Illustration of the working of on-off skyhook control strategy.

Switching Mode		Damping force	
		Passive	Semi-active
1	 $v_2 \geq 0$ $(v_2 - v_1) \geq 0$		on-state 
2	 $v_2 < 0$ $(v_2 - v_1) > 0$		off-state 
3	 $v_2 > 0$ $(v_2 - v_1) < 0$		off-state 
4	 $v_2 \leq 0$ $(v_2 - v_1) \leq 0$		on-state 

In the second phase, the sprung mass moves downwards and two masses separate from each other. In this condition, again damper is expanded, and sprung mass is pulled down that means damping force works negatively in the same direction as sprung mass movement and support it. Therefore, control strategy switches to the low level of damping in order to minimize the undesirable damping force. In the third phase, the sprung mass moves upwards, and two masses come together. In this condition, the compressed damper pulls up the sprung mass. In this mode, damping force works negatively in the same direction as sprung mass movement and supports this mass. Therefore, control strategy switches again to the low level of damping in order to minimize the undesirable damping force.

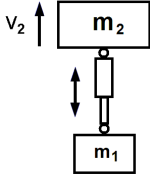
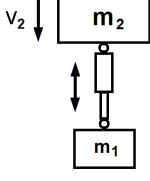
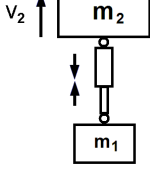
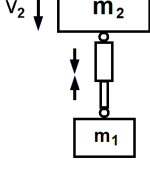
Finally, in the fourth phase, the sprung mass moves downwards, and two masses come together. In this condition, the compressed damper pulls up the sprung mass. In this mode, damping force works usefully against sprung mass movement. Therefore, control strategy switches to the high level of damping in order to magnify the useful damping force. To sum up, semi-active damper is tuned in the high level of damping, as damper force can be useful for the damping of the sprung mass vibration. In opposition, semi-active damper is tuned in the low damping level as the damper force is against damping of the sprung mass vibration.

After the description of the control strategy, at this point, the method of applying the control signals to the actuators should be determined. As mentioned before, the actuator of each suspension unit is a double-acting cylinder with a throttle system on each side of it. As experimental observations, it was found as the flowing oil toward the cylinder was throttled, a vacuum effect was occurred in the cylinder, which was a disturbing phenomenon in hydro-pneumatic suspension. On the other hand, this effect did not appear during the throttling of the pressurized oil coming from the cylinder.

Therefore, as a design rule in this investigation, the high damping command of the controller is applied to the throttle system of the just one side of the cylinder. It is the side that oil is leaving the cylinder. The created damping level is the same as the determined value, regardless of the cylinder side. Table 3-11 illustrates control commands in the four control phases with respect to this rule. As shown, with the positive relative velocity, the control command is applied to the throttle system of the rod side, and with the negative relative velocity, the control command is applied to the throttle system of the head side.

Based on the table 3-11, the Simulink model of skyhook control strategy is built (Fig. 3-39). The inputs of this model are the absolute velocities of the sprung and unsprung masses, and the outputs of the model are control commands, which are applied to both the throttling systems of the head and rod sides of the cylinder. After building the controller model, in order to examine its function, two sinusoidal waves were applied to the model as the test input. Figure 3-40 shows the result of this test. The inputs waves and both rod and piston cylinder control commands are shown in this chart. As shown, the outputs of the model are created correctly based on the determined control approach.

Table 3-11 On-off skyhook control commands for the double-acting hydro-pneumatic cylinder.

Switching Mode	Damping State	Head Side	Rod Side
<p>1</p>  $v_2 \geq 0$ $(v_2 - v_1) \geq 0$	<i>Hight</i>	<i>off</i>	<i>on</i>
<p>2</p>  $v_2 < 0$ $(v_2 - v_1) > 0$	<i>Low</i>	<i>off</i>	<i>off</i>
<p>3</p>  $v_2 > 0$ $(v_2 - v_1) < 0$	<i>Low</i>	<i>off</i>	<i>off</i>
<p>4</p>  $v_2 \leq 0$ $(v_2 - v_1) \leq 0$	<i>Hight</i>	<i>on</i>	<i>off</i>

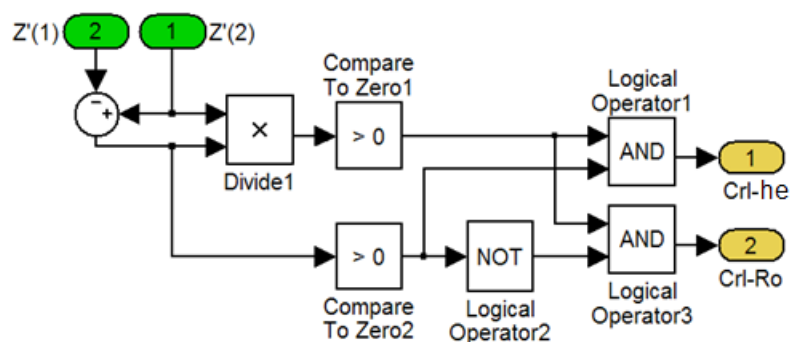


Figure 3-39 Simulink model of skyhook on-off controller for one suspension unit.

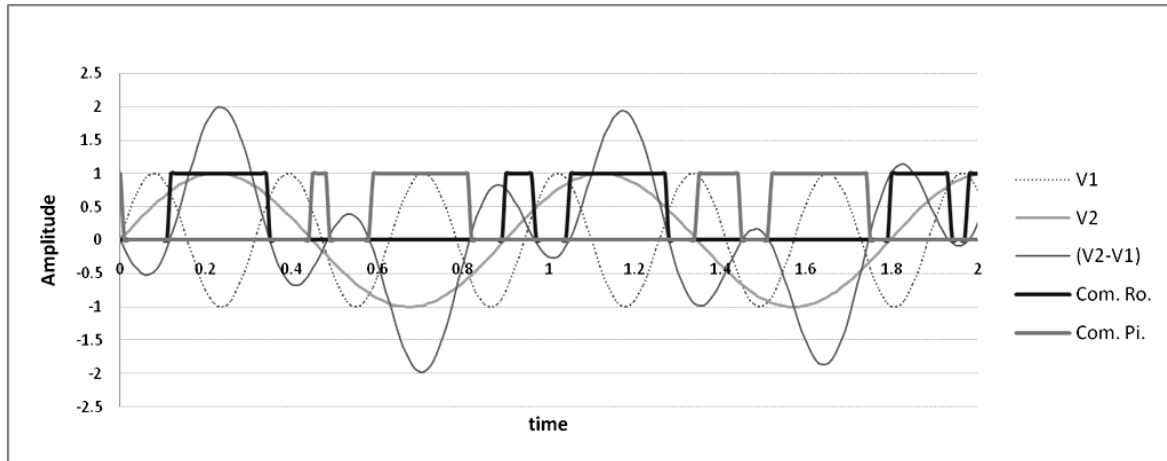


Figure 3-40 Control command for the rod and head cylinder sides using two sinusoidal waves as the input of control.

Figure 3-41 also shows how the controller model is joined to the full vehicle model. Absolute velocities of the sprung mass and unsprung mass in the rear suspension units are used as the input of the controller model. The outputs of the model are sent to the tractor model. These outputs are the commands of the head and rod cylinder side of the tractor model. The commands are applied to the models of the hydro-pneumatic rear suspension of the tractor. This model is described in detail in section 3.2.4.

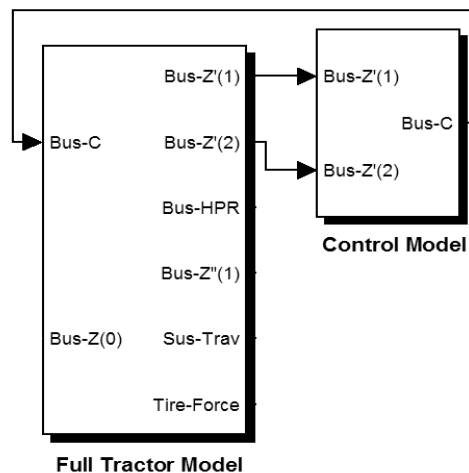


Figure 3-41 Connection of the Simulink control model to the full tractor model.

After the modeling of the controller and joining this model to the full tractor model, the full tractor model is ready to be used for the simulation tests. However, the proper design for the tests is needed and must be determined before. This subject will be presented in chapter 5. In addition, the result of the simulation tests will be presented in chapter 6. However, before presenting these chapters, the prototype phase of this study will be presented in the following chapter.

Chapter 4

Development of the Semi-active Suspension

In the previous chapter, modeling of the semi-active suspension system was presented. The created overall model was a virtual prototype that was used for the simulation study of the system. In addition to the simulation study, experimental study is also intended in this investigation. For this purpose, first, an actual prototype of the system is needed. This chapter describes the development of this physical prototype.

This prototype is indeed the physical version of the virtual prototype, presented in chapter 3, and has the same structure. This structure is illustrated in figure 4-1. As shown, the physical prototype is a test-tractor attaching to the control system consists of three components: sensors, actuator, and controller. The sensors measure the required parameters of the test-tractor dynamics and send them to the controller. The controller used for this system is a digital controller.

Therefore first, the sensor signals are converted to digital signals, then these digital signals enter to the controller. After that, based on the skyhook on-off control strategy written by computer software, the controller produces the control commands of high-low damping. These commands apply to the valves of the actuator system through a relay system. All these steps are performed in a close control loop that creates the semi-active control of the suspension system.

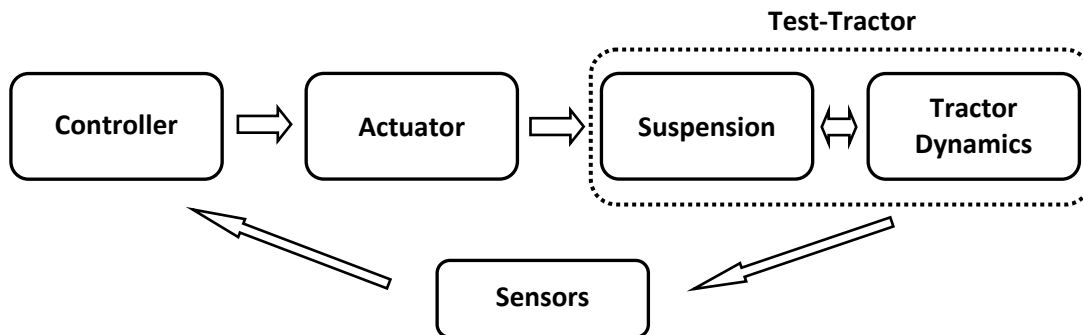


Figure 4-1 Structure of the actual prototype of the control system.

In this chapter, development of the physical prototype is presented in four parts: test-tractor, actuator, sensors, and controller. At the first part, the tractor used as a test-tractor is

introduced. Then, building the actuator system that is the hydro-pneumatic rear suspension of the test-tractor with a controllable damping system is presented. After that, the sensors of the control system and installation of them on the test-tractor are explained. At the end, development of the hardware and the software parts of the controller is described.

4.1 Test-Tractor

A semi-active controller prototype cannot be evaluated by itself. It can be evaluated, when the semi-active controller is applied to the suspension of a tractor, and the influence of this system on the dynamics of the tractor is measured. Therefore, as the first step of prototype developing, a tractor was determined as the test-tractor of the system. As stated in section 2.6.6, the test-tractor used for this investigation was TUB-Trac (Fig. 4-2).

This tractor was indeed MB-1600 tractor that was converted to a full suspension tractor by attaching a hydro-pneumatic suspension on the rear axle. This work was performed before at the TU Berlin - Department Machinery System Design as a research project, and after that, it is called TUB-Trac and used for research works in suspension area as a test-tractor. Figure 4-2 shows this tractor and relevant rear and front axle suspensions.



Figure 4-2 Test-tractor with the conventional suspension of the front axle and the hydro-pneumatic suspension of the rear axle.

This tractor is a full suspension tractor with a hydro-pneumatic suspension for the rear axle. A full suspension system is considered as the most complete passive suspensions for a tractor. As the next step, the application of an active suspension is defined. This provides better suspension performance, which is the objective of this investigation. On the other hand, the hydro-pneumatic suspension can be converted simply to an active suspension system. This is possible because of the simplification in building the actuation

system (refer to section 2.5 for more detail). Therefore, this tractor was selected as a proper test-tractor for this study, and its hydro-pneumatic rear suspension was equipped with the physical prototype of the semi-active control system. Next section describes the actuation system of the semi-active system that was developed on the hydro-pneumatic rear suspension of the test-tractor.

4.2 Hydraulic Actuator

In an active suspension system, the actuator is a part of the system between the controller and the suspension that applies an external force, determined by the controller, to the suspension of the vehicle. Depend on the control type, there are different kinds of actuators. In a semi-active suspension with skyhook on-off control strategy, the actuator is a controllable damper with the high and low damping levels. This system was used for this investigation.

In order to use the test-tractor as a prototype in this study, the semi-active control was applied to the hydro-pneumatic rear suspension of the test-tractor. For this purpose, the actuator of semi-active system was added to this suspension system. Figure 4-3 shows the circuit of the hydro-pneumatic suspension including two separate suspension units. Each unit was equipped with an actuation system that was a controllable throttling system, consisted of a throttle and a valve, which stood in parallel. By controlling the valve, the double damping level was created. In addition to controllable throttling system, each suspension unit consisted of a hydraulic cylinder, two accumulators. Table 4-1 identifies all these components.

As shown in figure 4-4, all these components except cylinders were installed on a board on the rear part of the tractor. The cylinders were placed between the wheel and chassis in the position of the conventional springs and dampers (Fig. 4-5), because in a hydro-pneumatic suspension system, the cylinders generate both the damping and spring forces. Since these cylinders work with just vertical forces, lateral forces must be nullified from it. For this purpose, in the test-tractor, for the cylinders connection to the chassis, a joint-type linkage was used (Fig. 4-6). Because of this connection, there was a relative small movement between the cylinders and chassis, and therefore, the connection of the cylinders to the hydraulic board was created by the elastic pipes (Fig. 4-5).

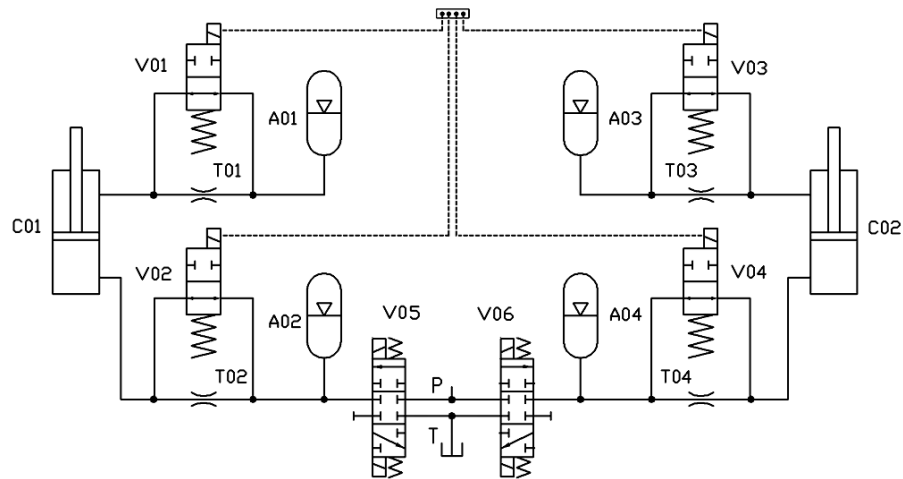


Figure 4-3 Hydraulic circuit of the hydro-pneumatic suspension with controllable damping system.

Table 4-1 Hydro-pneumatic suspension components in respect with figure 4-5.

No.	Component	Side	Unit	Sym.	No.	Component	Side	Unit	Sym.
1	hydraulic cylinder	-	left	C01	10	throttle	head	right	T04
2	hydraulic cylinder	-	right	C02	11	parallel valve	rod	left	V01
3	accumulator	rod	left	A01	12	parallel valve	head	left	V02
4	accumulator	head	left	A02	13	parallel valve	rod	right	V03
5	accumulator	rod	right	A03	14	parallel valve	head	right	V04
6	accumulator	head	right	A04	15	leveling valve	-	left	V05
7	throttle	rod	left	T01	16	leveling valve	-	right	V06
8	throttle	head	left	T02	17	elastic cylinder pipes	-	-	-
9	throttle	rod	right	T03	18	steel pipes	-	-	-

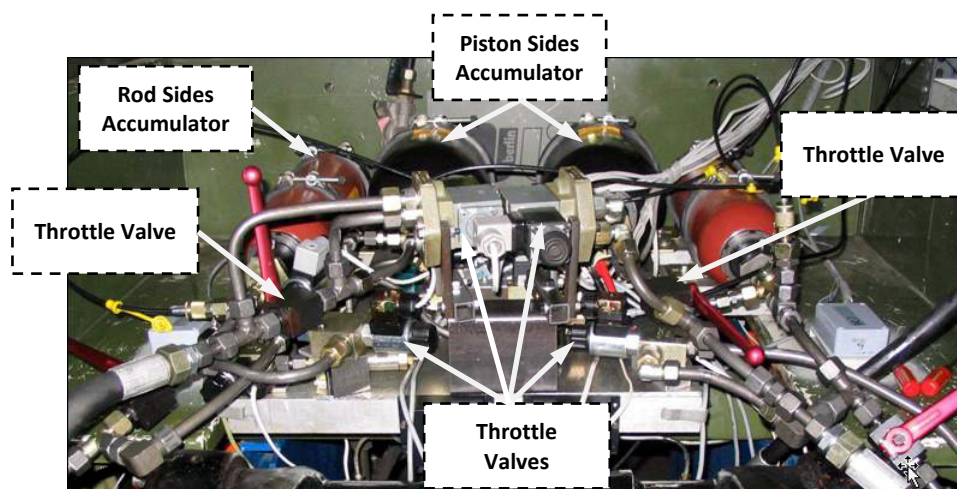


Figure 4-4 Hydraulic components of the hydro-pneumatic rear suspension with controllable damping system.

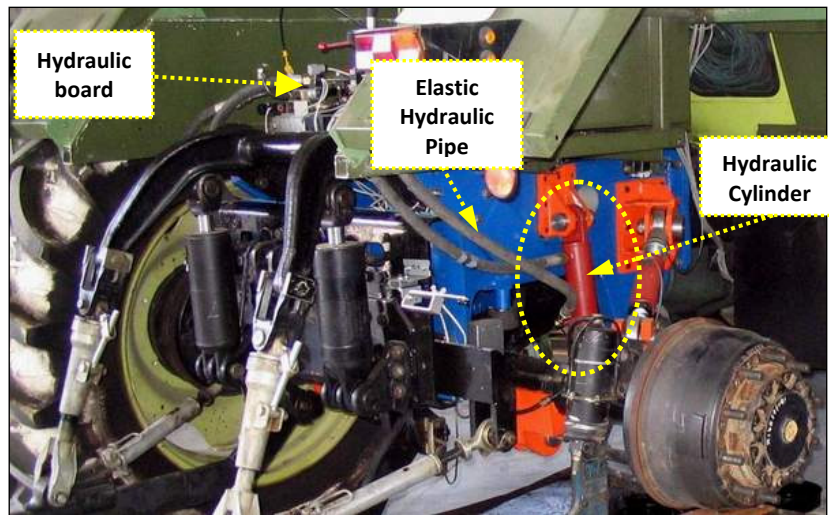


Figure 4-5 Position of the hydraulic cylinder in the rear axle suspension of the tractor.

These cylinders were specialized hydro-pneumatic suspension cylinders, which were equipped with a special seal system in order to provide a low friction level. The cylinders used for rear axle suspension were double-acting type providing the feasibility of controlling on both sides of the cylinder. Likewise, in this investigation, the throttling system was applied to both sides of the cylinder.

Another point about the cylinders is the throttling effect of their ports. As stated chapter 3, this throttling effect was considered in the design calculation of the damper for the system as the only throttling effect of the system in the mode of low-level damping. Figure 4-6 shows these cylinder ports. The detailed specification of the cylinder such as the piston area, ports cross-section, and friction force are presented along with simulation parameters in appendix E4.

Specific property of the hydro-pneumatic suspension that was used for this study was the control ability of the damping level of the suspension. This ability was created in the prototype by mean of a special throttling system comprised of a throttle and a parallel valve (Fig. 4-4 and Fig. 4-7). Working of this system was described in section 3.2.2. The throttle used in the system was an adjustable throttle-valve providing the high damping level and passive damping level for the suspension. This valve also provided the possibility of testing of other damping levels for these two damping modes. Determination of the proper value for these two damping levels was described in section 3.2.6.

The valves, standing in parallel with the throttles, were the only controllable elements of the system that provide the ability of controlling the damping level of the

system. The implementation of this system is illustrated in figure 4-7, which is consistent with the hydraulic circuit shown in figure 4-3. In the throttling system, as the valve was turned on, a parallel way was created for oil flow. The throttle cross-section of the valve was so much that by opening this parallel way, the total pressure drop of throttling system fell into a negligible value, and as a result, the damping effect of throttling system was removed, and just the cylinder ports provided a low throttle effect for the low level of damping.

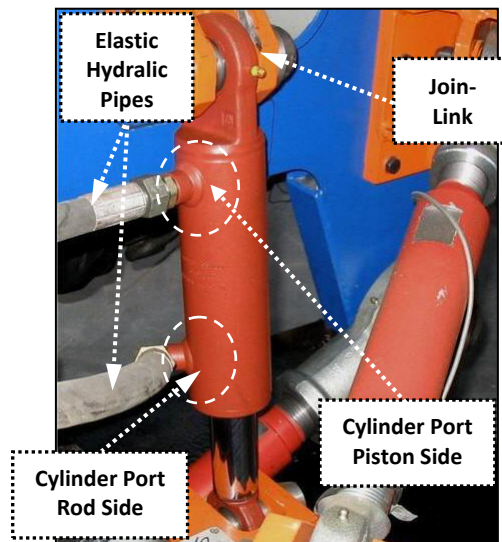


Figure 4-6 Hydraulic cylinder and head/rod side ports.

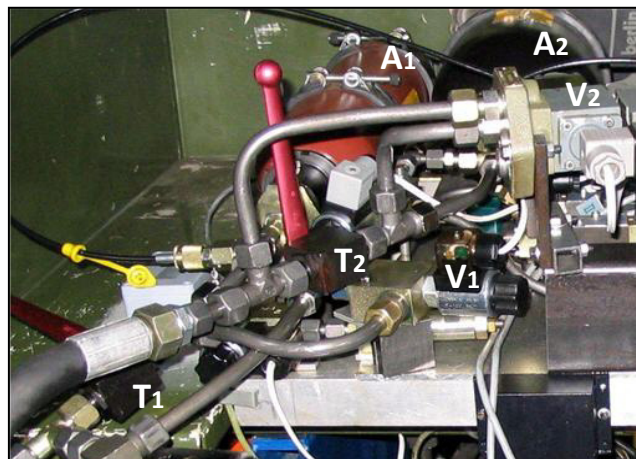


Figure 4-7 A view of throttling system used for controlling the damping level of the suspension, T: throttles, V: valves, A: accumulators.

In order to simplify the work of the throttle damping system, figure 4-8 shows the equal electrical circuit of the controllable throttling system. The resistors are equivalent to the pressure drop sources of the throttle and valve, and the valve is considered as a relay in series with a low value resistor showing the low pressure drop of the valve. As relay is turned

on, the low value resistor stands in parallel to the high value resistor of the throttle. This decreases completely the total resistance, so that just the resistor of the cylinder port stays in the circuit.

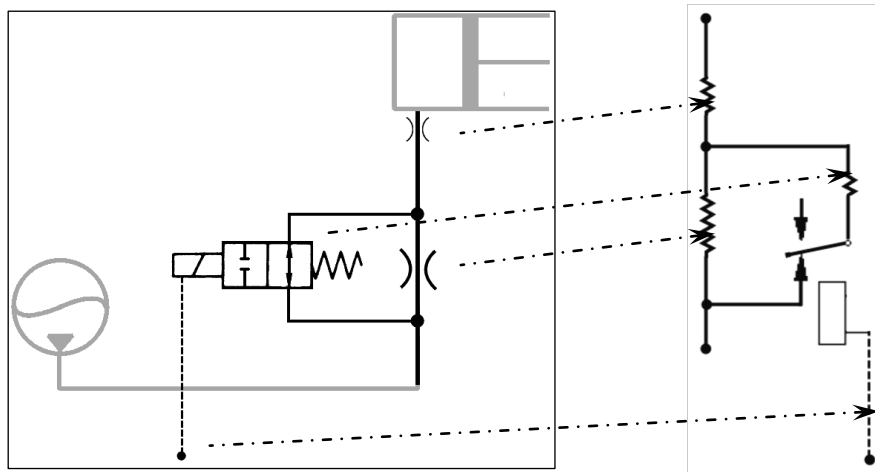


Figure 4-8 Throttle damping system with equivalent electrical circuit.

As a result, the calculation of total pressure drop for two damping levels can be derived from the equal electric circuit as follow:

"High" Mode,

$$\Delta P_{total} = \Delta P_{port} + \Delta P_{throttle}$$

4-1

"Low" Mode,

$$\Delta P_{total} = \Delta P_{port} + \frac{\Delta P_{throttle} \cdot \Delta P_{valve}}{\Delta P_{throttle} + \Delta P_{valve}} \cong \Delta P_{port}$$

Therefore, for selecting the valves, there was no need to calculate the quantity of their throttling effect and just the throttle cross-section of the valve had to be in a size that the total pressure drop would be negligible. With this design, the throttling effect of this part of the system was removed. The characteristic curves of the 2-way solenoid valves used for controllable throttling system, was derived from relevant hydraulic handbooks. These curves indicate the relation between the pressure drop and flow rate of the valves and were used in order to determine the throttling effect of the valves in different flow rates. This was done to ensure that in the mode of low damping, the throttling effect of the parallel throttle set was negligible. In other words, the parallel throttle set was equal to a piece of hydraulic pipe connection in this mode.

In addition to throttle electro-valves, there are two other directional solenoid valves in the hydraulic circuit (V05 and V06 in figure 4-3). These valves were used by auto leveling control system as an actuation system to adjust the suspension height of the tractor. These

valves were used in a way that by receiving the control commands, the head side of the cylinder was connected to the pressurized oil. This filled the cylinder and increased the suspension height. On the other hand, in order to decrease the suspension height, the cylinders were discharged by connecting to the oil tank via the valves. More detail about load leveling will be given in section 4.5.2.

Another component of a hydro-pneumatic suspension is the accumulator, which creates the spring force of the system. The accumulators used for the system were bladder-type, which provides a good dynamic response in hydro-pneumatic suspension (refer to Fig. 4-4 and 4-7). Volume capacity of the accumulators was selected so that to cover the maximum volume of the cylinder. Moreover, the pre-charge gas pressures of the accumulators were adjusted by adding pressurized nitrogen gas with respect to the determined values mentioned in appendix E4. At this point, after the description of actuation system, the controller components of the prototype will be explained in the following sections.

4.3 Velocity Sensors

In order to find the require sensors for the semi-active suspension system, it should be referred to Section 3.3 that describes skyhook on-off control strategy used for the semi-active suspension. Looking at table 3-11, the needed parameters can be identified that are the absolute velocity of the tractor body (i.e. sprung mass) and the relative velocity between the tractor body and wheel (i.e. unsprung mass). On the prototype, each unit of the semi-active suspension was considered independent and, in order to measure the velocity of the sprung mass (m_2), the velocity of the corners of the tractor body was measured (Fig 4-9). Moreover, in order to measure the velocity of the unsprung mass (m_1), the velocity of the corners of the rear axle was measured.

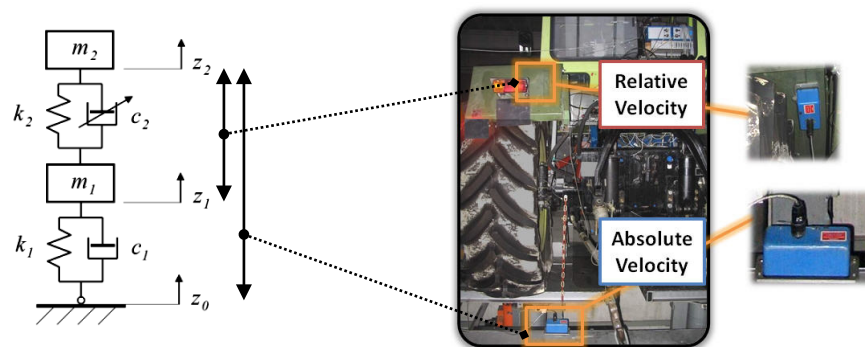


Figure 4-9 Using velocity sensors for the on-off semi-active control on the rear axle suspension.

One technique used for measuring the absolute velocity is to derive it from the absolute accelerometer signals. For this purpose, the absolute acceleration of the tractor body is measured by an accelerometer. Then, accelerometer signals are integrated in order to achieve the corresponding velocity signals. The integration could be performed either digitally by a computer or in analog by an integrator circuit. However, because of the necessary signal integrating, this method is considered as a difficult method and associated with errors.

In this investigation, the experimental tests were performed on a suspension test rig, and it was not needed to move the tractor during the tests. Therefore, it was possible to measure the absolute velocity directly by velocity sensors. For this purpose, a cable-type of velocity transducers was used in order to measure the absolute velocity of the tractor body. This sensor was fixed on the ground, and then, cable of the sensor was fixed to the directly upside point of the tractor body (Fig. 4-9).

In order to measure the relative velocity between the tractor body and wheel, again, a cable-type of velocity transducers was installed on the tractor mudguard, and then, the cable was fixed to the directly downside point of the wheel (Fig. 4-9). Technical data of this transducer is presented in appendix C2. The velocity signal of this transducer was out of noise, linear and self-energizing. In this way, a proper signal for the control system was provided. In spite of this, in order to remove the effect of the high frequency vibrations on the vibrations signal, an external low pass filter with the cut-off frequency of 25 Hz was used. This filtered the transducers signals before applying them to the controller.

4.4 Controller Hardware

Development of the components of the control system including test-tractor, actuator, and sensors were described in the previous section. At this point, development of the controller is explained. Figure 4-10 illustrates the structure of the used controller for this investigation. This controller was indeed a personal computer with control software that was connected to the control input-output via an interface card.

As the input of control, the analog signals of the velocity transducers were applied to the interface card, while this interface card worked just with digital signals. Therefore, an ADC circuit was used in order to covert the analog signals to the digital ones before entering to the interface card. On the other hand, the interface card was not able to drive the solenoid valves directly. Though the digital output signal of the interface card was matched

to the input signal of the on-off valves, interface card output was not enough powerful to operate the solenoid valves directly. Therefore, an electronic relay system was used to amplify interface card output signal.

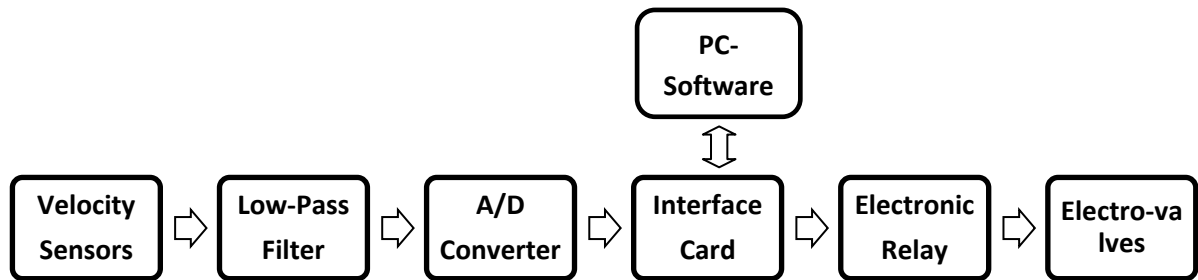


Figure 4-10 Schematic of the control hardware of the semi-active suspension system.

In the following section, development and function of the hardware components of the control system will be presented. At first, the A/D converter circuit is described. Then, interface card and the electronic relay system are explained.

4.4.1 A/D Converter

Generated signals of the velocity transducers were analog, while the computer-based controller could work just with digital inputs. Therefore, transducers signals had to be firstly converted to digital signals. At first, the internal ADC, present in the interface card was considered. The primary test of this circuit showed that a considerable delay was put on the control loop, and control bandwidth was reduced after using this converter. On the other hand, for skyhook on-off control strategy, just the sign of absolute and relative velocities was needed not the value of them (refer to equation 3-27). Therefore, a special external electronic circuit was developed only in order to distinguish the sign of velocities signals. Based on the sign of velocities signals, this circuit created a digital code in the outputs. This circuit had simpler function than a usual A/D converter, worked very faster, and had no affect the control bandwidth.

The electronic circuit of this external A/D converter that is in fact a voltage comparator using fast electronic elements is shown in figure 4-11. The analog signal entering to this circuit is in the range of -2V until 2V. First, Op-Amp (Op 1) centers the velocity signal at 2.5 V and limits it to the voltage range of 0 - 5V. Then, this signal is applied to the two other Op-Amps, which works as voltage comparator. If the transducer signal is negative (indicating the negative velocity), Op-Amp 2 generates a “1” digital signal in its output (out

1), and if the transducer signal is positive, which indicated the positive velocity, Op-Amp 3 generates a “1” digital signal in its output (out 2). Figure 4-12 shows the output of the circuit for a sinusoidal wave input.

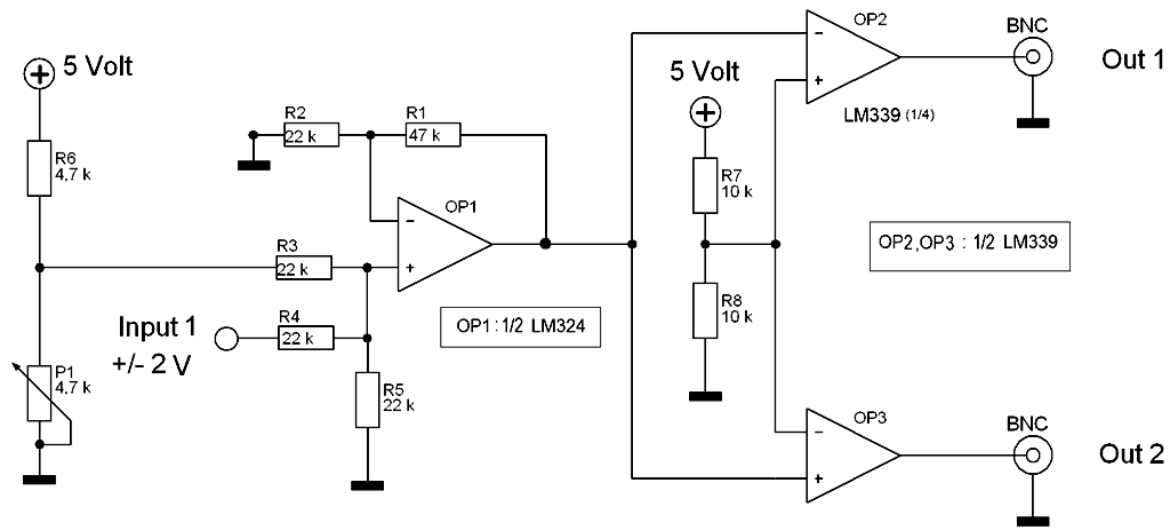


Figure 4-11 Electronic circuit of a ADC unit.

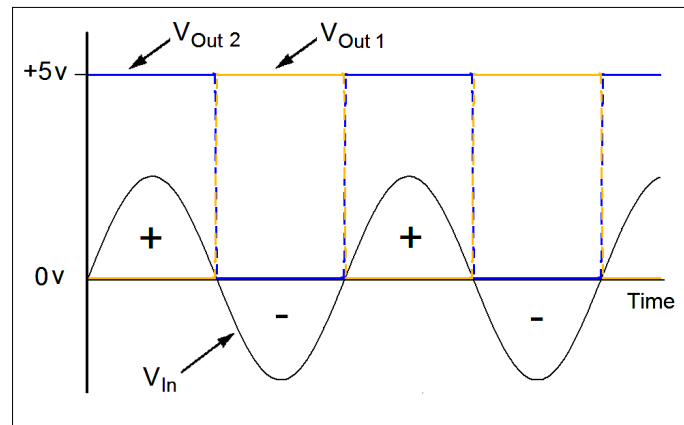


Figure 4-12 Digital output of the ADC circuit, entering a sinusoidal wave input.

Such an ADC circuit was used for each velocity transducer signal. Therefore, the four units of this circuit were used for the four velocities signals coming from the velocities sensors of the system. The output digital signal was fitting to the input of the interface card, and it could be applied directly.

4.4.2 Interface Card

The digital controller in this investigation was a personal computer that was communicated to the inputs and outputs of control via an interface card. The interface card used for this investigation was a data acquisition card (NI-DAQ) from National Instruments,

providing different digital-analog ports for the controller. Figure 4-13 illustrates the internal structure of this card, and figure 4-14 shows external construction of it. The detailed technical data of this card is presented in appendix C3.

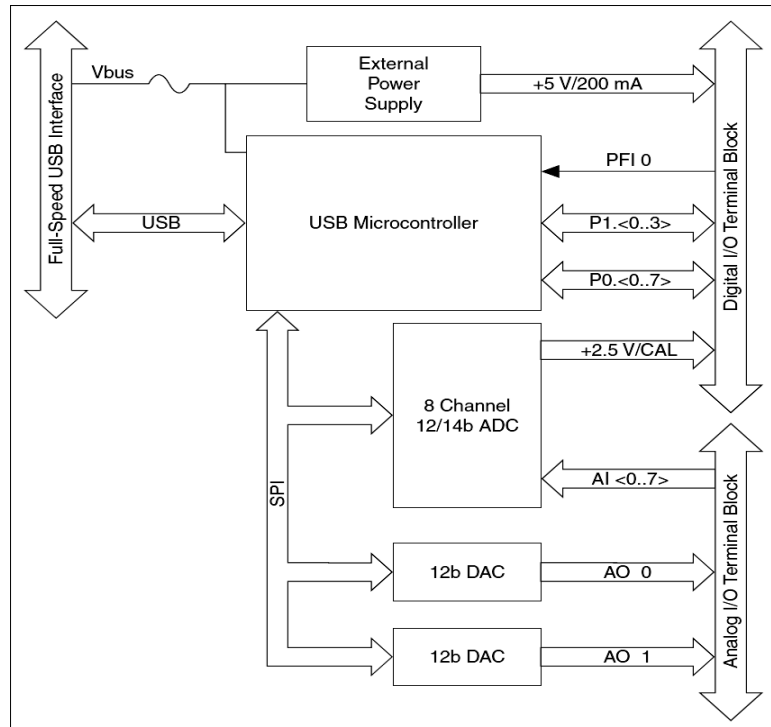


Figure 4-13 NI-DAC Interface card internal structure.

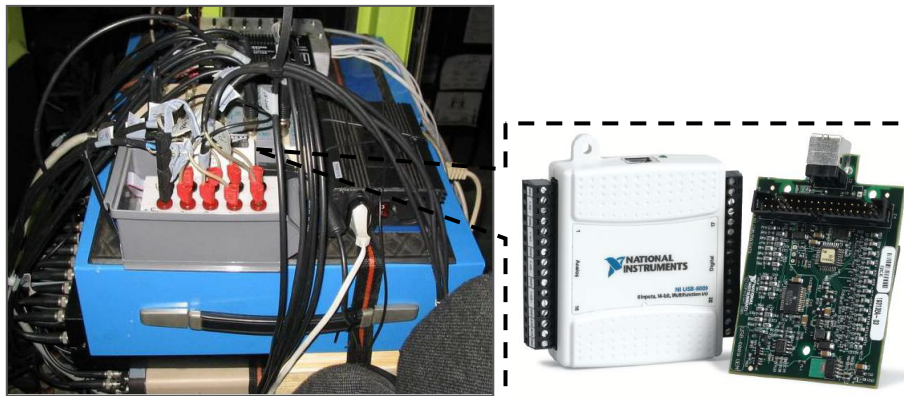


Figure 4-14 NI-DAC Interface card and relevant connection to the input-output devices.

This interface card uses a computer driver set called DAQ mxBase. As this software is installed, a new function set called mxBase is added to the function palette of LabVIEW software. This new set contains the mxBase functions of “Open”, “Read”, “Write”, and “Close”. LabVIEW is the software that the program of the control strategy was written by (refer to Fig. 4-18). In this program, these new functions were used in order to link the

controller program to the inputs and outputs of the card, which were indeed the control inputs, and outputs.

As shown in figure 4-13, the core of this interface card is a controller that communicates with the computer through a USB port and provides the digital inputs and outputs for the computer. Besides this controller, there are A/D and D/A converters. By these converters, the card can receive the analog inputs and create analog outputs. However, they were not used in the suspension controller, because the bandwidth of the card would be decreased until 10 kHz after using these converters, and the controller bandwidth would be reduced largely. Therefore, instead of the internal ADC, an external ADC was developed and used for converting the control inputs. This external converter was described in the previous section. By using the external converter, just the digital ports of the interface card were used. This led that interface card worked with high sampling rate, so that, the effect of card delay in control bandwidth was negligible.

The interface card was placed in the driver cabin beside other electronic components so that it could be connected directly to the input-output of the devices (refer to Fig. 5-20). Since the computer was placed out of the tractor, its communication with the interface card was made by means of a long USB cable.

4.4.3 Electronic Relay System

Control output signals from the interface card were not enough powerful so as to be applied directly to the solenoid valves. Therefore, this output signals were amplified firstly by a relay system. Since the conventional electro-mechanic relays are not enough fast for the control system, an electronic relay circuit was applied. Figure 4-15 shows the circuit of the one unit of the electronic relay system.

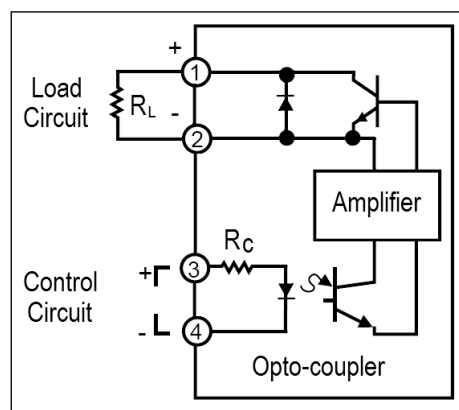


Figure 4-15 The electronic relay circuit used for driving the solenoid valves of the actuators.

In this circuit, the output signal of the interface card passes through the opto-coupler to an amplifier. Then, output of this amplifier put into the “base” connection of a power transistor in order to turn the transistor on. This power transistor works as a switch in this circuit and could afford until 5 amperes, which was enough for switching the solenoid valves. Using an opto-coupler in this circuit provided a complete isolation between the valve circuit and control circuit that protected interface card ports. In addition, a diode connecting to the output of the circuit protected the power transistor from the high voltage signals, which come from the solenoid valve as it was turning off. This occurred because of an inductance effect in the valve’s solenoids.

In the practice circuit, each unit of the relay circuits was placed in a red capsule. Figure 4-16 shows the developed electronic relay system including 10 relay channels, which were enough in order to cover all the output channels of the system. Table 4-2 presents the technical data of these electronic relay units.

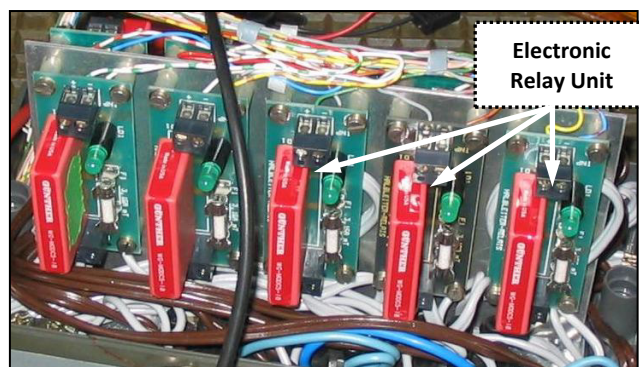


Figure 4-16 Developed electronic relay system.

Table 4-2 Technical data of the electronic relay system.

Control Circuit (Input)		Load Circuit (Output)	
Voltage	3-24 V	Voltage	3-60 V-DC
Current	Max. 24 mA by 24V	Current	0.01-3A, shock current: 5A 1s

4.5 Controller Software

In this investigation, a personal computer was used as the controller of the system. This computer was connected to an I/O card in order to communicate with the output and input of the control. Using special software, this computer was able to execute the strategy of control. The controller read the inputs and generated a command based on the control

strategy to put into the actuator. Then, the three main components of the control system were; input, output, and the control strategy. The inputs of control were the transducers signals of the absolute velocity of the tractor body and the relative velocities between the wheels and body of the tractor. Moreover, the outputs of the controller were switching signals, which were applied to the valves of both sides of the hydraulic cylinders. The third part is the control strategy of the semi-active suspension control, which was the skyhook on-off control strategy in this study. The input and output devices of the control system were presented in the previous sections.

The software of the controller performs the control strategy. In this section, this software is described. The flowchart of the control strategy is illustrated in figure 4-17. This flowchart is created based on the description of the control strategy, which was presented in detail in section 3.3.

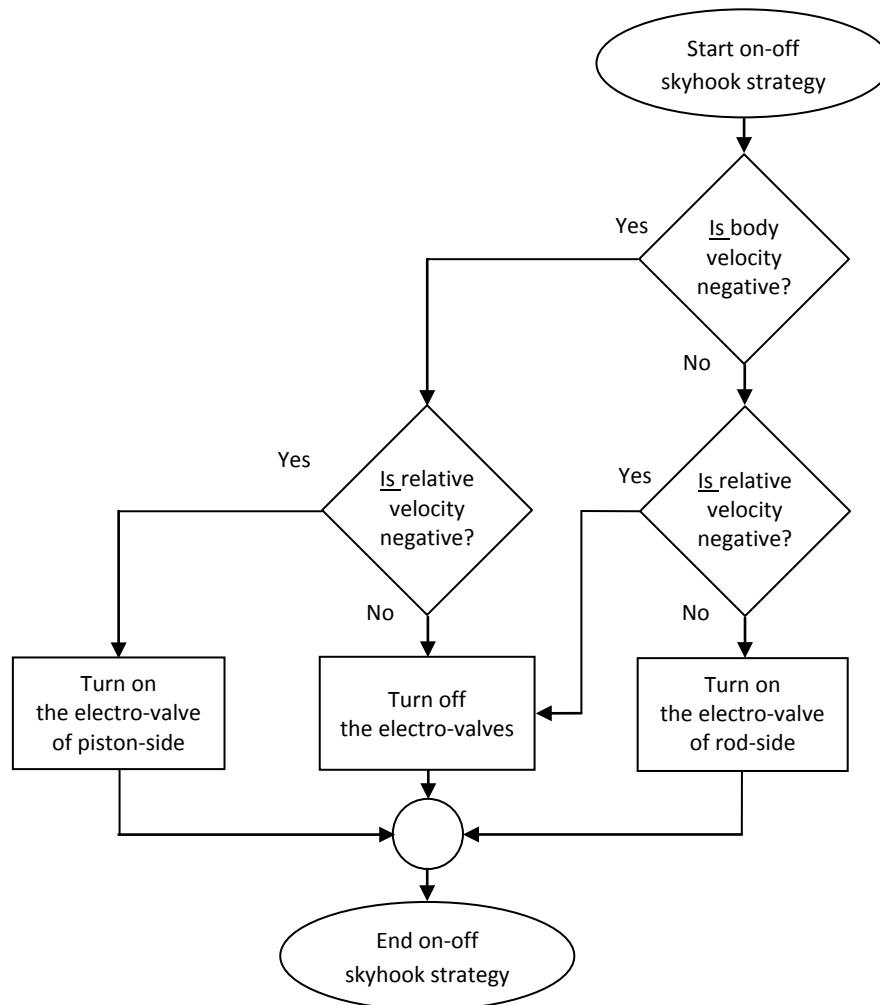


Figure 4-17 Flowchart of skyhook on-off control strategy.

The computer programming for the controller was done in LabVIEW software, which is a graphical programming language from National Instruments used for writing the instrumentation programs. This software was used for the controller, because it was matched completely with the NI-DAQ interface card, recommended by the card manufacturer. As mentioned, this card was driven by software called DAQ mxBase. As this software was installed, a new function set was added to LabVIEW software. This provided an access to the input and output ports of the interface card, which were equal to the inputs and outputs of the control.

Figure 4-18 shows a screen captured from the diagram of the controller program, which was a LabVIEW program. This program consisted of two similar controller units, which were used for the right and left suspension units of the rear axle suspension. Each controller unit was made of the three parts: input, control logic, and output.

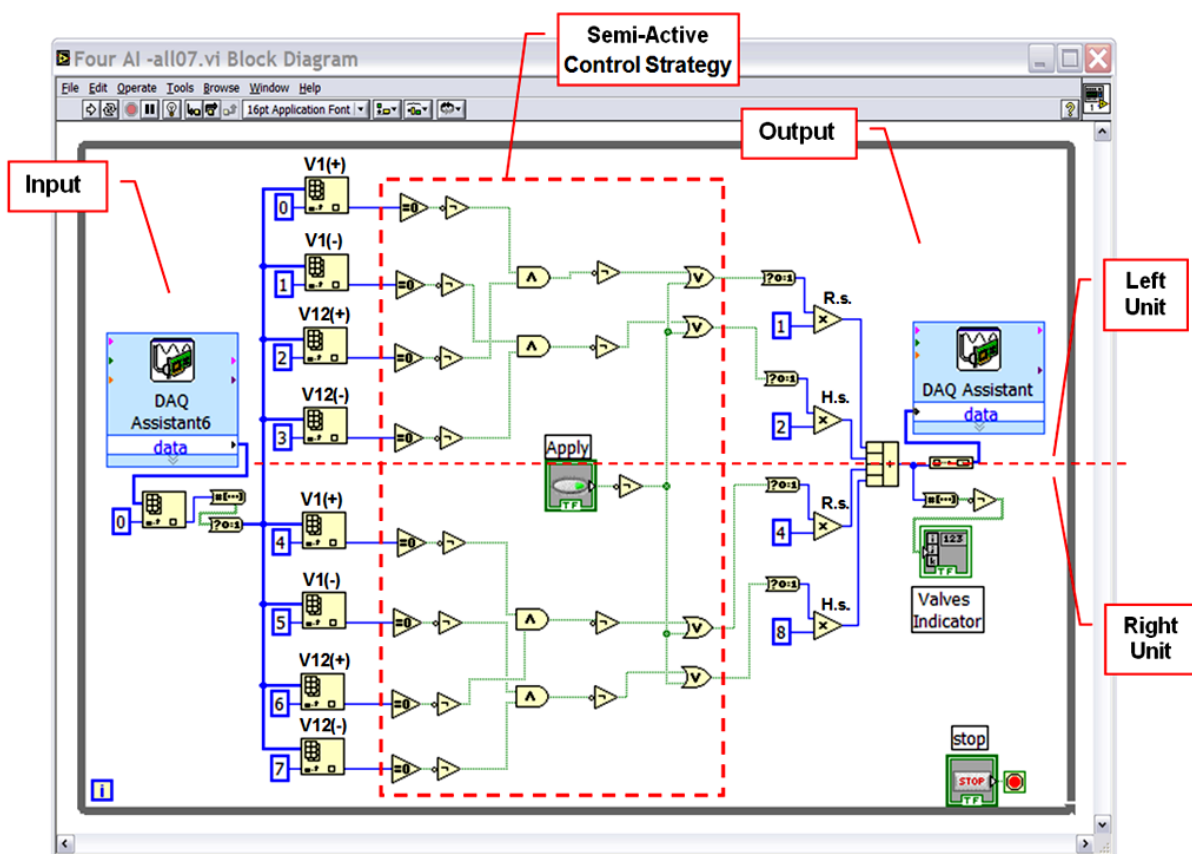


Figure 4-18 Block Diagram of the LabVIEW program of the semi-active controller.

The control inputs were the converted digital signals from the velocity transducers signals producing by A/D circuit. In this circuit, there were two digital outputs for each velocity sensor, which were applied to the two digital input ports of the I/O card. These

signals appeared on the two inputs of the program. Each one of this inputs indicated the positive or negative sign of the vertical suspension velocities. For example as shown in figure 4-18, the first input port (i.e. number zero) was used for indicating the positive sign, and the second input port (i.e. number one) was used for indicating the negative sign of the absolute velocity of the left corner of the tractor body. In this way, eight input digital ports were used in the program for the sensors.

Since all inputs were digital signal, the control strategy part of the program was created by using the logic elements, which were based on the flowchart of skyhook on-off control strategy showed in figure 4-17. The outputs of the program were command signals for controlling the valves of the hydraulic cylinder sides. These commands were four digital signals written on the four digital output ports. These signals appeared on the output ports of the card. These outputs, through the driving relays, put into the valves.

In LabVIEW software, for each program there is a front panel that is created in order to communicate with the operator during the program execution. Figure 4-19 shows a screen capture of the front panel of the controller LabVIEW program, consisting of different indicators and controls buttons. This front panel was used in order to perform the primary calibrations on the sensors and monitoring the control process of system during the tests.

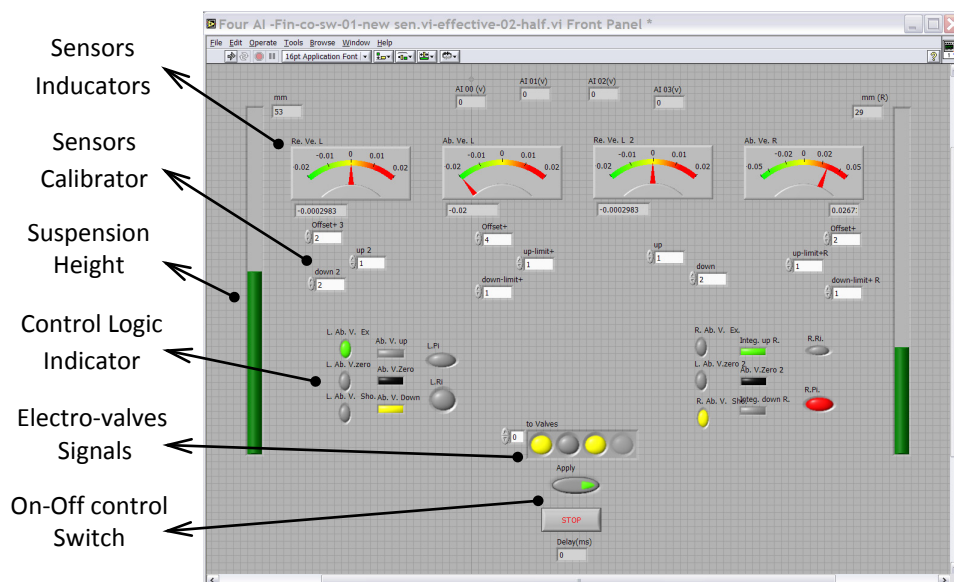


Figure 4-19 Front panel of the LabVIEW program of the semi-active controller.

4.6 Load Level Control

The main objective of this study is to employ active suspensions in order to improve performance of tractor suspensions. For accomplishing this objective, a semi-active suspension was used in order to provide a dynamic control on the operation of the tractor suspension. In addition to this system, another control system was also used for providing a static control on the operation of the suspension. This system, which is called load-leveling system, adjusts the suspension height of a tractor after a change in the static load.

This system is capable to provide a significant improvement in suspension performance. The details of this active suspension system, including advantages of the system in improving of the suspension performance, were presented in section 2.2.2. This system has particularly a great potential for agricultural tractors, which works with a wide range of load variations. For example, in some tractors such as TUB-Trac, the three-point hitch is fixed to the chassis. Now, if a heavy implement such as a plough is attached to them, the mass of the tractor body will change mainly that leads to a fall in suspension height (Fig. 4-20-a). In this condition, the suspension height can be kept constant by using load-leveling control regardless of load changes in a tractor (Fig. 4-20-b).

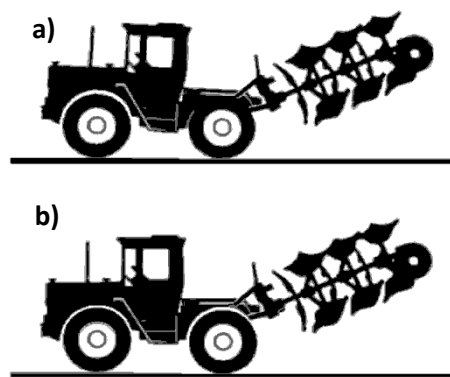


Figure 4-20 Effect of load changing on the tractor suspension

a) Without control b) With load leveling control.

Figure 4-21 illustrates the structure of the load leveling control system developed in this study. The inputs of the system were received from the displacement sensors measuring the suspension height. The signals of these sensors were filtered firstly by a low-pass filter in order to remove the dynamic variations in suspension height. After that, the static suspension height was compared with the suspension height, which was adjusted sooner as

the desired primary height. If the static height changing occurred, and it continued for a specific period, the system recognized it as a static change in suspension height and sent proper output signals to the actuator in order to change the suspension height into the primary value.

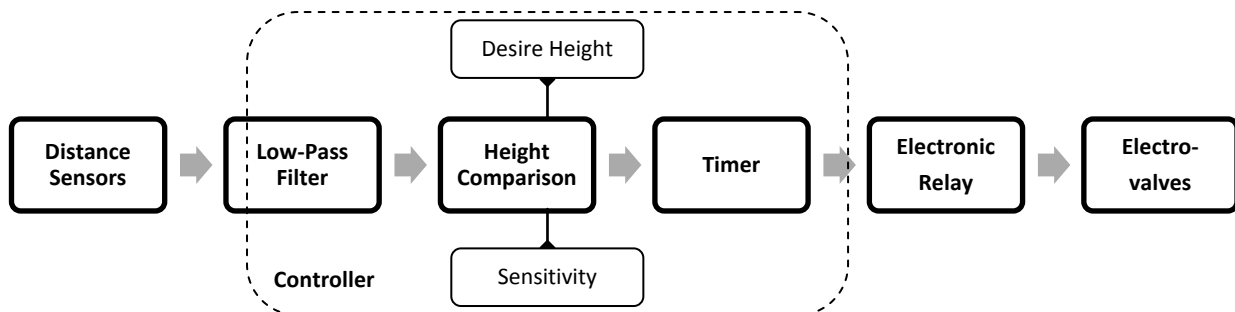


Figure 4-21 Block diagram of the load leveling control system.

For load leveling control system, a hardware configuration similar to the semi-active suspension control was used. In figure 4-22, the configuration of this system is shown. The controller of the system was the same computer as the semi-active controller with a new interface card and separate control software. Since the bandwidth of the load-leveling controller was largely lower than the bandwidth of the semi-active controller, the priority in computer response was set on the semi-active control over the load leveling control, so no interrupt occurred in operation of the semi-active controller.

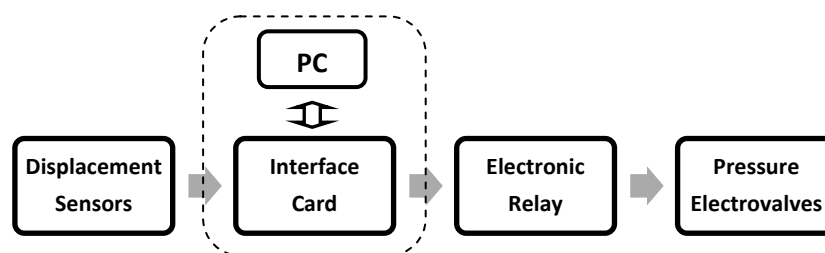


Figure 4-22 Block diagram of the load leveling control system.

The program of the load-leveling controller was created in LabVIEW software. In this software, instead of the external ADC circuit controller, the internal ADC component of the interface card was used, and low-pass filter were performed by controller software. This led to increase the delay of the controller loop. Since a low bandwidth control was needed for this system, the delays created by these components did not disturb the system.

Figure 4-23 illustrates the block diagram of this program that consists of six parts: input, low-pass filter, comparator I, timer, comparator II, and output. The first part includes two A/D converters to convert the analog signals of the displacement sensors to digital signals. These sensors were used for measurement of the suspension height. The second part is a low-pass filter with the cut-off frequency of 0.1 Hz, which was used to remove the signals of the dynamic change in suspension height. The third part is a comparator that lets the operator determines the primary height of the suspension. In addition, the sensitivity of the controller in responding to the static change in suspension height could be adjustable in this part.

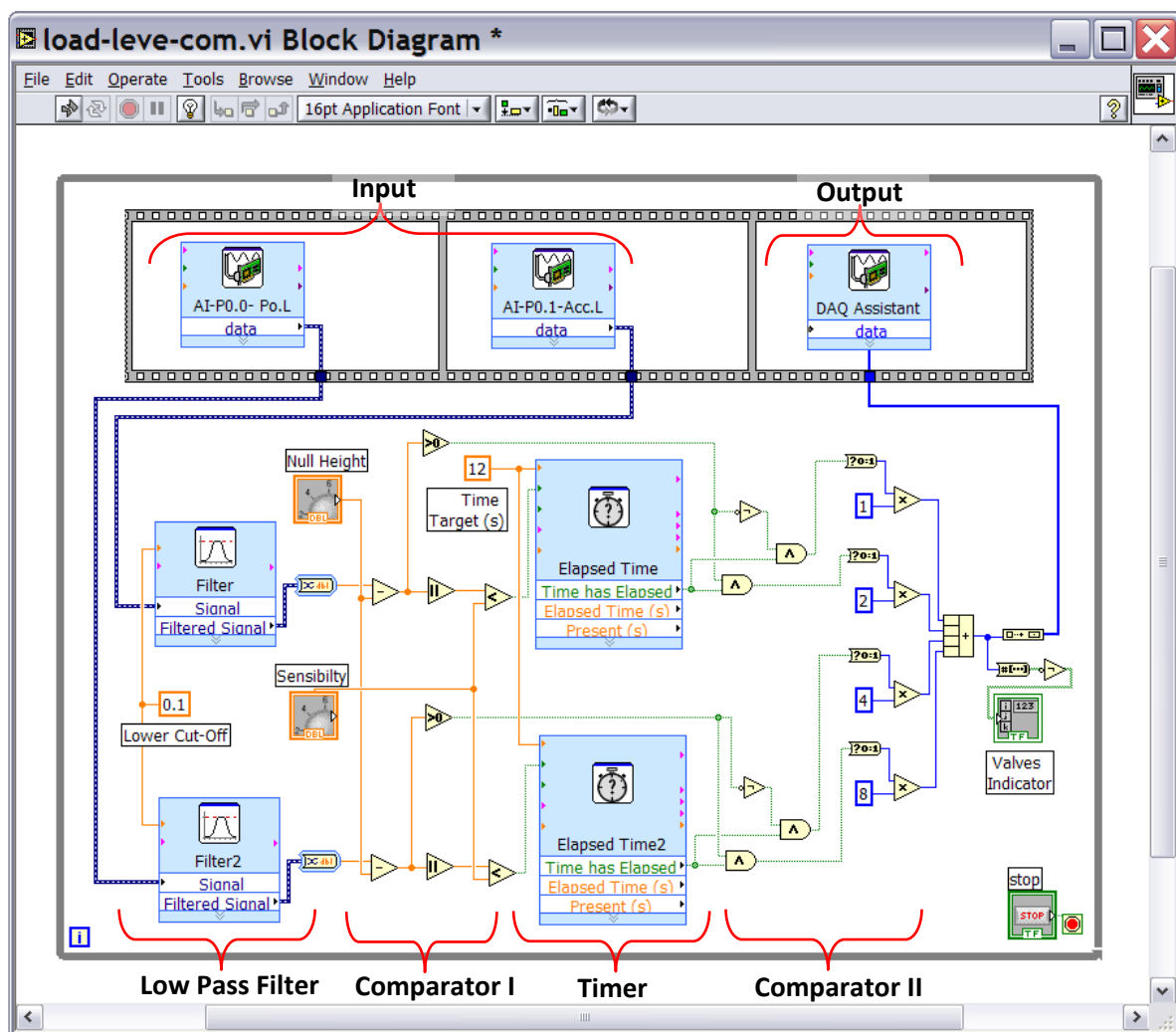


Figure 4-23 Block diagram of LabVIEW program of the load leveling controller.

The forth part of the software is a timer that was used in order to measure the duration of static changes in suspension height to ensure that the change was not just a

transient one. The fifth part after receiving the output signal of the timer, created the proper commands into the valves with the intention of running the cylinders so as to correct the suspension height. This part compared continuously the suspension height with primary height. This caused that the cylinders kept running until the height was corrected. The sixth part is the output part that sent the control commands to the output of the interface card.

The hydraulic circuit of the hydro-pneumatic suspension for the rear axle was presented in section 4.2 in figure 4-3. The directional solenoid valves that received these commands were the valves number 5 and 6 in this circuit. As the suspension height should be increased, the hydraulic oil was pressurized to the head side of the cylinder via these valves. On the contrary, the initial pressure of the head side of the cylinder was decreased by directing the oil to the tank as the suspension height should be decreased.

In semi-active control, a cable-type of velocity transducers was used to measure the relative velocity of the suspension. These sensors can measure the displacement as well (appendix C2). The displacement signals of these sensors were used as the input of the load-leveling controller.

As the load leveling control system works with a very low frequency, evaluation of this system was performed by applying an extra load to the system. Then, it was observed if the reaction of the control system was correct and the tractor body became again level after the delay time. These tests showed the correct operation of the system.

In chapter 4, development of the prototype of the full suspension tractor was described. This prototype contained the semi-active and load leveling control system on the rear axle suspension. In the next chapter, the test setup, which was indeed the preparation for the evaluation system tests, will be presented.

Chapter 5

Simulation and Experimental Test

After building the computer model and developing the virtual prototype, the simulation and experimental tests can be performed. However, the tests should be designed, and their details should be determined before. In this chapter, the design and performance of the simulation tests and experimental tests are described.

5.1 Test Design

An objective of this investigation is the evaluation of the new suspension system. To begin with accomplishing the evaluation, a proper test design should be determined. General steps of the tests are illustrated in figure 5-1. The first step was the application of the test input to the test-tractor in order to excite the suspension system. In the second step, by preparing the system and applying the test input to the system, the test was performed. As the third step, the outcomes of the tests, which were the time history curves of the output parameters, were read as the test output. This data was saved by a data logger to use them later for the final step, which was the data analysis. By analyzing the data, the results of the tests are concluded.

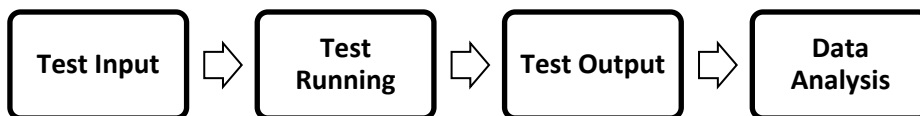


Figure 5-1 Process of the test implementation.

The test design and test plan will be described in the following sections. First, the test-output are determined. These outputs are the parameters that evaluation criteria of the system are inferred from them. Then, the data reduction methods are explained. After that, test-input used for suspension excitation is described. Finally, all these cases of the test design are considered for making the plan of the tests.

5.1.1 Test Output

In order to design a test, the output of the test should be determined initially. The output of a test depends on the goal of the performing the test. In this study, the goal was to evaluate the performance of the new suspension system. Therefore, the criteria of a suspension performance should be determined initially. These criteria were considered the ride comfort and vehicle handling of the tractor. The definition and importance of these factors were stated in section 2.1.1 and 2.1.2 .

Ride comfort, implying the comfort of the driver, depends on the vibration of the tractor body. Therefore, the accelerations of the tractor body including “Heave”, “Pitch”, and “Roll” accelerations were measured. Vehicle handling, involving vehicle stability and safety, depends on the road contact of the tires, which is affected by the tractor body and wheel vibrations. This parameter is evaluated by measuring the vertical dynamic force of the tire contact called in short form “dynamic tire force”. Besides the two parameters, another parameter is considered. This parameter is maximum suspension travel, which is related to the constructional design of a suspension system and indicates the required suspension stroke in the design of the suspension.

5.1.2 Data Reduction

From the evaluation tests, two groups of the time-domain and frequency-domain results were achieved. In order to perform the vibration analysis of the new suspension, these results should be studied. For this purpose, the two main analysis method of amplitude-based and frequency-based were used for the test data reduction, which will be described in the following sections.

5.1.2.1 Amplitude-Based Analysis

Amplitude-based analysis is used normally for the data reduction purpose in order to derive a quantity indicating the magnitude characteristic of a data series. The most used expressions for the amplitude of a set of data is root-mean-square that is often abbreviated as “RMS”. This quantitative parameter, presenting the average of data magnitudes is used for the analysis of the vibrations data. This indicates the energy of the vibrations.

For example, a more powerful vibration has higher RMS. RMS analysis of a set of data is defined mathematically as:

$$[t, a(t)] \rightarrow RMS(a) = \sqrt{\frac{1}{T} \int_0^T a^2(t) dt} \quad 5-1$$

Practicable formulation used for data analysis is defined as:

$$RMS = \frac{\sqrt{(a_1^2 + a_2^2 + \dots + a_n^2)}}{n} \quad 5-2$$

a_i is the measured data, and n is the number of test samples.

Looking at the formulation, it can be stated that the unit for the RMS value of a data series is the same as the data unit. For example, the RMS unit of acceleration data is $[m/s^2]$. In addition to RMS, another method is used for amplitude-based analysis. This method is maximum peak-to-peak with the abbreviation of “MPTP” that is determined by subtracting the minimum value of data from the maximum data value and is defined as:

$$[t, a(t)] \rightarrow PTP(a) = \text{maximum value of } (a) - \text{minimum value of } (a)$$

This analysis is used for the analysis of the suspension travel data in order to obtain the needed suspension length for the design consideration of suspensions. An example of this analysis is presented in figure 5-2, showing the maximum peak-to-peak value of the suspension travel.

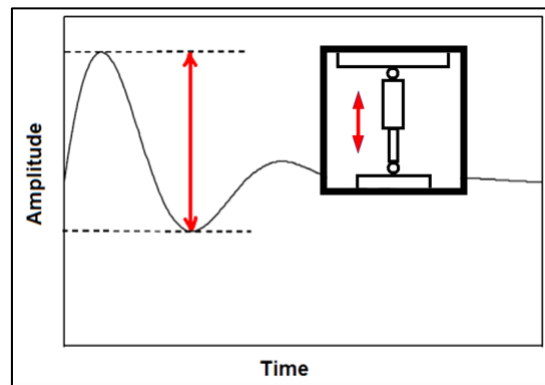


Figure 5-2 Maximum peak-to-peak value of suspension travel.

5.1.2.2 Frequency-Based Analysis

RMS analysis of a data series provides an average quantity of them. For example, RMS value of the acceleration data of the body of a vehicle indicates the average quantity of

ride comfort. In order to understand the quantity of ride comfort in different frequency ranges, in addition to amplitude-based analysis, a frequency-based analysis is needed.

The common method in frequency analysis is spectrum analysis that presents a graphical illustration from the different exciting frequencies derived from the time history data along with the amplitude of each frequency. These graphs provide a useful tool in order to recognize the different frequency components of a data series. In this study, a particular spectrum method called “Power Spectral Density” or as abbreviation “PSD” is used that instead of amplitude, presents the average of the vibration power.

PSD is defined mathematically as the average of the Fourier transform magnitude squared, over a large time interval as follows:

$$S_x(f) = \lim_{T \rightarrow \infty} E \left\{ \frac{1}{2T} \left| \int_{-T}^T x(t) e^{-j2\pi ft} dt \right|^2 \right\} \quad 5-3$$

The power of $x(t)$ in the range of (f_1-f_2) is defined as:

$$P_{12} = \int_{f_2}^{f_1} S_x(f) df \quad 5-4$$

In a PSD graph, the x-axis is the frequency with the unit of [Hz], and the y-axis is the PSD value. The unit of the PSD values is resulting from its formulation that is the quarter of data quantity divided by frequency unit. For example, for acceleration data, the PSD unit is $\frac{(m/s^2)^2}{Hz}$.

In practice, estimating methods are used for sampling discrete data to perform the PSD analysis. A standard way is to use a window function in “Discrete Fourier Transform” or DFT. A discrete data is obtained effectively by a window $w[n]$ function that selects a finite-length (e.g. N samples) of $x[n]$ from the continuous signal as follows:

$$v[n] = w[n] \cdot x[n] \quad 5-5$$

The FFT of the sampled data is defined as:

$$V(k) = \sum_{n=0}^{N-1} w[n] \cdot x[n] e^{-i2\pi F_k n} \quad 5-6$$

Where, N is the number of samples. As simplification, an estimation method can be used for the calculation of the power spectrum as follows:

$$P(k) = \frac{1}{\sum_{n=0}^{N-1} (w[n])^2} |V(k)|^2 \quad 5-7$$

There are some different window functions. The simple one is the “Rectangular” window, defined as:

$$w[n] = 1 \quad 5-8$$

In this study, the window function of “Hanning” is used, because it provides good frequency resolution and leakage protection with fair amplitude accuracy. Having these advantages, this function is became the most commonly used window functions for random signals (Ziemer, Tranter, & Fannin, 1998). This function is defined as:

$$w[n] = \frac{1}{2} \left[1 - \cos \left(\frac{2\pi n}{N-1} \right) \right] \quad 5-9$$

5.1.3 Test Input

In order to evaluate the performance of the suspension system, response of the system to a suspension excitation should be studied. Exciting of the suspension is performed by the test input, which is indeed simulation of the road input. This input is a vertical displacement wave that applies to the tires and through them excites the suspension system.

In evaluating tests, in addition to the time domain, the frequency domain of the system is also considered. Because of this, the test input must provide all the frequency range of the suspension vibrations. There are different kinds of inputs waves used as the suspension excitation for the tests. Figure 5-3 indicates the three main categories of them, which are random, swept-frequency, and pulse inputs.

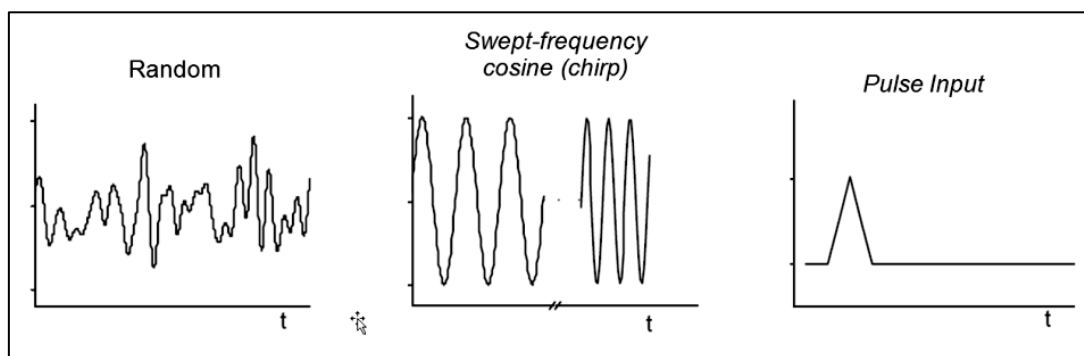


Figure 5-3 Different input signal, used for the frequency response analysis.

For this investigation, the pulse signal was used as input signal (Fig. 5-4). This input was used for the simulation and experimental tests. Frequency of the input pulse was 10 Hz.

This value was selected based on the practical considerations of the test input in the experimental tests, which were performed using a suspension test rig. The determined pulse signal with this frequency was sufficient to cover the required bandwidth of the suspension vibrations.

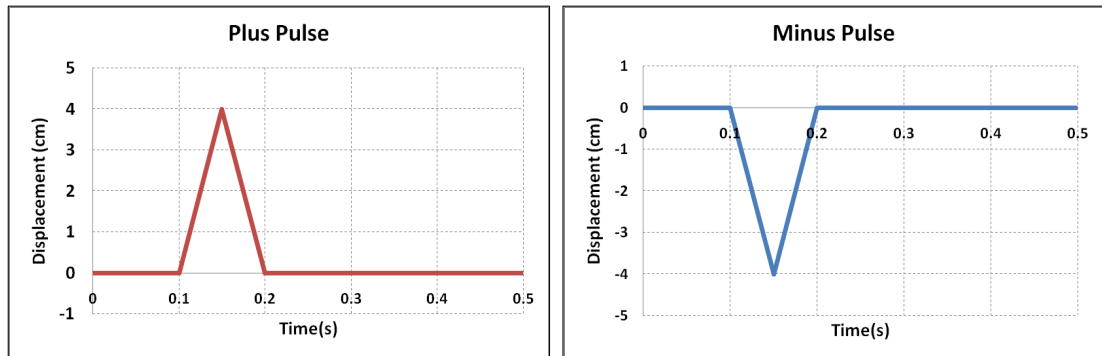





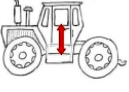











Figure 5-4 The positive and negative pulse used for the test input.

Table 5-1 Three input modes used for the tests and the relevant pulses applying to the wheels.

Input Mode		Pulse to Wheel			
		Front Left	Front Right	Rear Left	Rear Right
	Roll				
	Heave				
	Pitch				

As mentioned before, the tests criteria were the parameters of the tractor body vibrations including the vertical vibration (i.e. heave) and the rotational vibration (i.e. pitch and roll) of the tractor body and the parameters of the vertical vibration (i.e. hip-hop) of the wheels. In order to examine these parameters, the test input was designed so as to provide a direct excitation on each one of these parameters. For this purpose, the input pulses were applied to the four tires of the tractor in three special orders called: roll, heave, and pitch modes. These inputs create direct excitations for the vertical and rotational vibrations. Table 5-1 shows these three input modes and determines the direction (i.e. positive or negative) of each pulse, which is applied to a tire in order to perform the three input modes.

5.1.4 Test Plan

In the previous sections, the test input, output, and data reduction were determined. At this point, the plan of the whole tests including the simulation and experimental tests can be formulated. In this plan, the inputs and outputs of each test should be determined. In addition, the measuring parameters and data reduction method of each test should be resolved.

Table 5-2 presents a plan for the tests including inputs, outputs, measuring parameters, and data reduction method for each test. This plan consists of two similar test groups; the first with passive suspension mode and the second with semi-active suspension mode, that are considered concerning to the main objective of this study as evaluation of the new suspension by comparing it with conventional passive suspension.

On the other hand, model validation is an objective of this investigation. In order to perform the model validation, the results of the simulation tests should be compared with the experimental tests. Therefore, it is needed that the test design for the simulation and experimental tests would be similar. This includes the test input, test output, and the test plan. However, the repetitions of the two test groups are different. This issue will be discussed in the following sections. As shown in table 5-2, there is a similar plan for both groups of the tests. At the final columns of the table, results of the simulation and experimental tests are shown separately.

There are three types of outputs for the tests. The first one includes the heave, pitch, and roll accelerations of the tractor body, which are used for evaluating the ride comfort. The second one is the dynamic tire vertical forces, which are used for evaluating the handling ability of the tractor, and the third one is the suspension travel, which is considered for suspension design consideration.

The corresponding test inputs to the test outputs are also determined in table 5-2. The roll input mode is used for the body roll acceleration and the heave input mode is used for body heave acceleration. The input mode of pitch is considered for the dynamic tire force and suspension travel, in addition to body pitch acceleration.

In the table of the test plan, the data reduction method for each output of the tests is determined. For the heave, pitch, and roll accelerations of the tractor body both RMS and PSD as amplitude and frequency based analysis are considered. Similar analysis is considered for the dynamic tire force, and for the suspension travel, MPTP amplitude-based analysis is

determined. In the last column of the table, the final reduced data of the tests are listed. Repetition of each test is not considered in this table. This subject will be explained in the following section during the description of the simulation and experimental tests.

Table 5-2 Detailed tests plan.

Test	Suspension Mode	Input	Measuring Parameter	Output	Data Analysis	(Exp.) Data Nr.	(Sim.) Data Nr.
T01	Passive	Roll	Body corners acc.	Roll acc.	RMS & PSD	e1	s1
						e2	s2
T02	Passive	Pitch	1-Body corners acc. 2-Wheels acc. 3-Sus. travel	Pitch acc.	RMS & PSD	e3	s3
				Tire force	RMS & PSD	e4	s4
						e5	s5
				Sus. travel	MPTP	e6	s6
T03	Passive	Heave	Body corners acc.	Heave acc.	RMS & PSD	e7	s7
						e8	s8
T04	Semi-active	Roll	Body corners acc.	Roll acc.	RMS & PSD	e9	s9
						e10	s10
T05	Semi-active	Pitch	1-Body corners acc. 2-Wheels acc. 3-Sus. travel	Pitch acc.	RMS & PSD	e11	s11
				Tire force	RMS & PSD	e12	s12
						e13	s13
				Sus. travel	MPTP	e14	s14
T06	Semi-active	Heave	Body corners acc.	Heave acc.	RMS & PSD	e15	s15
						e16	s16
T07	Passive	Roll	Body corners acc.	Roll acc.	RMS & PSD	e17	s17
						e18	s18

In this section, the test plan was presented. The input, output, and data reduction method of the tests were also explained. At this point, the tests can be performed. In the following sections, performance of the simulation and experimental tests will be described.

5.2 Simulation Tests

Figure 5-5 shows the procedure of the simulation tests. In the previous sections, the test plan, test input, test output, and data reduction were explained before. In this section, performing of the simulation tests is presented. First, the preparation of the full tractor Simulink model for these tests is explained. Then, the execution of the tests is described.

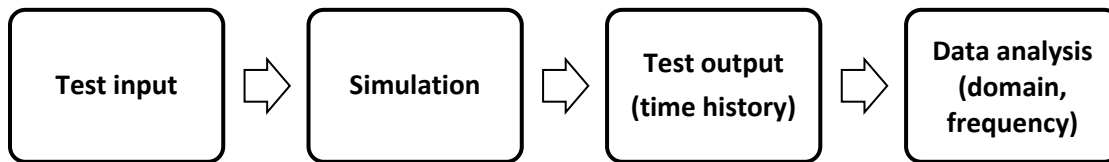


Figure 5-5 Simulation test process.

5.2.1 Final Simulation Model

In chapter 3, the procedure of building the full tractor model was presented, and at the end of this procedure, the full tractor model was built. In addition, the test design was prepared in past sections. At this point, the simulation tests can be performed.

The final Simulink model is created by joining the tractor suspension model, including sprung and unsprung models, to the controller model (refer to section 3.1.6 and 3.3). In addition, a new road simulator model is added to the full model in order to apply the determined test input to the model. In the end, a new output model is added to the full model for logging the determined test output. Figure 5-6 shows the final Simulink model prepared for the simulation tests. As shown, the new blocks of the test input and output are added to the main block of the tractor suspension.

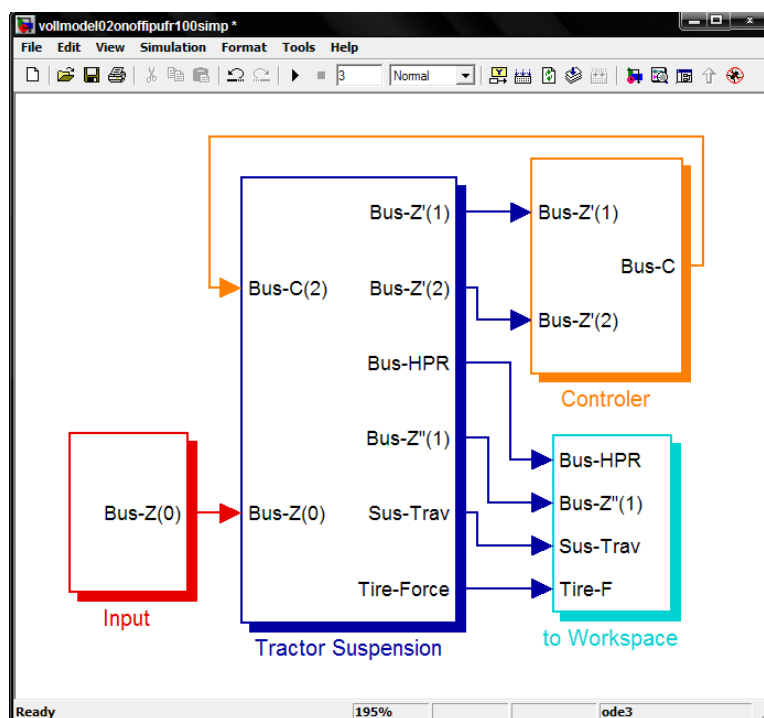


Figure 5-6 The final Simulink model used for the simulation tests.

Figure 5-7 shows the Simulink model of the test-input simulator. This model is created based on the input test defined in section 5.1.3. Using the Simulink block of “signal builder” and based on the figure 5.4, the simulator of the input signal is built. In addition, the produced pulse is divided into four tractor tires according to the table 5-1 in order to simulate three input modes.

Input Mode	Suspension Unit			
	fl	fr	rl	rr
Roll	+1	-1	+1	-1
Heave	+1	+1	+1	+1
Pitch	-1	-1	+1	+1

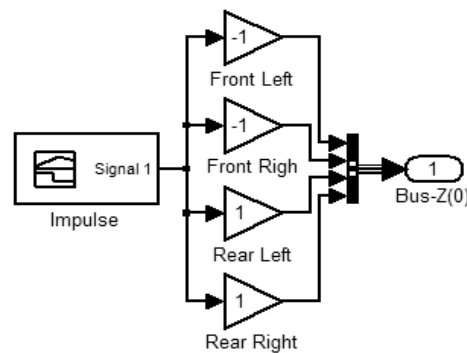


Figure 5-7 Simulink model of the test input simulator with the relevant input-modes coefficients.

For logging the outputs of the simulation tests, the determined parameters are sent directly to the “workspace” and saved as time history data. However, the dynamic tire forces are not available as the direct parameters in the model, and they are calculated through other parameters. After the calculation of these data, they are sent to the workspace and saved as time history data. Figure 5-8 indicates the Simulink model of the calculator of the dynamic tire force. The inputs of this model are the displacement of the road simulator and the displacement of the wheel.

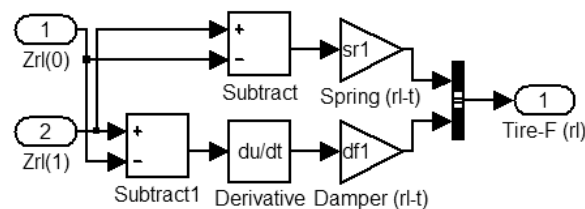


Figure 5-8 Simulink calculator of the dynamic tire force.

As stated in the test plan, the two suspension modes of the passive and semi-active are used for the tests. The model of the semi-active controller was explained before. In order to create the passive mode, the controller model is adjusted so as to provide a constant damping level. This is performed by applying a constant throttling cross-section to the model of the hydro-pneumatic suspension. This provides an average damping-ratio of 0.5 for the passive suspension mode. At this point, after all these preparations, the Simulink model is ready for performing the simulation tests, which will be explained in the following section.

5.2.2 Simulation Test Performing

The simulation tests were performed by using a MATLAB m-file in order to manage all steps of the simulation tests. Figure 5-9 shows the process of the simulation tests using the m-file. First, the m-file defines the parameter of the simulation. This provides the possibility to define all the parameters separately from the Simulink model. In addition, modification of the parameters can be performed without changing the Simulink model. Then, m-file runs the Simulink model. After finishing the simulation, the m-file analyzes the output of the tests, and finally, the m-file presents the results of analysis numerically and graphically. The content of this m-file is presented in appendix D1.

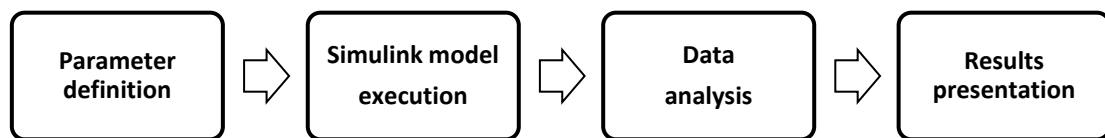


Figure 5-9 Flow chart of the MATLAB m-file used for simulation tests.

Running configuration of the Simulink model is presented in table 5-3. Running option of “Fixed-step” was preferred over “Variable-step” with the intention of providing a constant sampling rate for the whole simulation tests, because referring to equation 5-2 and 5-6, the RMS and PSD results of analysis are depended to the sampling rate. Value of the fixed step was determined 0.01 second that is similar to the sampling rate of the experimental test. The running method of “Ode 3” was also selected as a standard method with the aim of creating convergence simulation running. The duration time of each simulation test was determined 3 second, which was selected after observing the time history of the primary simulations. Likewise, in the experimental tests, the main vibration was damped completely after this period.

Table 5-3 Simulink software configuration used for the simulation tests.

Solver Parameters	
Type:	Fixed-step
Method:	Ode 3 (Bogacki-Shampine)
Fixed-step size:	0.01 sec.
Simulation time:	3 sec.

The simulation tests, based on the test plan, were performed in two categories: passive suspension mode and semi-active suspension mode. Adjusting a test input, the test was performed once in the semi-active suspension mode. Then, the second corresponding test was performed with the same input in the passive suspension mode. Since no random function was used in the model and simulation, the repetition of each simulation test was not required. However, in order to ensure the repeatability and correctness of the tests, each simulation test was repeated once.

5.3 Experimental Tests

The building a prototype for the system was explained in chapter 4. This model was used for the experimental tests. The test plan of the experimental tests was similar to the simulation tests. Before performing the experimental tests, the necessary preparation was organized. Figure 5-10 illustrates the configuration of the experimental tests. In order to create the test input and test output in the experimental tests, two new components of excitation unit and data logging unit were used. The excitation unit provided the test input in order to excite the suspension system, and data logger was used in order to measure the output parameter and to save them. These data were analyzed in the next step.

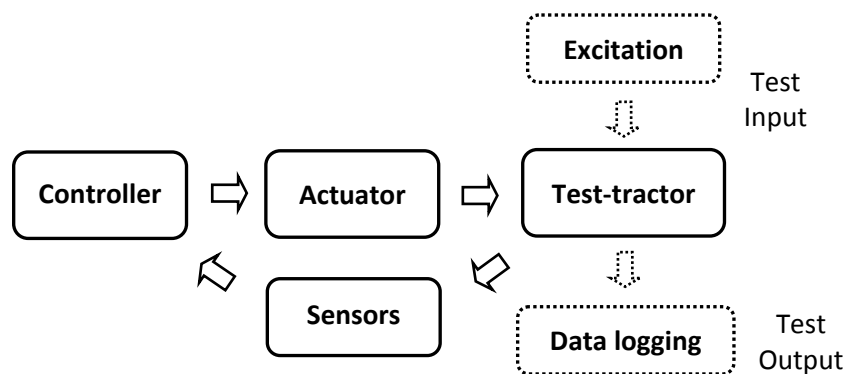


Figure 5-10 Experimental test configuration.

In this section, first, the suspension test rig used for applying the test input to the test-tractor is explained. Then, the data logging system used for measuring and saving the test output is described. After that, the operation check of the control system is explained, and finally, performing of the experimental tests is presented.

5.3.1 Full Suspension Test Rig

For performing the experimental tests and applying the test input to the test-tractor, there were two options: field testing and laboratory testing. As this study was the first attempt in evaluating the new suspension system after the creation of it, the first option was considered as the best choice. This option was the performing of laboratory tests by using a suspension test rig. For this purpose, the suspension test rig at the TU Berlin - Department Machinery System Design was used as a road input simulator. By using these facilities, it was possible to perform the test excitation and data logging accurately and without different error sources, which exist in typical field testing.

This suspension test rig consists of four hydraulic shakers. As shown in figure 5-11, the tractor stayed on the test rig so that each shaker was placed under one wheel, and so the wheels could be excited individually. The framework of the test rig is mounted on a foundation via an air suspension system in order to isolate ground from the test rig vibrations.

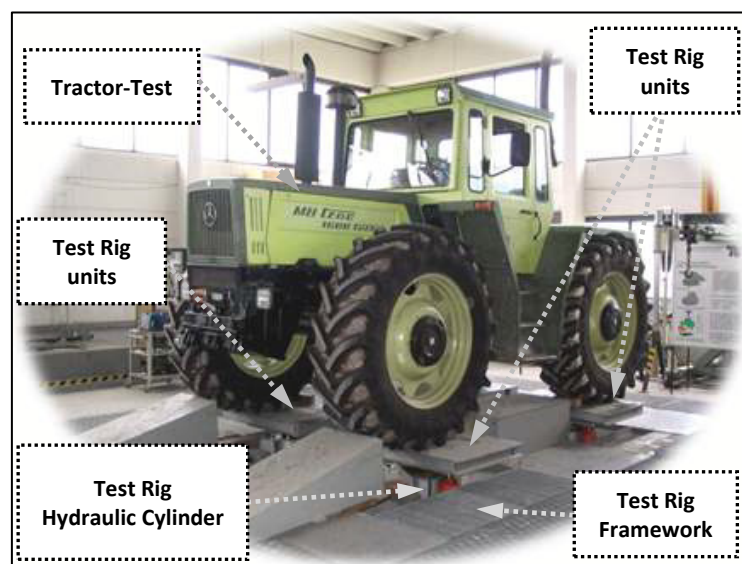


Figure 5-11 Test-tractor standing on the full suspension test rig.

The control center of the suspension test rig is shown in figure 5-12. This system is able to control each hydraulic shaker independently with individual waveform and amplitude. The input of each shaker can be adjusted separately. Each shaker is indeed a double-acting hydraulic cylinder, controlled by a servo-valve. This servo-valve receives command signal from the control center. Technical data of the suspension test rig is presented in appendix B.

For applying the determined input signal to the suspension test rig, a function generator was used to create proper signals correspondent to the input signal illustrated in figure (5-4). Amplitude and waveform of the control commands, which were sent to the shakers, were monitored by an oscilloscope (Fig. 5-12). Amplitude of the input test created by shaker was adjusted to the value of plus or minus five cm. Then, this input signal was applied to each shaker with a special order, which was indicated before in table 5-1.

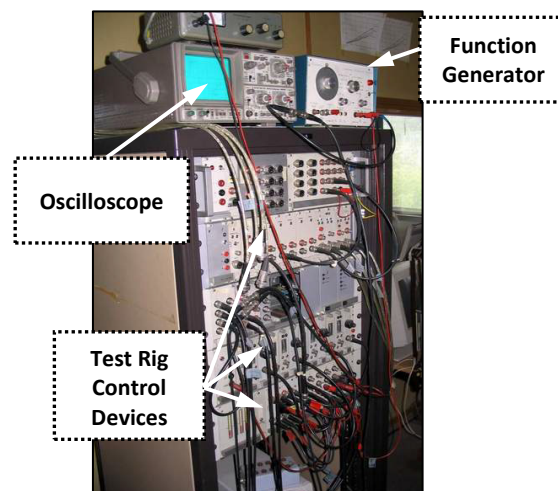


Figure 5-12 Equipment of the control system of the full suspension test rig.

The suspension test rig was used for applying the test inputs to the test tractor. For output of tests, a data acquisition system was used in order to gather the data from the output parameters of tests. This subject will be described in the following section.

5.3.2 Data Acquisition System

Data acquisition system conducted two functions: measurement and data logging. The output parameters of the tests were measured by using suitable sensors, and the signals of these sensors were saved by data logger as time history data. These saved data were later analyzed in order to derive the test results.

The data acquisition system used for this research was a PC-based system including a laptop computer connecting to a sensory set-up via an ADC interface card (Fig. 5-13 and 5-14). The sensory set-up consisted of the sensors, signal conditioner, and a low-pass filter. The sensors measured the determined parameters. The signals of the sensors were converted firstly to the proper type of signals, because signals of the sensors should be compatible with the inputs of the interface card. For this purpose, a signal conditioner was used.

Conditioning of the signals was composed of sensor excitation, sensor isolation, and signal amplification. Before signals enter to the card, they were passed through a 20Hz low-pass filter. This filter separated the signals of the sensors from the noise and from the high frequency signals, which are not related to the suspension operation. Then, the sensory signals were converted to digital signals by using ADC card and after that, were saved by computer as time history data. The saved data was later transferred to another PC in order to perform the needed analysis on them.

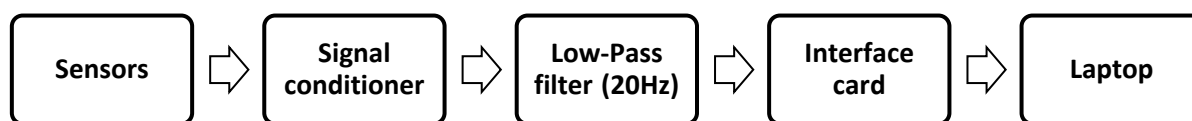


Figure 5-13 Components of the data acquisition system.

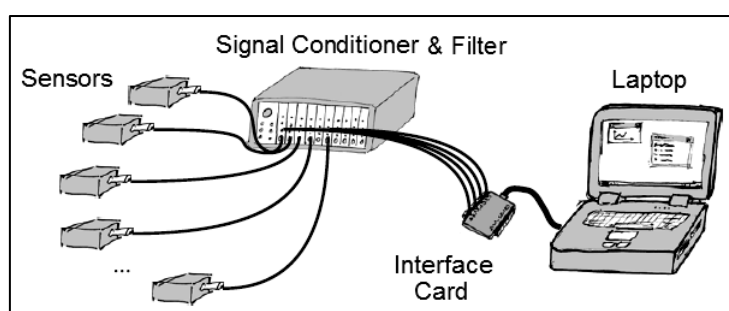


Figure 5-14 Schematic configuration of the data acquisition system (Thiebes P. , 2006).

The ADC interface Card used for data logger system was PCI-BASE300 from BMC Company working with the nextView NT Software. This cart was equipped with 16 analog inputs with the resolution of 16 bits. The sampling rate of the data logging system was 100 Hz. Technical data of this card is presented in appendix C5.

As mentioned, the output parameters of the tests were measured by data acquisition system. These outputs were chosen based on the performance criteria. The output parameters were accelerations of the center of gravity of the tractor body, dynamic tire force, and suspension travel (section 5.1.1). However, except the suspension travel, it was not possible to measure these parameters directly. Therefore in order to acquire these parameters, initially some related parameters were measured. Then based on these values and using relevant equation, the main parameters were derived. This procedure is illustrated in figure 5-15.

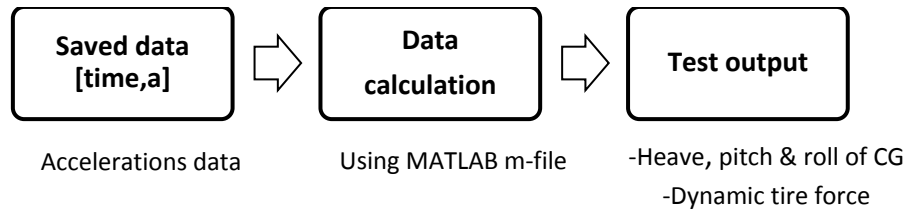


Figure 5-15 Analysis procedure of the experimental data.

The acceleration of the center of gravity of the tractor body including heave, pitch, and roll acceleration were calculated based on the vertical acceleration data, measured on the body corners. The calculation was accomplished by using the following equations, which are taken from section 3.1.5 based on the figure 3-6.

$$\begin{cases} z''_{2fl} = z''_{cg} - l_f \cdot \theta'' + t_l \cdot \phi'' \\ z''_{2fr} = z''_{cg} - l_f \cdot \theta'' - t_r \cdot \phi'' \\ z''_{2rl} = z''_{cg} + l_r \cdot \theta'' + t_l \cdot \phi'' \\ z''_{2rr} = z''_{cg} + l_r \cdot \theta'' - t_r \cdot \phi'' \end{cases} \quad 5-10$$

In order to solve this system of linear equations, they were represented in the matrix form as:

$$A \cdot X = B$$

The unknown matrix X consisted of the accelerations of the center of gravity, and constant matrix B consisted of the vertical accelerations of the body corners. Matrix A also consisted of the dimensional parameters of the tractor. So, the system of linear equations was presented as:

$$\begin{bmatrix} 1 & -l_f & t_l \\ 1 & -l_f & -t_r \\ 1 & l_r & t_l \end{bmatrix} \begin{bmatrix} z_{cg}'' \\ \theta'' \\ \phi'' \end{bmatrix} = \begin{bmatrix} z_{2fl}'' \\ z_{2fr}'' \\ z_{2rl}'' \end{bmatrix} \quad 5-11$$

By multiplication of the two sides of the equation by the inverse of the matrix of the dimensional parameters (i.e. A), the system of linear equations was solved, and the matrix of the accelerations of the center of gravity (i.e. X) was obtained as:

$$X = A^{-1} \cdot B \quad 5-12$$

In addition to the acceleration on the center of gravity, the dynamic tire force should be calculated from the measured parameters. For this purpose, the formulation of the quarter car model (i.e. the equations of the sprung and unsprung masses) from section 3.1.2 was used as follow:

$$\begin{aligned} +m_2 z_2'' + F_{k_2} + F_{c_2} &= 0 \\ +m_1 z_1'' + F_{k_1} + F_{c_1} - F_{k_2} - F_{c_2} &= 0 \end{aligned}$$

After some manipulations, a new equation was resulted as:

$$F_t = +m_2 z_2'' + F_{k_1} + F_{c_1} + m_1 z_1'' = 0 \quad 5-13$$

On the other hand, the dynamic tire force was equal as:

$$F_t = -F_{k_1} - F_{c_1} \quad 5-14$$

Therefore, the dynamic tire force was obtained based on the vertical accelerations of the wheel and body corner as:

$$F_t = +m_2 z_2'' + m_1 z_1'' \quad 5-15$$

By writing a m-file in MATLAB the mentioned calculations of the body acceleration and dynamic tire force were performed overall experimental data. This program read the measured parameters, which were saved by data logger before. Then, by using the formulation explained in this section, it gives the time history of the calculated parameters. This m-file is presented in appendix D2.

As mentioned, the output parameters were obtained indirectly some other measurable parameters. The list of these measured parameters is presented in table 5-4. Four accelerometers, placed on the corners of the tractor body, were used to measure the

absolute vertical accelerations of the tractor body. Four other accelerometers, placed on each corner of the axles near the wheels, were used to measure the absolute vertical acceleration of the four wheels of the tractor (Fig. 5-16).

Table 5-4 Measured parameters of the test-tractor by data logger.

Parameter	Symbol	Channel	Measuring Place	
Absolute Acceleration	HLU	analog 01	rear left	axle corners
	HRU	analog 02	rear right	axle corners
	VLU	analog 03	front left	axle corners
	VRU	analog 04	front right	axle corners
	HLO	analog 05	rear left	body corners
	HRO	analog 06	rear right	body corners
	VLO	analog 07	front left	body corners
	VRO	analog 08	front right	body corners
Relative Displacement	HLW	analog 09	rear left	suspension unit
	HRW	analog 10	rear right	suspension unit

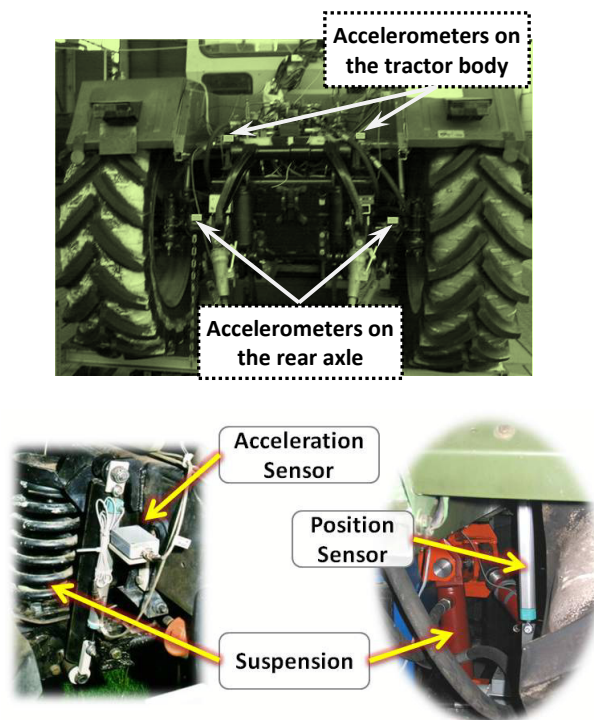


Figure 5-16 The acceleration and displacement sensors used for data acquisition system.

For measuring suspension travel, two displacement sensors were employed. For measuring the displacement, linear resistor-type of the position transducers were used (Fig. 5-16). Accelerometers were piezo-resistive type with the measuring range of $\pm 20g$ for the wheel acceleration and with the measuring range of $\pm 10g$ for the body acceleration. The detailed specifications of the acceleration sensor are given in appendix C1.

5.3.3 System Operation Check

Before using developed prototype for performing the experimental tests, relevant adjustment were done, and operation of the different components were proved separately. For this purpose, at first, the hydro-pneumatic suspension was re-examined. Different components of this system were considered separately. The proved parameters of these components were the initial gas pressure of the accumulators, primary suspension height, valves connections, and passive and semi-active modes of the throttle valves.

Suspension characteristic of the tires has a significant influence on the suspension performance of a tractor. This characteristic is directly dependent on the inflation pressures of tires. For more details about the suspension characteristic of the tires, please refer to section 2.5.1. Therefore, after the hydro-pneumatic suspension, tractor tires were proved to be with the correct determined inflation pressures. In addition, the data acquisition system including sensors, signal conditioner, and pc-based data logger were calibrated and confirmed.

At this point that the test-tractor was placed on the suspension test rig and was ready for the tests (Fig. 5-11), a check on the electronic components of the control system was done before performing the tests. For this purpose, the data logging system was arranged in order to measure the output of each component. Figure 5-17 shows the configuration of this primary test.

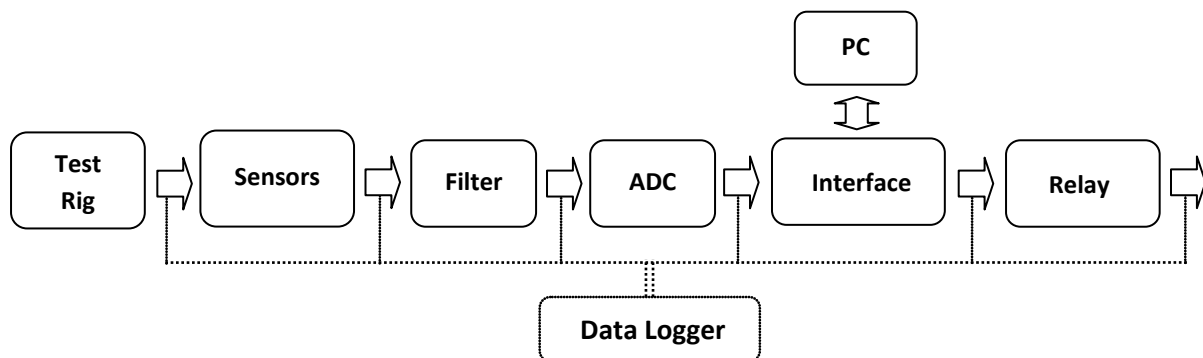


Figure 5-17 Configuration of the primary test of the control system.

The test was started with applying a test input to the suspension test rig. The data logger using a position sensor measured the real output of the test rig. Time-history data of the output signal of all components were saved by data logger. These components were sensors, low pass filter, A/D converter, interface card, and electronic relay. Using these data, after the test, operation of each component was examined.

For example, figure 5-18 shows the saved time history data measured by the absolute and relative velocity sensors that were used as the inputs of the tests along with the electronic relay signals as the output of control. As shown, the noise effect of the sensors signals caused some errors in the signals of the relays, which is applied to the valves in the real system. Recognizing this problem, in order to overcome against it a low-pass filter was used after the sensors in order to remove the noise part of the sensory signals.

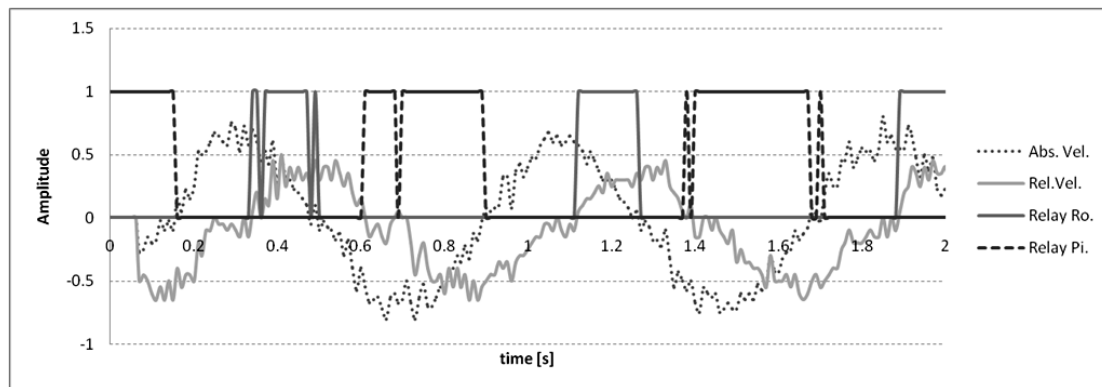


Figure 5-18 A result of the primary controller test, indicating mistakes in the relay signals due to the noise effect.

Another characteristic of the control system that should be revealed was the system bandwidth. The every part of control system worked in a close loop (Fig. 5-19). In order to determine system bandwidth, the spending time of each component was considered. In developing of the system, it was a challenge to fulfill the required control bandwidth.

Therefore, during the designing of the system, time response of each component of the system was carefully determined. The system consisted of two categories of components: the electronic components and the electro-mechanic components. The electronic components were PC, I/O card, electronic relay, A/D converter, and low-pass filter. The electro-mechanic components were the velocity transducers and solenoid valves.

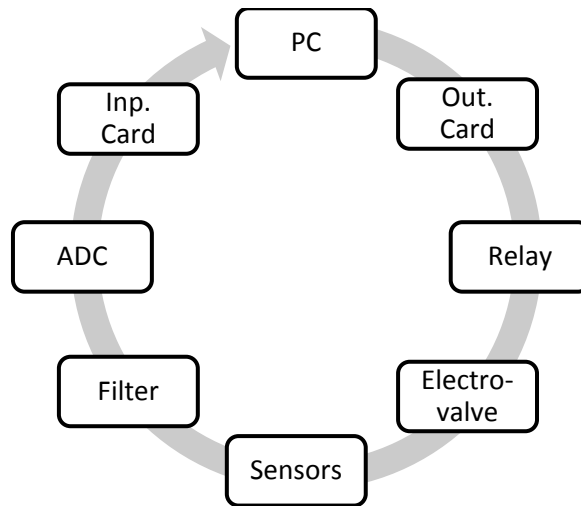


Figure 5-19 Semi-active close control loop.

By using fast electronic components, especially I/O card, A/D converter, and electronic relay, a high bandwidth value of about 300 Hz was achieved. This value measured by creating close loop running of the system without electro-mechanic components. Among electro-mechanic components, whereas the velocity transducers had no significant delay in their operation, the valves created main delay in the system. Therefore, the delay time of the valves was the single factor that established the bandwidth of the control system and was concerned in the selection of these valves.

The valve delay was studied during the valve modeling presented in section 3.2.2.4. The delays of the solenoid valves of this project were between 20 ms and 35 ms, referring to their data sheet. Therefore, the whole delay of the control loop was determined maximum 40 ms that meant that the bandwidth of the system was at least 25 Hz.

This bandwidth was acceptable for the control system in this research, because the goal of this research was the effective damping of the vibration of the tractor body. The natural frequencies of the tractor body, which were obtained from the primary tests, were maximum 2 Hz. On the other hand, the natural frequency of the wheels (i.e. unsprung mass) was 5 Hz. As a result, these frequencies were covered by 25 Hz bandwidth of the control system.

As described, by primary operation check of the system components, the correction of the system operation was confirmed, and necessary adjustment was performed. As the next step, the experimental tests were performed, which will be explained in the following section.

5.3.4 Experimental Test Performing

In order to perform the experimental evaluation of the new suspension system, the experimental tests were considered. For this purpose, as described in the previous chapter, a prototype of the system was built. A test plan was determined, and the related test setup was arranged. At the end, a check on system was performed. At this point, after all these preparations, the experimental tests could be begun.

For performing the experimental tests, the control equipments were placed all in the driver cabin (Fig. 5-20). These equipments consisted of interface card, low-pass filter, signal conditioner, and electronic relay system. After that, test-tractor was placed on the suspension test rig (Fig. 5-21).

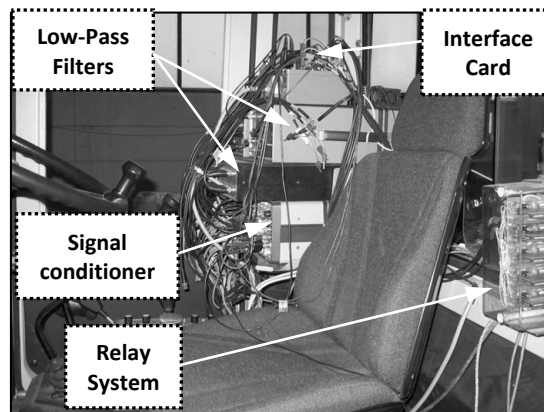


Figure 5-20 Electronic equipment installed in the tractor cabin used for the experimental test.

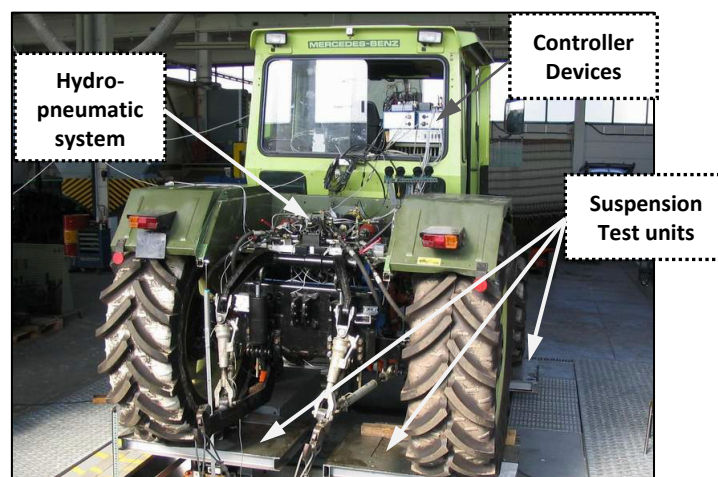


Figure 5-21 Rear view of the test-tractor standing on the full suspension test rig used for the experimental tests.

Interface card was connected to the controller PC via a long USB cable, which was placed in the controller room of the test rig (Fig. 5-22). Applying the proper input to the test rig, monitoring of the semi-active controller, and data logging system were performed from this room.

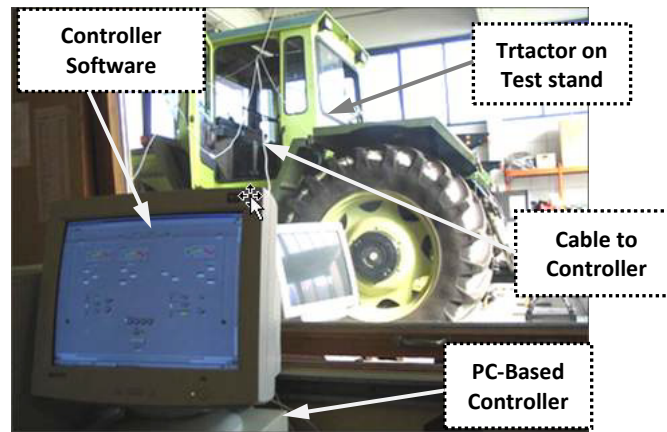


Figure 5-22 A view of the PC-based controller located in the test rig control cabin.

Performing of the experimental tests was based on the test plan presented in table 5-2. First, hydro-pneumatic rear suspension was tuned in the passive mode. For this purpose, the controller was turned off, and the throttle valve was tuned to the passive mode in order to provide the standard damping level. Then, the input mode was selected, and the controller of the suspension test rig was adjusted according to the arrangement in table 5-1.

After that, the data logger was turned on a new data file with specific name, and the test was performed by applying the “Roll” input signal to the test rig. The second repetition of the tests was performed after a period time in order to ensure that the vibrations of the tractor are damped completely. Then, the third and forth attempts were performed similarly, and finally, with closing the data file this test was finished.

The second and third test groups were performed with applying the “Pitch” and “Heave” input signals to the test rig. Each test category was performed similar to the “Roll” test. However, the data was saved with a new data file by data logger. Therefore, in the passive suspension mode, three data files including data of the 12 tests were achieved as the result of the tests.

After this test category of the passive suspension mode, the test category of the semi-active suspension mode was performed. For this propose, firstly, the hydro-pneumatic rear suspension was tuned on the semi-active mode. In this mode, the controller was tuned

on, and the throttle valve was tuned in the semi-active mode (i.e. low damping mode). Other steps of the test were similar to the test category of the passive mode. At the end, three data file including the data of the 12 tests, were achieved as the results of the tests.

As mentioned, each individual test was repeated four times in order to increase the reliability of the tests and decrease the influence of unexpected errors. For analyzing of the test data, the RMS, MPTP, and the PSD results of each repeat of the tests were calculated separately. Then, the average of the four repeats was considered as main result. These calculations were performed by using an m-file program in MATLAB software.

This program received the data files related to the four repeats of the experimental tests, and based on these data, calculated the output of the tests. The formulation of this calculation was presented in section 5.3.2. In addition, this program calculated the average values of the RMS, MPTP, and PSD analysis of the test outputs. The content of this m-file program is presented partly in appendix D1.

Chapter 6

Result

After describing the execution step of the simulation and experimental tests, in this chapter, the achieved results from these tests are presented. These results are presented in four groups, which are respectively: model validation results, ride comfort results, handling results, and suspension stroke results. At first, the results of the model validation are presented by comparison of the simulation tests results with the experimental tests results.

Then, performance of the new suspension system concerning the ride comfort of the tractor is evaluated by comparison of the passive suspension results with the semi-active suspension results for both the simulation and experimental tests. Likewise, the performance of the new suspension system concerning the handling capability of the tractor is evaluated. After that, the influence of the new suspension system on the suspension travel is examined by comparison of the passive suspension results with the semi-active suspension results for the simulation and experimental tests. Finally, all these results are summarized.

6.1 Model Validation

Along with the experimental and simulation studies, the validation of the simulation model was considered also as an objective of this research work. This was performed by comparison of the simulation result with the corresponding experimental results. After the validation of the model, the results of the simulation test could be used for the evaluation of the new suspension system by the simulation tests as well as the experimental tests. In addition, this model can be used for future developing investigations in the area of the suspension systems for agricultural tractors.

Figure 6-1 shows the procedure of the model validation. Each simulation result was compared with the corresponding experimental result. The simulation model was examined in order to recognize the weak points of the model and increase the correlations between simulation and experimental results.

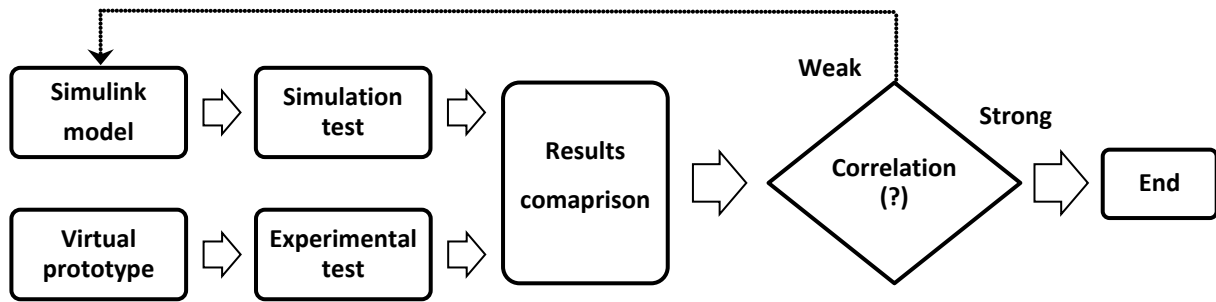


Figure 6-1 Model validation procedure.

Basically, low precise result appears in a simulation model because of the failure in the logic of the modeling or in the imprecise parameters of the simulation. In the validation process in this investigation, modification of the simulation model was performed by considering these two inaccuracy sources. For instance, in the case of the failure in modeling logic, after observing a low correlation in time and frequency domain results, it was realized that the hydraulic cylinder model should be modified by considering the friction effect in the model.

Therefore, as described in section 3.2.3, the model of the friction effect in the cylinders was built and added to the main cylinder model. In another case, observing low correlation in the natural frequency results led to consider a multi-body lumped-mass model for the tractor body model. In addition, parameters that are more accurate were derived for the tractor masses. These multi-body mass model and the relevant parameters are presented in appendix E.

The validation was performed based on the comparative results of the simulation and experimental tests in two categories of the time domain and frequency domain results. These results will be presented in the following sections. It should be noted that the simulation results of this part are the simulation results that were achieved after the model validation.

6.1.1 Amplitude-Based Validation

The amplitude-based validation of the model was performed using RMS values in the following formula. In this formula, which gives the percentage inaccuracy of the simulation results, experimental results are considered as the reference.

$$\text{Inaccuracy (\%)} = \left| \frac{\text{Simulation(RMS)} - \text{Average of Experiments(RMS)}}{\text{Average of Experiments(RMS)}} \times 100 \right| \quad 6-1$$

Considering passive suspension mode, the inaccuracies of all RMS results are presented in table 6-1. This table presents the percentage inaccuracies of the tractor body accelerations, dynamic tire force, and MPTP.

Table 6-1 Comparison between simulation and experimental results in the passive suspension mode.

Parameter mode	Units	Simulation	Experiment	Inaccuracy (%)
Body acceleration Heave	RMS [m/s ²]	0.577	0.698	17.3
Body acceleration Pitch	RMS [rad/s ²]	0.478	0.565	15.4
Body acceleration Roll	RMS [rad/s ²]	0.296	0.371	20.2
Dynamic tire force	RMS [N]	1267.6	1444.7	12.3
Suspension travel	MPTP [m]	0.065	0.061	6.6

Similarly, for the semi-active suspension mode, the inaccuracy related to the RMS and MPTP values of the simulation results are presented in table 6-2.

Table 6-2 Comparison between simulation and experimental results of the semi-active suspension.

Parameter Mode	Units	Simulation	Experiment	Inaccuracy (%)
Body acceleration Heave	RMS [m/s ²]	0.523	0.653	19.9
Body acceleration Pitch	RMS [rad/s ²]	0.427	0.519	17.7
Body acceleration Roll	RMS [rad/s ²]	0.257	0.335	23.3
Dynamic tire force	RMS [N]	1190.3	1381.8	13.9
Suspension travel	MPTP [m]	0.074	0.072	2.8

These results show indeed the accuracy of the model after the correction and improvement of the model. As shown, the accuracy of the simulation results in the passive mode is minimum 79 % and in the semi-active mode is minimum 77 %. These results indicate a good agreement between simulation and experimental time domain results. In the semi-

active results, the accuracy of the results are not reduced more than 4.2 % that. This represents the good accuracy in simulation model of the controller and actuators.

6.1.2 Frequency-Based Validation

The frequency-based validation of the model was performed by comparing the PSD graphs of the simulation results and experimental results. This comparison evaluated the correlation of the model in different frequency areas helping to recognize the model weak point. Figures 6-2 shows the PSD graphs derived from the heave body acceleration of the simulation and experimental tests in the passive suspension mode. Figure 6-3 shows the similar graphs of the semi-active suspension mode. These graphs are presented here as typical graphs. Some other graphs are presented in appendix A1.

In principle, the frequency range related to the vehicle suspension is 0 - 20 Hz. In this research, primary observation on the PSD results of the simulation and experimental tests showed that the major vibrations occurred in the first half areas of this frequency range. Therefore, in order to illustrate higher graph resolution, the PSD graphs in this thesis are just presented in the frequency range of 0 – 12 Hz, such as the following PSD graphs.

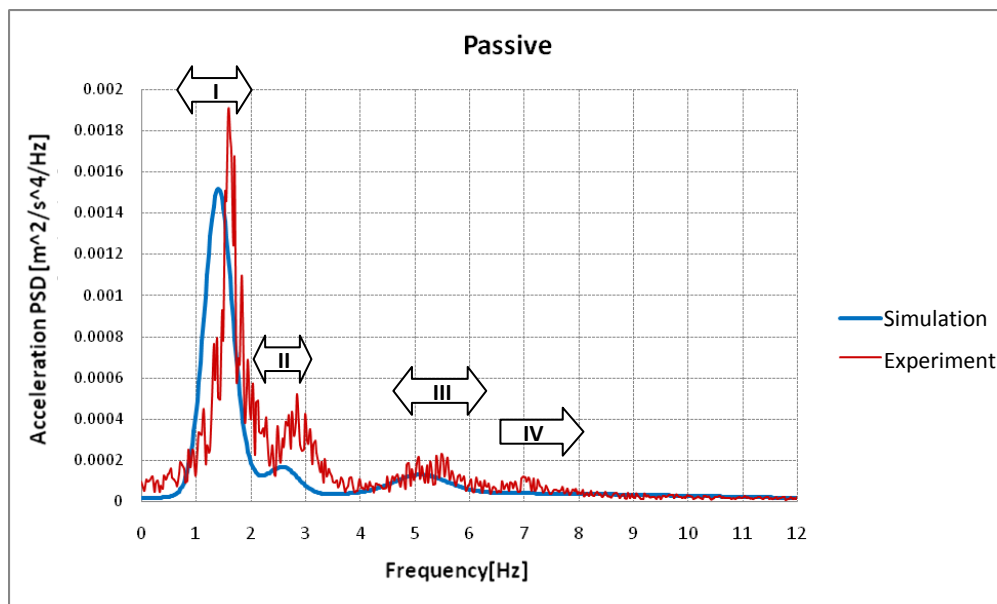


Figure 6-2 Comparison between the simulation and experimental frequency responses of the tractor body acceleration in the passive suspension mode.

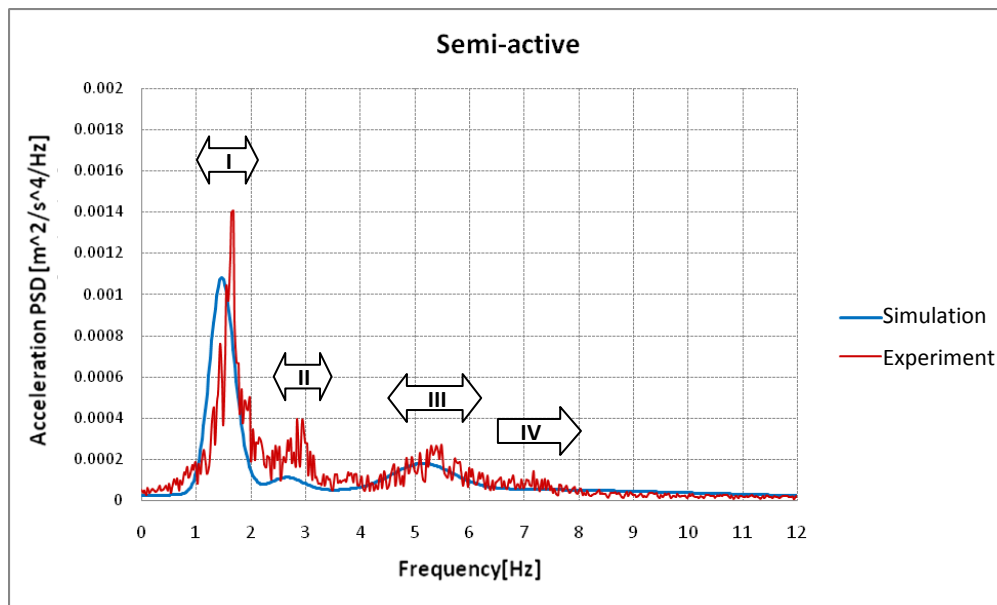


Figure 6-3 Comparison between the simulation and experimental frequency responses of the tractor body acceleration in the semi-active suspension mode.

These results are indeed the comparison of the experimental result with the results of the validated simulation model. As the first different, simulation curve is smooth and experimental curve is jagged. This is so, because the tractor body model was simplified to the lumped solid-mass model, whereas in reality, tractor body consists of mass-components (i.e. multi-body) with elastic connection. However, as shown the main curves demonstrate a good agreement. In order to analyze these graphs, the frequency area is divided into four areas.

The first area is the frequency range from 0.5 to 2 Hz, containing tractor body (sprung mass) natural frequencies. As shown, there is a good agreement between two curves, and just the frequency of the peak amplitude is a little different. The quantity of this difference will present in the end of this section.

The second area is the frequency range from 2 to 4 Hz. This area is placed between the two areas of the natural frequencies of the sprung mass and unsprung mass. As shown, in this area on the experimental curve, there is an unknown peak amplitude. Before the validation of the model, in the simulation curve, this peak did not exist. An estimated computation showed that the frequency of this peak (~3 Hz) is comparable with natural frequency of the tractor body when there would be solid connection between the body and wheel. Primary experimental observation indicated that this peak occurred because of the slip-stick effect in the suspension elements. In order to provide a better agreement between

simulation and experiment curves in this area, the friction model of the cylinder was added to the main model (described in section 3.2.3). After that, a similar peak appeared in the simulation curve in this area (Fig. 6-2, 6-3).

The third area is the frequency range between 4 and 6.5 Hz. This area contains particularly the natural frequency of the wheels (i.e. unsprung mass). As shown, there is a good agreement between the two curves, and just the frequency of the peak amplitude is a small amount different. The quantity of this difference will be presented in the end of this section.

Frequency range further than 6.5 Hz is the fourth area, which contains the natural frequencies related to the minor mass-components of the tractor. Except a minor peak amplitude in the experimental curve, there is no considerable peak in this area. This peak is indeed the natural frequency of the cabin, which is attached to the tractor body through a rubber connection operating as a semi-suspension and has its individual natural frequency. Since this system had not significant effect on the results of the experimental tests, it was not considered in the simulation model. Consequently, the effect related to this system does not exist in the simulation curve.

As shown from the PSD graphs, the experimental curves show generally a little higher amplitude than simulation curve. As shown before, this phenomenon was more obvious in the amplitude-based results of the validation. As mentioned, in the validation procedure, some modifications in modeling logic and the model parameters were done, such as adding the friction model, adding the multi-body mass model, and using the more accurate mass parameters. Therefore, a better agreement between general amplitude level of the simulation and experimental results was achieved. This improvement was particularly notable in the second area of the PSD graph that was affected by the static friction factor in the suspension system.

The frequency-based method for validation of the model is the comparison of the different natural frequencies of the tractor, which are derived from the simulation and experimental tests. As mentioned before, corresponding to each degree of freedom of the model, a natural frequency can be derived from the simulation results. Therefore, seven natural frequencies related to the seven degrees of freedom of the model are considered. Heave, pitch, and roll motion of the tractor body are three of them, and the rest four frequencies are the natural frequencies of the four tractor wheels. Since the tires and mass

parameters of the four wheels are similar, the four natural frequencies of the wheels are the same, and in validation study, the frequency of the just one of them is considered.

Table 6-3 presents the five natural frequencies, derived from the simulation and experimental results. Percentage validation of the simulation results are also presented in this table. As seen, these percentage results are at least 67 %, showing an acceptable agreement between simulation and experimental natural frequencies.

Table 6-3 Comparison between simulation and experimental natural frequencies of the tractor.

Vibration Mode	Natural Frequency		Min. Validation [%]
	Experiment [Hz]	Simulation [Hz]	
Body Heave	≈ 1.6	1.4	78
Body Pitch	≈ 1.7	1.6	84
Body Roll	≈ 1.0	0.8	67
Wheel Hop	≈ 5.4	5.1	88

In the whole, after attaining acceptable correlations between the time domain and frequency domain results of the simulation and experimental tests, the model validation was completed, so that it can be used in order to simulate the dynamic behavior of an agricultural tractor by focusing on the suspension system. After this validation, the results of the simulation tests were used for the evaluation of the new suspension system besides the experimental tests, as the secondary reference. This led to a more accurate system evaluation. In the following sections, these results will be presented.

6.2 Ride Comfort Evaluation

The first criterion for evaluating the semi-active suspension is the ride comfort. For this purpose, as stated before, accelerations of the tractor body were considered. The performance of the new suspension system was evaluated by comparing the time domain and frequency domain results of the passive suspension mode with the semi-active suspension mode. In this section, the results of the simulation tests and then, the results of the experimental tests are given. In each part, the time domain results and the frequency domain results of the tests are presented.

6.2.1 Simulation Result

Evaluation of the suspension system, based on the time domain results, was performed by comparing the RMS value of accelerations. In order to quantify this comparison, the following equation was used for calculating the percentage improvement of ride comfort. The accelerations magnitudes on the center of gravity of the tractor body are presented in table 6-4. This data were obtained from the simulation tests. These include the heave, pitch, and roll accelerations of the passive and semi-active suspension.

In addition, improvement of ride comfort, based on the RMS values of accelerations is denoted in percentage by means of equation 6-2, which is presented in the last column of this table.

$$improvement\ (\%) = \left| \frac{(semi - active\ RMS) - (passive\ RMS)}{passive\ RMS} \right| \times 100 \quad 6-2$$

Table 6-4 Simulation RMS results of the tractor body accelerations with passive and semi-active suspension.

Body Acceleration	Units	Passive (RMS)	Semi-active (RMS)	Improvement [%]
Heave	[m/s ²]	0.577	0.523	9.4
Pitch	[rad/s ²]	0.478	0.427	10.7
Roll	[rad/s ²]	0.296	0.257	13.3

As shown, the improvements are between 9.4 % and 13.3 %. Considering that the semi-active control was applied just to the rear suspension of the tractor, these results indicate a good performance for the new suspension in reducing the accelerations level on the tractor body, and means that a considerable improvement in the ride comfort of the tractor was achieved.

The RMS analysis gave quantitative information about the average performance of the system. After that, in order to examine the detailed operation of the semi-active system in different frequency ranges, the frequency analysis of data was considered, which was performed by study of the related PSD graphs. Figure 6-4 shows on of these graphs derived from the vertical acceleration on the tractor body in the passive and semi-active suspension modes.

As seen, the frequency area of this graph can be divided into four ranges. The first area is the frequency range between 0.5 and 2 Hz, which contains the natural frequencies of the tractor body (i.e. sprung mass). As shown, the best performance of the semi-active suspension in reduction of the acceleration occurs in this area. The peak of the curve in this area shows the natural frequency related to the vertical movement of the tractor body. As shown, this frequency is 1.4 Hz. Likewise; the natural frequencies related to the rotational movements of the tractor body in the simulation tests were derived. These frequencies were mentioned in the validation section before.

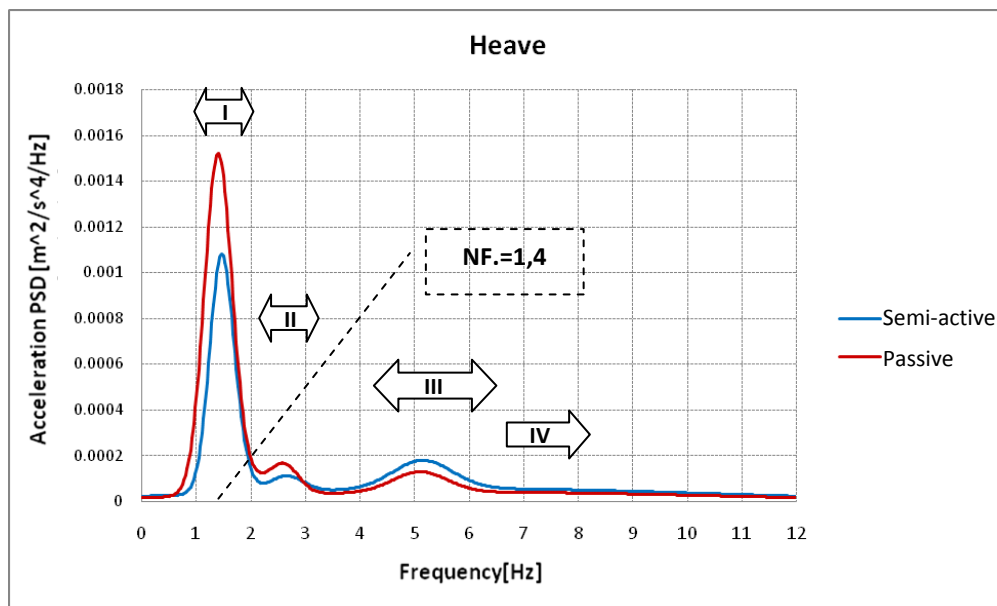


Figure 6-4 Comparison between semi-active and passive frequency responses of the tractor body acceleration in the simulation test.

The second area is the frequency range from 2 to 4 Hz, placed between the two areas of the natural frequencies of the sprung mass and unsprung mass. As mentioned, the peak amplitude in this area appears because of the friction-effect, which was considered in the model of the hydro-pneumatic suspension. As shown, the performance of the semi-active suspension in this area is also considerable and reduces the acceleration.

The third area is the frequency range between 4 and 6.5 Hz, containing the wheel (i.e. unsprung mass) natural frequency. As shown, the semi-active is not reduced the acceleration in this area. This happened because of the principle of the sky-hook control strategy that concentrates on the controlling the tractor body vibration, and not on the vibration of the wheels, which is the exciting source of the tractor body in this area. More discussion in this theme is presented in section of “handling result”. The fourth area is the

frequency range further than 6.5 Hz, which contains the natural frequencies related to the minor mass-components of the tractor. In this area no major vibration is appeared. Therefore, this area had not a significant role in performance of the semi-active suspension.

As shown, the semi-active suspension improved the ride comfort just in the first and the second frequency ranges, and improvement in the rest ranges was not achieved. However, based on the RMS results, the semi-active improved the whole ride comfort. The PSD graphs derived from the rotational accelerations of the tractor body are presented in appendix A2. These include the results of both the passive and semi-active suspension modes, which are derived from the simulation tests.

6.2.2 Experimental Result

Similar to the simulation result, the time domain-based evaluation of the suspension was performed by comparing the RMS value of accelerations. In order to quantify this comparison, the changes of ride comfort are denoted in percentages. Results related to the accelerations at the center of gravity of the tractor body are presented in table 6-5. These results are the heave, pitch, and roll accelerations of the passive and semi-active suspension modes, which are obtained from the experimental tests. In addition, percentage influence of the semi-active suspension on ride comfort is calculated based on the RMS value of the accelerations and is presented in the last column of this table.

Table 6-5 Experimental RMS results of the tractor body accelerations with passive and semi-active suspension.

Body Acceleration	Units	Passive (RMS)	Semi-active (RMS)	Improvement [%]
Heave	[m/s ²]	0.698	0.653	6.4
Pitch	[rad/s ²]	0.565	0.519	8.2
Roll	[rad/s ²]	0.371	0.335	9.7

As shown, the improvements are between 6.4 % and 9.7 %. Even if these results are not strong as simulation results, considering that the semi-active control was applied just to the rear suspension of the tractor, these values indicate still an acceptable performance. As a result, the new suspension was able to reduce the tractor body accelerations, and consequently, it improved the ride comfort capability of the tractor.

Similar to simulation results, for experimental results, the frequency domain analysis was considered in addition to the evaluation based on the time domain results. By frequency domain analysis, the detailed operation of the semi-active system in different frequency ranges was examined. This was performed based on the related PSD graphs. Figure 6-5 shows the PSD graphs derived from the vertical acceleration of the tractor body in the passive and semi-active suspension modes, derived from the experimental tests.

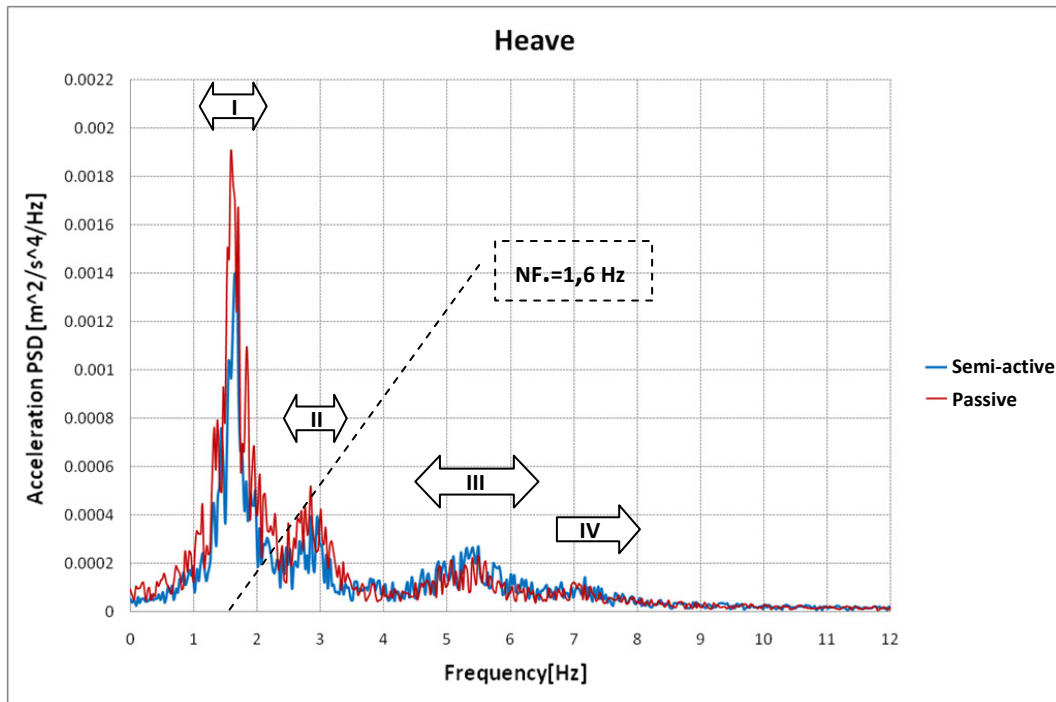


Figure 6-5 Comparison between semi-active and passive frequency responses of the tractor body acceleration in the experimental test.

As seen, the frequency area of this graph is divided again into four ranges. The first area is the frequency range from 0.5 to 2 Hz, containing the natural frequencies of the tractor body (i.e. sprung mass). The peak of the curve in this area shows the natural frequency related to the vertical movement of the tractor body. As shown, this frequency is 1.6 Hz. The natural frequencies of the body rotational movements were derived similarly in the experimental tests. These data were presented in the validation section. As shown, the best performance of the semi-active suspension in reduction of the acceleration occurs in this area.

The second area is the frequency range of 2-4 Hz, located between the two areas of the natural frequencies related to the sprung mass and unsprung mass. As mentioned, the peak amplitude in this area appeared because of a friction effect. As shown the performance

of the semi-active suspension in this area is also considerable and reduces the acceleration significantly.

The third area is the frequency range from 4 to 6.5 Hz. This area contains the natural frequency of the wheels (i.e. unsprung masses). As shown, in this area, the acceleration level was not reduced by the semi-active suspension. This happened because of two reasons. First, the sky-hook control strategy in principle, concentrates on controlling the tractor body vibration and not on controlling the wheel vibration, which is the source of the vibration appearing in this frequency area. More discussion in this theme is presented in section of “handling result”.

Secondly, a practicable rate was selected for the bandwidth of the controller with the purpose of controlling the vibrations in the frequency range related to the tractor body motions (i.e. first range). Therefore, as the frequency range goes far from the first range, the control ability of the semi-active suspension reduced, and the suspension operation slanted to a passive suspension. Despite the low performance of the semi-active suspension in the third area, the overall performance of the system in controlling the vibration of the tractor body was positive. This conclusion was obtained based on the related RMS results.

The fourth area is the frequency range further than 6.5 Hz, containing the natural frequencies related to the minor mass-components of the tractor. In this area, no significant vibration is observed. On the other hand, as explained, in this area the semi-active suspension has no direct control. Therefore, this area is not considered important in performance evaluation of the semi-active suspension.

Results of the experimental tests, similarly to the simulation results, revealed that the semi-active suspension improved the ride comfort of the tractor. This improvement was created particularly in the first and the second frequency ranges, and improvement in the rest ranges was not achieved. However, the RMS results indicated that semi-active improved the overall ride comfort. The PSD graphs derived from the rotational accelerations of the tractor body are presented in appendix A3. These are the results of the experimental tests in the passive and semi-active suspension modes.

6.3 Handling Evaluation

In order to evaluate the performance of the semi-active suspension, after ride comfort, the handling capability of the tractor was investigated. As stated before, in order to quantify the handling, vertical dynamic tire contact-force was measured. Similar to the ride

comfort study, by comparing the time domain and frequency domain results of the suspension in the two modes of the passive and semi-active, the new suspension system was evaluated. In this section, results of the simulation tests and experimental tests are presented. In each part, the time domain results and frequency domain results are given. These parts include the results of the two modes of the passive and semi-active suspension.

6.3.1 Simulation Result

Time domain analysis is performed based on the comparison of the RMS results of the vertical dynamic tire force. The average of the RMS values derived from the dynamic tire force of the tractor rear wheels are presented in table 6-6. These simulation results are given for the two passive and semi-active suspension modes. In order to quantify this comparison, the percentage improvement of ride comfort is given in the table as well.

Table 6-6 Simulation results of the dynamic tire force in the passive and semi-active suspension mode.

Dynamic Tire Force	Passive	Semi-active	Units
RMS	1267.6	1186.3	[N]
Improvement	6.4		[%]

As shown, the improvement of 6.4 % is gained. This result is considerable, because the semi-active control was applied just to the rear suspension of the tractor and not to all four wheels. On the other hand, since the skyhook control strategy is focused principally on the vibration control of the vehicle body and not on the vibration control of the wheels. Referring to the achieved result, the semi-active suspension was able to reduce the dynamic tire force of the tractor significantly, and the handling capability of the tractor was improved consequently.

The frequency-response results of the tractor body accelerations studied for ride comfort investigation showed that in the third frequency range, which was related to the vibration of the wheels, no positive performance by semi-active system was achieved. This result was matched to the basic function of sky-hook strategy. However, the RMS results of the dynamic tire force indicated that the new suspension had positive influence on the handling capability of the tractor. In order to clarify this specious inconsistency, the frequency-response of the dynamic tire force was studied.

The results of the frequency-based analysis of the dynamic tire force are presented as the PSD graphs. Figure 6-6 shows one of these graphs derived from the dynamic tire force of the tractor in passive and semi-active suspension modes, related to the simulation tests.

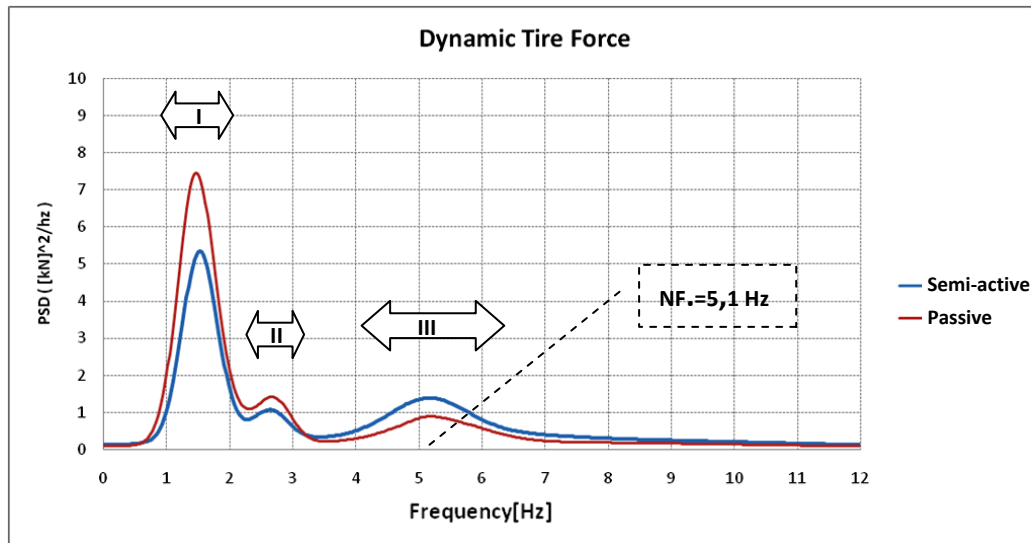


Figure 6-6 Comparison between semi-active and passive frequency responses of the dynamic tire force in the simulation test.

As seen, the frequency area of this graph is divided into three ranges. The first area is the frequency range of 1 - 2 Hz, containing the natural frequencies of the tractor body (i.e. sprung mass). As shown, the best performance of the semi-active suspension in reducing the dynamic tire force was achieved in this area. The second area is the frequency range of 2 - 3 Hz, which is the area between two natural frequencies areas related to the sprung mass and unsprung mass. As mentioned, the peak amplitude in this area appeared because of the function of the friction model. As shown, the performance of the semi-active suspension in this area was also considerable and reduced the amplitude of the dynamic tire force.

The third area is the frequency range from 4 to 6.5 Hz. This contains the natural frequency of the wheels (i.e. unsprung masses). The peak of the curve in this area shows the natural frequency related to the vertical motion of the tractor wheel that this frequency is 5.1 Hz. As shown, the dynamic tire force was not reduced by the semi-active in this area, whereas based on the RMS results, the dynamic tire force was reduced, and handling was improved.

The dynamic tire force is affected directly by the two factors of the vehicle body vibration and wheel (i.e. unsprung mass) vibration (refer to section 5.3.2). Therefore, these two factors were considered in order to investigate the influence of the semi-active

suspension on the dynamic tire force. The PSD graphs related to the tractor body accelerations showed that the semi-active suspension controlled notably the vibration of the tractor body in the first frequency range. In order to examine the effect of the semi-active suspension on the wheel vibration, the PSD graph derived from the vertical acceleration of the wheels was studied.

Figure 6-7 shows the PSD graphs derived from the wheel acceleration in passive and semi-active suspension modes, obtained from the simulation tests. In this graph two frequency ranges is considered. The first one is the area including the natural frequencies of the tractor body motions, and the second one is the area of the natural frequency related to the wheel motion. As seen, in the first area, the role of the semi-active suspension in reduction of the wheels acceleration is slightly positive. However, this effect in the third area is significantly negative. This occurred because of the basics of sky-hook control strategy that is focused on the vibration control of the body of a vehicle.

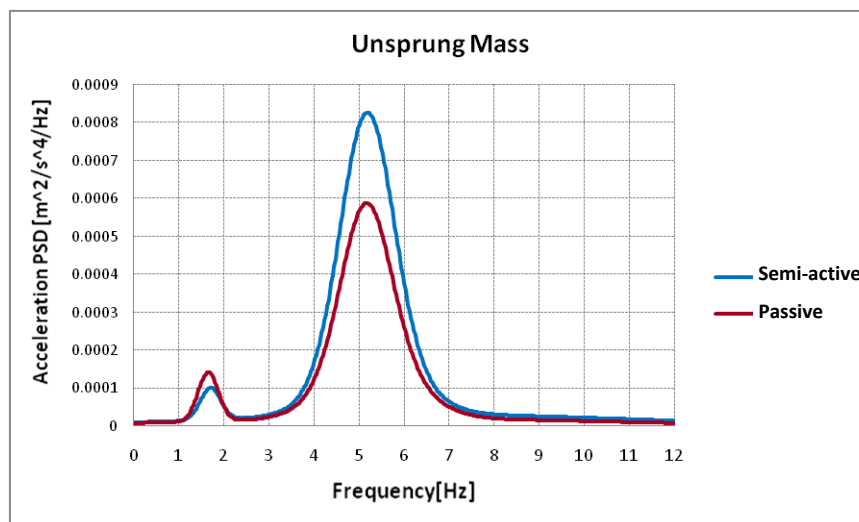


Figure 6-7 Comparison between semi-active and passive frequency responses of the unsprung mass (i.e. wheel) acceleration in the simulation test.

The negative effect on the wheel vibration was observable in the third frequency range (i.e. wheel natural frequency area) of all the PSD graphs. However, this effect was always small in comparison with the positive performance of the semi-active suspension on the first frequency range (i.e. tractor body natural frequencies area). After looking at equation 5-15 and considering that the mass of the tractor body is higher than unsprung mass, it can be understood why the influence of the body vibration is greater than the factor of the wheel vibration. This is the reason that the overall performance of the system in

controlling of the dynamic tire force was positive. This issue was observable especially in the result of the dynamic tire force, as the dynamic tire force were improved significantly in spite of the increase in the wheel acceleration. This was also approved in the RMS results of the dynamic tire force.

6.3.2 Experimental Result

The average of the RMS values derived from the dynamic tire force of the rear wheels are presented in table 6-7. These values are the results in the passive and semi-active suspension modes and derived from the experimental tests. In order to quantify the comparison of these two results, the percentage improvement is presented in the table as well. This value indicates indeed the improvement of ride comfort, achieved by the new semi-active suspension.

Table 6-7 Experimental results of the dynamic tire force in the passive and semi-active suspension mode.

Dynamic Tire Force	Passive	Semi-active	Units
RMS	1444.7	1381.8	[N]
Improvement	4.3		[%]

As shown, the improvement of 4.3 % is achieved. This result is not as strong as simulation result, but it is still considerable, because as mentioned, the semi-active control was employed just in the rear suspension of the tractor and not for the complete four wheels. In addition, the skyhook control strategy is focused principally on the control of the body vibration of a vehicle and not on the control of the wheels vibration. This result also showed that in the experimental tests, the dynamic tire force of the tractor was reduced by the semi-active suspension. Consequently, the handling capability of the tractor was improved.

Performance of the semi-active suspension in reduction of the dynamic tire force in different frequency ranges was studied by the frequency-response of the dynamic tire force. Figure 6-8 shows the PSD graphs derived from the dynamic tire force of the tractor in the passive and semi-active suspension modes, achieved from the experimental tests.

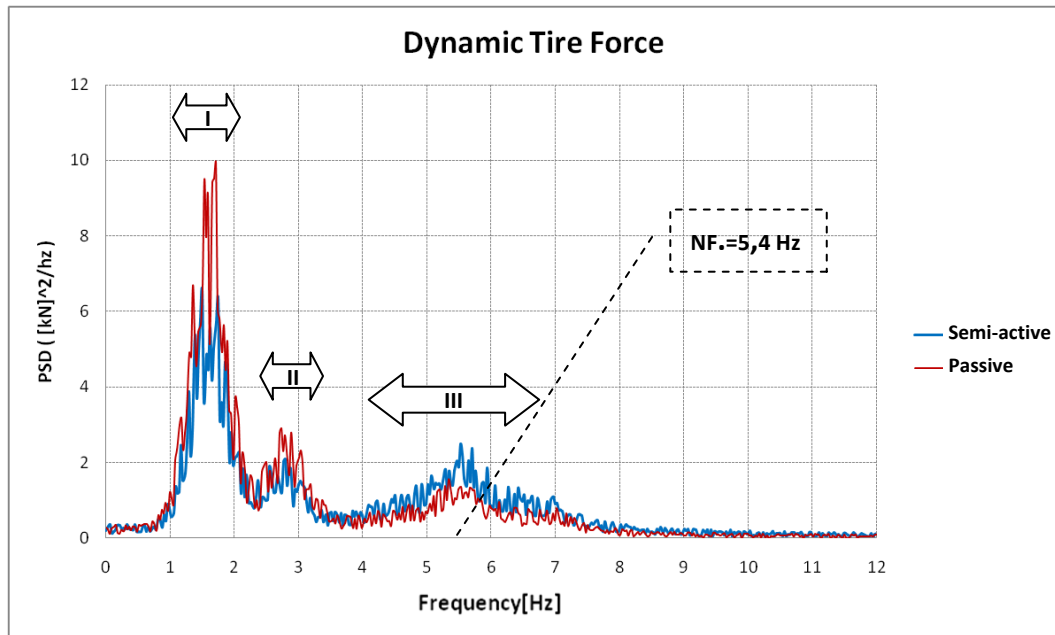


Figure 6-8 Comparison between semi-active and passive frequency responses of the dynamic tire force in the experimental test.

As seen, the frequency area of this graph is divided into three ranges. The first area is the frequency range of 1 - 2 Hz, containing the natural frequencies of the tractor body (i.e. sprung mass). As shown, the best performance of the semi-active suspension in reduction of the dynamic tire force was gained in this area. The second area is the frequency range from 2 to 3.5 Hz. This area is located between two groups of the natural frequencies areas of the sprung mass and natural frequencies areas of the unsprung masses. As mentioned, the peak in this area appeared because of the friction-effect in the suspension elements. As shown, performance of the semi-active suspension is also acceptable in this area, and the amplitude of the dynamic tire force is reduced.

The third area is the frequency range from 4.5 to 7 Hz, which includes the natural frequency of the wheels (i.e. unsprung masses). The peak of the curve in this area shows the natural frequency related to the vertical motion of the tractor wheel. As shown, this frequency is 5.4 Hz. In the third area, the dynamic tire force was not reduced by the semi-active. However, the RMS results indicated that in general, the dynamic tire force was not increased, but also a significant improvement in vehicle handling was achieved.

As mentioned, the dynamic tire force is affected directly by the two factors of the body vibration and wheel vibration of a vehicle. The PSD graphs of the tractor body accelerations showed that the semi-active suspension controlled remarkably the vibration of the tractor body in the first frequency range. The PSD graphs of the tractor body

accelerations and dynamic tire force indicated that the effect of the semi-active suspension on the reduction of the wheels acceleration in the third area was significantly negative. This effect occurred because of the control logic of sky-hook strategy that is concentrated on the vibration control of the body of a vehicle. However, using practicable sky-hook strategy moderated this focus, and leads to improve the vibration control of the wheels partially as well.

The semi-active suspension increased the wheels acceleration. This has just a slight negative construction effect on the wheels. However, the indirect effect of this phenomenon on the dynamic tire force is important, and it affects significantly on the handling of the vehicle. This negative effect was recognizable in the third frequency range (i.e. wheel natural frequency area) of all the PSD graphs. However, this effect was always small in comparison with the positive performance of the semi-active suspension in the first frequency range (i.e. tractor body natural frequencies area). This fact that the factor of the body vibration has stronger effect than the wheel effect led to overall positive performance of the system, particularly in reducing the dynamic tire force. This was also approved by the RMS results of the dynamic tire force.

As whole, results of the experimental tests revealed similar to simulation results that the semi-active suspension improved the handling capability as well as the ride comfort of the tractor. This improvement was created particularly in the first frequency ranges, and improvement in the third ranges was not achieved. Although, the RMS results indicated that the semi-active reduced the total dynamic tire force of the tractor and so, improved the handling capability.

6.4 Suspension Travel Evaluation

After the examination of ride comfort and handling as the dynamic parameters of the tractor, a constructional parameter of suspension systems was considered in order to evaluate the performance of the new suspension system. In design of a suspension system, the available place between the vehicle chassis and each wheel used for suspension elements is limited. Therefore, in design of a suspension system, this factor must be considered. The related factor is the stroke of a suspension. Lower required stroke is considered as an advantage in suspension design, because means that less suspension place is needed. With conversion a passive suspension to an active suspension, this factor may be

changed. So, in this research, the effect of this semi-active suspension on the stroke of the suspension was examined. In this part, result of this examination obtained from the simulation and experimental tests are presented.

The maximum stroke of a suspension is the key factor in the suspension design. Therefore, the maximum peak-to-peak of the suspension travel, with the abbreviation of “MPTP”, was considered as the measuring value in this study. The calculation method of this parameter was described in section 5.1.2.1.

The average MPTP values of the suspension travel of the rear suspension-units in the passive and semi-active suspension mode are presented in table 6-8 and 6-9. These results are obtained from the simulation and experimental tests. The percentage change in the suspension travel in comparison with passive system is presented also in the tables.

Table 6-8 Simulation results of the suspension travel in the passive and semi-active suspension mode.

Suspension Travel	Passive	Semi-active	Units
MPTP	0.065	0.074	[m]
Variation	14		[%]

Table 6-9 Experimental results of the suspension travel in the passive and semi-active suspension mode.

Suspension Travel	Passive	Semi-active	Units
MPTP	0.061	0.072	[m]
Variation	18		[%]

These results indicate that using semi-active suspension, the suspension travel was increased 14 % in the simulation tests and 18 % in the experimental tests in comparison with passive values. This negative effect of the semi-active system is related to the basic operation of skyhook approach that focuses on the control on the body vibration of a vehicle. This is gained at the cost of a poor control on the wheel vibration and consequently, undesirable higher suspension travel. However, this rise in the suspension travel implies a need for some centimeters more space for suspension elements that is not considered as a notable limiting factor.

6.5 Result Summary

In order to evaluate the semi-active suspension, two groups of the simulation tests and experimental tests with a similar plan were performed. In each group, three series of tests with the three different input tests were used. Evaluation of the new suspension was done by comparing the passive and semi-active suspension modes. Therefore, each test was performed once in the passive mode and then, in the semi-active mode. The achieved data from these tests in the two suspension modes were analyzed in order to derive the amplitude and frequency based results of the system. These results were presented in the RMS values and the frequency domain graphs. The frequency-domain graphs were used in order to investigate the vibration characteristic of the suspension system in different frequency ranges of the system bandwidth.

Vibration control of the tractor body, particularly in the area of the body natural frequencies, was considered as priority motive for using an active suspension for tractors. The control strategy used for the semi-active suspension was selected considering this concern. In evaluation of the semi-active suspension, the ride comfort capability of the tractor was considered as the first criterion. For this purpose, accelerations of the tractor body were measured, and the influence of the new suspension system on the ride comfort capability of the tractor was evaluated by comparing the results of the passive and semi-active suspension modes. The following charts show the summary results related to the tractor body accelerations, acquired from the simulation and experimental tests.

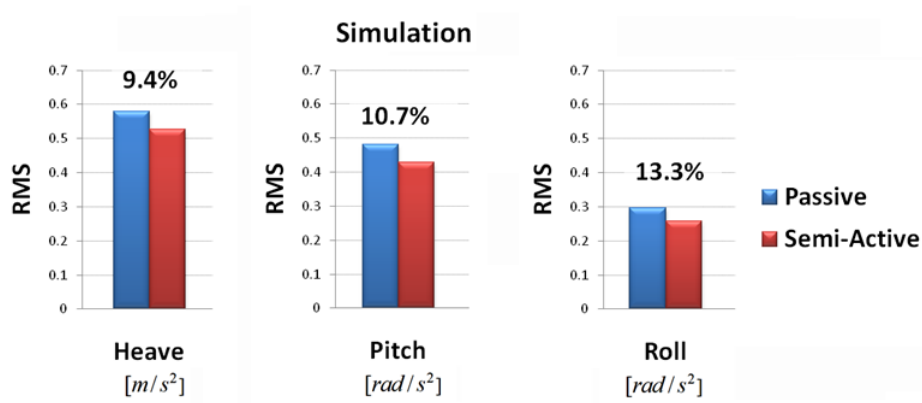


Figure 6-9 Comparison between RMS results of the tractor body accelerations in the simulation tests.

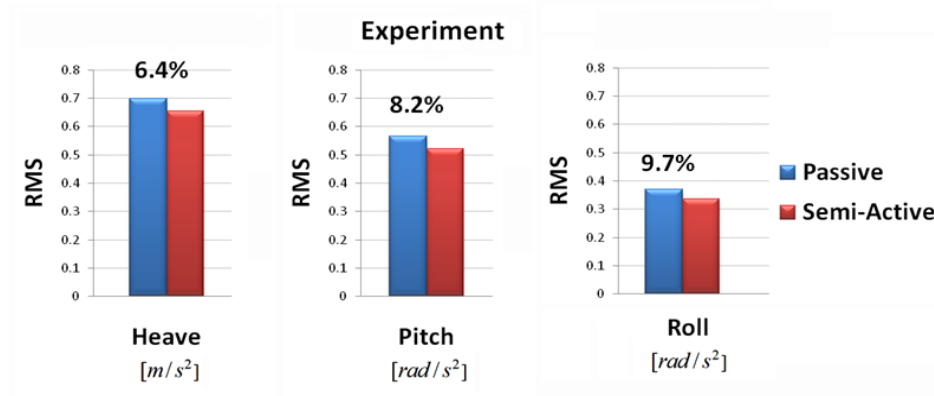


Figure 6-10 Comparison between RMS results of the tractor body accelerations in the experimental tests.

After ride comfort, improvement of the handling capability was the main goal of applying active suspensions to the suspension system of tractors. In order to evaluate the performance of the new suspension system in this respect, the vertical dynamic contact-force of the tractor's tires was considered as the quantifier parameter, and the effect of the new suspension system in handling capability of the tractor was examined. This was performed by comparing the dynamic contact-force results of the passive suspension with the semi-active suspension modes. The subsequent charts show the summary results related to the dynamic tire force of the tractor, obtained from the simulation and experimental tests.

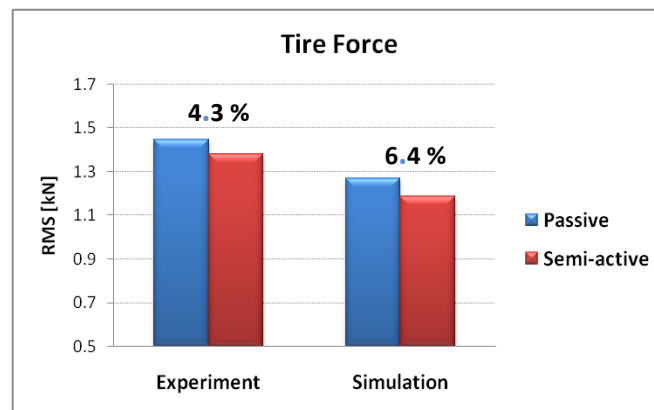


Figure 6-11 Comparison between the RMS results of the dynamic tire force in the simulation and experimental tests.

After the examination of ride comfort and handling as the dynamic parameters of the tractor, maximum suspension travel was considered as a constructional criterion in order to evaluate the new suspension system. For this purpose, the suspension travel in the passive and semi-active suspension modes was compared in order to examine the effect of this

semi-active suspension on the stroke of the suspension. The following charts show the summary results related to the maximum suspension, acquired from the simulation and experimental tests.

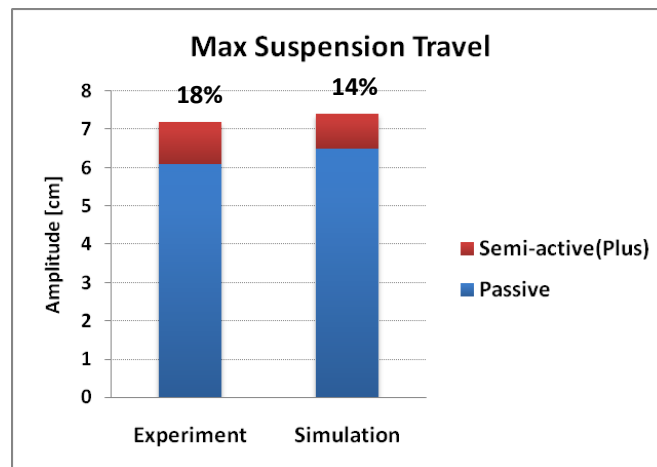


Figure 6-12 Comparison between the MPTP results of the suspension travel in the simulation and experimental tests.

Table 6-10 presents the result of a comparative study with the intention of evaluating the performance of the semi-active suspension in the simulation tests and experimental tests. In this table, the whole measured parameters are considered. A view of these results reveals that the simulation results in comparison with the experimental results indicated always a better performance for the new suspension system. In addition, after referring to the RMS results, it was realized that the simulation results had lower magnitude than corresponding experimental results.

Table 6-10 Difference in performance of the semi-active suspension in the simulation and experimental tests.

Parameter Mode		Improvement (%)	
		Simulation	Experiment
Body Acceleration	Heave	9.4	6.4
Body Acceleration	Pitch	10.7	8.2
Body Acceleration	Roll	13.3	9.7
Dynamic Tire Force		6.1	4.3
Suspension Travel		14	18

These results illustrate that the simulation model is inclined to present the ideal feature of the system, and some practical negative factors in the experimental tests are not considered. Even if in the validation of the model, some new concerns, such as the cylinder static friction model and the multi-body lumped mass model of the tractor body, were recognized and added to the model. Based on the tests results and observation, author supposed that the complex friction effect present in the suspension components was the main disturbing factor.

This effect caused also that in the experimental tests, the low damping level of the semi-active suspension was in practice higher than the determined value. This indicates that reducing the friction forces in a suspension system leads to a more efficiency for a semi-active suspension.

Chapter 7

Conclusion

This chapter is intended to summarize the work, which was done for this thesis, and to present the conclusions, which were achieved from this study. The chapter is concluded with several suggestions for future research in order to extend this work.

7.1 Summary and Conclusions

Main objective of this research was to improve suspension performance of agricultural tractors by using a proper active suspension system. In order to accomplish this objective, the background of the research was studied initially. This study leads to choose a proper active suspension system for agricultural tractors. For evaluation of this new suspension system, two approaches of the computer simulation testing and experimental testing were used.

In order to perform the evaluation tests, the design and plan of the simulation and experimental tests were determined. The output of the tests was the acceleration data of the tractor body and wheel. These data were analyzed in order to obtain the time and frequency domain results of the vibration modes. These results were used in order to evaluate the ride comfort and handling ability of the tractor. Based on the investigations done for this thesis, the following conclusions are drawn:

- Idea of active suspension for agricultural tractors. In this research, available options for an active system for the chassis suspension of agricultural tractors were studied. As the best choice, a semi-active suspension with the control strategy of “on-off skyhook” was selected.
- Modeling of the new suspension system. For this purpose, a computer model of the tractor counting the suspension model, using MATLAB-Simulink program, was built. The model consisted of the test-tractor model and the semi-active suspension model. The semi-active suspension model was composed of three sub-model models: controller, actuator, and sensor models.

- Development of the prototype of the new suspension system. In order to perform the practical evaluation of this new system, the full suspension test-tractor of TU-Trac with hydro-pneumatic rear suspension was determined. A prototype of the new suspension system was developed and then, on the rear axle suspension of the test-tractor was installed. The prototype consisted of three parts: set of the sensors, hydraulic actuators, and electronic controller.
- Design of the tests. In order to evaluate the performance of the new suspension by simulation and experimental testing, design and plan of the tests were determined. The suspension system was excited by the three set of impulse inputs, which were applied to the four tractor's wheels. Each test was performed in the two suspension modes of the passive and semi-active.
- Operation of a suspension test rig for performing the tests. In order to perform an accurate test in the experimental tests, the suspension test rig at the TU Berlin - Department Machinery System Design was employed. This test rig used to simulate three different road inputs in order to excite the suspension system in order to perform the evaluation tests.
- Model validation. The overall model was validated by comparing the simulation results with experimental results. In the highest deviations, there was 77 % correlation between the simulation RMS results and the experimental results, indicating good validity of the model. Referring to the PSD results, frequency response of the simulation results had acceptable correlation with experimental results. These results from the validation indicated that the simulation model was able to simulate the dynamic behavior of the suspension system of tractors and estimate the vibration transmission accurately.
- Examination of the tractor ride comfort. The comparison between passive and semi-active results in the simulation and experimental tests demonstrated that the accelerations of the tractor body were reduced until 13 % in the simulation tests and 10% in the experimental test by using the new suspension system. These results implied that a significant improvement in the ride comfort of the tractor was achieved.
- Examination of the tractor handling. The comparison between passive and semi-active results in the simulation and experimental tests indicated that the average of

the tractor dynamic tire force was reduced until 6.5 % in the simulation tests and 4.5 % in the experimental tests by using the new suspension system. These results implied that an acceptable improvement in tractor handling was achieved.

- Examination of the suspension travel. The results indicated that using the semi-active suspension was increased 14 % the suspension travel in the simulation test and 18 % in the experimental test. Considering the overall suspension stroke, this increase in the suspension travel indicated a need for some centimeters more space for suspension elements that was not considered as a notable limiting factor.

7.2 Recommendations

The specific recommendations that can be expanded on this investigation and follow it are stated as:

- Use of a hybrid active suspension for the agricultural tractors. These vehicles drive on the different road conditions such as asphalt street and field way. They perform different operations such as fast-duty fieldwork, heavy-duty fieldwork, and stationary work. A typical semi-active suspension is not capable to cover all these different conditions. By using an adaptive suspension together with the semi-active suspension, the suspension parameters can be changed largely after a major change in the working condition, and then, the semi-active suspension can provide an efficient performance for the agricultural tractor in the different working conditions.
- An idea for the adaptive suspension system is the use of the driver command sensors for the semi-active suspension. This can be performed by involving these data in the control loop in order to provide prediction of the maneuver inputs entering to the suspension system. These sensors could install on the break pedal, gas pedal, and steering wheel in order to measure the break, accelerating, and turning commands. Another similar idea is to analyze the frequency response of the acceleration on the wheels as the input of the adaptive control in order to realize general road excitations. In addition, similar to the research of (Hansson P. , 1996), the preview sensors installing on the front axle can be used in order to predict the road inputs entering to the rear axle. This extra sensory information can be added to the control loop of the semi-active suspension system as is shown in figure 7-1.

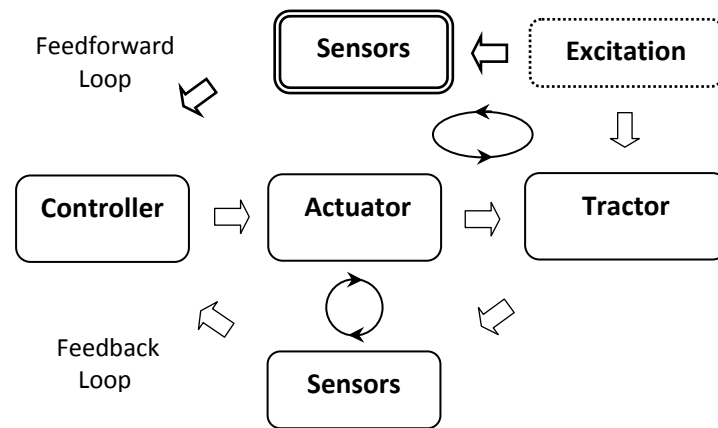


Figure 7-1 Driver command sensors for the semi-active control loop in order to provide a more efficient control.

- In extreme driving conditions or in station work, using the chassis suspension system for tractor may lead to an instability situation. Then, a blockage mode can be useful for the suspension system of tractors. In this research, in the hydro-pneumatic suspension the double-acting cylinders were used.

In order to apply the suspension blockage mode to each unit, two hydraulic valves can be simply added to the hydro-pneumatic circuit, between the accumulators and cylinder in both sides of the double-acting cylinders. As these valves are off, the cylinder inlets are closed, and the cylinder is blocked. Because of the position of these valves between the accumulators and cylinder, the throttling effect of them must be considered in the design of the semi-active suspension system explained in section 3.2.2.

- Different damping ratio can be evaluated for the high and low levels of damping related to the on-off sky-hook strategy.
- The influence of the semi-active controller bandwidth on the suspension performance can be investigated.
- In addition to the rear axle suspension, the semi-active suspension can be applied to the front axle suspension of the tractor, and then, performance of a full semi-active suspension for agricultural tractors can be evaluated.
- In addition to on-off skyhook, efficiency of other control strategies can be examined for the semi-active suspension of the tractor. Some of these methods were mentioned in section 2.3.

- Using the validated model as virtual prototype for developing investigation. This includes naturally all the recommended objects here.
- The full tractor model, which was created in this research, can be improved and developed as follow:
 - A more accurate model can be built for the tractor body by considering the elasticity of the masses of the body and the connections among them.
 - A more accurate tire model can be built considering tire pressure and other tire parameters. In this research, it was indicated that the model of the tires have significant influence on the simulation accuracy.
 - Friction effect can be considered in modeling of more suspension components.
 - Model of the sensors can be built considering possible happening errors.
- The benefits of MR dampers can be evaluated for the actuator of a semi-active suspension. The main advantage of these dampers is its very low response delay that can increase the bandwidth of the control system.
- There is friction effect in the different elements of a semi-active suspension. The effect of these frictions on the suspension performance can be investigated.
- In this study, a test rig was used in order to evaluate the active suspension system. Since this study was the first step of the examination of the new suspension, the test rig was used to eliminate the different errors occurring during the typical field tests. As the next step, the tests can be performed by driving the test-tractor on the different types of roads. This can be performed by simulation using a road model before. For this purpose, a challenging point is the measurement of the absolute velocity that is needed for skyhook control strategy. This subject should be studied as well to achieve to a sure method.

References

- Abd El-Tawwab, A. M. (1997). *Twin-Accumulator Suspension System*. Warrendale: Society of Automotive Engineers: SAE Technical paper no.970384.
- Adams, B. T. (2002). *Central Tire Inflation For Agricultural Vehicles*. Ph.D. Dissertation, University of Illinois, USA.
- Ahmadian, M. (1997). Semiactive Control of Multiple Degree of Freedom Systems. *Proceedings of Design Engineering Technical Conferences*.
- Ahmadian, M., & Pare, C. A. (2000). A Quarter-Car Experimental Analysis of Alternative Semiactive Control Methods. *Journal of Intelligent Material Systems and Structures*, 11 (8), 604-612.
- Al-Holou, N., Joo, D. S., & Shaout, A. (1996). The Development of Fuzzy Logic Based Controller for Semi-Active Suspension System. *Proceedings of the 37th Midwest Symposium on Circuits and Systems*, (pp. 1373-1376).
- Baillie, A. S. (1999). *Development of a Fuzzy Logic Controller For an Active Suspension of an Off-Road Vehicle Fitted with Terrain Preview*. Master Thesis, Royal Military College of Canada, Kingston, Ontario.
- Barak, P. (1989). Design and Evaluation of Adjustable Automobile Suspension. *SAE Paper 890089*.
- Barak, P. (1991). *Magic Numbers in Design of Suspension for Passenger Cars*. SAE Technical Papers Series, n. 878, pp.53-88.
- Barr, A., & Ray, J. (1996). Control of an active suspension using fuzzy logic. *Proceedings of the Fifth IEEE International Conference on Fuzzy Systems*, 1, pp. 42-48.
- Bastow, D. (1987). *Car Suspension and Handling*. Pentech Press Limited, London.
- Bauer, W. (2007). *Hydropneumatische Federungssysteme*. Springer.
- Blundell, M. (1999). The Modelling and Simulation of Vehicle Handling Part 3: Tire Modelling. *Journal of Multi-body Dynamics*, 214 (1), 1-32.
- Boileau, P.-E., & Rakheja, S. (1990). Vibration attenuation performance of suspension seats for off-road forestry vehicles. *International Journal of Industrial Ergonomics*, 5, 275-291.
- Boonchanta, P. (1982). *Comparisons of Active, Passive, and Semiactive Suspensions for Ground Vehicles*. Ph. D. Dissertation, University of California, Davis, CA, USA.
- Burton, A., Truscott, A., & Wellstead, P. (1995). Analysis, Modelling and Control of an Advanced Automotive Self-Levelling Suspension System. *IEE Proc.-Control Theory Appl.*, 142 (2), 129-139.
- Carter, A. K. (1998). *Transient Motion Control of Passive and Semiactive Damping for Vehicle Suspensions*. Master Thesis, Virginia Tech., Blacksburg, Virginia, USA.

Chalasani, R. (Dec.1986). Ride Performance Potential of Active Suspension Systems-Part I:Simplified Analysis Based on a Quarter-Car Model. *Proceedings of 1986 ASME Winter Annual Meeting*. Los Angeles, CA.

Chalasani, R. (1986). Ride Performance Potential of Active Suspension Systems-Part II: Comprehensive Analysis Based on a Full-Car Model. *ASME Symposium on Simulation and Control of Ground Vehicles and Transportation Systems*, 80 (2), 187-204.

Chaudhary, S. (1998). *Ride a Roll Performance Analysis of a Vehicle with spring Loaded Interconnected Hydro-Pneumatic Suspension*. Master Thesis, Concordia University, Montreal, Quebec, Canada.

Claar, P., Sheth, P., Marley, S., & Buchele, W. (1980). Agricultural tractor chassis suspension system for improved ride comfort. *ASAE Paper*, 80, 1565.

Class. (2006). Retrieved 2006, from www.claas.de

Crolla, D. A., & Abdel-Hady, M. B. (1991). Semi-Active Suspension Control for a Full Vehicle Model. *SAE (Society of Automotive Engineers) Transactions*, 100 (6), 1660-1666.

Deakin, A., Crolla, D., & Shovlin, A. (1997). Power Consumption in Ride of a Combat Support Vehicle Slow-Active Suspension. *SAE Special Publication*, vol.38.

Deutz. (2006). Retrieved June 2006, from Deutz Tractors: <http://www.deutz-fahr.de>

Donahue, M. D. (1998). *Implementation of an Active Suspension, Preview Controller for Improved Ride Comfort*. Master Thesis, University of California, Berkeley, USA.

Efatpenah, K., Beno, J. H., & Nichols, J. H. (2000). Energy Requirements of a Passive and an Electromechanical Active Suspension System. *Vehicle System Dynamics*, 34 (6), 437-458.

Elmadany, E. M., & Abduljabbar, Z. (1999). Linear Quadratic Gaussian Control of a Quarter-Car Suspension. *Vehicle System Dynamics*, 32 (6), 479-497.

Eulenbach, D. (2003). *Stand und Entwicklungstrends hydropneumatischer Niveauregelsysteme*. Haus der Technik, Essen, Germany.

FASTRAC. (2007). *JCB FASTRAC*. Retrieved April 2007, from <http://www.jcb.com/products/MachineOverview.aspx>

Festo. (2003). *Hydraulics Basic Level*. Denkendorf, Germany: Festo.

Fodor, M., & Redfield, R. (1995). Resistance Control, Semi-Active Damping Performance. *Advanced Automotive Technologies American Society of Mechanical Engineers, Dynamic Systems and Control Division*, 161-169.

Giliomee, C. L. (2003). *Analysis of a Four State Switchable Hydro-Pneumatic Spring and Damper System*. Master Thesis, University of Pretoria, South Africa.

Gillespie, T. (1992). *Fundamentals of Vehicle Dynamics*. USA: SAE.

- Giua, A., Savastano, A., Seatzu, C., & Usai, G. (1998). Approximation of an Optimal Gain Switching Active Law with a Semiactive Suspension. *IEEE Conference on Control Applications- Proceedings*, Piscataway, NJ, USA, 248-252.
- Goehlich, H. (1984). The Development of Tractors and Other Agricultural Vehicles. *J. agric. Engng Res.*, 29, 3-16.
- Göhlich, H., Hauck, M., & von Holst, C. (1999). Fahrdynamik – Fahrsicherheit – Fahrerplatz. *Jahrbuch Agrartechnik*. 11, pp. 61 – 69. Landwirtschaftsverlag Münster, 1999.
- Goncalves, F. (2001). *Dynamic Analysis of Semiactive Control Techniques for Vehicle Applications*. Master Thesis, Virginia Tech., Blacksburg, Virginia, USA.
- Gunston, T. (2000). The Definition of Suitable Input Motions for Testing Suspension Seat End-stop Impact Performance. *34th meeting of the U.K. Group on Human Response to Vibration*, (pp. 127-137).
- Hansen, M. R., & Andersen, T. O. (2003). Active Damping of Oscillations in Off Road Vehicles. *8th Scandinavian Intl Conference on Fluid Power*, 2, 1073-1085.
- Hansson, P. A. (1995). Optimization of Agricultural Tractor Cab Suspension Using the Evolution Method. *Computers and Electronics in Agriculture*, 12, 35-49.
- Hansson, P. (1995). Optimization of Agricultural Tractor Cab Suspension Using the Evolution Method. *Computers and Electronics in Agriculture*, 12, 35-49.
- Hansson, P. (1996). Rear axle suspensions with controlled damping on agricultural tractors. *Computers and Electronics in Agriculture*, 15, 123-147.
- Hauck, M. (2001). *Geregelte Dämpfung für Traktor-Fahrersitze*. Ph.D. Dissertation, TU-Berlin, Germany.
- Heo, S., Park, K., & Hwang, S. (2000). Performance and Design Consideration for Continuously Controlled Semi-Active Suspension Systems. *International Journal of Vehicle Design*, 23 (3), 376-389.
- Hilmes, R. (1982). Dreissig Jahre Kampfpanzerentwicklung (1950-1980). *Soldat und Technik* 6, 324-329.
- Hilton, D. J., & Moran, P. (1975). Experiments in Improving Tractor Operator Ride by Means of a Cab Suspension. *J. agric. Engng Res.*, 20 (4), 433-448.
- Hoppe, U. (2006). *Einfluss der Hinterachsfederung auf die Fahrdynamik von Traktoren*. Ph.D. Dissertation, TU-Berlin, Germany.
- Hoppe-, U., & Meyer, H. J. (2005). Entwicklung und Realisierung eines vollgefederten Traktors. *Tagung Landtechnik 2005, VDI Verlag, Düsseldorf*.
- Hoppe-01, U. (2004). Stand der Technik und aktuelle Entwicklungen bei der Traktorfederung. *Neue Landwirtschaft*, 5, 43-46.
- Horton, D., & Crolla, D. (1984). Designing Off-Road Vehicles with Good Ride Behavior. *Proceedings of the 8th International Conference of the ISTVS*. 1, pp. 171-184. Amsterdam, The Netherlands: Elsevier Science.

Hyvärinen, J. P. (2004). *The Improvement of Full Vehicle Semi-active Suspension Through Kinematical Model*. Ph.D. Dissertation, University of Oulu, Finland.

ISO2631. (1974). *Mechanical Vibration and Shock - Evaluation of Human Exposure to Whole Body Vibrations*. Part 1: General Requirement, ISO 2631-1, The International Organisation for Standardisation.

ISO5008. (1979). *Agricultural wheeled tractors and field machinery - Measurement of whole-body vibration of the operator*. The International Organisation for Standardisation.

Jalili, N. (2002). A Comparative Study and Analysis of Semi-Active Vibration-Control Systems. *Journal of Vibration and Acoustics*, 124, 593-605.

Jamei, M. (2002). *Symbiotic Revolution-Based Design of Fuzzy Inference System with Application to Active Suspension system*. Ph.D. Dissertation, University of Sheffield, Great Britain.

Jonh.Deere. (2005). Retrieved April 2005, from John Deere Tractors:
http://www.deere.com/en_US/ProductCatalog

Kaczmarek, R. (1984). Central Tire Inflation Systems (CTIS) – A means to enhance vehicle mobility. *Proceedings of the 8th International Conference of the ISTVS*. 3, pp. 1255-1271. Amsterdam, The Netherlands: Elsevier Science.

Kaplick, C. (1995). *Verifikation und Bewertung fahrdynamischer Traktor Simulationsmodelle*. Ph.D. Dissertation, TU-Berlin, Germany.

Kaplick, C. (1995). *Verifikation und Bewertung fahrdynamischer Traktor Simulationsmodelle*. Ph.D. Dissertation, TU-Berlin, Germany.

Karnopp, D., & Heess, G. (1991). Electronically Controllable Vehicle Suspension. *Vehicle System Dynamics* 20, 207-217.

Karnopp, D., & Margolis, D. (1984). Adaptive suspension concept for road vehicles. *Vehicle System Dynamics*, 13 (3), 145-160.

Karnopp, D., Crosby, M. J., & Harwood, R. A. (1974). Vibration Control Using Semi-Active Force Generators. *ASME Journal of Engineering for Industry*, 96 (2), 619-626.

Kauß, W. (1981). *Aktive, hydraulische Schwingungsisolierung des Fahrerplatzes ungefederter, geländegängiger Fahrzeuge*. Ph.D. Dissertation, TU-Berlin, Germany.

Kauss, W., & Weigelt, H. (1980). Die gefederte Traktorkabine - verbesserter Schwingungsschutz und Fahrkomfort. *Landtechnik*, 9, 396-401.

Kising, A. (1988). *A Dynamische Eigenschaften von Traktor-Reifen*. Ph.D. Dissertation, TU-Berlin, Germany.

Langlois, R., Anderson, R., & Hanna, D. (1991). Implementing Preview Control on an Off-Road Vehicle with Active Suspension. *Proceedings 12th IAVSD Symposium on the Dynamics of Vehicles*. France, Lyon, Swets and Zeitlinger.

- Lehmann, K. (2004). *Analyse von Niveauregelungssystemen für Traktoren*. Diplomarbeit, TU-Berlin, Germany.
- Lehtonen, T., & Juhala, M. (2006). Predicting the ride behaviour of a suspended agricultural tractor. *International Journal of Vehicle Systems Modelling and Testing*, 1 (1-2), 131-142.
- Lizell, M. (1990). *Dynamic levelling for ground vehicles*. Ph.D. Dissertation, Norstedts tryckeri, Stockholm, Sweden.
- Mäkelä, K. (1999). *Characterization and performance of electrorheological fluids based on pine oils*. VTT publications 385, Espoo.
- Margolis, D. (1982). The Response of Active and Semiactive Suspensions to Realistic Feedback Signals. *Vehicle System Dynamics*, 11 (5-6), 267-282.
- Margolis, D., & Nobles, C. M. (1991). Semi-Active Heave and Roll Control for Large Off-Road Vehicles. *SAE Special Publications. n 892*, 25-34.
- Marsili, A., Ragni, L., Santoro, G., & Servadio, G. (2002). Innovative Systems to Reduce Vibrations on Agricultural Tractors: Comparative Analysis of Acceleration Transmitted Through the Driving Seat. *Biosystems Engineering*, 81 (1), 35-47.
- Masi, J. W. (2001). *Effect of Control Techniques on the Performance of Semiactive Dampers*. Masters Thesis, Virginia Polytechnic Institute, Blacksburg, Virginia.
- McLellan, N. (1998). *On the Development of a Real-Time Embedded Digital Controller for Heavy Truck Semiactive Suspensions*. Master Thesis, Virginia Tech., Blacksburg, Virginia, USA.
- McMichael, S. C. (1981). *The Simulation and Spectral Analysis of A Motorcycle Model with a Semiactive On-Off rear Shock Absorber*. Ph.D.Dissertation, University of California, Davis, CA, USA.
- Meller, T. (1987). *Self-Energizing Hydropneumatic Levelling System*. SAE Technical paper no 780052, Warrendale: Society of Automotive Engineers.
- Meyer, H. J. (2005). *Ölhydraulik und Pneumatik II*. Vorlesungsumdruck, TU-Berlin, Germany.
- Meyer, H. (2006). *Konstruktion von Maschinensystemen*. Vorlesungsskript, TU-Berlin.
- Meyer, H. (2004). *Mobile Arbeitsmaschinen*. Vorlesungsskript, TU-Berlin, Germany.
- Meyer, H. (2004). Schwingungsentkopplung bei Landmaschinen. *Landtechnik*, 1, 24–25.
- Miller, L. (1988). Tuning Passive, Semi-Active, and Fully Active Suspension Systems. *Proceedings of the 27th IEEE Conference on Decision and Control*, 3, pp. 2047 - 2053.
- Mitschke, M. (1984). *Dynamik der Kraftfahrzeuge* (2 ed., Vol. B). Berlin: Springer.
- Müller, N. (2001). *Einfluss der Hinterachsfederung auf die Fahrsicherheit und den Fahrkomfort von Ackerschleppern*. Forschungsbericht, TU-Berlin, Germany.
- New-Holland. (2005). Retrieved March 2005, from New Holland Tractors: <http://www.newholland.com/home.asp>

- Nobles, C. M., & Miller, L. R. (1985). The Design and Development of a Semi-Active Suspension for a Military Tank. *SAE Technical Paper Series No. 881133* .
- Paré, C. A. (1998). *Experimental Evaluation of Semiactive Magneto-Rheological Suspensions for Passenger Vehicles*. Master Thesis, Faculty of the Virginia Polytechnic Institute, Blacksburg, Virginia.
- Pickel, P. (1993). *Simulation fahrdynamischer Eigenschaften von Traktoren*. Ph.D. Dissertation, TU-Berlin, Germany.
- Pickel, P., Kaplick, P., & Göhlich, H. (1990). Welche Chancen haben gefederte Traktoren? *Landtechnik*, 10 (90), 363-366.
- Profi. (2007). Sicherer und Komfortabler Arbeiten mit Einem Gefederten Schlepper. *Profi Test (Tractors Profi and Farm Machinery)*, 2/99, 10-18.
- Rhenius, K. T. (1983). Erhöhte Arbeitsgeschwindigkeiten und Schleppertechnik:Wo liegen die Grenzen? *Landtechnik*, 38 (11), 466-469.
- Rill, G., Slag, D., & Wilks, E. (1992). Improvement of Dynamic Wheel Loads and Ride Quality of Heavy Agricultural Tractors by Suspending Front Axls. *Heavy Vehicle and Roads-Technology,Safety and Policy*, Telford, London, 116-121.
- Rolvag, T. (2004). *Design and optimization of Suspension Systems and Components*. Norwegian University of Science and Technology NTNU.
- SAE. (1992). *Measurement of Whole Body Vibration of the Seated Operator of Off-Highway Work Machines*. SAE J1013, Society of Automotive Engineers, Warrendale, PA.
- Sampson, D. J. (2000). *Active Roll Control of Articulated Heavy Vehicles*. Ph.D. Dissertation, Cambridge University, Cambridge, UK.
- Satoh, M., Fukushima, N., Akatsu, Y., Fujimura, I., & Fukuyama, K. (1990). An Active Suspension Employing an Electrohydraulic Pressure Control System. *Proceedings of the 29th IEEE Conference on Decision and Control*.
- Scarlett, A. J., Price, J. S., & Stayner, R. M. (2007). Whole-Body Vibration: Evaluation of Emission and Exposure Levels Arising from Agricultural Tractors. *Journal of terramechanics*, 44 (1), 65-73.
- Siekmann, H. (2003). *Strömungslehre für den Maschinenbau*. Springer.
- Simon, D. (2001). *An Investigation of the Effectiveness of Skyhook Suspensions for Controlling Roll Dynamics of Sport Utility Vehicles Using Magneto-Rheological Dampers*. Ph.D. Dissertation, Virginia Tech., Blacksburg, Virginia, USA.
- Soliman, A., & Crolla, D. A. (1996). Preview control of a semi-active suspension system. *International Journal of Vehicle Design*, 17 (4), 384-397.
- Standards. (2004). *Vehicle Standards Bulletin VSB 11*. Department of Transport and Regional Services. Canberra: Vehicle Safety Standards.
- Stayner, R. M., & Bean, A. G. *Tractor Ride Investigations. A survey of vibration experienced by drivers during field work*. Natn. Inst. agric. Engng Dept. Note DN/E/578/1445.

- Stein, G., & Ballo, I. (1991). Active Vibration Control System for the Driver's Seat for Off-road Vehicles. *Vehicle System Dynamics*, 57-78.
- Suggs, C., & Huang, B. (1969). Tractor Cab Suspension Design and Scale Model Simulation. *Trans.ASAE*, 12, 283-289.
- Thiebes, P. (2006). *Fahrdynamik eines vollgefederten Traktors Hybride Modellierung, Simulationsvalidierung*. Diplomarbeit, TU-Berlin, Germany.
- Thiebes, P., Müller, P., & Gericke, K. (2005). *Konstruktion und Analyse eines Traktorrahmens zur Aufnahme einer gefederten Hinterachse*. Projektarbeit, TU-Berlin, Germany.
- Thoreson, M. J. (2003). *Mathematical Optimisation of the Suspension System of an Off-Road Vehicle for Ride Comfort and Handling*. Master Thesis, University of Pretoria, Pretoria.
- Titli, A., & Roukieh, S. (1995). Design of Active and Semi-Active Automotive Suspension Using Fuzzy Logic. *Proceedings of the 12th Triennial World Congress of the International Federation of Automatic Control*, 3, pp. 73-77. Pergamon, Oxford, UK.
- Ulrich, A. (1983). *Untersuchung zur Fahrdynamik von Traktoren mit und ohne Anbaugerät*. Ph.D. Dissertation, TU-Berlin, Germany.
- Uriarte, C. (2007). *Studie verschiedener Regelstrategien für die adaptive Dämpfung einer Kabinenfederung*. Analytische Studienarbeit, TU-Berlin, Germany.
- Valášek, M., Novak, M., Sika, Z., & Vaculin, O. (1997). Extended ground-hook – new concept of semiactive active control of truck's suspension. *Vehicle system dynamics*, 27 (5-6), 289-303.
- Valtra. (2005). Retrieved March 2005, from Valtra Tractors: <http://www.valtra.com>
- Vaughan, J. E. (2004). *Active and Semi-Active Control to Counter Vehicle Payload Variation*. Master Thesis, Georgia Institute of Technology, USA.
- Vessonen, I., & Järviluoma, M. (2001). Simulation Based Design of Mobile Machine Vibration Control and Active Cabin Suspension Prototype. *VTT Symposium 209*, (pp. 121-139). Espoo, Finland.
- Von Holst, C. (2000). *Vergleich von Reifenmodellen zur Simulation der Fahrdynamik von Traktoren*. Ph.D. Dissertation, TU-Berlin, Germany.
- Weigelt, H. (1987). *Schwingungseigenschaften Vorderachsgefederter Landwirtschaftlicher Traktoren*. Ph.D. Dissertation, TU-Berlin, Germany.
- Williams, R. A. (1994). Electronically Controlled Automotive Suspensions. *Computing & Control Engineering Journal*, 143-148.
- Yi, K., & Hedrick, K. (1993). Dynamic Tire Force Control by Semiactive Suspensions. *Journal of Dynamic Systems Measurement & Control-Transactions of the ASME*, 115 (3), 465-474.
- Zadeh, L. A. (1965). "Fuzzy Sets,". *Information and Control*, 8, 338-353.
- Ziemer, R. E., Tranter, W. H., & Fannin, D. R. (1998). *Signals & Systems*. New Jersey: Prentice Hall.

Appendices

Appendix A: Rest PSD Graphs

A.1: Passive, Experiment-Simulation

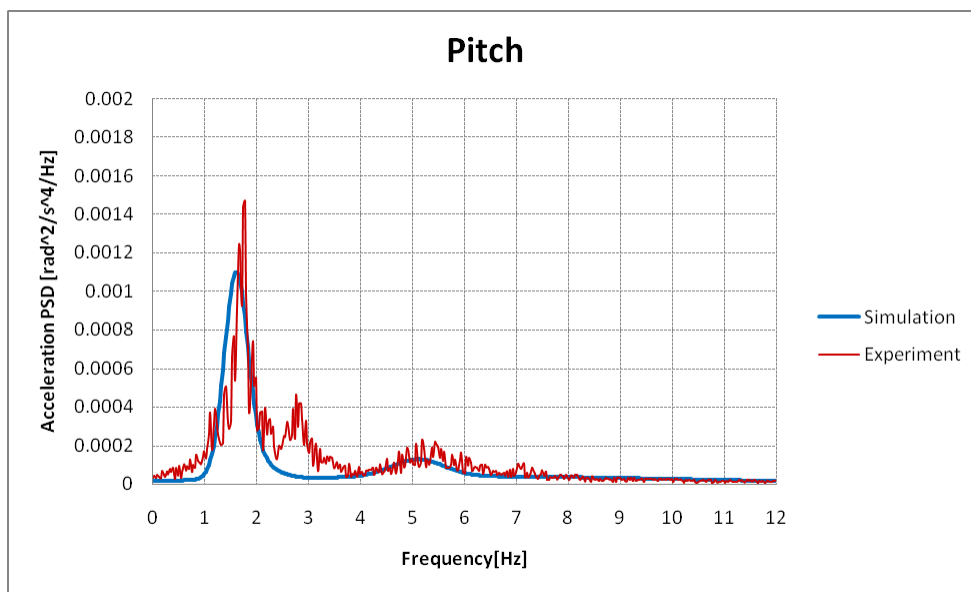


Figure A-1: Comparison between simulation and experimental frequency responses of the tractor body “pitch” acceleration.

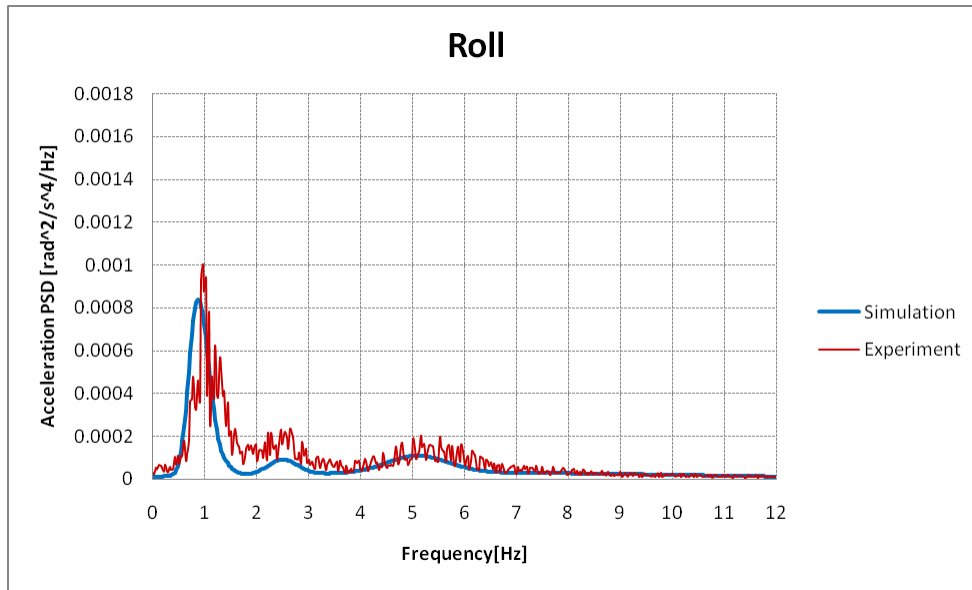


Figure A-2: Comparison between simulation and experimental frequency responses of the tractor body “roll” acceleration.

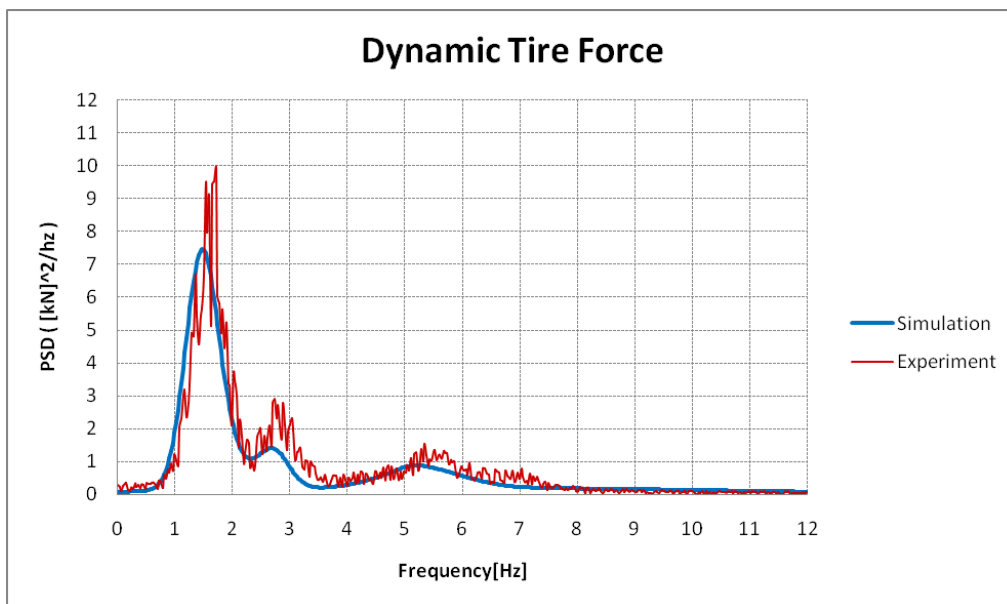


Figure A-3: Comparison between simulation and experimental frequency responses of the dynamic tire force.

A.2: Simulation, Passive-Semi active

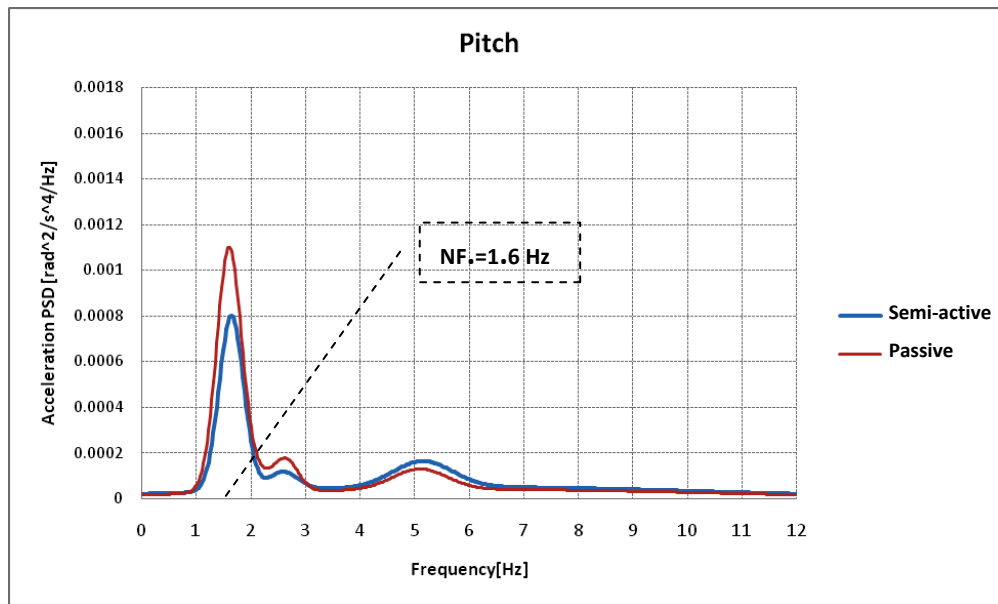


Figure A-4: Comparison between semi-active and passive frequency responses of the tractor body “pitch” acceleration in the simulation test.

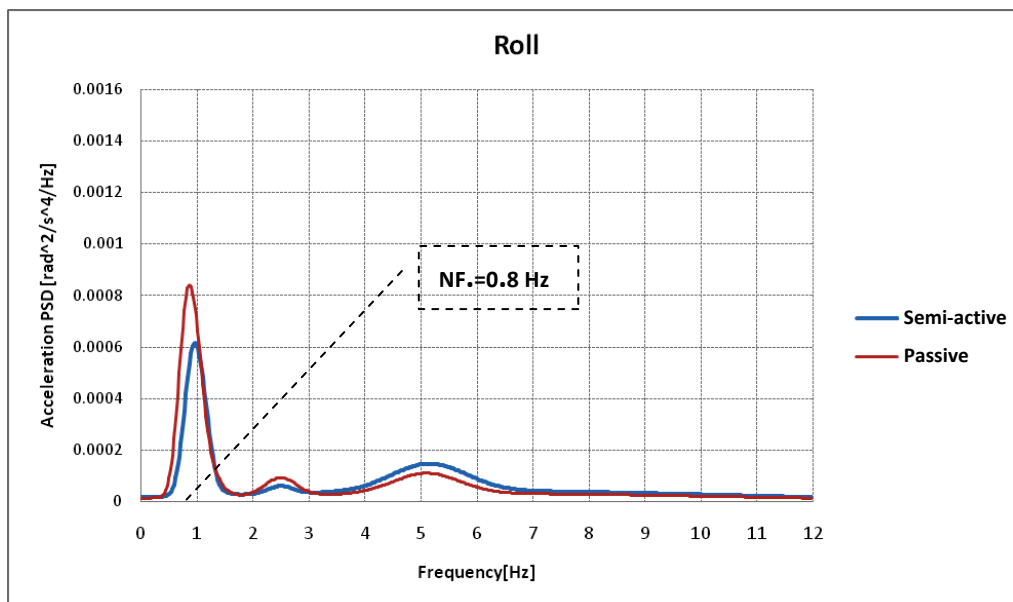


Figure A-5: Comparison between semi-active and passive frequency responses of the tractor body “roll” acceleration in the simulation test.

A.3: Experiment, Passive-Semi active

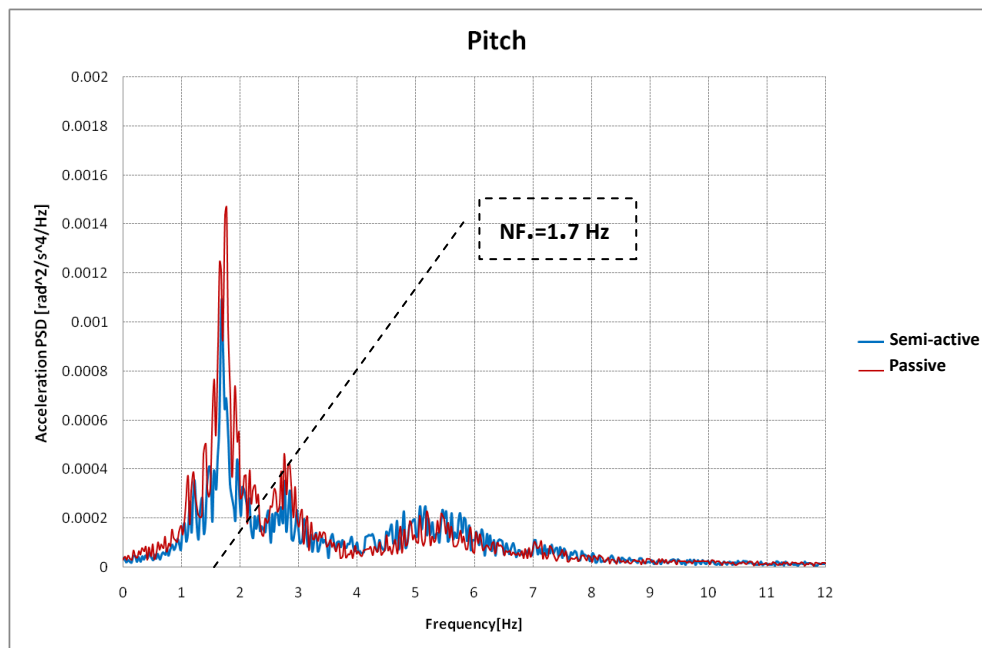


Figure A-6: Comparison between semi-active and passive frequency responses of the tractor body “pitch” acceleration in the experimental test.

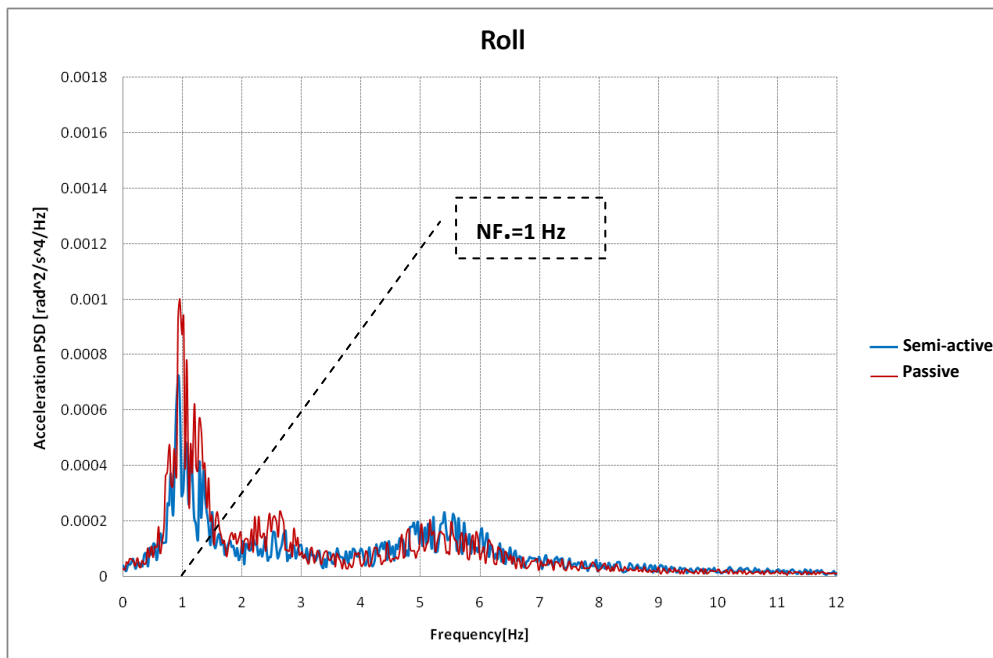


Figure A-7: Comparison between semi-active and passive frequency responses of the tractor body “roll” acceleration in the experimental test.

Appendix B: Suspension Test Rig

Technical data of the Full Suspension Test Rig

1- Hydraulic Cylinder		
Piston diameter		80 mm
Piston-rod diameter		60 mm
Max. stroke		80 mm
Max. piston speed		± 90 mm
2- Hydraulic Pumps		
Power		2,45 kW
Pressure		280 bar
Rate of flow		180 l/min
3- Valves*		
Nominal rate of flow at $\Delta p=70$ bar		100 l/min
Nominal filter rate		5 μm
4- Fundament**		
Mass		90.000 kg
Response frequency		1 Hz
5- Frequency Range		
Upper limiting frequency		~ 10 Hz
6- Load		
Max. vehicle mass		6000 kg
* Servo-valve Bosch 0814-SMV2/100		
** The fundament is mounted on air springs.		

Appendix C: Measurement System

C.1: Accelerometer Sensor

SENSORS

Accelerometer Sensor Model 3021

OEM Accelerometer Piezoresistive Low Cost

Features

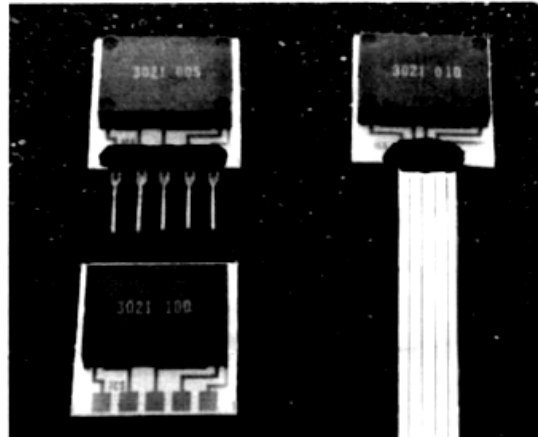
- DC Response
- Wide Bandwidth
- High Sensitivity
- Built-In Damping
- Miniature Size
- Low Mass
- Built-In Overrange Stops
- Solid State Reliability
- Ease of Mounting

Typical Applications

- Automotive Suspension Control
- Automotive Braking Control
- Machine Tool Monitoring
- Industrial Vibration Monitoring
- Computer Peripherals
- Modal Analysis
- Security Systems Motion Detection
- Aerospace Flight Navigation
- Robotic Motion Control
- Medical Patient Activity Monitoring
- Appliance Control
- Military Arming and Fuzing

Standard Ranges

- ± 5g
- ± 10g
- ± 20g
- ± 50g
- ± 100g



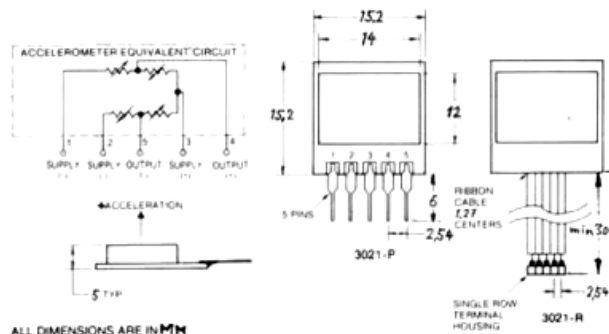
Description

The Model 3021 is the first in a family of general purpose, solid-state, piezoresistive accelerometers and is packaged on a ceramic substrate. It is intended for use where small size, excellent performance, and low cost are required.

The accelerometer consists of a micromachined silicon mass suspended by multiple beams to a silicon frame. Piezoresistors located in the beams change their resistance as the motion of the suspended mass changes the strain in the beams. Silicon caps on the top and the bottom of the device are added to provide over-range stops and increased durability. As a result of this unique three-layer silicon structure, accelerometers with a very low profile and low mass can be batch fabricated at a very low cost. An added feature is built-in damping, which allows a wide useable bandwidth to be achieved.

The device is available in standard acceleration ranges from $\pm 5g$ to $\pm 100g$. Custom ranges from $\pm 2g$ to $\pm 500g$ are also available. Device performance characteristics and packaging can be easily tailored to meet the requirements of specific applications.

Connections/Dimensions



DELTA Regeltechnik GmbH

Türkenstraße 11 · D-8000 München 2

Telefon (0 89) 28 20 43 · Telex 5 29 345 dema d · Telefax (0 89) 28 35 09

Model 3021

Accelerometer

Performance Specifications

Supply = 5 Volts & Ambient Temperature = 25°C (Unless otherwise specified)

PARAMETER	RANGE				
	± 5g	± 10g	± 20g	± 50g	± 100g
Frequency Response (-5%)	0-350 Hz	0-500 Hz	0-700 Hz	0-1050 Hz	0-1600 Hz
Mounted Resonant Frequency (±15%)	600 Hz	850 Hz	1200 Hz	1800 Hz	2750 Hz

PARAMETER	ALL RANGES				
	MIN	TYP	MAX	UNITS	NOTES
Full Scale Output Span	30	50		±mV	1
Zero Acceleration Output		5	25	±mV	
Damping Factor		.707			3
Non-Linearity and Hysteresis		0.2	1	±%Span	4
Transverse Sensitivity		1	3	±%Span	
Input & Output Resistance		3500	5000	Ω	
Temperature Coefficient - Span		0.3	2.0	±%Span	2.5
Temperature Coefficient - Zero		0.3	2.0	±%Span	2.5
Temperature Coefficient - Resistance		0.22		%/°C	2.5
Supply Voltage		5.0	10.0	VDC	
Output Noise		1.0		μV p-p	
Output Load Resistance	2			MΩ	6
Acceleration Limits (Any Direction)		20X		Rated	
Operating Temperature	-40°C to +125°C				
Storage Temperature	-55°C to +150°C				
Weight (Excluding Cable)	1.2 Grams				

Notes

1. Positive voltage for positive acceleration; negative voltage for negative acceleration.
2. For compensation information, see Technical Note TN-009.
3. Damping factor is controlled to within ±10% over operating temperature range. Alternate damping ratios are available on a special order basis.
4. Best Fit Straight Line linearity. For full scale ranges of 10g or less, the maximum non-linearity is ±2%.
5. Temperature range: 0-50°C in reference to 25°C.
6. Prevents increase of TC-Span and sensitivity decrease due to output loading.
7. Various electrical connections are available: R = ribbon cable, P = pins, N = none.

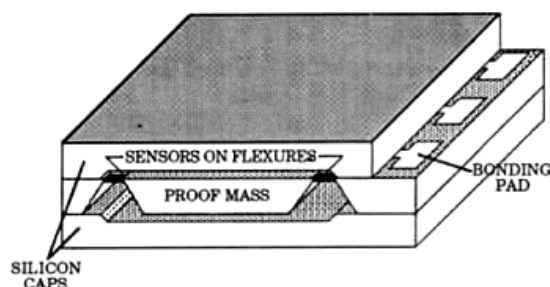
Ordering Information

3021 - 010 - R

Electrical Connection (R,P,N - see Note 7)

Acceleration Range

Model



Cut-away view of double-cantilever accelerometer structure

DELTA

Regeltechnische Bauteile

Telefon (0 89) 28 20 43
Telex 5 29 345 dema d
Telefax (0 89) 28 35 09

Türkenstraße 11
D-8000 München 2

C.2: Velocity and Position Sensor

VP SERIES LINEAR VELOCITY AND POSITION

Simultaneous velocity and position measurement

The VP series combines a self-generating tachometer and a precision potentiometer to give an output of both velocity and analog position. Standard position output is a voltage divider circuit. Outputs optionally available are the bridge circuit, 4-20 mA, 0-10 VDC, and ± 10 VDC. See PB, P420, P510 and P1010 series data sheets for specifications.



SPECIFICATIONS

General

Positional Linearity	
2", 3", 4" & 5" Ranges	$\pm 0.25\%$ Full Scale
10", 15", 20" & 25" Ranges	$\pm 0.15\%$ Full Scale
All other ranges	$\pm 0.10\%$ Full Scale
Repeatability ¹	$\pm 0.015\%$ Full Scale
Positional Resolution	Essentially Infinite
Construction	Aluminum Cover & Baseplate
Sensing Device	Tacho-Generator—Velocity
Precision Potentiometer—Position	
Connector	MS3102A-14S-6P
Wire Rope	$\varnothing 0.016$ Stainless Steel
Wire Rope Tension	See Table 6
Wire Rope Inbound Acceleration	See Table 6
Weight	1.96 lb. (0.89 Kg) to 50"
	2.20 lb. (1.00 Kg) 60" & 80"
Dimensional Information	See Supplemental Data ¹ , Fig. 3
Options and Accessories	See Supplemental Data ¹

Environmental

Thermal Coefficient of potentiometer	± 100 PPM/ $^{\circ}$ C max.
Operating temperature	-40° C to 95° C
Operating humidity	95% R.H. max. non-condensing
Vibration	15 G's 0.1 ms max.
Shock	50 G's 0.1 ms max.
Ingress Protection	NEMA 1, IP-40

FOOTNOTES TO SPECIFICATIONS

1. Supplemental Data section located at end of Standard Series pages.

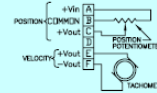
Electrical (Position)

Input Impedance ("A" Circuit)	$1000\Omega \pm 10\%$
Excitation Voltage	25 Volts Max. AC or DC
Output Voltage	$\frac{990}{\text{Range in Inches}}$ mV/V/inch
(Use total measurement range in calculation)	
	$\frac{990}{\text{Range in mm.}}$ mV/V/mm

Electrical (Velocity)

Output	See Table 6
Linearity	Within 0.10% of Output Voltage
Ripple	3% Max.
Output Impedance	350 Ω

CONNECTION DIAGRAM

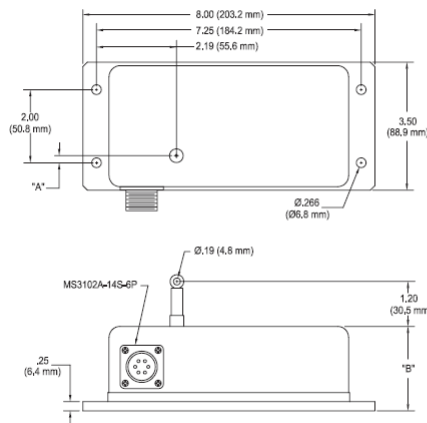


POSITIVE OUTPUT OCCURS WITH WIRE ROPE EXTENDING

TABLE 6

MEASUREMENT RANGE	VELOCITY OUTPUT		WIRE ROPE TENSION		WIRE ROPE ACCEL	WEIGHT	
(inch)	(mV per in/sec)	(mV per cm/sec)	(oz)	(N)	(Gs)	(lb)	(Kg)
2, 10	200	78	34	9.5	33	1.20	0.54
3, 15, 30	136	53	24	6.7	30	1.20	0.54
4, 20, 40	102	40	24	6.7	36	1.20	0.54
5, 25, 50	82	32	34	9.5	33	1.20	0.54
60	69	27	24	6.7	27	1.54	0.70
80	52	20	19	5.3	16	1.54	0.70

ALL MEASUREMENT RANGES



RANGE	"A"		"B"	
	(in)	(mm)	(in)	(mm)
2", 10"	0.66	16.8	2.25	57.0
3", 15", 30"	0.51	12.9	2.25	57.0
4", 20", 40"	0.35	8.8	2.25	57.0
5", 25", 50"	0.19	4.8	2.25	57.0
60"	0.04	1.0	3.25	82.6
80"	-0.28	-7.1	3.25	82.6

C.3: Interface USB Card 6008/6009

Specifications

Typical at 25 °C unless otherwise noted.

Analog Input

Absolute accuracy, single-ended

Range	Typical at 25 °C (mV)	Maximum (0 to 55 °C) (mV)
±10	14.7	138

Absolute accuracy at full scale, differential¹

Range	Typical at 25 °C (mV)	Maximum (0 to 55 °C) (mV)
±20	14.7	138
±10	7.73	84.8
±5	4.28	58.4
±4	3.59	53.1
±2.5	2.56	45.1
±2	2.21	42.5
±1.25	1.70	38.9
±1	1.53	37.5

Number of channels..... 8 single-ended/4 differential
Type of ADC Successive approximation

ADC resolution (bits)

Module	Differential	Single-Ended
USB-6008	12	11
USB-6009	14	13

Maximum sampling rate (system dependent)

Module	Maximum Sampling Rate (kS/s)
USB-6008	10
USB-6009	48

Input range, single-ended..... ±10 V
Input range, differential..... ±20, ±10, ±5, ±4, ±2.5, ±2, ±1.25, ±1 V
Maximum working voltage ±10 V
Overvoltage protection ±35 V
FIFO buffer size 512 B
Timing resolution 41.67 ns (24 MHz timebase)
Timing accuracy 100 ppm of actual sample rate
Input impedance 144 k
Trigger source..... Software or external digital trigger
System noise..... 0.3 LSB_{rms} (±10 V range)

Analog Output

Absolute accuracy (no load) 7 mV typical, 36.4 mV maximum at full scale
Number of channels..... 2
Type of DAC Successive approximation
DAC resolution 12 bits
Maximum update rate 150 Hz, software-timed

Output range 0 to +5 V
Output impedance..... 50 Ω
Output current drive..... 5 mA
Power-on state 0 V
Slew rate..... 1 V/μs
Short-circuit current..... 50 mA

Digital I/O

Number of channels..... 12 total
8 (P0.<0..7>)
4 (P1.<0..3>)
Direction control Each channel individually programmable as input or output
Output driver type
USB-6008 Open-drain
USB-6009 Each channel individually programmable as push-pull or open-drain
Compatibility CMOS, TTL, LVTTL
Internal pull-up resistor 4.7 kΩ to +5 V
Power-on state Input (high impedance)
Absolute maximum voltage range..... -0.5 to +5.8 V

Digital logic levels

Level	Min	Max	Units
Input low voltage	-0.3	0.8	V
Input high voltage	2.0	5.8	V
Input leakage current	—	50	μA
Output low voltage (I = 8.5 mA)	—	0.8	V
Output high voltage (push-pull, I = -8.5 mA)	2.0	3.5	V
Output high voltage (open-drain, I = -0.6 mA, nominal)	2.0	5.0	V
Output high voltage (open-drain, I = -8.5 mA, with external pull-up resistor)	2.0	—	V

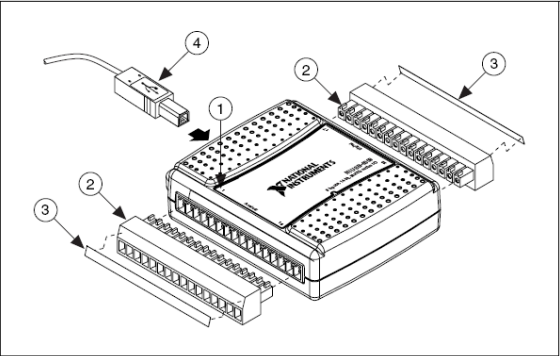
Counter

Number of counters 1
Resolution 32 bits
Counter measurements..... Edge counting (falling edge)
Pull-up resistor 4.7 kΩ to 5 V
Maximum input frequency..... 5 MHz
Minimum high pulse width..... 100 ns
Minimum low pulse width..... 100 ns
Input high voltage 2.0 V
Input low voltage 0.8 V

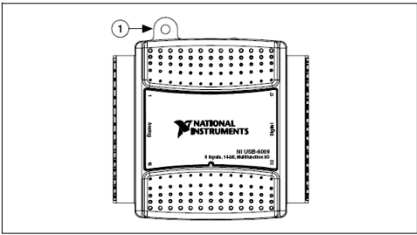
Power available at I/O connector

+5 V output (200 mA maximum) +5 V typical
+4.85 V minimum
+2.5 V output (1 mA maximum) +2.5 V typical
+2.5 V output accuracy 0.25% max
Voltage reference temperature drift... 50 ppm/°C max

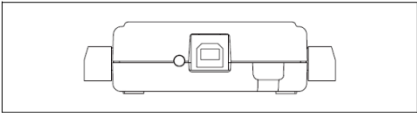
¹Input voltages may not exceed the working voltage range.



- 1 Overlay Label with Pin Orientation Guides 3 Signal Labels
2 Combicon Jack 4 USB Cable



1 USB Cable Strain Relief



Module	Terminal	Signal, Single-Ended Mode
	1	GND
	2	AI 0
	3	AI 4
	4	GND
	5	AI 1
	6	AI 5
	7	GND
	8	AI 2
	9	AI 6
	10	GND
	11	AI 3
	12	AI 7
	13	GND
	14	AO 0
	15	AO 1
	16	GND

Module	Terminal	Signal
	17	P0.0
	18	P0.1
	19	P0.2
	20	P0.3
	21	P0.4
	22	P0.5
	23	P0.6
	24	P0.7
	25	P1.0
	26	P1.1
	27	P1.2
	28	P1.3
	29	PF1.0
	30	+2.5 V
	31	+5 V
	32	GND

C.3: BMCM PCI-BASE50/300 Data Acquisition Card

PCI-BASE50/300

Data Acquisition and Processing Card for Mxx-Module



Features

- 2 slots for Mxx modules
=> up to 32 analog channels
- FIFO for rapid data acquisition
- PCI bus compatible (short PCI!)
- 16 or 32 digital channels

Applications

- acquisition of analog signals
- analog controls
- recording of digital events
- digital controls



BMC Messsysteme GmbH proudly presents the

... PCI-Multifunction Measuring Card ...

with a highly integrated and modular concept at an unbeatable price which allows the user to tackle any measuring task by assembling his individual measuring card. The MAD modules provide sampling rates of up to

... 333kHz ...

Depending on the application various modules are available for analog in- and outputs with resolutions of

... 12 or 16 Bit ...

The measured data can be simultaneously displayed and stored on the hard disk. The switch-over from one measuring range to another can be defined for each channel and does not influence the sampling rate.

... 16 or 32 digital
in-/ outputs respectively

are available on the PCI-BASE plate. This means that the base plate, without any analog module is a digital I/O card itself.

The

... modular concept ...

easily allows for

... 32 analog inputs ...

with resolutions of 12 or 16 Bit. In order to access the analog inputs 17..32, BMC Messsysteme offers a PC card cover with a 37pole Sub-D socket plus connecting cable.

At present the following analog input modules are available:

- MAD 12: 100kHz; 12 Bit
- MAD12f: 333kHz; 12 Bit
- MAD16: 100kHz; 16 Bit

These modules freely combine with each other or the following analog modules:

- MDA 12: 12 Bit, 2 outputs
- MDA 12-4: 12 Bit, 4 outputs
- MDA 16: 16 Bit, 2 outputs

We provide ActiveX controls STR-PCI for Windows® 95/98/2000/NT as well as the operator's software ST-PCI for the display, control and automation of analog and digital processes. These are included with the "Software Collection"-CD.

As the hardware component of the measuring data acquisition and analysis system NextView®/NT by BMC Messsysteme GmbH, the PCI-BASE50/300 offers superb performance under Windows® 95/98/2000 or NT and is available in the versions *Light*, *Professional* or *Client/Server*. A demo version is included.

Technical Data PCI-BASE50/300 (typical at 20°C and 5V Supply)

- Sampling Parameters (in connection with measuring and analysis software NextView®/NT)

	PCI-BASE50	PCI-BASE300
Max. cumulative sampling rate:	50kHz	330kHz
Digital input channels:	8	16
Digital output channels:	8	16
FIFO:	1kByte	4kByte
Memory depth:	depending on the RAM or HD space available (up to 4GByte)	
Trigger:	rising edge, falling edge, window trigger, logical trigger	
Prehistory:	0..99%	

• Digital In-/ Outputs

Level / digital IN R _i :	CMOS/TTL-level (0 = 0.0V..0.5V; 1 > 2.6V..5.0V) / 1MΩ
Digital IN surge resistant to:	60V DC
Digital OUT R _i / output current:	100Ω / 1mA

• Signal Connection

Analog In-/ Outputs (of MAD/MDA modules):	All channels are accessible at a 37pole Sub-D socket at the PC-card blende or via pin connectors.
Digital channels:	2x20pole pin connectors on the plate; The digital channels are brought out via the ZUKA16 (option).

• General Data

Power supply:	+5V from PCI-Bus, max. 500mA
Bus connection:	PCI-Bus
CE standards (EMC):	EN50081T1, EN50082T1, EN61010-1, max. 2kV ESD on the lines
Max. permiss. potentials:	60V DC acc. to VDE
Relative humidity:	0 – 90% (not condensing)
Size:	178 x 103 x 13,5 mm ³
Other:	ambient temp. 0..40°C, working temp. 0..70°C, storage temp. –25..85°C
Accessory (included):	PC blende for mounting
Other accessory:	connecting cable ZUKA16, current shunts ZUSP1000, all modules of the series MAD/MDA

• Software

Software (included):	STR-PCI (ActiveX Control) for programming under Windows® 95/98/2000/NT; operating programs ST-PCI; for displaying and controlling of analog and digital signals.
NextView®/NT:	Measuring and analysis software for the optimum performance of the measuring card.

Appendix D: MATLAB M-files

D.1: Perform Simulink Model and Data Reduction

```
clear variables, close all

% addpath 'C:\Programme\MATLAB7\work\work-Matlab';
%---Parameters determination
%Front suspension ,%Tyre ,%Hydro-pneumatic Suspension
%Tractor Mass and Moment of inertia ,%Tractor Dimensions
[t,x,y] = sim('vollmodel02onoffIpuf100simp');
%---(Data Analysis)
%---(RMS of the body Accelerations)
RMSORol=sqrt(mean(Rol.^2))
RMSOHea=sqrt(mean(Hea.^2))
RMSOPit=sqrt(mean(pit.^2))
%---RMS of the tire Force
RMSOTFrl=sqrt(mean(TFrl.^2)) %Tire Force
%---Pick to Pick of suspension Travel
ptp=max(STrl)-min(STrl)
%---1- PSD of the body Roll Acceleration
fs = 100; % Sampling frequency
T = 1/fs; % Sample time
L = size(Rol,1); % Length of the signal
NFFT = 2^nextpow2(L); % Next power of 2 from length of y
Win = hann(NFFT); % Window is a Hanning window of the length NFFT
f = fs/2*linspace(0,1,NFFT/2);
[mpsd f] = psd(Rol, NFFT, fs, Win, 0);
PSD = [2*mpsd/NFFT]; %Plot PSD Graph
figure (1), plot(f,PSD,'b','LineWidth',2)
aro2=1.2*max(PSD); axis([0 10 0 aro2]), grid minor
title('-Roll-'), xlabel('Frequency (Hz)'), ylabel('PSD (m2/ s4/ Hz)')
%---2-PSD of the body Pitch Acceleration
fs = 100; % Sampling frequency
T = 1/fs; % Sample time
L = size(pit,1); % Length of the signal
NFFT = 2^nextpow2(L); % Next power of 2 from length of y
Win = hann(NFFT); % Window is a Hanning window of the length NFFT
f = fs/2*linspace(0,1,NFFT/2);
[mpsd f] = psd(pit, NFFT, fs, Win, 0);
PSD = [2*mpsd/NFFT]; %Plot PSD Graph
figure (2), plot(f,PSD,'b','LineWidth',2)
```

```

aro2=1.2*max(PSD); axis([0 10 0 aro2]), grid minor

title('-Pitch-'), xlabel('Frequency (Hz)'), ylabel('PSD (m2/ s4/ Hz)')

%---3-PSD of the body Heave Acceleration
fs = 100; % Sampling frequency
T = 1/fs; % Sample time
L = size(Hea,1); % Length of the signal
NFFT = 2^nextpow2(L); % Next power of 2 from length of y
Win = hann(NFFT); % Window is a Hanning window of the length NFFT
f = fs/2*linspace(0,1,NFFT/2);

[mpsd f] = psd(Hea, NFFT, fs, Win, 0);
PSD = [2*mpsd/NFFT]; %Plot PSD Graph
figure (3), plot(f,PSD,'b','LineWidth',2)

aro2=1.2*max(PSD); axis([0 10 0 aro2]), grid minor

title('-Heave-'), xlabel('Frequency (Hz)'), ylabel('PSD (m2/ s4/ Hz)')

%---4-PSD of the wheels Acceleration
fs = 100; % Sampling frequency
T = 1/fs; % Sample time
L = size(Unrl,1); % Length of the signal
NFFT = 2^nextpow2(L); % Next power of 2 from length of y
Win = hann(NFFT); % Window is a Hanning window of the length NFFT
f = fs/2*linspace(0,1,NFFT/2);

[mpsd f] = psd(Unrl, NFFT, fs, Win, 0);
PSD = [2*mpsd/NFFT]; %Plot PSD Graph
figure (4), plot(f,PSD,'r','LineWidth',2)

aro2=1.2*max(PSD); axis([0 10 0 aro2]), grid minor

title('-Wheel rear-left-'), xlabel('Frequency (Hz)'), ylabel('PSD (m2/ s4/ Hz)')

%---5-PSD of the Dynamic Tire force
fs = 100; % Sampling frequency
T = 1/fs; % Sample time
L = size(TFrl,1); % Length of the signal
NFFT = 2^nextpow2(L); % Next power of 2 from length of y
Win = hann(NFFT); % Window is a Hanning window of the length NFFT
f = fs/2*linspace(0,1,NFFT/2);

[mpsd f] = psd(TFrl, NFFT, fs, Win, 0);
PSD = [2*mpsd/NFFT]; %Plot PSD Graph
figure (5), plot(f,PSD,'g','LineWidth',2)

aro2=1.2*max(PSD); axis([0 10 0 aro2]), grid minor

title('dynamic Tire force rl'), xlabel('Frequency (Hz)'), ylabel('PSD (N2/ Hz)')

```

D.2: Data Acquisition System (for Experimental Data)

%--- Acceleration on the Center of gravity of the tractor Body---

```
% Data Analyzer
% input, Output data files
path='C:\My Data\Studies\Mess-Technik\test Date\ASCII\';
rfile='one-pulse-hea.asc';
wfile='WHeave001.asc';

frpath=[path,rfile];

% Load input data file
DataM1=load (frpath);
MSize=size (DataM1);

si=MSize(1,1);

%Position of the Center of gravity of the tractor Body
%(Matrix a in 'AX=B' )
af=1.4;ar=1.4;tr=0.5;tl=0.5;
MDim = [1 -af tl; 1 ar tl; 1 ar -tr];
% Definition output Matrix
DataM2(si,7)=0;

%Loop
for n = 1:1:si
% Matrix B in 'AX=B'
% VLO=DataM(n,10) ,HLO=DataM(n,12) ,HRO=DataM(n,13)
MAcc= [DataM1(n,10);DataM1(n,12) ;DataM1(n,13)];

% System Equation solution
IA=inv(MDim);
X=IA*MAcc;

% outputfile matrix =[t,VLO,HLO,HRO,H,R,P]
t:time

%VLO:vertical acceleration on front left body corner
%HLO:vertical acceleration on rear left body corner
%HRO:vertical acceleration on rear right body corner
%H:Heave acceleration on body's Center of Gravitation
%R:Roll acceleration on body's Center of Gravitation
%P:Pitch acceleration on body's Center of Gravitation
DataM2(n,1)=DataM1(n,1);

DataM2(n,2)=DataM1(n,10);

DataM2(n,3)=DataM1(n,12);

DataM2(n,4)=DataM1(n,13);

DataM2(n,5)=X(1,1);

DataM2(n,6)=X(2,1);
```

```

DataM2(n,7)=X(3,1);
end
% Save Matrix 'DataM2' as a AscII file
fwpath=[path,wfile]
save(fwpath,'DataM2','-ASCII','-tabs')

%-----Tire Contact Force-----

%values of a quarter sprung mass and an unsprung mass
spm=mt/4; unm=axm/2
%Loop
for n = 1:1:si
% Read needed parameters
%zz2fl(n): sprung mass vertical acceleration of the front left corner
%zz2fr(n): sprung mass vertical of the front right corner
%zz2rl(n): sprung mass vertical of the rear left corner
%zz2rr(n): sprung mass vertical of the rear right corner
%zz1fl(n): unsprung mass vertical acceleration of the front left corner
%zz1fr(n): unsprung mass vertical of the front right corner
%zz1rl(n): unsprung mass vertical of the rear left corner
%zz1rr(n): unsprung mass vertical of the rear right corner
zz2fl(n)=DataM(n,1), zz1fl(n)=DataM(n,5);
zz2fr(n)=DataM(n,2), zz1fr(n)=DataM(n,6);
zz2rl(n)=DataM(n,3), zz1rl(n)=DataM(n,7);
zz2rr(n)=DataM(n,4), zz1rr(n)=DataM(n,8);
%Calculation
TFfl(n)=spm*zz2fl+unm*zz1fl; TFfr(n)=spm*zz2fr+unm*zz1fr
TFrl(n)=spm*zz2rl+unm*zz1rl; TFrr(n)=spm*zz2rr+unm*zz1rr
% outputfile matrix =[t, TFfl, TFfr, TFrl, TFrr]
t:time
% TFfl: vertical dynamic force of the front left tire
% TFfr: vertical dynamic force of the front right tire
% TFrl: vertical dynamic force of the rear left tire
% TFrr: vertical dynamic force of the rear right tire
DataM3(n,1)= DataM1(n,1);
DataM3(n,2)= TFfl(n);DataM3(n,3)= TFfr(n);
DataM3(n,4)= TFrl(n);DataM3(n,5)= TFrr(n);
end
% Save Matrix 'DataM3' as a AscII file
fwpath=[path,wfile]
save(fwpath,'DataM3','-ASCII','-tabs')

```

Appendix E: Vehicle-Suspension Model Parameters

E.2: Tractor Body Geometry, Mass and Inertia

Table E-1 : Tires static loads of the test-tractor

Ballast	Mass (kg)				Total
	lf	rf	lr	rr	
0	1200	1250	950	1100	4500
200	1150	1200	1100	1250	4700

Table E-2: Position of the CG of the test-tractor body relating to the axles and wheels.

Ballast	Dimension (mm)			
	af	ar	tr	tl
	CG to font axle	CG to rear axle	CG to right wheel	CG to left wheel
0	1289	1541	555	645
200kg	1415	1415	575	625

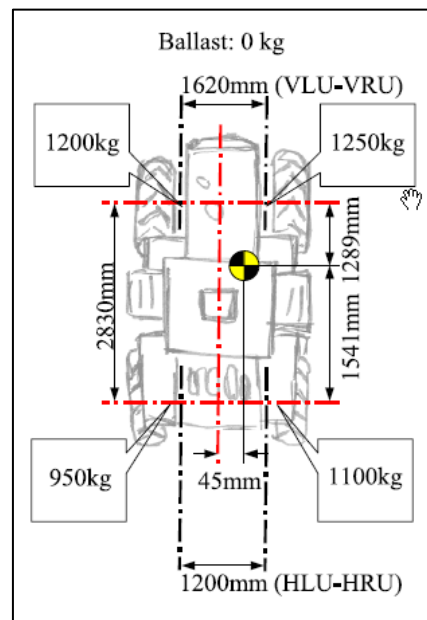


Figure E-1: Top view of the test-tractor with some relevant dimensions and tires static loads
(Thiebes P. , 2006).

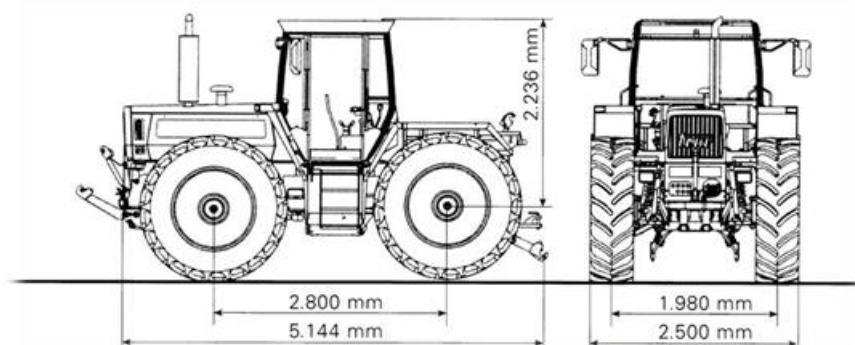


Figure E-2: Front and side view of the test-tractor with some relevant dimensions.

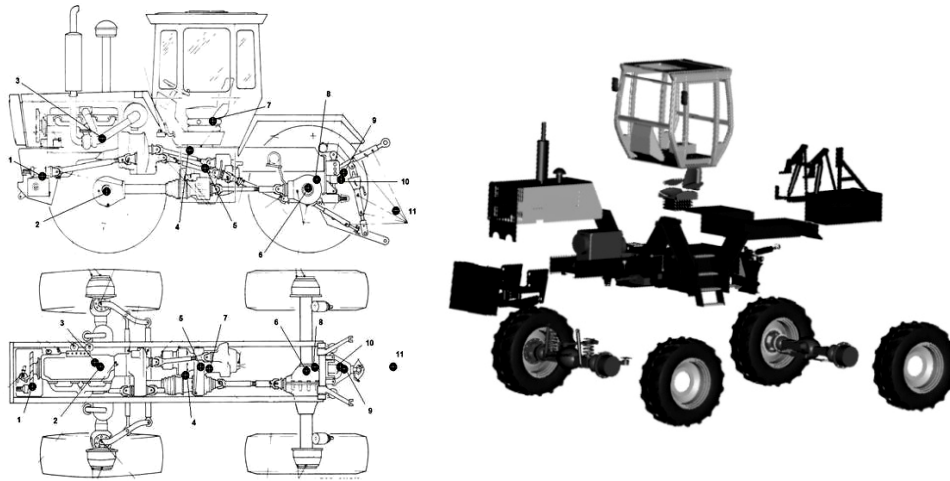


Figure E-3: Illustration of the major masses of the test-tractor with their center of gravity used for multi-body lump mass model.

x

Table E-3: Main mass-components of the test-tractor body with relevant mass, position of their CG and moment of inertia [derived from (Lehmann, 2004)].

Tractor Body Part		Mass [kg]	Position*			Inertia	
			x [m]	y [m]	z [m]	I_{xx} [kg.m ²]	I_{yy} [kg.m ²]
1	Main frame	1252	1.34	0.11	0.14	557.6	1952.7
2	Rear frame	365	-0.42	0.01	-0.25	58.1	30.5
3	Engine	585	2.56	-0.05	3	21	133
4	Transmission	820	1.13	0.09	-0.1	50	71
5	Cabin	755	1.02	0.02	0.53	360	359
6	Three-point hitch	258	-0.8	0.01	-0.16	61.6	48.8
7	Rear weights	250	-1.52	0.01	-0.67	64.3	138.5
8	PTO front	300	3.4	0.19	0	3.13	2.56
9	PTO rear	150	-0.76	0	-0.25	3.13	2.13
Sum			4735				
.* The coordinates are relative to a hypothetical point at end of the tractor							

Table E-4: The coordinate of the CG of the test-tractor body, calculated based on the main mass-components information from above table.

CG	x	y	z
$[m]$	1.064	0.056	0.404

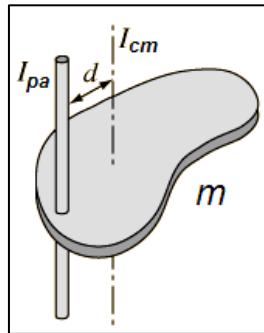


Figure E-4: The moment of inertia about an axis that is in parallel to the axis going across center of gravity. This is calculated by:

$$I_{\text{Parallel axis}} = I_{\text{Center of mass}} + md^2$$

Table E-5: Main mass-components of the test-tractor body with relevant longitudinal and lateral moments of inertia related to the CG of the tractor body.

	Tractor Body Part	I_{yy} $[kg.m^2]$	I_{xx} $[kg.m^2]$
1	Main frame	2430.9	895.0
2	Rear frame	622.4	297.4
3	Engine	1885.8	1540.9
4	Transmission	487.8	464.2
5	Cabin	459.8	458.9
6	Three-point hitch	551.2	207.6
7	Rear weights	838.1	333.0
8	PTO front	713.8	130.8
9	PTO rear	292.8	101.6
Sum		8282.5	4429.5

Table E-6: Parameters of the total mass and Inertia of the test-tractor body

Symbol	Description	Value	Units
M_t	Total body mass (unload)	6500	kg
I_{yy}	Moment of inertia (about pitch axis)	8282	$Kg.m^2$
I_{xx}	Moment of inertia (about roll axis)	4429	$Kg.m^2$

E.2: Tire/Axle properties

Table E-7: Tire Characteristic

Symbol	Description	Value	Units
M_{ur}	Rear tire /axle mass	430	kg
M_{uf}	Front tire /axle mass	440	kg
c_{Tr}	Rear tire damping coefficient	900	$N.s/m$
k_{Tr}	Rear tire stiffness	460,000	N/m
c_{Tf}	Front tire damping coefficient	920	$N.s/m$
k_{Tf}	Front tire stiffness	390,000	N/m
T_p	Tire inflation pressure	0.16	MPa

E.3: Front Suspension Properties

Table E-8: Front Suspension Parameter

Symbol	Description	Value	Units
k_f	Spring stiffness	125,000	N/m

E.4: Hydro-pneumatic Rear Suspension Properties

Table E-9: Parameters related to the hydro-pneumatic rear suspension of the test-tractor.

Symbol	Description	Value	Units
A_p	Piston area (head side)	3116	mm^2
A_r	Piston area (rod side)	1526	mm^2
c	Piston stroke	100	mm
p_o	Pre-charge gas pressure (head side)	1.00	MPa
p_o	Pre-charge gas pressure (rod side)	0.50	MPa
p_1	Initial pressure (head side)	4.55	MPa
p_1	Initial pressure (rod side)	1.75	MPa
V_o	Accumulator volume (head side)	4	dm^3 (L)
V_o	Accumulator volume (rod side)	2.5	dm^3 (L)
ρ	Density of the oil	900	kg/m^3
AT_p	Throttle cross-section (head side)	50	mm^2
AT_r	Throttle cross-section (rod side)	38	mm^2
AP_p	Cylinder port cross-section (head side)	55	mm^2
AP_r	Cylinder port cross-section (rod side)	41	mm^2
tp_a	Valve switching-on time (head side)	25	ms
tp_b	Valve switching-off time (head side)	35	ms
tr_a	Valve switching-on time (rod side)	20	ms
tr_b	Valve switching-off time (rod side)	30	ms
k	Polytrophic constant	1.35	-

Appendix F: Technical Data of MB Trac 1600 Turbo Tractor

Engine:

exhaust-driven turbocharger	direct injection, water-cooled
Power:	115 kW / 156 PS
Torque	530 Nm (54 kpm) in 1300-1700/min.
Fuel:	diesel
Cylinders	6
Total cylinders capacity	5958 cm ³
Rated RPMs:	2400 U/min
tank capacity	240 Liter

Transmission:

Forward:	14
Reverse	14

Dimensions:

maximum total weight	10000 kg
maximum weight on front axle	6020 kg
maximum weight on rear axle	6500 kg
empty weight	6320 kg
Length	4680 mm
width	2500 mm
Height	2930 mm
wheelbase	2650 mm
Ground clearance	580 mm
exterior width	2500 mm
turning radius	13,0 m

Hydraulics:

pump	gear type
nominal flow rate	57 l/min.
operating pressure	200 bar
travel speed	40km/h

Electrical:

Battery capacity	120 Ah
Battery volts	12 V

Tires:	520/70 R38
---------------	------------